Pairing Anaerobic Ammonia Oxidation with Newly Discovered Nitrite-Supplying Metabolisms for Enhanced Mainstream Nitrogen Removal

Kathryn I. Cogert

A dissertation

submitted in partial fulfillment of the

requirements for the degree of

Doctor of Philosophy

University of Washington

2020

Reading Committee:

Mari K.H. Winkler, Chair

David A. Stahl

Amy V. Mueller

Program Authorized to Offer Degree:

Civil and Environmental Engineering

UNIVERSITY OF WASHINGTON

ABSTRACT

Kathryn I. Cogert

Chair of the Supervisor Committee:

Professor Mari K.H. Winkler

Civil and Environmental Engineering

In wastewater treatment, sidestream nitrogen removal with anaerobic ammonia oxidation (anammox) has reduced cost, energy demand, and potentially greenhouse gas (GHG) emission as compared to conventional nitrification-denitrification However, under mainstream conditions, nitrite oxidizing bacteria (NOB) outcompete anammox bacteria for the nitrite produced by ammonia oxidizing bacteria (AOB). Therefore, nitrite production is the bottleneck in mainstream anammox nitrogen removal. The ultimate goal of this research was to evaluate the potential of three newly discovered nitrite-producing metabolisms for more reliable nitrite supply to anammox: nitrate-dependent denitrifying anaerobic methane oxidizing archaea (n-damo), ammonia oxidizing archaea (AOA), and complete ammonia oxidizing bacteria (comammox).

Nitrate-dependent denitrifying anaerobic methane oxidizing archaea (n-damo) anaerobically reduce nitrate with methane gas to produce nitrite that could support anammox nitrogen removal. AOB and NOB would produce nitrate aerobically for an anaerobic anammox and a n-damo compartment in which n-damo would convert some nitrate back to nitrite for anammox if supplied methane from anaerobic sludge digestion or a mainstream anaerobic membrane

bioreactor (AnMBR). A techno-economic analysis revealed that AnMBR/AOB/anammox systems reduced cost and GHG emissions the most, while the AnMBR/AOB/anammox/n-damo systems saw very similar reductions to the AnMBR/AOB/anammox system while simultaneously circumventing the risk of nitrate accumulation by NOB, potentially allowing easier aeration control.

Two newly discovered organisms of interest that could also supply nitrite to anammox under mainstream conditions are ammonia oxidizing archaea (AOA) and complete ammonia oxidizing bacteria (comammox), that are capable of ammonia and nitrite oxidation. AOA are known to co-operate with anammox in oxygen minimum zones (OMZs) where oxygen and ammonia (here considered as total ammonia plus ammonium) concentrations are low (similar to the mainstream) and counter-diffuse in opposite directions near the OMZ boundary. Low ammonia affinity AOA supply nitrite to anammox while outcompeting canonical NOB and AOB. AOA-anammox nitrogen removal was tested in both co-diffusing granular sludge and OMZ-like hollow fiber membrane aerated biofilm reactors (MABR). The AOA species *Nitrososphaera viennensis* was found only in the OMZ-like MABR environment while *Nitrospira* and anammox were abundant in both environments. Some of the *Nitrospira* detected were determined to be of comammox type. Similar to AOA, comammox have a high ammonia affinity but a low affinity for nitrite (their intermediate product) which gives anammox a competitive edge to access it. When comammox and anammox were inoculated into granular sludge and MABR reactors, co-operation between the two species was observed both experimentally and in theoretical models. Comammox abundance and nitrogen removal was higher in the MABR due to the same-counter-diffusing phenomenon that made low-affinity AOA a successful anammox partner in OMZs. It is

concluded that low-ammonia concentrations are essential to select for AOA- or comammox-anammox nitrogen removal.

In these nitrogen removal systems, online ammonium (NH_4^+) sensing would be highly advantageous, and thus a set of online electrodes targeting ions of interest were tested for their resiliency in anammox reactors. Polyvinyl chloride (PVC)-based potassium and ammonium electrodes were degraded in these reactors while poly-crystalline chloride probes did not. Potassium electrodes appeared to decay at the same rate in systems including active and inactivated granules while ammonium probes fouled faster in a biologically active system. These results motivate the need to understand the chemical effects of anammox granular sludge on ammonium probes.

In summary, novel processes for applying annamox in mainstream wastewater treatment were demonstrated and elucidated with modelling, bioreactor operations, and molecular analysis. The results showed that cooperation between these newly discovered nitrite producing species and anammox in wastewater treatment can lead to reduced energy requirements while meeting effluent limitations and mitigating our impact on the global nitrogen cycle.

TABLE OF CONTENTS

List of Figures ..... *vii*

List of Tables ..... *xi*

Chapter 1. Overview *1*

Chapter 2. Literature background *9*

2.1 Anammox in Wastewater Treatment 9

2.2 Two-Stage Anammox 12

2.3 One-Stage Anammox 13

2.4 NDAMO as an Anammox Partner 14

2.5 AOA as an Anammox Partner 16

2.6 A New Potential Partner: Comammox 17

Chapter 3. Reducing Cost and Environmental Impact of Wastewater Treatment with Denitrifying Methanotrophs, Anammox, and Mainstream Anaerobic Treatment *18*

3.1 Abstract 18

3.2 Abstract Art 19

3.3 Introduction 19

3.4 Materials & Methods 23

3.4.1 Calculating Differences in Greenhouse Gas Emissions and Cost 24

3.4.2 Scenario A: Conventional Nitrification/Denitrification..... 26

3.4.3 Scenario B: High Rate Activated Sludge & AOB/Anammox 26

3.4.4 Scenario C: AnMBR & AOB/Anammox 28

3.4.5 Scenario D: High Rate Activated Sludge, Anammox, & N-Damo..... 28

3.4.6 Scenario E: AnMBR, Anammox, & N-Damo 29

3.5 Results..... 29

3.5.1 Relative Difference in Greenhouse Gas Emissions 30

3.5.2 Relative Difference in Operational Cost..... 32

3.6 Discussion..... 34

3.6.1 Practical Control Concerns on Technology Selection 35

3.6.2 Impact of Nitrous Oxide Emissions on Results 36

3.6.3 Reduction in Greenhouse Gas Emissions and Cost 38

3.7 Supporting Information Available 40

Chapter 4. Replicating an Oxygen Minimum Zone in a Laboratory Microscosm Elucidates Partnerships between Anammox, Ammonia Oxidizing Archaea, and Nitrospira..... 41

4.1 Abstract..... 41

4.2 Introduction 42

4.3 Materials & Methods 44

4.3.1 Cultivation of Ammonia Oxidizing Organisms 44

4.3.2 Molecular Techniques 49

4.4 Results 51

4.4.1 *Metabolite Concentrations in Synthetic Environments* 51

4.4.2 Microbial Populations Present in Synthetic Environments 52

4.4.3 Microscopy of Synthetic Environment Biofilms 55

4.5 Discussion 55

4.5.1 Nitrogen Removal by AOA and Anammox Requires Counter-Diffusion 55

4.5.2 Comammox Presence in Co-Diffusing and Counter-Diffusing Environments 56

4.5.3 Potential for Anaerobic Nitrospira Activity 57

4.6 Supporting Information Available 60

Chapter 5. Comammox and Anammox Co-operate in both Co-Diffusing Granular Sludge and Counter-Diffusing Membrane Aerated Biofilm Reactors 61

5.1 Abstract 61

5.2 Abstract Art 62

5.3 Introduction 62

5.4 Materials and Methods 65

5.4.1 Cultivation of Ammonia Oxidizing Organisms 65

5.4.2 Determination of Kinetic Parameters of Nitrifying Species 66

5.4.3 Design, Operation, and Analysis of Co- and Counter- Diffusion Reactors 68

5.4.4 Theoretical Models 69

5.5 Results and Discussion 70

5.5.1 Nitrogen Removal Observed in Both Reactors 70

5.5.2 Comparing Measured Kinetic Parameters to Expected Values 72

5.5.3 Higher Abundance of Nitrifiers Leads to Higher Nitrogen Removal 73

5.5.4 Fish Microscopy Suggests a Possible Fate for Nitrate 76

5.5.5 Theoretical Co-operation of Comammox-Anammox at Varied Loading Conditions 78

5.5.6 Comparison of Theoretical and Experimental Results 83

5.6 Conclusions 83

5.7 Supporting Information Available 84

Chapter 6. Evaluating Impact of Anammox granular sludge on Ion Selective Electrodes 85

6.1 Introduction 85

6.2 Preliminary Work 86

6.3 Materials and Methods 90

6.3.1 Design of experimental setups 90

6.3.2 Abiotic granular sludge experiment 91

6.3.3 Nitric oxide experiment 91

6.3.4 Calibration of Sensors 92

6.3.5 Data Analysis Methods 93

6.4 Results & Discussion 93

6.4.1 Impact of Nitric Oxide on Sensors 93

6.4.2 Physical Abrasion with Inactive Granular Sludge 94

6.5 Supporting Information Available 96

Chapter 7. Conclusions and Future Outlook 97

References 103

Appendix A 1

Supplemental Results: Sensitivity Study of Pumping Demand on Results 32

Appendix B 1

Appendix C *1*

Appendix D *1*

LIST OF FIGURES

Figure 2-1. Anammox reactors have smaller footprints at both bench scale (a) and at pilot scale (b) in (Rotterdam, the Netherlands)[12] compared to traditional water resource recovery facilities with large clarifiers (c) in Seattle, WA, USA. 11

Figure 2-2. Reproduced from Hellinga et al., 1999.[14] The minimum sludge retention time (SRT) required to retain ammonium oxidizing bacteria (AOB), and nitrite oxidizing bacteria (NOB) in a reactor as a function of temperature demonstrates why it is possible to control the SRT to select for AOB over NOB only at high temperatures. 13

Figure 2-3. Ideal anammox granular sludge from a one-stage anammox system in the theoretical (a) and confirmed with FISH microscopy (b)[37]. 14

Figure 2-4. Interaction between DAMO and Anammox[45].....15

Figure 2-5. Ammonia, oxygen, and nitrite affinities for various nitrifying organisms[17,20,40]. 17

Figure 3-1. Overview of techno-economic-environmental feasibility study. 19

Figure 3-2. (A, the base case) traditional nitrification/denitrification. (B) High Rate Activated Sludge (HRAS) and AOB/anammox for nitrogen removal. (C) Anaerobic Membrane Bioreactor (AnMBR) and AOB/anammox (D) HRAS and nitrification/anammox/n-damo for nitrogen removal, and (E) AnMBR and nitrification/anammox/n-damo. 27

Figure 3-3. The reduction in GHG emissions possible by implementing four different theoretical treatment technologies; HRAS and partial nitritation-anammox (3-3.1), AnMBR and partial nitritation-anammox (3-3.2), HRAS and anammox/n-damo nitrogen removal (3-3.3) and AnMBR and anammox/n-damo nitrogen removal (3-3.4) versus Modified Ludzack-Ettinger, MLE, also referred to as conventional nitrification/denitrification. Calculations are performed assuming a plant flowrate of 60 th m3/day. Greenhouse gases are reported in

equivalent kg CO2/m3/day saved or additional kg CO2/m3/day. Reduction is shown in blue and increase is shown in red as defined by the color key. 30

Figure 3-4. The estimated cost saved by implementing four different theoretical treatment technologies; HRAS and partial nitritation-anammox (3.1), AnMBR and partial nitritation-anammox (3.2), HRAS and anammox/n-damo nitrogen removal (3.3) and AnMBR and anammox/n-damo nitrogen removal (3.4) versus Modified Ludzack-Ettinger, MLE, also referred to as conventional nitrification/denitrification. Calculations are performed assuming a plant flowrate of 60 th m3/day. USD saved or additional USD cost per m3 per day shown in blue and red respectively as defined by the color key. 33

Figure 3-5. Conceptual diagrams describing the ideal use cases for the theoretical technologies in this study's results. (a) The AnMBR/anammox scenario had slightly lower cost metrics than the AnMBR/anammox/n-damo scenarios at nearly all conditions. However, due to the aeration management complexity of the anammox only system, the AnMBR/anammox/n-damo scheme may be the most beneficial to operational cost. (b) The ideal technology to minimize greenhouse gas emissions is variable and dependent on both nutrient ratios and influent concentrations. 38

Figure 1-1. Schematics of the small-scale co-diffusion (left) and counter-diffusion (right) environments. Air and N_2 gas were mixed before being filtered and fed into the co-diffusion environment. In the counter-diffusion environment, nitrogen gas was directly added to bulk liquid in the 2nd phase of operation that is emphasized in this study. 48

Figure 1-2. Performance of AOA inoculated anammox when ammonia was the only nitrogen source available in both a co-diffusing environment (left) and counter-diffusing environment (right). The measured nitrogen removed (– • –) was near the concentration of ammonia fed into the synthetic environment (–, grey), indicating a high rate of nitrogen loss in the system. 52

Figure 1-3. The relative abundance of aerobic nitrifiers in biofilms, after termination of operation of both the co-diffusing environment (n=2) (left) and counter diffusing environment (n=1) (right), was evaluated using both 16S sequencing (top) and qPCR primers (bottom). New primers designed to target the *amoA* of *N. viennensis* and a general *amoB* primer set for *Nitrospira* were used to target AOA and comammox, respectively. 53

Figure 1-4. Absolute abundance of anammox measured in the biofilms of the co- and counter- diffusing environments after operation ceased, using qPCR primers designed to target the 16S rRNA gene of anammox. 54

Figure 1-5. FISH images of the biofilms present in the co-diffusing granular system (left) and counter-diffusion membrane system (right). Archaea are stained with blue (cy5), Anammox cells are hybridized with red (cy3), and *Nitrospira* is stained with green (fluorescein). 55

Figure 1-6. Hypothesized co-operation between *Nitrospira* and anammox. Anammox produces nitrate (NO_3^-) via the anammox nitrogen removal pathway and formate ($CHOO^-$) via the carbon fixing reverse acetyl-CoA pathway for *Nitrospira* to anaerobically reduce nitrate to nitrite (NO_2^-), which support anammox and allow full N removal. Such a scheme could be possible in the anaerobic conditions present in either a co-diffusion or counter-diffusion environment. 59

Figure 5-1. Concepts behind co-diffusing anammox granular sludge and counter-diffusing membrane aerated biofilm reactors (MABRs). 62

Figure 5-2. Pictures of both the small-scale anammox granular reactor (left) and the MABR while in operation. 68

Figure 5-3. The long-term operational performance of both the granular sludge reactor and MABR inoculated with comammox and anammox. 71

Figure 5-4. Final relative abundance of aerobic nitrifiers in biofilms present in both the granular sludge reactor (left) and MABR (right). 74

Figure 5-5. Abundance of comammox in both the granular sludge reactor (left) and the MABR (right) as detected by general qPCR *amoB Nitrospira* primers after operation was completed. 75

Figure 5-6. Anammox abundance in the granular sludge reactor (left) and MABR (right) as measured by qPCR targeting the 16S rRNA anammox gene. 76

Figure 5-7. Fluorescent in-situ hybridization (FISH) microscopy of the biofilms from both the granular sludge reactor (left) and MABR (right) after operation was finished. Probes targeting anammox (Cy 3, red), AOB (Cy 5, blue), and *Nitrospira* (Fluorescein, green) were used. 77

Figure 5-8. Theoretical performance (top) and microbial composition (bottom) of co-diffusing anammox granular sludge inoculated with comammox with changing dissolved oxygen (left) and influent ammonia concentrations (right). 79

Figure 5-9. Theoretical performance and microbial composition of counter-diffusing anammox MABR inoculated with comammox with changing dissolved oxygen (left) and influent ammonia concentrations (right).....82

Figure 7-1. Sensors were placed in an anammox granular sludge reactor (left) where they were observed to degrade (right).....87

Figure 7-2. Schematics of the experimental conditions in which sensors were tested. (A) a control system aerated with compressed air, (B) a biologically inert granular sludge system mixed with compressed air,and (C) a system without granular sludge sparged with 1000 ppm nitric oxide.....90

Figure 7-3. After approximately four days of exposure to 1000 ppm nitric oxide, little sensor decay was observed in the chloride (left), potassium (middle), or ammonium (right) sensors. 94

Figure 7-4. Sensor drift over time for ammonium, potassium, and chloride sensors in the abiotic granular system, operating reactor, and control.....95

LIST OF TABLES

Table 5-1. Oxygen uptake kinetics of N. inopinata 73

Table 7-1. Calibration slopes (mV/decade) of sensors before and after long-term exposure to active anammox biomass. 87

Table 7-2. Description of sensors used in Anammox reactor. 88

Table 7-3. Concentrations in μM in the multi-salt set of calibrating solution used after 14 days of exposure to active anammox granular sludge. 88

ACKNOWLEDGEMENTS

This dissertation represents a period of my life of immense scientific, professional, and personal growth which could not have been possible without the support of many wonderful people. First, I would to thank my advisor, Prof. Mari Winkler for her encouragement and guidance throughout my time as a graduate student at UW. She has been an excellent role model as a visionary leader and an interdisciplinary engineer/scientist and her direct communication tempered with patience brought the quality of my work to new heights. I also would like to extend deep thanks to my entire committee, Prof. Dave Stahl, Prof. Amy Mueller, and Prof. Dave Beck. I am immensely grateful to Dave Stahl for his incisive questions that inspired me and taught me how to be a better scientist. Amy Mueller's patience, flexibility, and relentless positivity in the face of seemingly disappointing results is energizing and her attention to detail always provided me with valuable learning opportunities. I could not have made it to the finish line without the personal and professional advice given to me by Dave Beck, and his expertise in computer science and bioinformatics has been very relevant to my work and provided a valuable perspective on my data I would not have received otherwise and

I was very fortunate to work alongside many brilliant minds during my time at Benjamin Hall who provided valuable insight into my work in the form of casual conversation across lab benches (including but not limited to): Maxwell Armenta, Sam Bryson, John Carter, Nick Elliot, Bruce Godfrey, Jessica Hardwicke, Matthieu Landreau, Kelley Meinhardt, Frederick von Netzer, Kota Nishiguchi, Wei Qin, Madelyn Shaprio, Levi Straka, Dave Vuono, Ting Xie, Ryan Ziels, and many more that I may have forgotten to list here. I want to give an additional special thanks to my "Science Sister" Stephany Wei, who started her PhD about the same time as me, and was an immense source of support and knowledge as we made our way through our degrees together

and has become a lifelong friend. I am also grateful to have had the opportunity to supervise many gifted master's students and undergraduates: Laura Orschler, Kumari Soni, Lukas Keller, Kateryna Gomozsova, Carter Gears, Maria Abando, and Kim Tran. I have and will continue to enjoy following their progress and careers.

This work was supported by the Valle Scholarship, the U.S. Environmental Protection Agency through the Science To Achieve Results Fellowship [Contract #: 83929101], and the Defense Advanced Research Project Agency [Contract #: HR0011-17-2-0064], the Paul L. Busch award, and the University of Washington.

I am grateful for the constant encouragement from my greater community. I would have not made the amount of progress I did without mentorship from other professors like Prof. Jim Pfaendtner, Prof. Renata Bura, and others. Additionally, I am so lucky to be supported and loved by friends as kind, thoughtful, and empathetic as Julie Mendel, Tim Dobbs, Michelle Lee, Julie Brower, Sarah Vorpahl, and many others. I am also lucky to have the Alton and LeeAnn Cogert as my family, and I thank them for (and return) their love and support over the past thirty years. Finally, I would like to acknowledge Boltzmann the Dog, who I loved watching while his owner, Jim Pfaendtner, was away. Boltzmann is not good at science, but very good at tug of war and cheering up graduate students.

Chapter 1. OVERVIEW

The nitrogen cycle is one of the most important elemental cycles on earth. Human activities have severely disrupted the cycle through excessive nitrogen discharge to aquatic and terrestrial environments. When nitrogen is discharged untreated into water bodies, it can lead to eutrophication, a phenomenon which decimates aquatic biodiversity, promotes invasive species, and costs $2.2 billion annually in the US[1,2]. The removal of nitrogen from point sources, such as wastewater, is accomplished in wastewater resource recovery facilities (WRRFs). However, nitrogen removal is expensive and produces greenhouse gases like carbon dioxide, methane, and nitrous oxide[3]. As wastewater treatment accounts for 2% of the U.S energy budget,[4] improving the carbon footprint of technologies that treat wastewater is a topic of great interest.

Nitrogen removal is most traditionally accomplished with a combination of nitrification and denitrification, requiring energy intensive aeration that accounts for approximately 50% of the net energy budget of wastewater treatment[4]. Influent ammonia (NH_3 and NH_4^+) first undergoes nitrification in two steps. Ammonia is first oxidized to nitrite (NO_2^-) by ammonia oxidizing bacteria (AOB), and NO_2^- is then oxidized to nitrate (NO_3^-) by nitrite oxidizing bacteria (NOB). Nitrification requires aeration blowers, which consume a lot of energy, to supply oxygen to AOB and NOB[4]. The formed nitrate is reduced to di-nitrogen gas by denitrifying heterotrophs that require an organic carbon source. If there is not enough organic carbon present in the wastewater, it must be added externally, usually as methanol or glycerol, at a cost to the facility[5]. Denitrification has a high biomass yield and therefore costly and energy intensive sludge handling equipment is required for sludge de-watering and landfilling or incineration[6]. In addition to these drawbacks, conventional nitrification/denitrification occurs in flocs that are

recycled through different aerobic and anaerobic tanks, resulting in costly recycle flows. Moreover, given the small density difference between sludge flocs and water, space-consuming settling tanks are required to separate the treated wastewater from the sludge.

Two innovations in the field of wastewater treatment over the last 20 years have begun to resolve these limitations (1) granular sludge reactor technologies and (2) nitrogen removal techniques based on anaerobic ammonia oxidation (anammox). In granular sludge technology, no separate settling tank is required and excessive recycle flows are avoided, resulting in a space reduction of up to 70%, capital cost savings of up to 30% and up to 25% less energy demand compared to conventional municipal wastewater treatment systems[7]. Anammox nitrogen removal is the anaerobic conversion of ammonia and nitrite, in about equimolar amounts, to nitrogen gas[8]. Anammox bacteria are autotrophic microorganisms that fix CO_2 as a carbon source for growth, therefore eliminating the need to add organic carbon for denitrification. They also have a much lower yield than heterotrophic denitrifiers, so anammox nitrogen removal systems reduce sludge production by up to 90%[9,10]. The total ammonia:nitrite ratio required for anammox nitrogen removal is supplied through a preceding partial-nitritation step in which 50% of the influent total ammonia is oxidized to nitrite (by AOB), while further oxidation to nitrate (by NOB) is prevented. 50% of the influent ammona remains unconverted and serves the anammox bacteria as an electron donor. Partial-nitritation/anammox processes result in substantial savings in aeration costs (up to 63%) and external carbon source addition costs (100%) and minimize CO_2 emissions and sludge production significantly[11]. Anammox can also form dense granules of 1-3mm in diameter that reduce the diffusion distance of substrates between different partner organisms offering a maximal microorganisms-to-space ratio and excellent settling properties, resulting in reduced tank volumes with smaller physical footprints[12]. AOB grow in the aerobic

outer rim of the anammox granule where they shield anammox in the granule interior from oxygen. Anammox is applied to treat reject water of anaerobic digesters in a sidestream that has high temperatures and carbon-to-nitrogen ratios too low support denitrification. Over 200 of these cost-efficient full-scale side stream treatment installations exist[13], with nitrogen removal reaching capacities of up to 10 $kgNH_3\text{-}N.m^{-3}.day^{-1}$, tenfold higher than conventional treatment systems[12].

Anammox offers an enormous opportunity to make future wastewater treatment more sustainable. However, in the mainstream, cold and low total ammonia (<20 °C, <100 mgN/L) conditions make it difficult to outselect NOB, which will compete with anammox for NO_2^{-5}. At high side-stream temperatures and ammonia replete concentrations present in the sidestream (~ 30 °C, >> 100 mgN/L), AOB grow faster than NOB. In addition, NOB are further inhibited by high free ammonia concentrations, so it is possible to tightly control sludge retention time (SRT) such that the faster growing AOB can be sustained while NOB are washed out[14,15]. However, this is only possible in the warm, ammonia rich, sidestream centrate. Alternately, it is possible to achieve anammox nitrogen removal in a single reactor of granular sludge with a low dissolved oxygen concentration in order to take advantage of AOB's higher affinity for oxygen than NOB[15]. However, low oxygen and ammonia concentrations hinder the rate of aerobic ammonia oxidation, resulting in poor nitrogen removal rates that are unacceptable in a mainstream system. Therefore, anammox requires a new partner organism capable of providing a more robust nitrite supply than AOB. **The ultimate goal of this research is to evaluate the viability of three newly discovered nitrite-producing organisms to improve nitrogen removal cost and environmental impact in mainstream wastewater treatment.** Chapter **2** provides an overview of literature relevant to this research, including an introduction to anammox nitrogen removal in

wastewater treatment and the current state of understanding of newly discovered nitrite-producing organisms as potential partners for anammox.

In **Chapter 3**, the theoretical potential of anammox to receive nitrite from newly discovered nitrite-driven anaerobic methane oxidizing archaea (n-damo) capable of converting nitrate to nitrite while anaerobically oxidizing methane, was explored in a techno-economic-environmental feasibility analysis. The potential operational savings and reduction in greenhouse gas emissions for four nitrogen and carbon removal designs that are as of yet untested at full-scale were reported. The largest environmental and economic benefits were seen with the implementation of a mainstream anaerobic membrane reactor (AnMBR) for carbon removal and the addition of n-damo to anammox nitrogen removal had only a small impact on greenhouse gas emissions while potentially alleviating the necessity to stop nitrification at nitrate, allowing easier aeration control.

In **Chapter 4**, ammonia oxidizing archaea (AOA) were explored. AOA is an aerobic ammonia oxidizing organism that has been observed to work with anammox in marine oxygen minimum zones causing up to 50% of marine nitrogen loss. Due to AOA's high affinity for ammonia, it is able to continue to supply nitrite to anammox at low oxygen conditions that would inhibit NOB and low ammonia and oxygen conditions that would inhibit AOB. In this chapter, AOA and anammox were inoculated together in two different mesocosms, a granular sludge system, in which ammonia and oxygen co-diffuse into a redox stratified biofilm, and a membrane aerated biofilm, in which oxygen and ammonia enter opposite sides of the biofilm, resulting in counter-diffusion. The counter-diffusion system was designed to mimic a marine oxygen minimum zone (OMZ), in which oxygen diffuses downward from the surface while ammonium originating from within the OMZ diffuses upward to the OMZ boundary layer. AOA were only able to co-operate

with anammox in the counter-diffusing environment, suggesting that counter-diffusion is essential for AOA-anammox nitrogen removal. Furthermore, the presence of a complete ammonia oxidizing (comammox) bacteria was detected. Comammox is another newly discovered organism capable of both ammonia and nitrite oxidation at oligotrophic conditions[16,17]. The emergence of a comammox population in these anammox systems demonstrated their potential to co-operate with anammox. Both systems observed high percentages of nitrogen removal and residual nitrogen left the system as ammonia, and not nitrite or nitrate. This result was surprising as anammox produces nitrate in its anabolic pathway[8]. There was also a high relative abundance of *Nitrospira* detected that could not be explained entirely by the presence of *Nitrospira* comammox. *Nitrospira* were also found in anaerobic regions of the biofilms. These findings together spurred the development of a new hypothesis which suggests the potential of a nitrate-cycling partnership between *Nitrospira* and anammox. *Nitrospira* could be performing their newly discovered anaerobic nitrate reducing pathway using formate as an electron donor[18], while anammox supply nitrate from ammonia oxidation and formate (an essential intermediate in the reverse acetyl-coA pathway possessed by anammox)[19] and nitrate (from anaerobic ammonia oxidation)[8].

This new hypothesis and the potential of comammox-anammox co-operation was further supported by the study described in **Chapter 5**, in which complete ammonia oxidizing bacteria (comammox), were inoculated with anammox in both an anammox granular sludge reactor and a membrane aerated biofilm reactor (MABR). Theoretical models were also used to better understand the population dynamics in these systems. In both theoretical and experimental work, comammox were found to co-operate with anammox in both reactors, though comammox abundance and fractional nitrogen removal were found to be higher in the MABR. This was

caused by the co-occurrence of the higher maximum oxygen concentration present in the MABR as compared to the granular sludge system and the simultaneously low ammonia concentrations near the membrane-biofilm interface. Low ammonia concentrations selected for the high affinity comammox while the higher oxygen concentrations enabled higher comammox activity resulting in more nitrite production for anammox. Anammox appeared to out-compete comammox for nitrite likely because of the nitrite affinities of anammox and comammox. The species of comammox used in this study, *Nitrospira inopinata*, have a worse affinity for nitrite (371 μM-NO_2^-)[17] than anammox (48-7.1 μM-NO_2^-)[8,20], which would allow anammox a competitive niche to access nitrite produced by comammox. The MABR out-performed maximum possible nitrogen removal predicted by the theoretical model, and the theoretical models predicted the presence of nitrite and nitrate in the effluent at all conditions, while neither the MABR nor the granular sludge reactor had nitrite or nitrate in their effluent. The experimental results are in line with the results from Chapter 4, in which no nitrite or nitrate was observed in the effluent of either the co- or counter-diffusing system. As *Nitrospira* was also found in the anaerobic regions of the comammox inoculated biofilms, the nitrate-cycling hypothesis posed in chapter 4 would explain the absence of nitrate and nitrite in the effluent of these systems as well. It would also explain the discrepancies between the theoretical model and the experimental model as the nitrate produced by anammox would be reduced back to nitrite and then be converted by anammox to di-nitrogen gas.

In order to select for either AOA or comammox as a nitrite source for anammox, low ammonia concentrations are required. In systems where the nitrogen loading rate is high, it is critical to simultaneously maintain a high nitrogen flux to ensure the necessary low total ammonia concentration is achieved. However, reliable mechanisms to control ammonia concentrations

online do not exist as current wet-lab methods are time and labor intensive while ion selective electrodes have been observed to foul much faster in nitrogen removal systems than in cleaner applications[21]. In **Chapter 6**, the impact of the abrading effect of anammox granular sludge on the delicate membranes of ion selective electrodes was evaluated. Ammonium, potassium, and chloride probes were kept in three aerated environments, an operating anammox granular sludge reactor, a compartment with biologically deactivated granular sludge, and a control compartment with no granular sludge. Decline in probe performance was measured as the decay in a probe's calibration curve slope over the course of at least 14 days in each environment. The performance of the poly-crystalline membrane chloride probe did not change significantly in any of the environments, while significant decay of both the PVC ammonium and potassium probes was observed in both the biologically deactivated and active granular sludge systems. While the potassium probes in the abiotic and biotic environments decayed at very similar rates, the ammonium probes decayed much faster in the operating granular sludge environment.

The methods, results, and conclusions of this study are presented in Chapter 3 as published papers and in Chapters 4,5, and 6 as manuscripts currently in preparation for submission. The key conclusions and future outlook of the technologies described are summarized in the concluding **Chapter 7**. Supplemental data for the research presented in Chapters 3-6 is presented in Appendices A-D

The publication associated with the research in **Chapter 3** is:

Cogert, K. I.; Ziels, R. M.; Winkler, M. K. H. Reducing Cost and Environmental Impact of Wastewater Treatment with Denitrifying Methanotrophs, Anammox, and Mainstream Anaerobic Treatment. *Environ. Sci. Technol.* **2019**. https://doi.org/10.1021/acs.est.9b04764.

The planned publication associated with the research in **Chapter 4** is:

Cogert, K. I.; Shapiro M.; Tran, K., Gottshal, E., Bryson, S., Rittman, B., Stahl D.A., Winkler, M. K. H., (2021) Replicating an Oxygen Minimum Zone in a Laboratory Microscosm Elucidates Partnerships between Anammox, Ammonia Oxidizing Archaea, and Nitrospira. *Prepared for submission to The ISME Journal.*

The planned publication associated with the research in **Chapter 5** is:

Cogert, K. I.; Shapiro M.; Tran, K., Qin, W., Rittman, B., Stahl D.A., Winkler, M. K. H., (2021). Comammox and Anammox Co-operate in both Co-Diffusing Granular Sludge and Counter-Diffusing Membrane Aerated Biofilm Reactors *Prepared for submission to Water Research.*

The planned publication associated with the research in **Chapter 6** is:

Cogert, K. I.; Mueller A. V., Winkler, M. K. H., (2021). Evaluating Impact of Anammox granular sludge Conditions on Ion Selective Electrodes. *Prepared for submission to Environmental Science & Technology Letters*

Chapter 2. LITERATURE BACKGROUND

2.1 ANAMMOX IN WASTEWATER TREATMENT

In 1977, E. Broda predicted the existence of a chemolithotrophic organism that would anaerobically oxidize ammonia and nitrite to produce nitrogen gas based on the standard Gibbs free energy of the reaction:[22]

$$NH_4^+ + 1.3\ NO_2^- \rightarrow N_2 + 2H_2O + 0.3\ NO_3^- \qquad \Delta G = -360\ kJ \qquad \text{Eqn 2-1}$$

These organisms, named anammox for their unique metabolism, were eventually discovered in a 23-L denitrifying fluidized bed reactor, and their metabolic stoichiometry was empirically determined in laboratory testing[23,24]:

$$NH_3 + 1.32\ NO_2^- + 0.07\ HCO_3^- + 0.13\ H^+ \rightarrow 1.02\ N_2 + 0.26\ NO_3^- + 0.07\ CH_2O_{0.5}N_{0.15} + 2.03\ H_2O \qquad \text{Eqn 2-2}$$

Since their discovery, anammox have been found to grow prolifically in the ocean[25,26]. Initially, it was thought that anammox had only a small role in the nitrogen cycle due to their slow doubling time (0.21 d^{-1})[27]. However, more recent analysis and theoretical modeling has shown anammox to be a major player in the ocean's nitrogen cycle, accounting for up to half of marine nitrogen loss[28–31]. Successfully enriched anammox are restricted to a group of microorganisms in the *Plantomycetes* phylum. There are five described candidatus anammox genera: Brocadia, Kuenenia, Anammoxoglobus, Jettenia, and Scalindua.[29] The ideal pH for their growth is between 6.7 and 8.3 with a pH optimum around 7.5[8,32]. The maximum conversion from anammox found in wastewater treatment is at 37 °C, though activity has been observed between 10- 45°C[33,34]. Nitrite is toxic to anammox in high enough concentration with half inhibition reported at approximately 5 mM in an anammox reactor[35].

In wastewater treatment, the implementation of anammox represents significant reduction in energy demand, greenhouse gas emissions, and operational cost. In traditional nitrogen removal, all influent nitrogen is completely oxidized from ammonia (NH_3) to nitrite (NO_2^-) by ammonia oxidizing bacteria (AOB) and then to nitrate (NO_3^-) by nitrite oxidizing bacteria (NOB) in the stoichiometries shown in equations 2 & 3.

$$NH_4^+ + 1.5\ O_2 \rightarrow NO_2^- + 2H^+ + H_2O \quad \text{Eqn 2-3}$$

$$NO_2^- + 0.5\ O_2 \rightarrow NO_3^- \quad \text{Eqn 2-4}$$

Nitrate is then reduced to di-nitrogen (N_2) gas by heterotrophic denitrifying bacteria that use organic carbon in the influent as an electron donor. While traditional nitrogen removal requires complete nitrification of nitrate by AOB and NOB, anammox nitrogen removal shortcuts the nitrogen cycle because it only requires partial-nitritation of ammonia to NO_2^- by AOB. Anammox then anaerobically oxidizes NH_3 and NO_2^- to N_2 at approximately a 1.3 NO_2^-/NH_3 molar ratio as shown in equation 2.[12,36,37] Short-cut anammox nitrogen removal has five key advantages over traditional nitrogen removal:

1) Anammox is autotrophic and does not require organic carbon, eliminating the necessity for expensive external organic carbon addition. This contrasts with conventional heterotrophic denitrification that may require additional organic carbon in the form of methanol or glycerol if the C/N ratio in the influent wastewater is too low.
2) Energy requirements for aeration are reduced by approximately 60%, as only partial conversion of influent total ammonia to nitrite is required[11], whereas in traditional nitrogen removal, complete nitrification of 100% of influent total ammonia is required prior to denitrification.

3) Sludge production is reduced by up to 90%, primarily because the biomass yield of anammox (0.07 gVSS/gN-N_2) is much lower than heterotrophic denitrifying bacteria (2.25 gVSS/gN-N_2)[5,8].

4) Lower emissions of CO_2 and N_2O greenhouse gases may be produced as autotrophic anammox do not respire CO_2 and cannot produce N_2O unlike heterotrophic denitrifying bacteria. The reduction of N_2O emission is especially notable since it has a global warming potential 298-times that of CO_2[38]. The exact reduction of N_2O gas in anammox granular sludge is under dispute. AOB, which are necessary to both conventional and anammox nitrogen removal, do produce N_2O gas, but the exact amounts under varying conditions are inconsistently reported.[39]

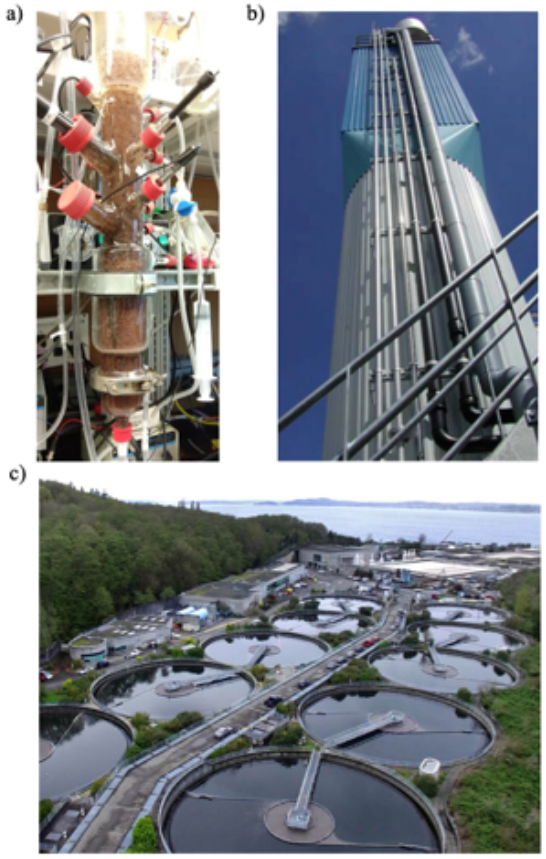

Figure 2-1. Anammox reactors have smaller footprints at both bench scale (a) and at pilot scale (b) in (Rotterdam, the Netherlands)[12] compared to traditional water resource recovery facilities with large clarifiers (c) in Seattle, WA, USA.

5) The physical footprint of the nitrogen removal system can be significantly reduced. Anammox can grow in large, dense, fast settling granules. Granular sludge is selected for over flocculant sludge by combining a short settling period (1-10 minutes) and shear force applied to the surface of the particles through mixing.[12] Together, these selection pressures result in large dense particles. The short settling time is accomplished in tall,

thing reactors (Figure 2-1a-b) that have a much smaller footprint than traditional clarifiers (Figure 2-1c) required to separate out flocculant denitrifying activated sludge from treated wastewater. Smaller footprints are especially beneficial to plants located in densely populated areas where real estate is a scarce resource.

However, the application of anammox in wastewater treatment is limited to treatment of sidestream centrate, the low volume stream (1% of volumetric flow) of warm (>30 °C), total ammonia rich (>>10 mM) reject water that is produced after dewatering sludge that has been anaerobically digested[5]. Under these warm high ammonia conditions, AOB are able to reliably supply anammox with nitrite, while at the comparably cold (< 20 °C), total ammonia deplete (< 5 mM) mainstream conditions, NOB outcompete AOB for oxygen and anammox for nitrite. There are currently two primary control strategies used to limit NOB activity in these systems; temperature driven control (two stage system) and oxygen driven control (single stage system).

2.2 TWO-STAGE ANAMMOX

In a two stage anammox system, aerobic and anaerobic species are separated in two reactor compartments. In the first compartment, approximately half of the influent total ammonia is aerobically oxidized to nitrite in a single reactor compartment. The ammonia / nitrite rich effluent is then used as influent for the anaerobic second stage in which anammox can grow and

remove nitrogen.

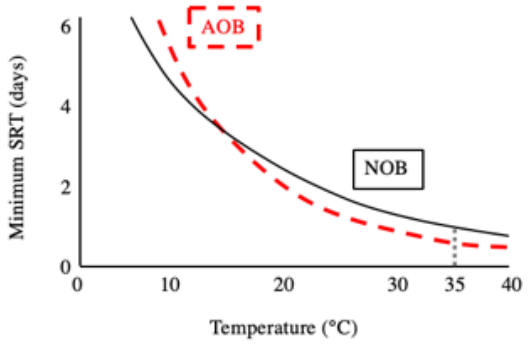

Figure 2-2. Reproduced from Hellinga et al., 1999.[14] The minimum sludge retention time (SRT) required to retain ammonium oxidizing bacteria (AOB), and nitrite oxidizing bacteria (NOB) in a reactor as a function of temperature demonstrates why it is possible to control the SRT to select for AOB over NOB only at high temperatures.

It is critical to control the first stage to select for AOB over NOB to avoid complete nitrification to nitrate. This is possible at the higher temperatures of the centrate from warm anaerobic digesters. At warm temperatures, AOB have a faster growth rate than NOB and the sludge retention time (SRT) of biomass in the nitrification tank can be controlled to retain AOB while NOB washout (Figure 2-2) in order to produce nitrite over nitrate for anammox.

2.3 ONE-STAGE ANAMMOX

As previously mentioned, anammox and AOB are able to form small granular sludge particles. This structure is beneficial not only for its fast settling time, but also provides a redox gradient such that there are both aerobic and anaerobic regions in the same reactor. On the granule's surface, AOB consume oxygen and produce nitrite, simultaneously supplying nitrite to anammox while shielding the obligate anaerobe, anammox, from oxygen (Figure 2-3).

However, selecting for AOB over NOB in granular sludge requires controlling the system at a low dissolved oxygen concentration (<0.5 mg O_2/L). AOB have a higher affinity for oxygen than NOB (0.3 mgO_2/L for AOB and 1.1 mgO_2/L for NOB),[40] so by controlling a system at low dissolved oxygen, AOB outcompete NOB for oxygen, allowing for complete nitrogen removal in a single stage.

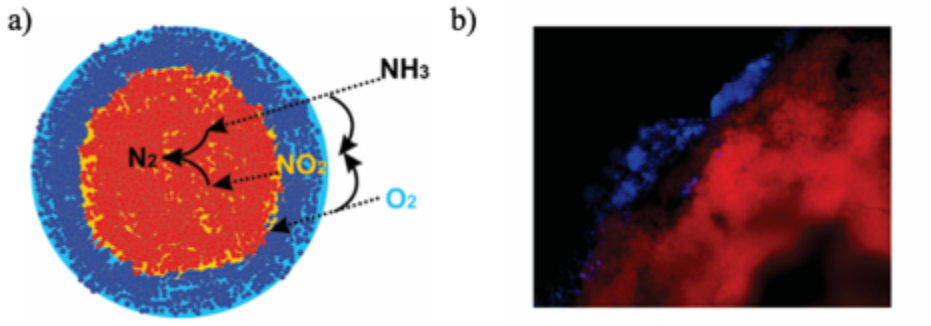

Figure 2-3. Ideal anammox granular sludge from a one-stage anammox system in the theoretical (a) and confirmed with FISH microscopy (b)[37].

However, at these low oxygen concentrations some ammonia remains untreated, resulting in residual ammonia in the effluent. This is acceptable in the sidestream treatment of anaerobic digester centrate, which makes up only 1% of volumetric flow, but high find ammonia effluent concentrations would violate permitted discharge limits in the mainstream that are governed by stringent requirements. A more robust configuration is needed to combine anammox with a process that can reliably supply nitrite to anammox while minimizing NOB activity and keeping nitrogen removal rates high enough to meet strict discharge permits. Three newly discovered organisms have such potential; nitrite-driven anaerobic methane oxidizing archaea (n-damo), ammonia oxidizing archaea (AOA), and complete ammonia oxidizing bacteria (comammox).

2.4 NDAMO AS AN ANAMMOX PARTNER

Nitrite-dependent anaerobic methane oxidizing (n-damo) archaea, or *Candidatus* Methanoperedens nitroreducens were first discovered in methane/nitrate/ammonia fed anaerobic methane oxidizing consortium inoculated with anammox (Figure 2-4)[41–44]. NDAMO archaea's metabolism anaerobically oxidizes methane using nitrate as an electron acceptor, producing nitrite[41]:

$$CH_4 + 4\ NO_3^- \rightarrow CO_2 + 4\ NO_2^- + 2\ H_2O \qquad \text{Eqn 2-5}$$

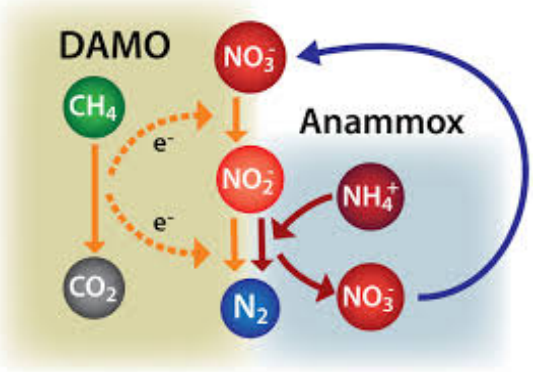

Figure 2-4. Interaction between DAMO and Anammox[45]

N-damo archaea are also found in culture with NDAMO bacteria, or *Candidatus* Methylomirabilis oxyfera, which anaerobically oxidized methane along with nitrite as an electron acceptor, producing N_2 gas. Even though n-damo bacteria and anammox are in competition for nitrite, modeling work has shown that n-damo bacteria would only survive in the presence of excess nitrite due to their lower affinity for nitrite than anammox[46].

These early successes in enhanced nitrogen and methane removal have inspired a lot of interest in adopting n-damo into a modified two-stage anammox nitrogen removal system for mainstream treatment.[11,43,47] Half of the influent total ammonia could undergo complete nitrification in the first stage by both AOB and NOB and would then be fed to the second anaerobic stage populated by anammox and n-damo along with the other half of the influent total ammonia. Co-operation between n-damo and anammox in anaerobic methane-fed conditions at small scale has been demonstrated[11]. Methane is often produced on-site at wastewater treatment plants during anaerobic digestion, either in an anaerobic mainstream digestion reactor or an anaerobic sludge digester, so it could be readily available to the second anaerobic stage.

2.5 AOA AS AN ANAMMOX PARTNER

The first ammonia-oxidizing archaeon was isolated from the rocky substratum of a saltwater tropical marine aquarium tank and named *Nitrosopumilus maritimus*[48]. It was the first cultivated representative of the ubiquitous marine Group 1 crenarchaeota and, like AOB, has the ability to grow chemolithoautotrophically by oxidizing ammonia to nitrite under mesophilic conditions. Today, many different species of AOA have been enriched or isolated from various environments, including marine, hot spring, soils, wastewater treatment plants, coal-tar contamination sites, and freshwater sediments[49–56].

AOA are frequently found in environments with low substrate (NH_3 and O_2) availability whereas AOB are commonly found in environments with higher substrate availability.[57] AOA have a remarkably high affinity for both oxygen and ammonia (Figure 2-5) and these low affinity constants make AOA a relative K-strategist when compared to R-strategist AOB. This makes AOA a potential candidate to replace AOB as the nitrite-supplying partner for anammox in mainstream wastewater treatment as AOA could continue to produce nitrite for anammox at low ammonia and low oxygen conditions unfavorable AOB and NOB. In fact, AOA have been detected in wastewater treatment plants with low dissolved oxygen levels and long sludge retention times.[58]

This work tested the potential application of AOA and anammox by using three different strains of AOA. Two enrichments were obtained from a freshwater lake sediment from Lake Acton and Lake Delaware (AC2 and DW1 respectively), and one from soil (*Nitrososphaera viennensis*). These strains were chosen because of they are freshwater species with high affinities for both oxygen and ammonia (Figure 2-5, top and middle).

2.6 A NEW POTENTIAL PARTNER: COMAMMOX

Comammox is the most recently discovered organism of those discussed here. All known species of comammox belong the genus *Nitrospira*, which also contains canonical NOB.[59] However, comammox is unique in that it encodes the ammonia monooxygenase subunits A, B and C, giving it the capability to perform ammonia oxidation in addition to canonical nitrite oxidation.[60] Nitrite is released extra-cellularly and then taken up again to produce nitrate. Like AOA, they have high affinities for oxygen and ammonia (Figure 2-5, top and middle). Despite their AOA-like affinity for oxygen and ammonia, their affinity for nitrite is low when compared to anammox (Figure 2-5, bottom). We hypothesize that in a co-culture of anammox and comammox at low oxygen/low ammonia conditions, anammox will outcompete comammox for the nitrite produced, resulting in high-rate nitrogen removal.

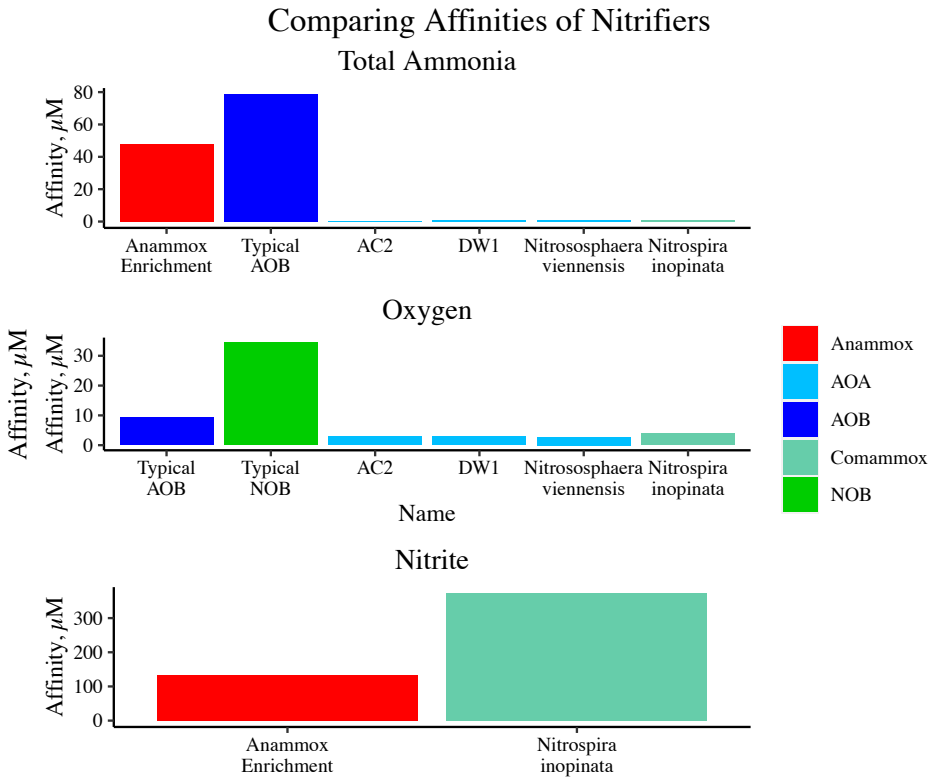

Figure 2-5. Ammonia, oxygen, and nitrite affinities for various nitrifying organisms[17,20,40].

Chapter 3. REDUCING COST AND ENVIRONMENTAL IMPACT OF WASTEWATER TREATMENT WITH DENITRIFYING METHANOTROPHS, ANAMMOX, AND MAINSTREAM ANAEROBIC TREATMENT

This work is published as:

Cogert, K. I.; Ziels, R. M.; Winkler, M. K. H. Reducing Cost and Environmental Impact of Wastewater Treatment with Denitrifying Methanotrophs, Anammox, and Mainstream Anaerobic Treatment. *Environ. Sci. Technol.* **2019**. https://doi.org/10.1021/acs.est.9b04764.

3.1 ABSTRACT

In water resource recovery facilities, sidestream biological nitrogen removal via anaerobic ammonium oxidation (anammox) is more energy and cost efficient than conventional nitrification-denitrification. However, under mainstream conditions, nitrite oxidizing bacteria (NOB) out-select anammox bacteria for nitrite produced by ammonium oxidizing bacteria (AOB). Therefore, nitrite production is the bottleneck in mainstream anammox nitrogen removal. Nitrate-dependent denitrifying anaerobic methane oxidizing archaea (n-damo) oxidize methane and reduce nitrate to nitrite. The nitrite supply challenge in mainstream anammox implementation could be solved with a microbial community of AOB, NOB, n-damo, and anammox with methane from anaerobic sludge digestion or a mainstream anaerobic membrane bioreactor (AnMBR). The cost and environmental impact of traditional nitrification/dentrification relative to AOB/anammox and AOB/anammox/n-damo systems, with and without an AnMBR were compared with a stoichiometric model. AnMBR implementation reduced costs and emission rates at moderate to high nutrient loading by lowering aeration and

sludge handling demands while increasing methane available for cogeneration. AnMBR/AOB/anammox systems reduced cost and GHG emission by up to \$0.303/d/m^3 and 1.72 kg equiv. CO_2/d/m^3, respectively, while AnMBR/AOB/anammox/n-damo systems saw a similar reduction of at least \$0.300/d/m^3 and 1.65 kg equiv. CO_2/d/m^3 in addition to alleviating the necessity to stop nitrification at nitrate, allowing easier aeration control.

3.2 ABSTRACT ART

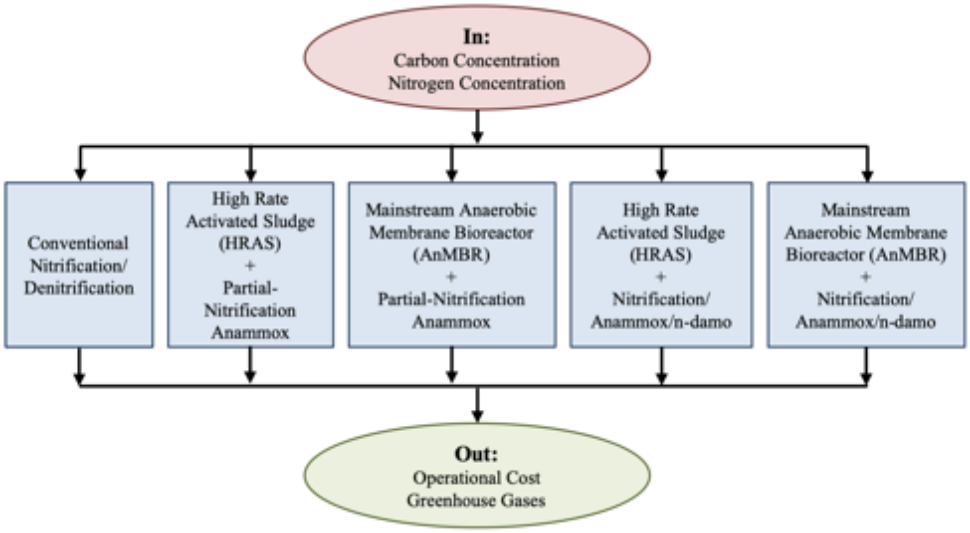

Figure 3-1. Overview of techno-economic-environmental feasibility study.

3.3 INTRODUCTION

Wastewater treatment accounts for 2% of the U.S energy budget.[61] Two major costs of water resource recovery facility (WRRF) operation are sludge handling, which can account for up to 60% of total operational cost, and aeration, which makes up 40-60% of energy usage[62,63]. Aeration demand is related to oxygen requirements of aerobic organisms consuming ammonium (NH_4-N) and organic carbon (measured in chemical oxygen demand or COD) in the influent. Sludge

handling requirements are driven by the biomass yield of organisms involved in the treatment process. Additionally, some WRRFs require external carbon addition for complete nitrogen removal if the COD/N influent ratio is too low for complete denitrification. Meanwhile, 0.5% of greenhouse gas (GHG) emissions produced in the U.S. are contributed by WRRFs[3]. Two primary GHGs of concern in WRRF operation are methane (CH_4) and carbon dioxide (CO_2)[64]. Although nitrous oxide (N_2O) is also a contributor to GHG emissions from WRRF (with a global warming potential 298-times that of CO_2) it is difficult to include N_2O into stoichiometric modelling as the microbial origin, amounts emitted, and conditions triggering its emission are controversial[39,65–68]. CH_4 has a global warming potential of approximately 34-times that of CO_2. Therefore even small quantities can greatly impact atmospheric quality[38]. Thus, reducing GHG emissions and energy consumption by wastewater treatment while maintaining high effluent water quality will be imperative to ensure long term air, water, and energy security.

In order to reduce the cost and carbon footprint of WRRF operation, much effort has been put into developing technologies that (1) demand minimal oxygen supply, (2) produce little sludge, and (3) require no external carbon addition for nutrient removal, while (4) reducing GHG emissions[69]. Anaerobic ammonia oxidizing (anammox) bacteria provide one such solution in nitrogen removal. Anammox bacteria are autotrophs that anaerobically oxidize ammonium to di-nitrogen gas utilizing nitrite as an electron acceptor, reducing aeration demands by nearly 60%, sludge production by 90%, and eliminating the need for external carbon[9,10,70] Anammox has been implemented for nitrogen removal in the side stream (1% of total volumetric flow) at many full-scale installations treating warm (>35°C) ammonium (NH_4^+) rich digester reject water.[71] Ammonium oxidizing bacteria (AOB) supply the nitrite (NO_2^-) for anammox while the competing activity of nitrite oxidizing bacteria (NOB) are suppressed by low dissolved oxygen

levels or free ammonia[72–74]. Implementation of anammox for mainstream nitrogen removal (99% of volumetric flow) with high-rate activated sludge carbon removal is gaining attention because it is theoretically posited to be an energy-neutral system as shown by other stoichiometric models[75]. However, anammox has been almost entirely limited to sidestream centrate treatment because of the difficulty limiting NOB activity at colder mainstream temperatures, while also meeting stringent nitrogen removal requirements[14,15,76]. A more robust configuration is needed to combine anammox with a process that can supply nitrite to anammox without relying on NOB out-selection.

A metabolic pathway that could be utilized to supply anammox with nitrite without NOB competition is nitrate-driven anaerobic methane oxidation (n-damo), in which a newly discovered archaea, *Ca. Methanoperedens nitroreducens*, are capable of using methane as an electron donor to reduce nitrate to nitrite:[41]

$$CH_4 + 4\ NO_3^- \rightarrow CO_2 + 4\ NO_2^- + 2\ H_2O \qquad \text{Eqn 3-1}$$

Previous work has demonstrated a sustained co-culture dominated by anammox and n-damo archaea capable of removing nitrogen,[41,4524,25] and bench scale studies have demonstrated complete high-rate nitrogen removal, outcompeting the nitrite-driven anaerobic methane oxidizing bacteria (*Ca. Methylomirabilis oxyfera*)[42–44]. N-damo bacteria and anammox are in direct competition for nitrite but modeling work has shown that n-damo bacteria are only able to survive in the presence of excess nitrite because they have a lower affinity for nitrite than anammox[46]. In a well-controlled n-damo archaea/anammox system, nitrite would be fully consumed, eliminating the environmental niche required for n-damo bacteria. Therefore, n-damo archaea/anammox nitrogen removal systems could theoretically be scaled up for mainstream nitrogen removal[77,78]. In this concept, half

of influent ammonium is oxidized to nitrate, reducing oxygen demand by 50%**.** The nitrate- and ammonium-rich streams are then fed to an anaerobic anammox/n-damo reactor supplied with methane. N-damo archaea reduce nitrate with methane, and the resulting nitrite is available for anammox bacteria to convert the remaining ammonium to di-nitrogen (N_2) gas. In such a system, methane could be supplied into the n-damo reactor either dissolved in solution or as a gas from biogas produced by anaerobic digestion[42,45].

Another new technology proposed for energy-neutral wastewater treatment is the anaerobic membrane bioreactor (AnMBR), which can provide a high methane yield while efficiently removing organic carbon with minimal sludge production[79–82]. AnMBR treatment holds great potential for the future of wastewater treatment, as it is predicted to produce more energy and thus have lower greenhouse gas emissions than high-rate activated sludge (HRAS) systems[83].

Organic carbon is converted into methane rich biogas for energy generation instead of being aerobically oxidized with high energy costs in HRAS [5]. Despite immense potential for lower operational costs, recent life cycle analysis research reveals that one major disadvantage to AnMBRs is downstream GHG emissions due to the high concentrations of dissolved methane in the effluent[83]. Yet, because n-damo archaea require a source of dissolved methane, AnMBRs could have a powerful synergy with n-damo/anammox systems, where simultaneous methane and ammonium removal is achieved anaerobically.

There has been little attempt to compare financial and environmental benefits of anammox paired with AnMBR or n-damo to existing secondary treatment technologies[84]. In this study, theoretical mainstream technologies (HRAS/anammox, AnMBR/anammox, HRAS/anammox/n-damo & AnMBR/anammox/n-damo) were compared to a traditional nitrification/denitrification system for

carbon and nitrogen removal. The impact of aeration demand, sludge handling, external carbon addition, and methane for energy generation on both economic and environmental feasibility was considered.

3.4 MATERIALS & METHODS

Five scenarios were investigated in this study: (A, base case) traditional nitrification/denitrification, (B) High Rate Activated Sludge (HRAS) COD removal followed by AOB/anammox (aerobic & anaerobic ammonium oxidation), (C) mainstream AnMBR followed by AOB/anammox, (D) HRAS followed by nitrification/anammox/n-damo, and (E) mainstream AnMBR (anaerobic membrane bioreactor) followed by nitrification/anammox/n-damo (Figure 3-1). Because the objective of this study was to examine theoretical nitrogen removal technologies and nitrogen removal is most challenging at low COD/N ratios, a wide range of typical nitrogen concentrations were explored (0.6-60 mgN-NH_4/L) while a moderate to low range of COD influent concentrations were explored (4-400 mg-COD/L). All calculations were done assuming a nominal plant flowrate of 60 th m^3/day. All COD was presumed 100% biologically degradable. All results were reported in comparison to the base case as a percent increase or decrease.

The model estimated how changes in oxygen demand, sludge production, biogas available for energy recovery, and external carbon addition (if applicable) influenced operational costs. Oxygen demand was estimated as the total oxygen required to remove maximum possible nitrogen and COD. The rate of biological decay can vary significantly, especially when comparing a highly controlled bench experiment to a full scale WRRF. Overestimating this value would lead to calculating an unrealistically low sludge production rate. Therefore, the rate of

decay was not included in calculations to ensure that sludge handling demands would not be underestimated. Biomass produced by all organisms involved in each scenario were considered to be waste activated sludge (WAS) fed to anaerobic digestion. A volatile solids reduction of 59% in the digester was assumed.[5] Methane production was assumed to be equivalent to 100% of the COD reduced in anaerobic sludge digestion and AnMBR. Biomass yield from sludge digestion was not considered. External carbon addition was only required if not enough COD was available for nitrogen removal.

3.4.1 Calculating Differences in Greenhouse Gas Emissions and Cost

The primary drivers of both cost and GHG emissions were assumed to be external COD added, oxygen demand, sludge produced, and methane produced. These metrics were combined together into an equivalent kg CO_2 emitted or cost in USD. Resulting GHG emission rates and costs were used as a direct comparison of the theoretical technologies explored in scenarios B-E to a conventional nitrification/denitrification plant by taking the difference in the calculated combined metrics (kgCO_2 or USD per day per m^3) in scenario A and subtracting it from the combined metrics calculated in scenarios B-E. The resulting value represents the relative difference in GHG emissions or cost between theoretical and conventional technologies (Figure 3-3 & Figure 3-4). Literature values for a plant with a nominal flowrate of 60 th m^3/day were used to estimate the contribution external COD added, oxygen demand, sludge produced, and methane produced to greenhouse gas emissions in equivalent kg CO_2 and operational cost in USD. The estimated calculations are provided in the supporting information, Table A1. It was assumed other factors contributing to cost and GHG emission (i.e. pumping demand, chemicals added, etc.) varied much less than those factors considered in this study.

GHG emission was estimated with CO_2 emissions originating from plant electrical demand, CO_2 released from external carbon added, and residual CH_4 emissions released from the plant. Energy demand due to aeration was calculated given the typical energy demand of an aeration blower to be 1.5 kWh/kg dissolved O_2[5,85]. Solids handling energy demand of the anaerobic digester and dewatering system were inferred to be 2.24 kWh/kgVSS given typical values[5,61]. Reproducible calculations for this value are provided in supporting information, Table A1. Electrical demand of 190 kWh/th m^3 for AnMBR operation in scenarios C & E and 26 kWh/th m^3 for mixing an anaerobic compartment in scenarios A, D, & E were also taken from literature and included[5,86]. Finally, the energy recovered from the cogeneration plant was calculated on a kg CH_4 produced basis given the lower heating value of biogas of 22400 kJ/m^3 and a cogeneration plant efficiency of 30%[5]. Additional electrical demands, like pumping requirements, were not included as they were assumed to be a minor contributor to operational costs and greenhouse gas emissions. The potential impact of this assumption on the results of this study was explored in a sensitivity study where the pumping demand of the theoretical scenarios B thru E was varied between 50-500% of the base case, scenario A. The impact of pumping demand on our results was determined to have only a minor impact (see Figures A9 & A10). The electrical demand was converted to offsite CO_2 emission using recent aggregate U.S. emission factors.[41] CO_2 from biogas cogeneration was not included. Biogenic CO_2 was only included if originating from oxidizing externally added COD, as the methanol and methane purchased by WRRFs typically originates from fossil fuels[87]. CH_4 emissions were estimated from the amount of residual methane emitted from the system and converted to equivalent CO_2[38,88].[11,43] N_2O is known to be a significant contributor to GHG, but N_2O metabolic pathways are too complex to be accurately reflected by a stoichiometric model[65–67]. It was therefore decided to omit N_2O production and consumption from this analysis.

Costs of (1) electrical demand on a per kWh basis, (2) landfilling sludge on a per kgVSS basis, and (3) external COD addition on a per kgO2 basis were calculated from literature and industry provided values and are presented in the supporting information, Table A1. The programming language R (version 3.5.2) in RStudio (1.1.419) was used for simulations and a detailed explanation of the models are given in the supporting information. The code used for this analysis can be accessed via the repository located at: https://github.com/cogerk/ndamo-econ.

3.4.2 Scenario A: Conventional Nitrification/Denitrification

Scenario A represents the base case scenario and describes a nitrification/denitrification system.[37] Influent was fed into an anoxic denitrification reactor, which received recycled nitrate from the nitrification reactor. If the COD/N in the influent was too low to remove all nitrogen, then supplemental COD was added. Conversely, if not enough nitrogen was present to remove all COD, residual COD was oxidized aerobically in the nitrification reactor.

3.4.3 Scenario B: High Rate Activated Sludge & AOB/Anammox

The anammox system in Scenario B was based on the system described by Sliekers et al.[16] currently in use at WRRFs worldwide for centrate treatment. The HRAS system was added to aerobically respire COD to CO_2 similar to the theoretical energy-neutral system described by Kartal et al.[20] In order to meet the anammox bacteria metabolic demands, 57% of influent nitrogen must undergo partial nitrification to generate 1.3 moles of nitrite per mole of ammonium (see Appendix A).

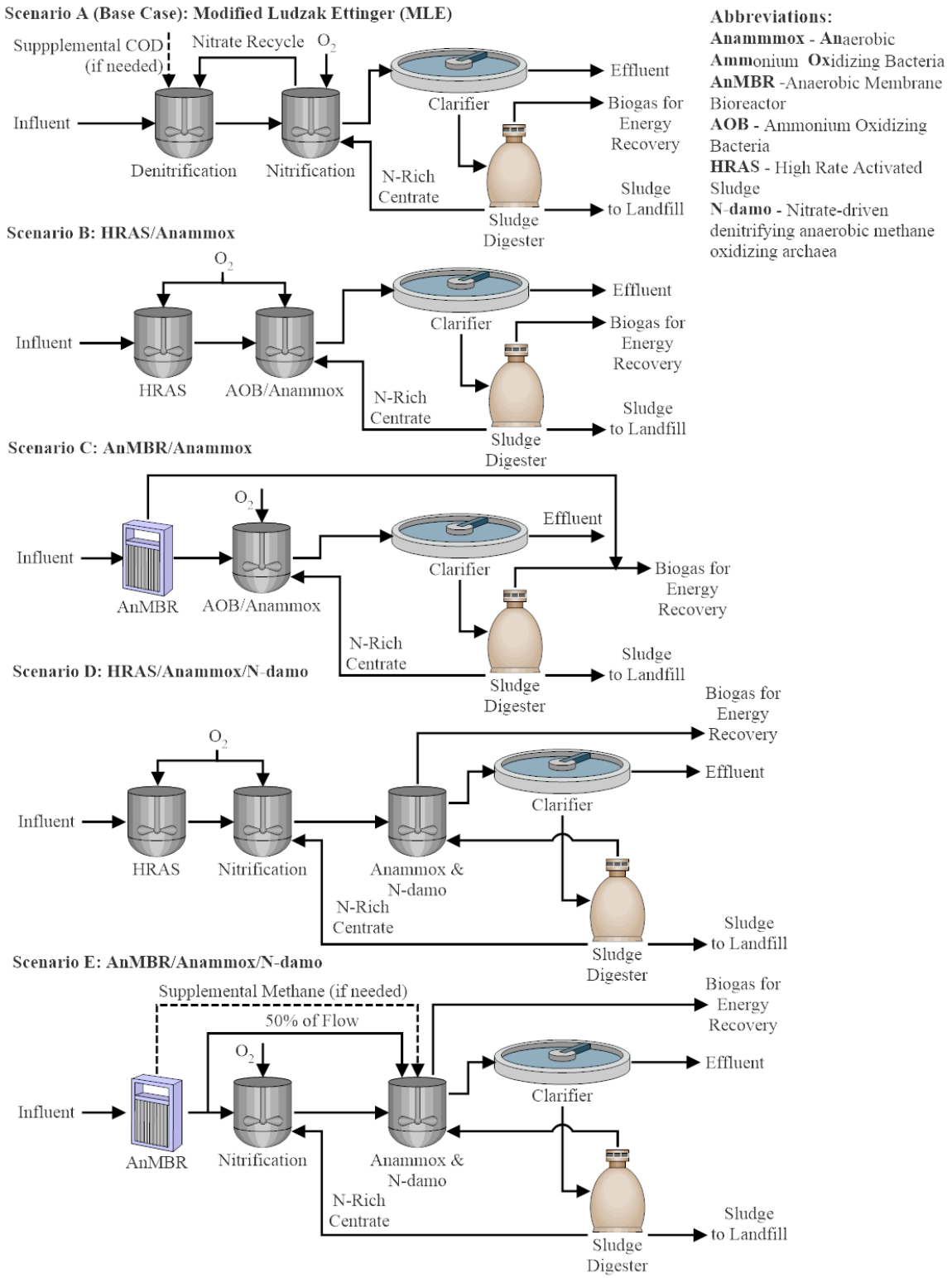

Figure 3-2. (A, the base case) traditional nitrification/denitrification. (B) High Rate Activated Sludge (HRAS) and AOB/anammox for nitrogen removal. (C) Anaerobic Membrane Bioreactor (AnMBR) and AOB/anammox (D) HRAS and nitrification/anammox/n-damo for nitrogen removal, and (E) AnMBR and nitrification/anammox/n-damo.

3.4.4 Scenario C: AnMBR & AOB/Anammox

Scenario C simulated a mainstream anaerobic membrane bioreactor (AnMBR) for the removal and recovery of organic carbon as biogas. Sludge input to anaerobic digestion was the sludge production from AnMBR and anammox/AOB reactors. The 190 kWh/th m^3 factor included for AnMBR operation represents electrical demand required for the scouring, mixing, and transmembrane pressure application of an AnMBR system.[40]

Dissolved methane concentration from AnMBR effluent was assumed to be 1.5 times the saturation concentration assuming the headspace is 62 %v/v methane[83]. Results from Daelman et al. were used to approximate the fate of dissolved methane in the aerated AOB/anammox reactor[89]. A binary scheme based on the biological kinetics of methanotrophs was used. At methane concentrations above the methanotroph affinity, (>5 mgCOD/L), methane would be 90% consumed by methanotrophs and the remaining 10% would be stripped. Below that threshold, 100% of methane would be stripped. It was assumed stripped methane exiting the AOB/anammox reactor was too dilute for energy recovery and escaped, contributing to GHG emissions. Residual dissolved methane not consumed by methanotrophs was also included in GHG emission calculations. All methane emissions were multiplied by 34 CO_2 equivalents based on the potency of methane as a GHG[38].

3.4.5 Scenario D: High Rate Activated Sludge, Anammox, & N-Damo

In this scenario, COD was removed with HRAS followed by nitrification where half of ammonium was oxidized to nitrate. The nitrate/ammonium rich effluent was fed into a n-damo/anammox reactor in which n-damo archaea supplied anammox bacteria with nitrite to remove ammonium. Methane required for nitrate reduction was supplied to n-damo archaea from

digester biogas and in all scenarios considered enough methane was available for 100% nitrogen removal, however if that were not the case methane could be externally purchased.

3.4.6 Scenario E: AnMBR, Anammox, & N-Damo

In scenario E, COD was removed anaerobically via AnMBR. Half of AnMBR effluent was fed to a nitrification reactor where ammonium was converted to nitrate. The remaining half was fed into a n-damo/anammox reactor where dissolved methane was available for n-damo. Oxygen consumption included nitrification and methane oxidation by aerobic methanotrophs. The amount of methane stripped from the nitrification reactor was calculated using the same assumption described in scenario C. Residual dissolved methane not consumed by methanotrophs or stripped from the nitrification reactor was included in the GHG emission calculation by multiplying the amount of methane by 34 CO_2 equivalents based on the potency of methane as a GHG[38].

3.5 RESULTS

The differences in GHG emission in kg equiv. CO_2 and operational cost in USD between each scenario (HRAS/Anammox, AnMBR/anammox, HRAS/anammox/n-damo, AnMBR/anammox/n-damo) and the base case (conventional nitrification/denitrification) are shown in Figure 3-3 & Figure 3-4, respectively. Similar comparisons of the oxygen demand, sludge production, external COD added, and methane production are available in the supporting information (Figures A6-A8).

3.5.1 Relative Difference in Greenhouse Gas Emissions

GHG emissions due to electrical consumption and escaped methane from WRRFs has a significant impact on total U.S. GHG emissions annually[89]. The GHG emissions produced due to electrical consumption, external COD addition, and escaped methane of scenarios B-E as they compared to the base case of conventional nitrification/denitrification were reported (Figure 3-3). As with the cost comparison, the two HRAS scenarios (Figure 3-3.1 and Figure 3-3.3) and two AnMBR scenarios (Figure 3-3.2 and Figure 3-3.4) appear to be almost identical suggesting that the economic driver for choosing either n-damo or anammox based processes is marginal. The addition of n-damo to an anammox system did not drastically change the GHG emission rate.

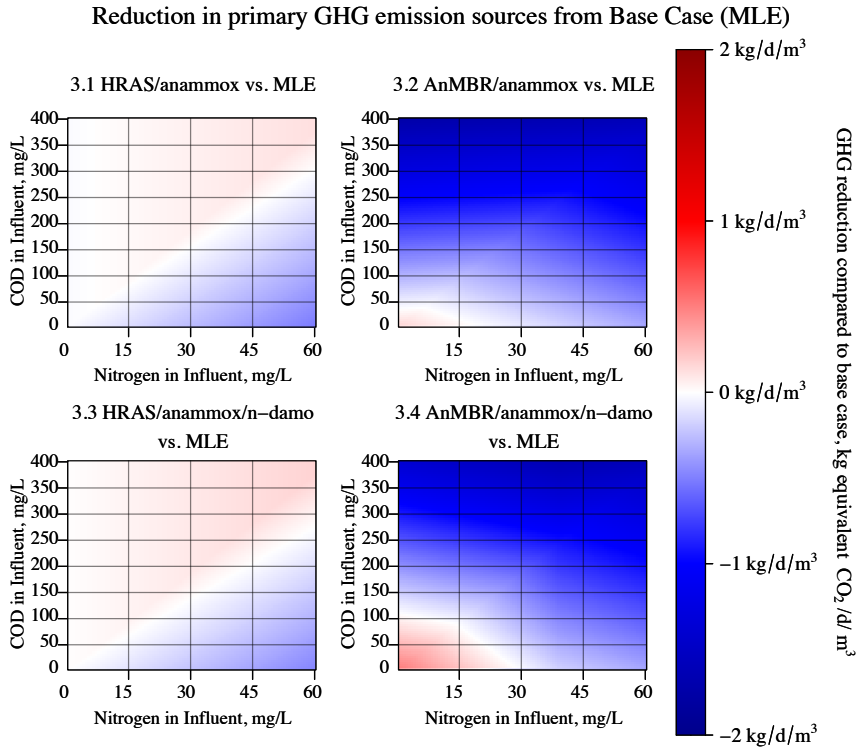

Figure 3-3. The reduction in GHG emissions possible by implementing four different theoretical treatment technologies; HRAS and partial nitritation-anammox (3-3.1), AnMBR and partial nitritation-anammox (3-3.2), HRAS and anammox/n-damo nitrogen removal (3-3.3) and AnMBR and anammox/n-damo nitrogen removal (3-3.4) versus Modified Ludzack-Ettinger, MLE, also referred to as conventional nitrification/denitrification. Calculations are performed assuming a plant flowrate of 60 th m3/day. Greenhouse gases are reported in equivalent kg CO2/m3/day saved or additional kg CO2/m3/day. Reduction is shown in blue and increase is shown in red as defined by the color key.

Anammox systems release slightly fewer GHGs than their anammox/n-damo counterparts (0.07-0.04 kg equiv. CO_2/d/m^3 at most conditions) due to extra electrical demand required to supply additional oxygen for full nitrification by NOB to support n-damo with nitrate, thus increasing CO_2 emissions due to electrical demand. In addition, extra sludge production by NOB and n-damo slightly increased GHG emissions due growth yields of the NOB and n-damo populations.

In both the HRAS/anammox and HRAS/anammox/n-damo scenarios, the relative difference in GHG emissions was highly dependent on the COD/N ratios. Emissions were strongly reduced at low COD/N ratios (up to 0.512 fewer kg equiv. CO_2/d/m^3 in the HRAS/anammox system and 0.474 fewer kg equiv. CO_2/d/m^3 in the HRAS/anammox/n-damo) and slightly increased at COD/N ratios > 5. At high ratios, relative emissions increased slightly with nitrogen loading rate (up to 0.122 more kg equiv. CO_2/d/m^3 in the HRAS/anammox system and 0.172 more kg equiv CO_2/d/m^3 in the HRAS/anammox/n-damo than the base case) due to the higher sludge production rate of aerobic heterotrophs (0.67 gVSS/gCOD) than denitrifying heterotrophs (0.44 gVSS/gCOD) and the additional oxygen demand required to aerobically remove COD that denitrification does not require. At high COD/N ratio and low nitrogen loading there is no significant difference between the HRAS scenarios and the base case. At these conditions in the conventional system, there is not enough COD available to support denitrification. Therefore, oxygen was used as an electron acceptor for COD oxidation like the HRAS system.

In both the AnMBR/anammox and AnMBR/anammox/n-damo scenarios (Figure 3-3.2 and Figure 3-3.4), difference in GHG emissions was dependent on the total nutrient loading. At moderate to high COD loading, enough methane for energy recovery was produced from the AnMBR to offset energy requirements and escaped methane emissions, resulting in dramatically lower GHG emissions than the base case (up to 1.72 fewer kg equiv. CO_2/d/m^3 in the

AnMBR/anammox system and up to 1.65 fewer kg equiv. CO_2/d/m^3 in the AnMBR/anammox/n-damo system). At high nitrogen and low COD loading, less methane was produced for energy recovery, but less methane escaped and anammox-based nitrogen removal resulted in lower oxygen demand and sludge production, resulting in lower GHG emissions at high nitrogen loading (up to 0.371 fewer kg equiv. CO_2/d/m^3 in the AnMBR/anammox system and 0.362 fewer kg equiv. CO_2/d/m^3 in the AnMBR/anammox/n-damo system). At low nitrogen and COD loading, electrical demands and methane production are all minimal, so GHG emissions were dominated by escaped methane, resulting in higher emissions in both AnMBR systems as compared to the base case (up to 0.144 more kg equiv. CO_2/d/m^3 in the AnMBR/anammox system and 0.489 more kg equiv. CO_2/d/m^3). At low loading rates, ~0.35 more kg equiv. CO_2/d/m^3 was emitted from the AnMBR/anammox/n-damo system (Figure 3-3.4) then the AnMBR/anammox system (Figure 3-3.2) because n-damo did not consume all dissolved methane from the AnMBR effluent at low influent nitrogen concentrations, whereas that methane was oxidized by aerobic methanotrophs to CO_2 in AnMBR/anammox systems. The electrical demand required to operate an AnMBR or anaerobic compartments played only a minor role at nearly all conditions.

3.5.2 Relative Difference in Operational Cost

AnMBR, anammox, and n-damo have all been suggested as less expensive alternatives to conventional nitrification/denitrification[75,77,78,83]. The estimated relative difference in cost between all alternatives to a conventional system (shown in Figure 3-4) follows the same trends in relative difference in GHG emissions (Figure 3-3). This is understandable given that both operational cost and GHG emissions were assumed to have the same primary drivers: oxygen

demand, sludge production, external COD addition, and methane production for cogeneration. However, unlike the GHG emission results reported in Figure 3-3, both AnMBR systems appear

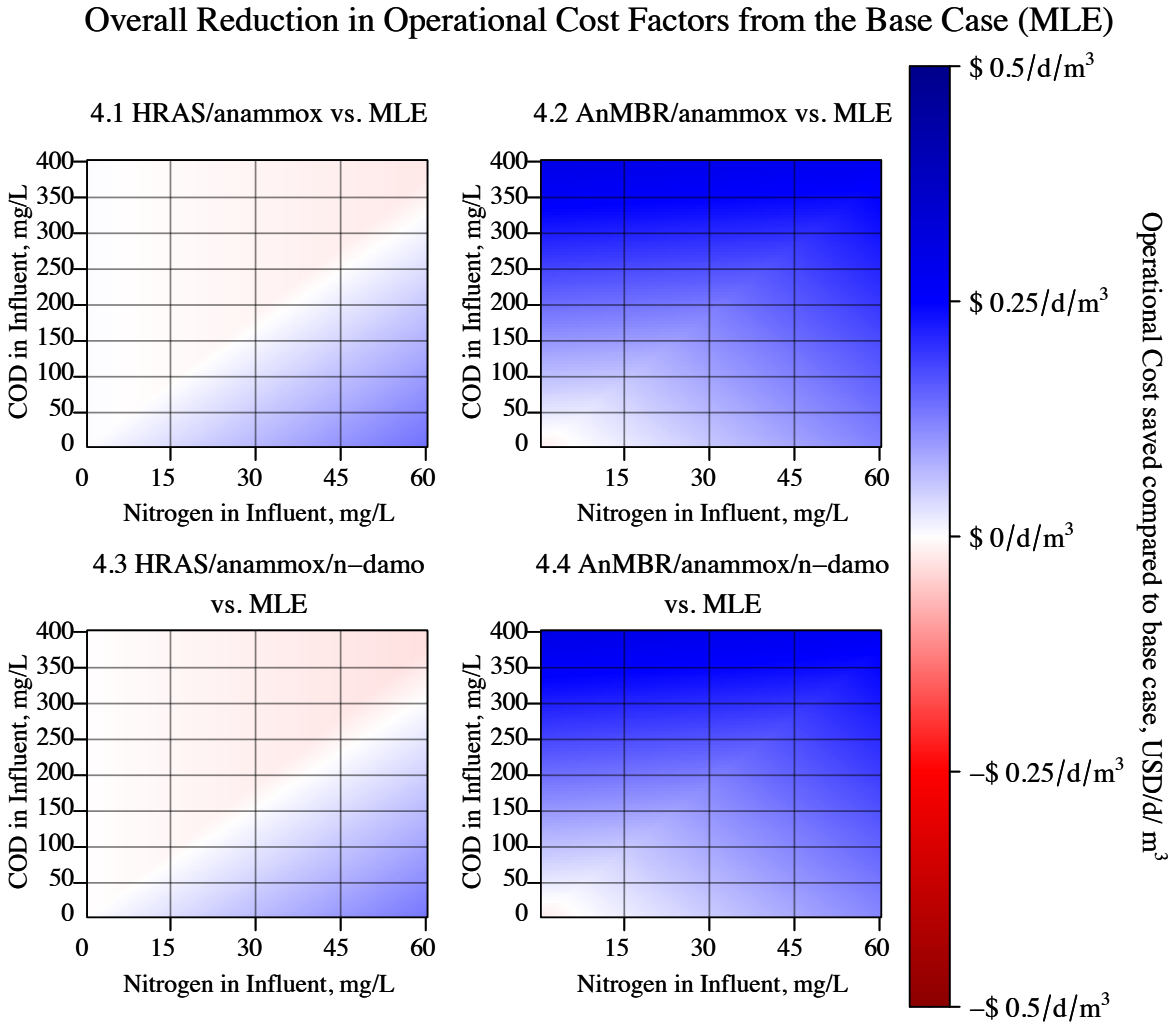

Figure 3-4. The estimated cost saved by implementing four different theoretical treatment technologies; HRAS and partial nitritation-anammox (3.1), AnMBR and partial nitritation-anammox (3.2), HRAS and anammox/n-damo nitrogen removal (3.3) and AnMBR and anammox/n-damo nitrogen removal (3.4) versus Modified Ludzack-Ettinger, MLE, also referred to as conventional nitrification/denitrification. Calculations are performed assuming a plant flowrate of 60 th m3/day. USD saved or additional USD cost per m3 per day shown in blue and red respectively as defined by the color key.

to be a better option than the conventional system at low nitrogen and carbon loading rates. At the lowest possible loading, 4 gCOD/m^3 and 0.6 gN/m^3 the AnMBR/anammox system (Figure 3-4.2) cost only \$0.13 more per day per m^3 and the AnMBR/anammox/n-damo (Figure 3-4.4)

system cost only up to \$0.15 more per day per m^3. At these very low loading rates, a plant would likely not employ nutrient removal. Meanwhile, at high COD loading, the costs for AnMBR/anammox and AnMBR/anammox/n-damo are almost the same: up to \$0.303 and \$0.300 less per day per m^3, respectively.

The costs for the two HRAS systems were very dependent on COD/N ratio. At low COD/N ratios the HRAS/anammox (Figure 3-4.1) system cost up to \$0.139 less per day while the HRAS/anammox/n-damo (Figure 3-4.2) system cost up to \$0.133 less per day to operate primarily because the base case required costly additional carbon addition at low COD/N ratios while the HRAS systems did not.At COD/N ratios above 5, the conventional system did not require additional carbon addition, which made HRAS systems slightly more expensive to operate then the base case, and cost increased with total nitrogen loading (up to \$0.021 more per day per m^3 in the HRAS/anammox system and up to \$0.030 more per day per m^3in the HRAS/anammox/n-damo system).

3.6 DISCUSSION

At moderate to high COD loading rates, the AnMBR systems released fewer GHGs and cost less than the HRAS and base case scenarios, suggesting switching to an AnMBR/anammox scheme would save operational cost and lower GHG emissions for WRRFs at these high COD conditions. By directly converting COD to methane in the mainstream, enough methane could theoretically be produced to offset not only energy demands but also the impact of escaped methane. At low COD loading rates with low COD/N ratios, the HRAS systems were cheaper and released fewer GHGs than the base case and even AnMBR systems at some loading rates, suggesting switching to an HRAS/anammox system would save operational cost and lower GHG

emissions for WRRFs at low COD/N ratios. This result is in line with other similar analysis performed on anammox/HRAS systems[75]. In both n-damo scenarios, enough methane was produced from either mainstream or sludge anaerobic digestion to supply n-damo enough carbon to convert all nitrate to nitrite. However, at COD/N ratios less than 5, the base case required the addition of external methanol, increasing both cost and GHGs as any added methanol would yield CO_2 that an autotrophic nitrogen removal scheme would not.

Anammox and anammox/n-damo systems perform very similarly because in both cases about half of ammonium is anaerobically oxidized, thus reducing aeration demand. N-damo systems demand slightly more oxygen because full nitrification instead of partial nitritation is required and together NOB and n-damo growth yields contribute to a slight increase in sludge production as well. However, these metrics do not take into account how anammox/n-damo nitrogen removal affects the control complexity through less strict aeration management. AnMBR/AOB/anammox systems reduced cost and GHG emission by up to \$0.303/d/m^3 and 1.72 kg equiv. CO_2/d/m^3, respectively, while AnMBR/AOB/anammox/n-damo systems saw a similar reduction of at least \$0.300/d/m^3 and 1.65 kg equiv. CO_2/d/m^3

3.6.1 Practical Control Concerns on Technology Selection

N-damo/anammox nitrogen has yet to be tested at full or pilot scales, but has been shown to remove nitrogen at a high rate at bench-scale[41,43,88,90]. Scale-up remains a source of uncertainty for any new technology, and n-damo is unlikely to be an exception. The ideal reactor design may be driven by the mass transfer rate of methane[91]. Additionally, it is unknown how impurities in the biogas, such as hydrogen sulfide, will limit n-damo[5]. However, this work illustrates the potential savings and GHG reduction possible by bringing anammox nitrogen removal to the

mainstream with the help of n-damo archaea. Implementation of anammox under mainstream conditions has so far been largely impractical due to nitrate accumulation by NOB[92]. While n-damo has not been tested at full scale, n-damo systems would theoretically obviate the need for stringent oxygen control required to limit NOB activity with only a 16% increase in oxygen consumption as compared to anammox only systems (equations A-42 thru A-43 in Appendix A). While the AnMBR/AOB/anammox system resulted in reductions of GHG emissions and cost of up to 1.72 kg equiv. $CO_2/d/m^3$reduction in GHGs and \$0.303/d/m^3 as compared to the base case, n-damo systems do not require a stringent aeration control and still provide a substantial reductions of up to 1.65 kg equiv. $CO_2/d/m^3$ in GHGs and \$0.300/d/m^3 in cost as compared to the base case. Additionally, nitrate-consuming n-damo could prevent nitrate accumulation as occurs in AOB/anammox systems due to the stoichiometry of the anammox pathway limiting the maximum possible nitrogen removal efficiency to 87% (see reaction A-1 on page S3 in SI).[10]

3.6.2 Impact of Nitrous Oxide Emissions on Results

N_2O remains a major factor of uncertainty in any quantification of GHG emissions from wastewater treatment due to both global warming potential (298 times more potent than CO_2) and variability in emission rates[38]. In conventional nitrification/denitrification, N_2O emissions can vary between 0 to 14.6% of influent nitrogen and can be affected by factors as diverse as COD/N ratio, pH, nitrite concentration, dissolved oxygen concentration, sudden increase in ammonium concentrations, and even size and scale of the nitrogen removal system[68]. In a conventional system, N_2O is produced through three mechanisms, nitrifier denitrification and hydroxylamine oxidation, both performed by autotrophic ammonium oxidizing organisms (AOB, ammonium oxidizing archaea, and complete ammonium oxidizing NOB) in the nitrification reactor, and incomplete denitrification, performed by heterotrophic denitrifying

organisms[39,83,93,94]. N_2O emissions from denitrification at minimum COD/N ratios (~5) have been measured between 8-4% of influent nitrogen and decreases as COD/N ratios increase[95]. Meanwhile, N_2O emissions in AOB/anammox reactors like those in scenarios B & C range vary between 1-2% of influent nitrogen and should be independent of the COD/N ratio in plant influent as all COD is removed first to select for an autotrophic population[96,97]. Anammox alone cannot produce N_2O, however supporting heterotrophic populations in an anammox reactor have been measured to release 0.056-0.6% of influent nitrogen as N_2O[98,99]. Most N_2O emissions in an AOB/anammox system are likely from AOB as these systems are controlled at low dissolved oxygen which has been shown to lead to increased N_2O emissions from AOB[98,100,101].

As complete nitrification does not require low dissolved oxygen concentration to inhibit NOB, the n-damo based systems (scenarios D & E) might reduce emissions as compared to the partial nitritation/anammox systems (scenarios B & C). Moreover, n-damo/anammox nitrogen removal could possibly yield lower N_2O emissions than a conventional system, especially at low COD/N ratios. The n-damo genome includes a nitrous oxide reductase gene, but the role of this enzyme in-situ and N_2O emission rates from anammox/n-damo reactors has yet to be explored[41]. The current state of research on these next generation nitrogen removal technologies does not allow an accurate estimation of N_2O emissions and how it impacts the total GHG emissions from a WRRF. However, it is possible that at COD/N ratios near the minimum requirement for denitrification, N_2O emission rates from these systems could be comparable or even improved by the addition of an anaerobic anammox/n-damo systems. However, due to a lack of understanding of N_2O emissions from an anammox/n-damo systems, a clear conclusion cannot yet be made. Despite this limitation, these results show how vital better understanding these systems through pilot scale and full-scale studies could be to reducing GHG emissions from WRRFs.

3.6.3 Reduction in Greenhouse Gas Emissions and Cost

GHG emission and operational cost were found to depend on both nutrient loading and ratio. At high COD concentrations, both AnMBR scenarios with and without n-damo scenarios saw reduced GHGs and cost due to energy recovery from biogas production. Adding n-damo to an anammox process, while still a theoretical possibility, could reduce control complexity of aeration managment, so it is recommended as the preferred technology at high COD concentration independent of nitrogen concentration (Figure 3-5b). At low COD,

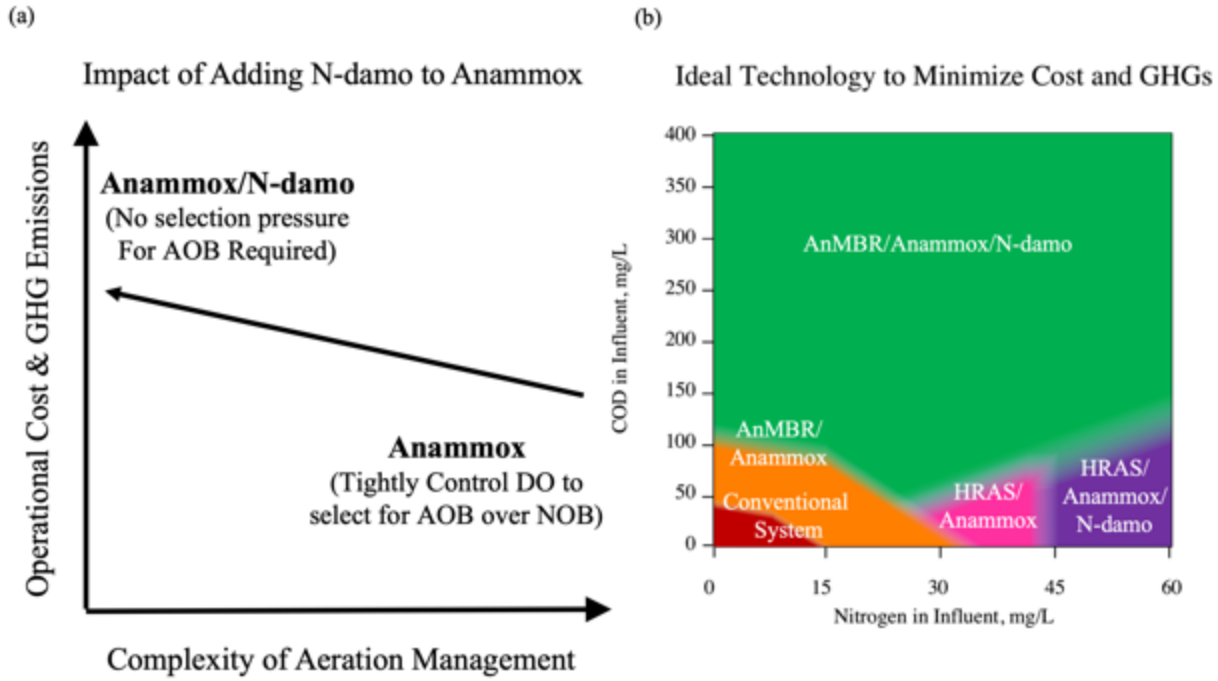

Figure 3-5. Conceptual diagrams describing the ideal use cases for the theoretical technologies in this study's results. (a) The AnMBR/anammox scenario had slightly lower cost metrics than the AnMBR/anammox/n-damo scenarios at nearly all conditions. However, due to the aeration management complexity of the anammox only system, the AnMBR/anammox/n-damo scheme may be the most beneficial to operational cost. (b) The ideal technology to minimize greenhouse gas emissions is variable and dependent on both nutrient ratios and influent concentrations.

AnMBR/anammox/n-damo saw more GHG emissions than the base case as n-damo was unable to consume all dissolved methane with available nitrogen in the AnMBR effluent. In the AnMBR/anammox scenario nearly all dissolved methane was oxidized to carbon dioxide by

methane oxidizing bacteria in the nitrification reactor. Therefore, AnMBR/anammox is recommended as the preferred application at moderate to low nitrogen and moderate COD concentrations. At low COD/N ratios, HRAS scenarios had the lowest cost and GHG emissions as anammox lowered electrical demand (Figure 3-5b). Adding n-damo only marginally increased greenhouse gas emissions while alleviating the necessity to stop nitrification at nitrite, allowing easier aeration control. N-damo is therefore considered to be preferential at very high nitrogen concentrations. Meanwhile, plants treating dilute wastewater streams will likely see minimal benefit from these new technologies and traditional nitrification/denitrification may be the best application if nutrient removal is required at these low concentrations.

This study demonstrates that AnMBR paired with n-damo/anammox nitrogen removal could be a powerful, albeit relatively unexplored, wastewater treatment scheme. Previous studies have demonstrated the potential of mainstream AnMBR treatment, but have pointed out drawbacks associated with the GHG emissions from rogue dissolved methane emissions[83]. At high nutrient concentration, GHG emissions from AnMBR could be offset by energy recovery from biogas. With the addition of n-damo to an AnMBR/annamox system, greenhouse gases are lowered further as n-damo can simultaneously remove dissolved methane while supplying nitrogen-removing anammox with the required nitrite. Even though nitrogen removal by anammox/n-damo has not yet been accomplished at full or pilot scale, these results, along with the demonstrated success of anammox/n-damo at bench scale, begin to quantify the value of developing mainstream anammox and anammox/n-damo technologies at full scale.

3.7 SUPPORTING INFORMATION AVAILABLE

- Detailed description of models used, sample calculations, and estimating calculations, sensitivity studies, and additional results from this work are available in Appendix A.

Chapter 4. REPLICATING AN OXYGEN MINIMUM ZONE IN A LABORATORY MICROSCOSM ELUCIDATES PARTNERSHIPS BETWEEN ANAMMOX, AMMONIA OXIDIZING ARCHAEA, AND *NITROSPIRA*

4.1 ABSTRACT

This study compares the microbial community composition and fate of nitrogen within co-cultured aerobic and anaerobic ammonia oxidizing microbial populations of both co-diffusing and counter-diffusing small-scale laboratory mesocosm setups. Typically, some accumulation of nitrate occurs due to production of nitrate by anammox, however in both environments no nitrate was detected. 16S rRNA gene sequencing and qPCR results using newly developed primers for the ammonia oxidizng archaea (AOA) *Nitrososphaera viennensis* amoA primers showed AOA was only present in the counter-diffusing environment while *Nitrospira* (including some comammox) and anammox were abundant in both environments. FISH probes targeting *Nitrospira* showed high abundance in anoxic or microoxic biofilm regions, suggesting that some *Nitrospira* follow an anaerobic lifestyle. Given this unusual distribution and no nitrate in the effluent, we hypothesize that anammox supplies nitrate from its nitrogen removal pathway and formate from its CO_2 fixation pathway to *Nitrospira*, which uses formate as an electron donor for anaerobic nitrate reduction to nitrite, which is in turn utilized by anammox for nitrogen removal. The counter-diffusive biofilm here appears to replicate the syntrophic relationship observed in marine oxygen minimum zones where and anammox cooperate and *Nitrospira* are present in high concentrations while nitrate concentrations are low.

4.2 INTRODUCTION

Human activities have significantly disrupted the global nitrogen cycle by accelerating the rate of fixed nitrogen loss in marine environments.[102,103] Anthropogenic nutrient input to marine systems has resulted in an increased incidence of Oxygen Minimum Zones (OMZs) in the oceans which has expanded the ecological niche for both denitrifiers and anammox, two organisms capable of producing nitrogen gas under anoxic conditions, and two primary sources of marine gaseous nitrogen production.[104] Both theoretical models and *in situ* measurements have suggested that anammox is responsible for 30-50% of net nitrogen loss in the ocean, and in some regions, anammox activity rates are even higher.[25,26,105]

Anaerobic ammonia oxidation (anammox), is an autotrophic metabolism performed by five candidate genera within the *Plantomycetes* phylum: Brocadia, Kuenenia, Anammoxoglobus, Jettenia, and Scalindua.[29] Ammonia and nitrite are consumed in a ~1:1.3 molar ratio to produce one mole nitrogen gas and 0.3 moles nitrate per mole of ammonia consumed. Ammonia is abundant in nature, but the anammox electron acceptor, nitrite,[22,106] must be produced to sustain anammox activity, which is most commonly supplied by aerobic ammonia oxidizing bacteria and/or archaea (AOB, AOA).[30,107]

AOA and anammox cooperate near the boundary of OMZs where oxygen diffuses downward from the surface while mineralized ammonia originating from within the OMZ diffuses upward toward the boundary.[30,108,109] This counter diffusive supply of substrate results in low ammonia and high oxygen concentrations on the oxygenated side of the OMZ boundary where AOA consume oxygen and produce nitrite. On the anoxic or near-anoxic side of the OMZ boundary, anammox receive nitrite from AOA and thrive in the higher ammonia concentrations originating

from deep within the OMZ.[30] These counter diffusive fluxes in substrates offer an ideal environment for AOA-anammox co-operation, as anammox have a high affinity for nitrite ($K_{NO2,AMX}$ = 48 μM)[20] and AOA possess high affinities for both total ammonia and oxygen ($K_{NH3+NH4,AOA}$ = 0.134 μM, $K_{O2,AOA}$= 2-4 μM)[110,111] as compared to AOB ($K_{NH4+NH3,AOB}$ = 150 μM, $K_{O2,AOB}$ = 15 μM)[112]. Mechanistic models have confirmed observations from OMZs showing that AOA and anammox co-operation requires counter-diffusion of ammonia and oxygen, but a laboratory mesocosm scale system promoting these conditions is lacking.[20,113] Similar to the OMZ, a lab system should support conditions in which AOA are allowed to grow in an oxygen rich/ammonia deplete region to supply nitrite to an oxygen deplete/ rich region where anammox can follow an anaerobic lifestyle.

In contrast, co-diffusion of and oxygen through a biofilm has long been shown to favor a population of anammox and AOB in engineered settings.[13,27,114] Worldwide, more than 200 wastewater treatment plants employ an AOB-anammox based nitrogen removal scheme in high ammonia digester centrate sidestreams.[115] In these systems, AOB and anammox grow together in spherical biofilms called granules.[116,117] AOB grow on the granule periphery where they consume oxygen and convert ammonia to nitrite.[37,118] By controlling the system at a low dissolved oxygen (~10-75 μM),[27] AOB and anammox are able to outcompete nitrite oxidizing bacteria (NOB) for oxygen and nitrite, respectively, due to the comparatively poor affinities of NOB for oxygen ($K_{O2,AOB}$ = 0.5, $K_{O2,NOB}$ = 0.9).[112,119] The nitrite and residual ammonia then co-diffuse into the interior anoxic core of the granule, where anammox convert ammonia along with produced nitrite to di-nitrogen gas. AOB-anammox partnerships function well in the ammonia-rich sidestream (influent concentration >>10 mM NH_3, 1% of the volumetric flow). Due to major cost savings, it is appealing to apply anammox nitrogen removal to the ammonia deplete

mainstream (influent concentration 2-5 mM NH_3, 99% of the volumetric flow).[5] In order to suppress NOB, oxygen concentrations must remain low (<35 μM O_2), similar to marine OMZs. Because AOB growth rate is a function of both ammonia and oxygen concentrations, AOB activity drops at these low oxygen OMZ-like conditions. Because AOB activity drops, not enough nitrite is supplied to keep up with the stringent nitrogen removal requirements of the mainstream (< 200 μM).[115] However, if these wastewater treatment systems were to mimic the natural environments in which anammox is found, a population of AOA would theoretically be better suited to continue to supply nitrite at the very low ammonia and oxygen concentrations present at mainstream conditions.[13]

In this study, we explored nitrifier population dynamics and nitrogen removal in two types of redox-stratified mesocosms: co-diffusive and counter-diffusive.[120,121] While the co-diffusion system made use of the previously described granular sludge, the counter-diffusive system is novel. Oxygen is fed through a hollow fiber membrane fiber submerged in ammonia rich medium, resulting in substrates counter-diffusing across a biofilm comprised of anammox and AOA. The established microenvironment mimics OMZ-like conditions of oxygen diffusing into an ammonia-rich hypoxic/anoxic interior, demonstrating the viability of bio-mimicking a marine OMZ to improve nitrogen removal in wastewater treatment.

4.3 MATERIALS & METHODS

4.3.1 Cultivation of Ammonia Oxidizing Organisms

Cultivation of AOA and anammox was required prior to operation of the environmental mesocosms in this experiment. AOA strains originating from sediment of the shores of Lake Acton (AC2) and Lake Delaware (DW1) were provided by Miami University.[50] The AOA pure

culture *Nitrososphaera viennensis* was received from the Deutsche Sammlung von Mikroorganismen und Zellkulturen GmbH (DSM 26422). Suspended cultures of *N. viennensis* were maintained with an added 10 μM sodium pyruvate to enhance growth rate as reported by Tourna M., Stieglmeier M., Spang A., Könneke M., Schintlmeister A., Urich T., et al.[51] All strains were maintained at 30 °C under low light conditions in 1 mM ammonia. A mineral salts media very similar to that used by Bollmann A., French E., & Laanbroek H.J. was used, with exception of the trace elements solution and EDTA. Instead, 1 ml/L of the trace elements solution previously used to grow marine AOA *N. maritimus* and a 7.5 μM concentration of EDTA ferric sodium salt were supplemeted.[48,50] Culture growth was assumed to be reflected by nitrite production as ammonia was consumed. Ammonia, nitrite, and total oxidized nitrogen measurements were determined with the Thermo Fisher Scientific (Waltham, MA USA) Gallery Analyzer with assays purchased from Thermo Fisher for the ammonia, nitrite, and TON (total oxidized nitrogen) tests. The nitrate concentration was calculated as the difference between concentrations of total oxidized nitrogen and nitrite. A culture was considered to be in late exponential phase when at least 75% of ammonia (0.75 mM) had been converted to nitrite and after 95% of ammonia had been consumed. AOA were concentrated by filtration, collecting cells on 0.2 μm track-etched polycarbonate membrane filters from1 L cultures. Anammox was obtained from a granular sludge centrate treatment system of a wastewater treatment plant in Sluisjesdijk, Rotterdam. The Netherlands.[12] For the counter-diffusion experiment, anammox granules were homogenized with a Bio-Gen (Cambridge, MA USA) Pro200 Electronic Tissue Grinder at 50% power for 1-2 minutes to create a dense dispersed could be sorbed to surface modified hollow fiber membranes as described below.

In addition to AOA and anammox, it was necessary to explore the metabolic versatility of another ammonia oxidizing organism, complete ammonia oxidizing bacteria (comammox). A pure culture of comammox *N. inopinata* was used to examine possible production of nitrite from nitrate by a potential formate-oxidizing pathway of comammox. Comammox, like other *Nitrospira*, have been shown to be abundant in regions with low oxygen concentration.[122,123] *Nitrospira moscoviennensis* has been observed to simultaneously consume nitrate and formate while producing nitrite in the absence of oxygen.[18] Therefore, the same activity was explored in *N. inopinata*. Cells were grown in AOA media described above containing 1 mM ammonia until almost all ammonia had been oxidized to nitrate at late exponential phase. Twenty mL of this culture was then used to inoculate 200 L of medium supplemented with 1 mM formate and nitrogen species were monitored over the course of 5 days of incubation.

Design and Operation of Co-Diffusion Environment

Anammox granular sludge is a co-diffusing environment in which ammonia and oxygen diffuse together through a redox-stratified spherical biofilm from the bulk liquid through the aerobic shell, where ammonia oxidizers grow, into of the granule into the anoxic interior, where anammox grow. As such, it was necessary to concentrate and attach a culture of AOA onto the surface of granular sludge. This was achieved through the adsorption of suspended culture AOA onto the surface of powdered activated carbon (PAC), which was subsequently adsorbed onto the surface of anammox granular sludge that had been cultivated under anaerobic conditions for six months. Powdered activated carbon was ordered from Thermo Fisher Scientific (Cat. No. C272-500, Lot. No. 116757). Prior to using the PAC, it was thoroughly rinsed in 1% HCl and then in milliQ water, autoclaved, filtered w/ 2.5 μm particle retention pore size (Whatman Cat. No. 1442-110, Maidstone, UK) and dried at 100 °C overnight to minimize presence of contaminants.

To check the adsorption of AOA onto PAC, 100 mL of late-exponential phase DW1 culture was stained by adding 40 µL of a fluorescent nucleic acid stain, SYBR™ Green (Thermo Fisher Scientific Ref. No. S7585) directly to the culture. After mixing and brief incubation (~60 seconds), 0.3 grams of PAC were added to the stained culture. An autoclaved magnetic stir bar was used to keep PAC suspended in the culture. A 20 µL sample was then put on a microscope slide and examined under a FITC filter. This was repeated after 24 hours (Figure B1a-b).

PAC was added to anammox granular sludge and allowed a brief (~10 minutes) incubation time for adsorption. Unattached PAC was removed with a tap water wash, allowing only a short (~ 2 min) settling period between washes. Washing and decanting was repeated until the water was relatively clear, indicating most unattached PAC was washed out. A sample of granules was kept on a shaker at 200 RPM for two weeks to evaluate the ability of PAC to remain on the granules (Figure B1c-d).

A 0.5 mL aliquot of the AOA-enriched-PAC-dosed anammox granules was then placed in a 20 mL working volume column, and continuously fed with sterile ammonia media (4.5 mL/hr). Initially, the influent ammonia concentration was increased to keep up with the nitrogen removal rate. However, to avoid ammonia accumulation, the influent ammonia concentration was stepped down back to 1mM. All columns were continuously aerated with dissolved oxygen controlled between 2-5 µM. Gas was filtered through a 0.3 micron filter as it entered and left the column (Figure 4-1, left). Samples for ammonia, nitrite, and nitrate measurements were taken three times per week. The chemical oxygen demand (COD) of the entering and exiting spent medium was evaluated on days 72 (co-diffusion) and 31(counter-diffusion) to check for any potential denitrification activity using the Hach™ (Loveland, CO USA) COD Digestion Vials, Low Range.

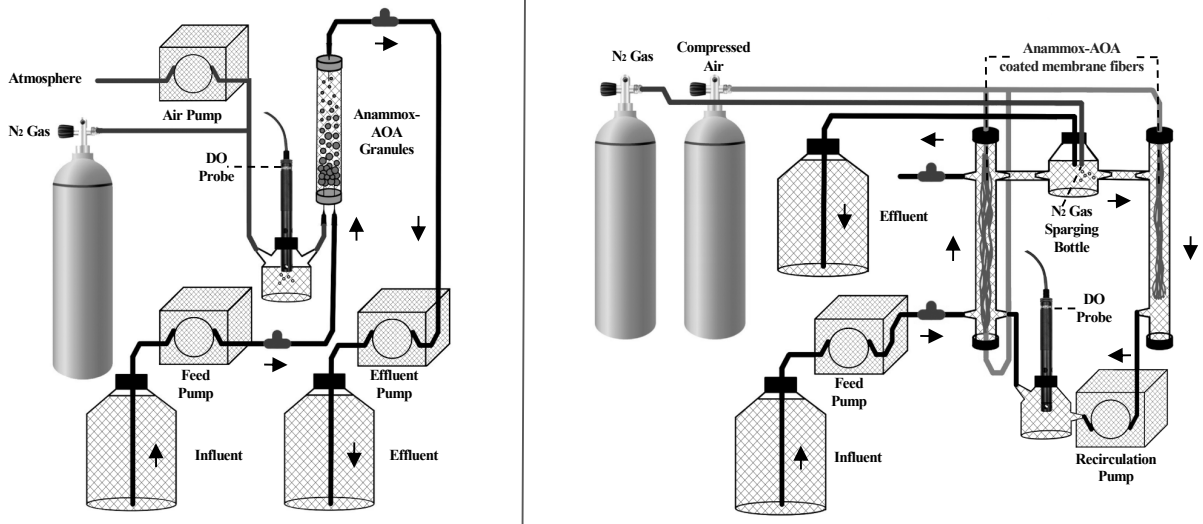

Figure 4-1. Schematics of the small-scale co-diffusion (left) and counter-diffusion (right) environments. Air and N_2 gas were mixed before being filtered and fed into the co-diffusion environment. In the counter-diffusion environment, nitrogen gas was directly added to bulk liquid in the 2nd phase of operation that is emphasized in this study.

Design and Operation of Synthetic Counter-Diffusion Environment

Composite hollow fiber membranes taken from a STERAPORE™ unit (Model No. 20M3400A, Mitsubishi Chemical Corp. Tokyo, Japan) were potted in small 1 cm diameter tubes with 1838 B/A green epoxy adhesive Scotch-Weld ™ (3M, Saint Paul, MN USA) to create a leak-tight enclosure. Fibers were coated with ten layers of poly-L-lysine to enhance cell attachment to the fibers. Once the poly-L-lysine layers fully dried onto the membranes, it was submerged in a small volume (~25 mL) of concentrated mixed AOA culture and allowed to incubate on a low RPM shaker for 30 minutes. Then, approximately 25 mL of the homogenized anammox mixture was added and allowed to attach to the membranes for another 30 minutes.

The system had two membrane modules, one double-ended membrane module, such that gas could flow freely through each strand, and one single-ended, such that oxygen could enter the

one end, but only leave through the membrane fiber. Both modules had ~40 hollow fiber membrane strands (Figure 4-1, right). Oxygen flow rate from the compressed air canister was kept very low throughout operation (1-2 psi). In the first phase of the experiment, nitrogen gas was connected to the pressure equalization vent on the media bottle to ensure anaerobic media was fed to this system. In the second stage, nitrogen gas was added to the mixing bottle between the two columns as shown in Figure 4-1, ensuring an anaerobic boundary between the bulk liquid and the biofilm edge. In both phases, dissolved oxygen (DO) was measured to be at or below the detection limit with a Vernier Optical DO Probe (Beaverton, OR USA). Homogeneous conditions in the bulk fluid were established by a 200 ml/min recirculation pump. Media was fed through a pump at a rate of 15 ml/hr and the total system volume was estimated to be about 400 mL. Sampling was done at the three-way sample ports, shown Figure 4-1. Ammonia, nitrite, and nitrate measurements were taken three times per week.

4.3.2 Molecular Techniques

Biofilm samples were stored for DNA extraction and fluorescent in-situ hybridization (FISH). The membrane fibers were removed from the reactor at the end of the experiment and then cut into smaller pieces. The granular sludge allowed sample collection throughout the experiment and granules were stored at days 0, 31, and 118 of operation. DNA was extracted using the DNeasy PowerBiofilm Kit (QIAGEN, Hilden, Germany) and quantified with both the Thermo Fisher NanoDrop 1000 Spectrophotometer and the Thermo Fisher Qubit dsDNA High Sensitivity assay. Illumina (MiSeq 2 x 300PE) sequencing of the V4-V5 region of the 16S rRNA gene using primers 515F-Y (5′-GTGYCAGCMGCCGCGGTAA)[124] and 926R (5'-CCGYCAATTYMTTTRAGTTT)[125] with 20k reads per assay was performed by Molecular Research Laboratories (Shallowater, TX USA). Analysis of sequencing data was performed with

the USEARCH v11 package; unoise3 was used to select OTUs and taxonomy was assigned with the sintax command using the RDP 16S training database (release 11).[126–129] Comammox and anammox presence were evaluated with qPCR using comammox amoB primers (148F and 485R)[130] and 16S anammox primers (818F[131] and 1040R[132]). A standard for the anammox 16S rRNA gene was constructed by cloning the amplicon for the 808 to 1066 gene region using 808F[132] and 1066R[131] into the pCR™4-TOPO® TA vector (TOPO® TA Cloning® Kit, Invitrogen™, Carlsbad, CA USA) and validating the construct by sequencing (Eurofins Scientific, Luxembourg). For quantification of the comammox amoB gene, a plasmid containing the targeted sequence in *N. inopinata* was used as a standard.

Primers to identify the *N. viennensis* AmoA gene were selected by identifying conserved regions in the *amoA* gene after alignment of sequences with two other AOA strains, AC2 and DW1.[133] Sequence regions that contained at least two mismatches from the other two *amoA* sequences and were selected for primer sequences (Table B2). For each of the three *amoA* sequences, the complete gene sequence was synthesized and cloned within the pUC18 plasmid (ordered from BIOBASIC®). qPCR tests with all three plasmids showed specific amplification of the *N. viennensis amoA* gene by the primers. For quantification the pUC18-*N.viennensis amoA* construct was used as a standard.

Samples for FISH were washed in phosphate buffered solution pH 7.0 (PBS) and soaked in 4% paraformaldehyde solution for 2 hours before being stored in a mixture of 98% ethanol and PBS. Three different probes designed to hybridize with *Nitrospira* were used per sample (Fluorescein, green), anammox (Cyanine 5, red), and general archaea (Cyanine 3, blue). Hybridization was done with 35% formamide hybridization buffer and 80 µM NaCl washing buffer. Details of the

FISH probes, qPCR primers and experimental conditions are available in the supplemental material (Tables B1 & B2).

4.4 RESULTS

4.4.1 *Metabolite Concentrations in Synthetic Environments*

Effluent concentrations of the nitrogen species from both synthetic environments along with the fed ammonia concentration are illustrated in Figure 4-2. The concentration of ammonia supplied to the co-diffusing synthetic environment was increased once nitrogen loss was near complete, in order to build up biomass of the co-culture. When effluent ammonia concentrations remained high, the influent ammonia concentration was stepped back down to promote an oligotrophic environment. The counter-diffusion system was fed anoxic media for 69 days with compressed air supplied to the hollow fiber membrane bundles. During that time, nitrate concentration in the effluent slowly increased (Figure B2). This was likely due to oxygen penetrating too far into the biofilm, creating an aerobic volume fraction within the biofilm too high to support an anammox population. After 69 days, nitrogen gas was added directly to the bulk fluid, as is shown in Figure 4-2, to reduce the bulk liquid dissolved oxygen concentration, effectively decreasing the biofilm's aerobic volume fraction. After adding nitrogen gas to the system, nitrogen removal dramatically improved and nitrate and nitrite effluent concentrations dropped to nearly zero. Figure 4-2 shows the performance during the 2nd phase only. No consumption of COD was found when COD measurements were taken on day 72 for the co-diffusion and on day 31 for the counter-diffusion environments. In the counter-diffusion system, on average 90% removal was observed during stable operation. In the co-diffusion system, on average 76% removal was observed during stable operation.

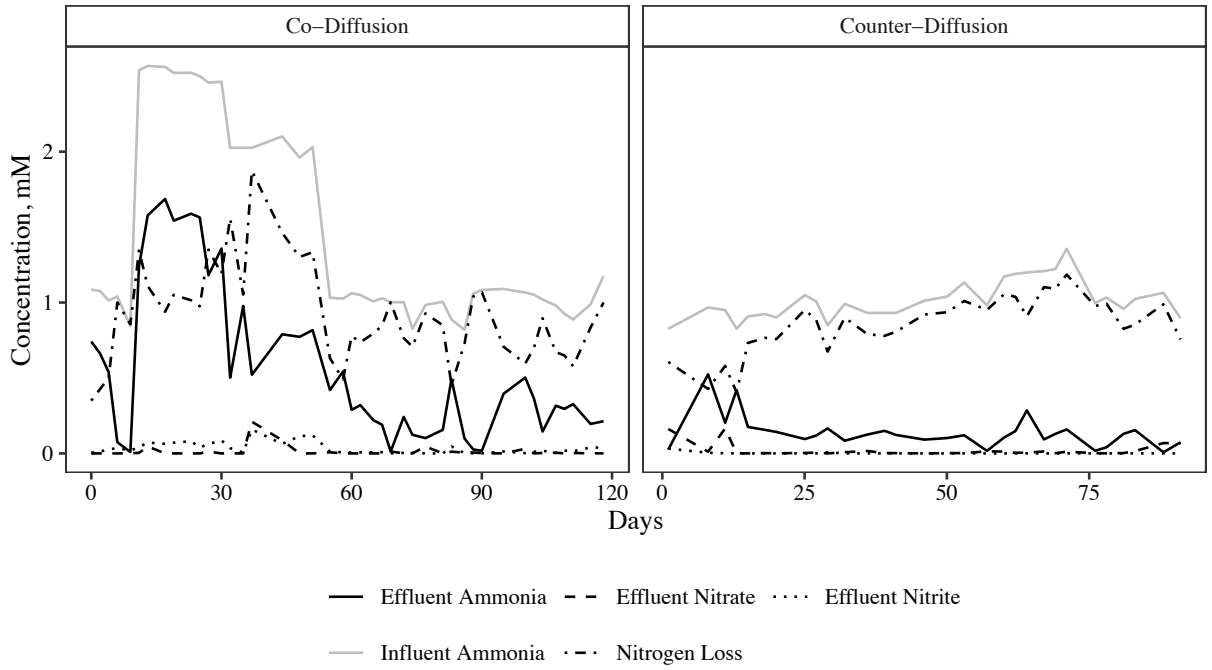

Figure 4-2. Performance of AOA inoculated anammox when ammonia was the only nitrogen source available in both a co-diffusing environment (left) and counter-diffusing environment (right). The measured nitrogen removed (– • –) was near the concentration of ammonia fed into the synthetic environment (–, grey), indicating a high rate of nitrogen loss in the system.

In addition to the long-term performance of these mesocosms, simultaneous nitrite production and nitrate reduction were observed during the short-term incubation of pure comammox with 1 mM formate and ammonia and some residual nitrate (~0.1 mM) under anoxic conditions. Nitrite produced (107 ± 14 μM) was roughly equivalent to the sum of ammonium (28.6 ± 7 μM) and nitrate (83.3 ± 17 μM) consumed in the culture.

4.4.2 Microbial Populations Present in Synthetic Environments

Abundances for all aerobic nitrifiers present in the biofilms after operation ceased were measured with both 16S rRNA gene sequencing and verified with qPCR (Figure 4-3). Both sequencing and qPCR demonstrated a high abundance of AOA as *N. viennensis* in the counter-diffusing environment and effective absence in the co-diffusing environment. Sequencing results indicated that prior to operation, almost 10% of the reads from the co-diffusing environment

belonged to the inoculated AOA species (Figure B3). High abundance of an uncharacterized *Nitrospira* taxa were also found in the sequencing results for both systems. Since 16S rRNA gene sequencing does not provide enough resolution to differentiate between comammox and canonical NOB, qPCR was required to evaluate the presence of the *amoB* diagnostic of comammox. Low abundances of comammox were found in both environments when checked with qPCR using general primers designed to target all known *Nitrospira* amoB genes[130]. Gel electrophoresis was performed with the qPCR product from the co-diffusion environment to confirm that the amplicon size matched the expected target length (Figure B3). Sequencing results at days 0, 31, and 118 of the co-diffusion environment are available in the supplemental material (Figure B4).

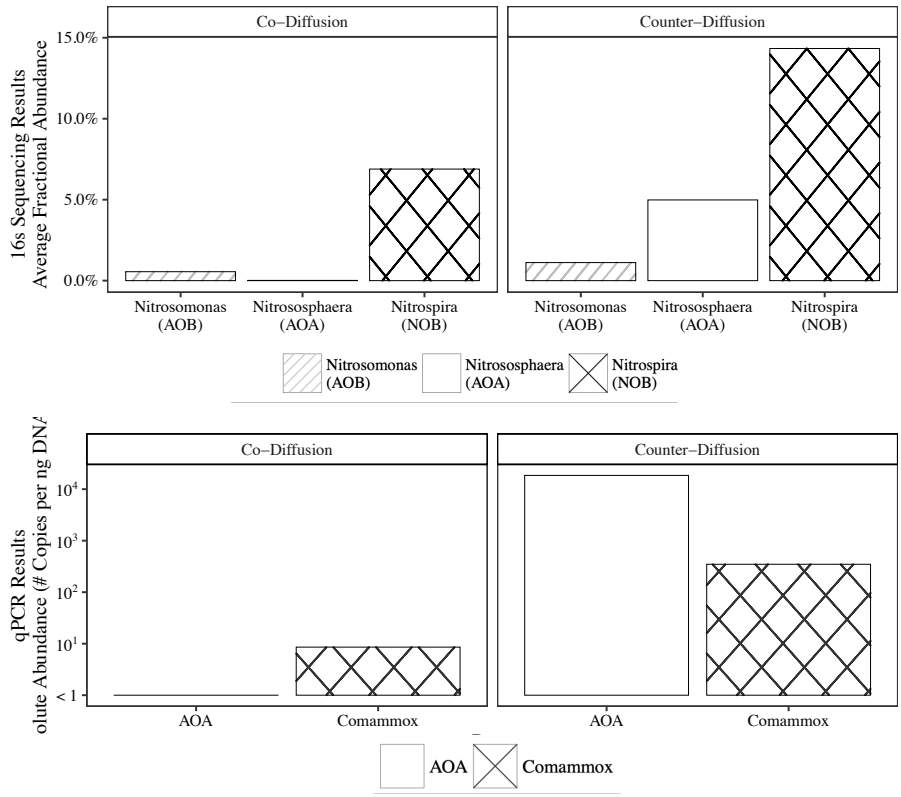

Figure 4-3. The relative abundance of aerobic nitrifiers in biofilms, after termination of operation of both the co-diffusing environment (n=2) (left) and counter diffusing environment (n=1) (right), was evaluated using both 16S sequencing (top) and qPCR primers (bottom). New primers designed to target the *amoA* of *N. viennensis* and a general *amoB* primer set for *Nitrospira* were used to target AOA and comammox, respectively.

The relative abundance of anammox measured via 16S rRNA gene sequencing was low (<2%) however qPCR amplification of the anammox 16S rRNA gene showed anammox was clearly present in both systems Figure 4-4**Error! Reference source not found.**. This discrepancy could be caused by primer bias in the 16S rRNA sequencing process that may select against anammox.[124] This analysis also does not account for gene copy numbers, which has shown to be another source of error in 16S rRNA analysis.[134] Assuming 1-4 fgDNA/cell, the qPCR results suggest a similar relative abundance to the relative abundances shown in 16S rRNA sequencing in the counter-diffusing environment (0.16-0.10%), and a potentially higher relative abundance than described in 16S sequencing in the co-diffusing environment (12-1.5%). The complex nature of the anammox cell wall, which has been shown to consist of an additional layer of peptidoglycan beneath the gram-negative outer membrane, may lower DNA extraction efficiencies as compared to the other organisms present, lowering the relative anammox abundances detected.[135]

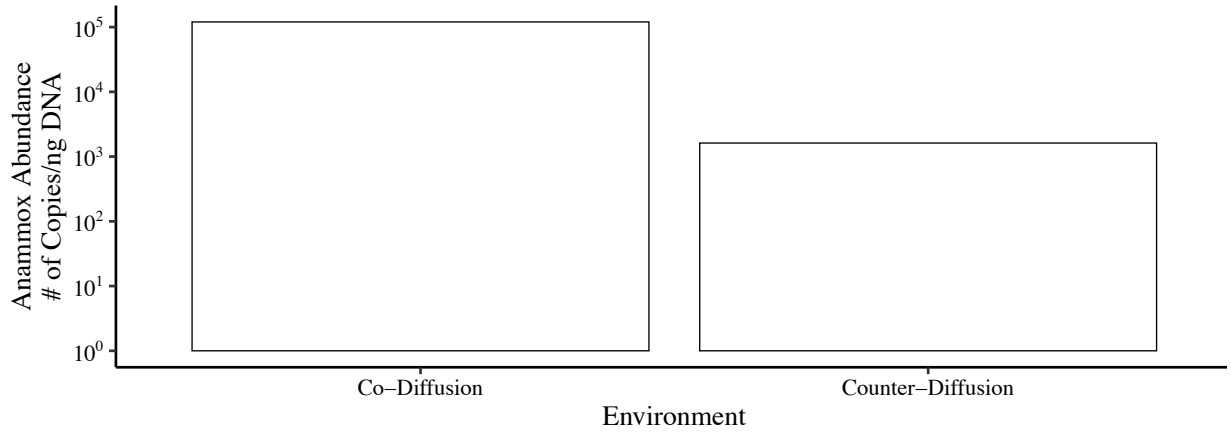

Figure 4-4. Absolute abundance of anammox measured in the biofilms of the co- and counter- diffusing environments after operation ceased, using qPCR primers designed to target the 16S rRNA gene of anammox.

Standard curves and melt curves of all qPCR results are included in supplementary information (Figures B7-B15).

4.4.3 Microscopy of Synthetic Environment Biofilms

FISH was performed on a cross section of the granules present in the co-diffusing system (Figure 4-5**Error! Reference source not found.**, left) and a cross section of a membrane fiber in the counter-diffusing system (Figure 4-5, right). Anammox (red), and *Nitrospira* (green) were clearly visible in both systems while archaea (blue) were more abundant in the counter-diffusing system. A live/dead stain of the exterior of a segment of membrane fiber showed co-association of living cells, with dead cells on the exterior of the membrane and the highest concentration of live cells on the face of the membrane fiber facing toward the bulk fluid (Figure B5).

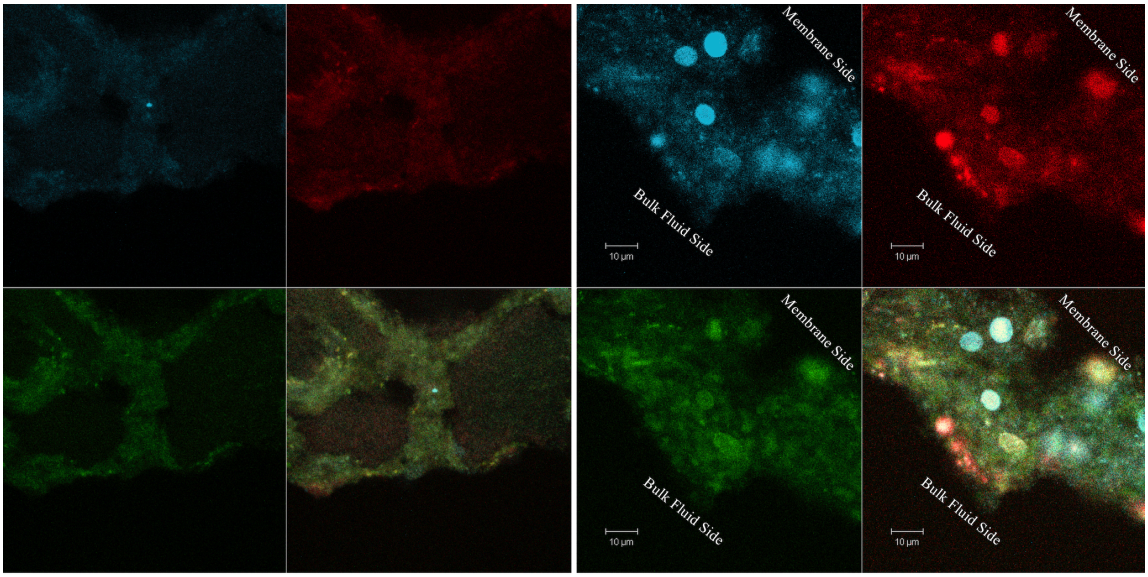

Figure 4-5. FISH images of the biofilms present in the co-diffusing granular system (left) and counter-diffusion membrane system (right). Archaea are stained with blue (cy5), Anammox cells are hybridized with red (cy3), and *Nitrospira* is stained with green (fluorescein).

4.5 DISCUSSION

4.5.1 Nitrogen Removal by AOA and Anammox Requires Counter-Diffusion

The counter diffusive environment was designed to mimic conditions within a typical OMZ, where ammonia and oxygen are supplied from opposite directions, a configuration known to

promote an AOA-anammox partnership.[20,136] While both the counter- and co-diffusion synthetic environments were found to remove nitrogen autotrophically through anammox, AOA were only present in the counter-diffusion environment with surprisingly low AOB abundances (<2%) and high *Nitrospira* abundance (7-14%) in both systems (Figure 4-3, top). FISH and qPCR analysis confirmed these findings (Figure 4-3, bottom and Figure 4-5). Recent theoretical models predicted that AOA would outcompete AOB in counter-diffusing systems because their high affinity for ammonia gives them a competitive edge.[20,136] Anammox consume most of the ammonia diffusing in from the anaerobic bulk liquid and oxygen diffuses into the biofilm attached to the hollow fiber membrane, resulting in low-ammonia/high-oxygen conditions near the base of the biofilm. These conditions favor AOA as they have a much higher affinity for ammonia than AOB, resulting in higher overall nitrogen removal.[111,112] FISH microscopy of the biofilm (Figure 4-5) supported this hypothesis, as the brightest clusters of anammox (red) were densest near the anaerobic bulk liquid exposed biofilm edge. The AOA (blue) were more abundant near the middle and base of the biofilm, where oxygen concentrations supported aerobic ammonia oxidization by AOA.

4.5.2 Comammox Presence in Co-Diffusing and Counter-Diffusing Environments

The high abundance of an unidentified *Nitrospira* taxa (Figure 4-3a) in both the co- (7%) and counter-diffusing (14%) environments was unexpected, given the low dissolved oxygen concentration measured in the co-diffusing environment (2-5 μM) and that no nitrate was found in the effluent of either system (Figure 4-2). Those *Nitrospira* might have included those capable of complete ammonia oxidation (comammox), but only partially oxidized ammonia to provide anammox with nitrite for ammonia removal.[16] Co-operation between anammox and comammox has been observed in synthetic microcosms, where ammonia and oxygen co-diffuse

together[137]. Comammox was found to be present in both biofilm systems, with higher abundance in the counter-diffusing system (Figure 4-3b). This finding is consistent with recent comammox ecology studies which show that comammox were more likely to be present in systems with long solids retention times, like those of the biofilms in these experiments.[130]

The observed higher comammox abundances in the counter-diffusing system provides additional context around other recent studies that report comammox preferably grow in low dissolved oxygen (DO) environments (6-31 μM).[59,138] This is in alignment with observations of higher comammox abundance in the counter-diffusing system that likely operated at higher maximum DO near the membrane-biofilm interface than the co-diffusive system, which was controlled at 2-5 μM. When these results are taken together in context with previous studies showing comammox is sensitive to DO, it suggests that there is an oxygen concentration, < 5 μM in this study, that begins to select against comammox while comammox will begin to dominate when DO increases above that concentration.

4.5.3 Potential for Anaerobic Nitrospira Activity

The copy numbers of comammox *amoB* detected with qPCR were lower than the abundances of *Nitrospira* detected with 16S rRNA gene sequencing, suggesting not all *Nitrospira* present were capable of complete ammonia oxidation (Figure 4-3). For example, in the counter-diffusing environment, far more copies of *N. viennensis amoA* were detected than comammox *amoB*, whereas the 16S rRNA gene sequencing results suggested that *Nitrospira* was three times as abundant as AOA. It is possible that the newly developed primers do not amplify all comammox organisms as more comammox species are still being discovered[122,139]. However, even considering primer bias, differences in 16S rRNA gene copy numbers, and other potential factors

contributing to error, the magnitude of the measured disparity cannot be ignored, and it is likely not all *Nitrospira* present were comammox. Though, it also seems unlikely that these *Nitrospira* were canonical NOB as the DO of the co-diffusion environment was controlled at 2-5μM, an order of magnitude lower than the reported affinity of *Nitrospira* for oxygen (~30 μM).[5,112,119] Nevertheless, this is not the first report of high abundances of *Nitrospira* under low oxygen conditions. *Nitropsira* have been shown to grow at DO concentrations as low as 2-5 uM in nitrification reactors within water resource recovery facilities.[123] FISH microscopy results show the *Nitrospira* (green) organisms were relatively uniformly distributed across oxic and anoxic regions of the biofilm (Figure 4-5).

Although *Nitrospira* and other nitrite oxidizing bacteria have traditionally been considered to be obligate aerobes, recent work has shown their capability of anaerobic metabolisms as well. *Nitrospira moscoviensis* has been shown to reduce nitrate to nitrite, using formate as an electron donor by reversing the activity of its nitrite oxioreductase (NXR) enzyme.[18] In this study, *N. inopinata* was found to be capable of the same metabolism as nitrate was consumed while nitrite was produced in the presence of anoxic conditions when fed 1 mM formate. Furthermore, several species of *Nitrobacter*, another genus of NOB, have been observed to perform dissimilatory nitrate reduction to ammonia (DNRA) under anoxic conditions.[140] No consumption of COD was measured in either the co- or counter-diffusing environments, so any heterotrophic metabolisms that occurred in these systems must have received COD from endogenous decay or CO_2 fixation by anammox or other autotrophs present. Theoretical calculations using the performance data from the counter-diffusing system and previously reported kinetic constants of AOA, anammox, and formate-reducing *Nitrospira* predict that 73% more COD would be required for the denitrification of anammox produced nitrate then could be produced by endogenous decay of

autotrophs.[5,8,18,20,141] The COD deficit leads us to consider the possibility of COD supplied via a CO_2 fixation pathway. Formate dehydrogenase has been observed to supply formate for DNRA in many organisms.[142] *Ca.* Brocadia sinica, the same genus detected in both counter- and co-diffusing environments, has genes for multiple nitrite/formate transporters and formate dehydrogenase[19,143,144]. Formate could be supplied by anammox via the reductive acetyl-CoA pathway, using formate dehydrogenase acting in the reductive direction. Recent metabolic network models built from metatranscriptomic data taken from anammox granular sludge have hypothesized that anammox supplies organic carbon as amines or EPS molecules, along with nitrate, to the heterotrophic populations present in anammox granular sludge (Figure B6).[145] Meanwhile, *Nitrospira* has been reported to be able to use formate and nitrate to form nitrite.[18] This would establish a syntrophic interaction in that anammox supplied both nitrate (NO_3^-) and formate ($CHOO^-$) to *Nitrospira* that then supported anammox with nitrite (NO_2^-) to perform ammonia (NH_3) oxidation to nitrogen gas (N_2) (Figure 4-6). This co-operation would be a viable hypothesis to explain the absence of nitrate in the effluents of both systems, as there is not enough COD available for typical heterotrophic denitrification (Table B5).

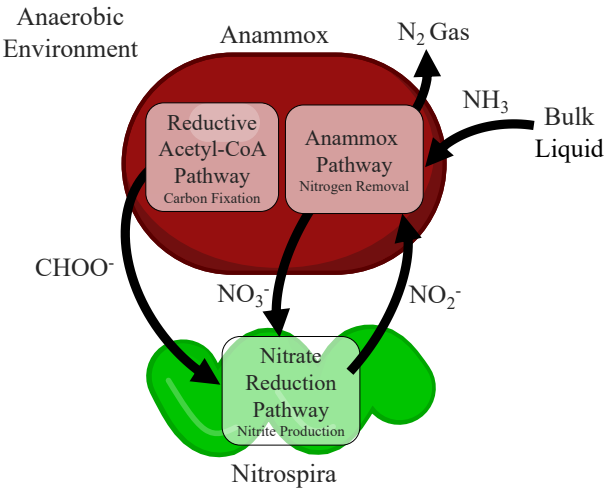

Figure 4-6. Hypothesized co-operation between *Nitrospira* and anammox. Anammox produces nitrate (NO_3^-) via the anammox nitrogen removal pathway and formate ($CHOO^-$) via the carbon fixing reverse acetyl-CoA pathway for *Nitrospira* to anaerobically reduce nitrate to nitrite (NO_2^-), which support anammox and allow full N removal. Such a scheme could be possible in the anaerobic conditions present in either a co-diffusion or counter-diffusion environment.

Quite strikingly the here investigated synthetic counter-diffusion ecosystem is comparable to the OMZ in that they both experience counter diffusive gradients, they both see AOA-anammox co-operation, they have similarly high abundances of NOB (up to 9% in OMZs, and 7-14% in this experiment), they receive little organic carbon, and they accumulate little nitrate, though in marine OMZs the major NOB is *Nitrospina.* [31,146,147] Anammox's competitive edge over any canonical NOB for nitrite is evidenced by the low nitrate concentrations in the effluent. This raises the question of whether *Nitrospina* (as observed in OMZs) can perform anaerobic nitrate reduction and likewise for the *Nitrospira* observed in this study.

Synthetic environment experiments like these allow us to better understand the ecological roles of the contributing microorganisms. In this experiment, we found a laboratory OMZ-like mesocosm replicated partnerships between AOA, NOB and anammox, demonstrating the capacity of lab-scale mesocosms as a tool to better understand and study OMZ environments. The laboratory mesocosm allowed us to identify two plausible novel nitrite-supplying pathways. Partial ammonia oxidation of comammox for anammox nitrogen removal, and anaerobic reduction of nitrate by *Nitrospira* supplying anammox with nitrite for nitrogen removal at very low oxygen loading rates in both counter and co-diffusing environments. We further found that counter-diffusion was essential to cultivating a partnership between AOA-anammox, which suggests a potential research pathway forward to implement AOA-anammox into wastewater treatment, ultimately achieving near 100% nitrogen removal at mainstream conditions.

4.6 SUPPORTING INFORMATION AVAILABLE

- Supplemental figures and tables referred to in this chapter are available.in Appendix B.

Chapter 5. COMAMMOX AND ANAMMOX CO-OPERATE IN BOTH CO-DIFFUSING GRANULAR SLUDGE AND COUNTER-DIFFUSING MEMBRANE AERATED BIOFILM REACTORS

5.1 ABSTRACT

In order to implement anammox into mainstream nitrogen removal, nitrite must be supplied at low ammonia (here considered as total NH_4^+ and NH_3) concentrations while suppressing activity of nitrite oxidizing bacteria (NOB). Recently discovered comammox are a complete oxidizing bacteria capable of both ammonia and nitrite (NO_2^-) oxidation and possess a high affinity for ammonia but a low affinity for nitrite, making them an attractive partner to supply nitrite to anammox at low ammonia mainstream conditions. Co-operation of comammox and anammox was tested by inoculating them both in two different reactor designs, a co-diffusing granular sludge reactor and a counter-diffusing membrane aerated biofilm reactor (MABR) and observing the nitrogen species in the effluent and the microbial populations after termination of operation. Theoretical models of these two systems were also ran at varying ammonia and oxygen concentrations. Theoretically and experimentally, comammox-anammox nitrogen removal occurred in both reactor designs, but higher nitrogen removal was observed in the counter-diffusing MABR than the co-diffusing anammox granular sludge reactor. This was likely because comammox were more active in the oxygen rich-ammonia poor membrane-aerated side of the biofilm in the MABR than the oxygen and ammonia poor aerobic shell of the granular sludge. While the theoretical model predicted the presence of nitrite and/or nitrate in the effluent at nearly all conditions, no nitrite or nitrate was observed in the experimental system. This result paired with the presence of *Nitrospira* in anaerobic regions of the biofilm suggests an anaerobic

lifestyle for the *Nitrospira*, in which we hypothesize that they consume nitrate and potentially organic carbon leaked by autotrophic anammox.

5.2 ABSTRACT ART

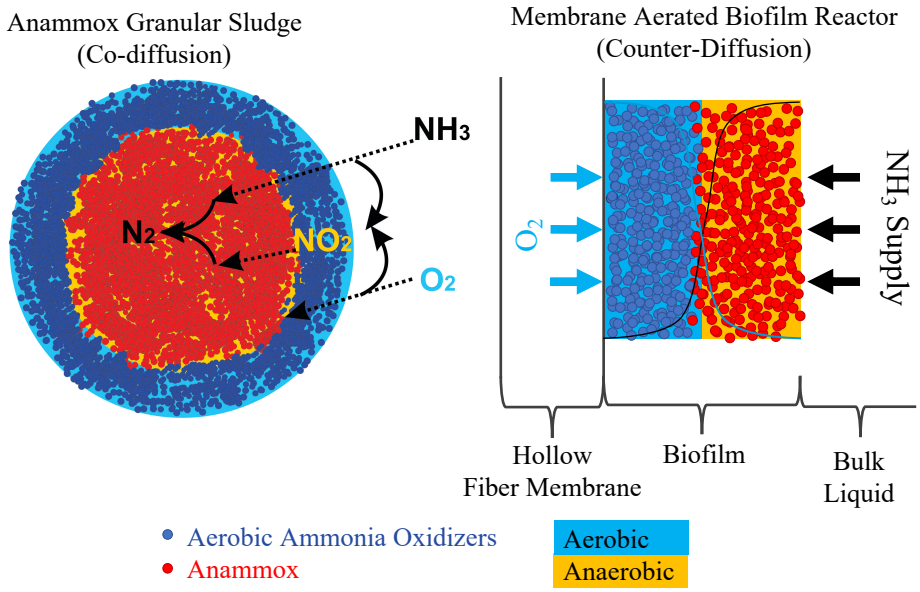

Figure 5-1. Concepts behind co-diffusing anammox granular sludge and counter-diffusing membrane aerated biofilm reactors (MABRs).

5.3 INTRODUCTION

The implementation of anaerobic ammonia oxidizers (anammox) has successfully lowered nitrogen removal costs in niche applications[12,148]. Anammox are autotrophic *Planctomyces* capable of shortcutting the nitrogen cycle by anaerobically oxidizing ammonia (in this study considered as total NH_4^+ and NH_3) with nitrite as an electron acceptor to form nitrogen gas[8]. In anammox nitrogen removal, ammonia oxidizing bacteria (AOB) supply nitrite (NO_2^-) for anammox (Figure 5-1, left)[72–74]. This syntrophic partnership is commonly referred to as partial-nitritation/anammox and can lower aeration demand by more than half, because only ~50% of the influent ammonia is required to be aerobically converted while the remainder is anaerobically

oxidized. The low biomass yield of autotrophic anammox and AOB bacteria reduce sludge production by up to 90% as compared to heterotrophic denitrifying organisms and eliminate the need for external carbon[9,70,149]. These organisms can also form dense granules with an aerobic shell populated by AOB, which provide the necessary nitrite to anammox that can grow in the anoxic inner core. Due to their size (1-3 mm), granules easily separate from other solids and therefore shorten settling times drastically and reduce tank volume by up to 70%[12].

Successful anammox-AOB nitrogen removal requires careful operational control to ensure that populations of AOB and anammox are selected over the nitrite oxidizing bacteria (NOB), which compete with AOB for oxygen and anammox for nitrite. If NOB become active in an anammox system, nitrite will be oxidized to nitrate, which is inaccessible to anammox's autotrophic pathway[150]. One strategy to suppress NOB activity involves operating the system at low dissolved oxygen (DO) concentrations. AOB have a higher affinity for oxygen than NOB, and thus are able to outcompete NOB for oxygen. Low DO control schemes have proven successful in the treatment of ammonia-rich sidestream anaerobic digester centrate (1% of volumetic flow, >1000 mgN/L-NH_3). However, in mainstream wastewater (99% of volumetric flow), ammonia concentrations are much lower (20-80 mgN/L-NH_3). The low oxygen concentrations required to select for AOB combined with the lower ammonia concentrations present in the mainstream throttle the activity of both AOB and anammox,[151] resulting in poor nitrogen removal in the mainstream with only a few exceptions.[13,15,70,115] It has therefore been of great interest to pair anammox with an ammonia oxidizing organism that thrives at low ammonia and low oxygen concentrations

Two such ammonia oxidizing organisms, comammox ($K_{NH3+NH4}^{CMX}$=9.1-15.4 µgN-NH_3+ NH_4^+/L reported for *Nitrospira inopinata*)[17] and ammonia oxidizing archaea (AOA, $K_{NH3+NH4}^{AOA}$=9.7-11.3

μgN-NH_3+ NH_4^+/L reported for *Nitrososphaera viennensis*),[20,152] have recently been discovered. In fact, marine AOA *Nitrosopumilus maritimus*, has an even higher ammonia affinity ($K_{NH3+NH4}^{AOA} = 1.85$ μgN-NH_3+ NH_4^+/L) Both have a much higher affinity for ammonia than AOB (K_{NH4}^{AOB} =2.19 mgN- NH_3+ NH_4^+//L) that would allow them to continue to supply nitrite to anammox at mainstream ammonia concentrations. In fact, AOA have been observed to work with anammox in oxygen minimum zones of the ocean where they contribute to up to 50% of marine nitrogen loss. Comammox are a complete ammonia oxidizing bacterium most closely related to NOB *Nitrospira* that are capable of ammonia oxidation in addition to canonical nitrite oxidation[16]. While comammox have a high affinity for ammonia, various kinetic studies have shown their nitrite affinity (K_{NO2}^{CMX} =6.65-0.19 g/m^3)[17,153] is similar to or worse than the anammox affinity for nitrite (K_{NO2}^{AMX} =0.67-0.10 g/m^3)[8,20]. These kinetic characteristics make comammox an ideal nitrite-supplying partner to anammox because they can oxidize ammonia low ammonia concentrations and anammox has opportunity to access comammox-produced nitrite. Comammox-anammox nitrogen removal has previously been observed in co-diffusing hydrogel beads,[137] and comammox-anammox partnerships were observed to develop without an initial inoculation of comammox in lab-scale anammox reactors inoculated with an anammox and AOA (see Chapter 4).

An alternate reactor design that may be well suited to application of anammox with a low-affinity ammonia oxidizing organism is the membrane aerated biofilm reactor (MABR). MABRs have been shown to achieve nitrification/denitrification at a pilot scale,[154] and autotrophic nitrogen removal with a population of AOB and anammox has been observed at lab-scale under strict intermittent aeration conditions[155,156]. In an anammox-AOB MABR, oxygen is supplied through small (~2 mm diameter) hollow fiber membranes while ammonia is supplied from the

bulk fluid, resulting in counter-diffusion of the two key substrates required for nitrogen removal. On the membrane side, the aerobic environment and low ammonia conditions are favorable to AOB. On the bulk fluid side, oxygen has been consumed by the AOB, which supply nitrite to the anammox, enabling them to grow in the anaerobic ammonia-rich conditions present near the bulk fluid. This set-up is ideal for low ammonia affinity AOA or comammox, which could thrive in the low ammonia aerobic side of the biofilm and supply nitrite at a higher rate than AOB to anammox in the anaerobic high ammonia side of the biofilm.

In this study, we explore the impact of reactor design on anammox-comammox co-operation theoretically and experimentally. Experimentally, co-diffusion and counter-diffusion are compared in a granular sludge reactor and an MABR respectively, both inoculated with comammox and anammox. The performance of these systems and the microbial communities that drive the nitrogen removal were measured. The experimental results are compared to theoretical results in granular sludge and MABR models, and the viability of comammox-anammox co-operation, especially in the MABR, was confirmed.

5.4 MATERIALS AND METHODS

5.4.1 Cultivation of Ammonia Oxidizing Organisms

Operation of both MABR and granular sludge reactors required healthy cultures of anammox and comammox. Anammox granular sludge originated from a reactor located in Sluisjesdijk, Rotterdam, The Netherlands which treats ammonia laden centrate of the adjacent wastewater treatment plant.[12] Upon arrival of the granular sludge in the lab, biomass was placed in plug-flow columns a 30 °C and fed synthetic wastewater to maintain activity. The comammox pure culture *N. inopinata* originated from the surface of a hot water covered metal pipe near a deep oil

exploration well in Aushiger, North Caucus, Russia and was provided by the University of Vienna [24]. Pure cultures of *N. inopinata* and *Nitrosomonas europaea* (ATCC® 19178™) were maintained in the dark at 30 °C in 14 mgN-NH_3/L ammonia media previously used to sustain ammonia oxidizing archaea cultures (Chapter 4).

5.4.2 Determination of Kinetic Parameters of Nitrifying Species

In order to create more descriptive theoretical models, kinetic parameters of both AOB (*N. europaea)* and comammox (*N. inopinata)* were determined. *Nitrosomonas europaea* was used in a nitrite inhibition experiment and grown at constant ammonia concentration and varying nitrite concentrations, similar to previous nitrite-inhibition experiments *N. inopinata*.[137] The rate of nitrite production by *N. europaea* was measured under varying nitrite concentrations (0.1, 0.125, 0.130, 0.132, 7, 14, 28, 70, 140, 280, 420, 560, 700, 1400 mgN/L) and constant ammonia concentration (14 mgN/L) in individual 100-mL batch cultures (Figure C6). The resulting calculated constant from experimental data was incorporated into the theoretical models described here.

In order to measure the oxygen affinity of *N. inopinata*, pure culture was maintained in liquid mineral medium at 30°C in the dark without shaking.[16] Growth was monitored by measuring ammonia consumption, nitrite production, and cell abundance. Cell counts were determined using Moviol–SYBR Green I staining protocol as previously reported[49] with a Zeiss epifluorescence microscope to count 15 random fields of view for each sample with 30 to 200 cells per field.

Oxygen uptake kinetic measurement of the late exponential *N. inopinata* cultures were carried out in custom-built 60 ml of glass chambers (Uniserse, Aarhus, Denmark) and instantaneous O_2

concentrations were measured using STOX oxygen microsensors (Unisense, Aarhus, Denmark). Briefly, *N. inopinata* cultures were grown with 1 mM ammonia at 30°C in batch culture, and ammonia, nitrite, and nitrate concentrations were monitored daily before cultures were subjected to oxygen uptake affinity measurement. Late exponential cultures were resuspended in ammonia and nitrite-free medium and transferred into a 60 ml of microrespirometry (MR) chamber so as to leave no headspace. MR experiments were performed in a water bath with a constant temperature set at 30°C. Concentrated ammonia or nitrite solutions were injected into the chamber via an injection port using a 10 µl Hamilton syringe to make the final substrate concentration to 1 mM. Stirring was applied at low stirring speeds of 100–150 rpm to maintain homogeneity of the cell suspension, and no cell aggregates or biofilms were observed during MR experiments. STOX oxygen microsensors were calibrated according to the manufacturer's instructions (Unisense). Sensors were plugged directly into a microsensor multimeter (Unisense) and were polarized for more than 1 day prior to use. Sensor signals were equilibrated until they became stable. Data were logged via the microsensor multimeter using SensorTrace Logger software (Unisense).

The oxygen kinetic constants ($K_{m(app)}$ and V_{max}) of *N. inopinata* were determined by fitting a Michaelis-Menten equation to O_2 uptake rates using the equation $V = (V_{max} \times [S]) \times (K_m + [S])^{-1}$. Here V is rate, V_{max} is the maximum rate (µM min^{-1}), K_m is the half saturation constant (µM), and [S] is oxygen concentration (µM). V_{max} was converted to specific rate by dividing the rate by cell number.

5.4.3 Design, Operation, and Analysis of Co- and Counter- Diffusion Reactors

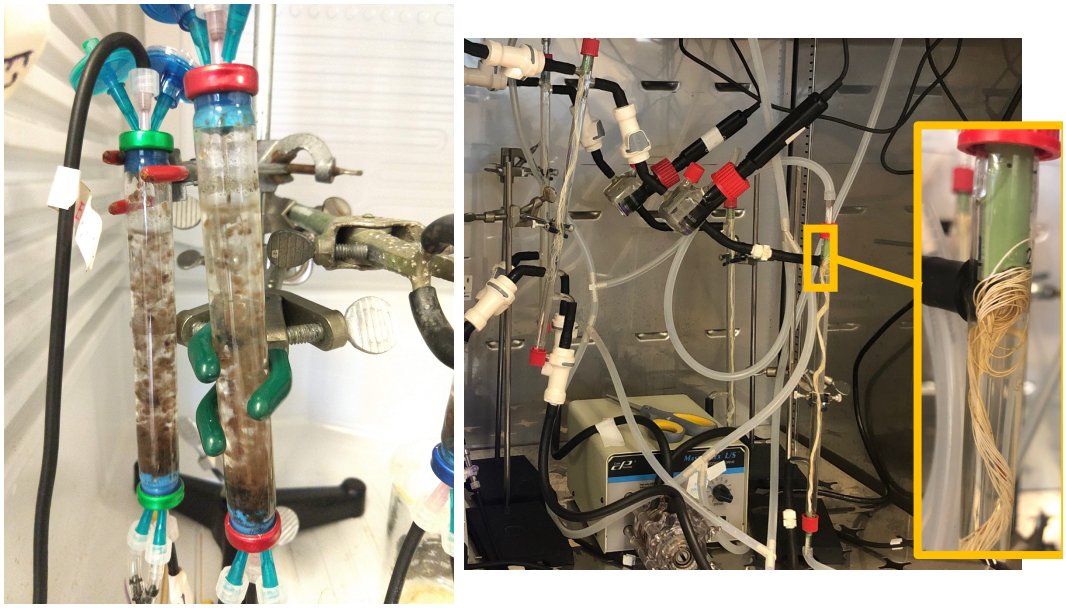

Anammox Granular Sludge Reactor

Membrane Aeraed Biofilm Reactor

Figure 5-2. Pictures of both the small-scale anammox granular reactor (left) and the MABR while in operation.

Two different reactor systems were designed and operated in order to evaluate the effects of reactor design on comammox-anammox nitrogen removal, an anammox granular sludge reactor and a MABR. For the granular sludge reactor, 1 L of a late exponential phase comammox culture was concentrated onto powdered activated carbon and then the comammox-sorbed activated carbon allowed to attach to a small volume (~5 mL) of anammox granular sludge with diameters between 1-3 mm. Sequencing results obtained from granular sludge just before and after inoculation (Figures C1 & C2) and flow cytometry cell counts of the suspended comammox culture before and after attachment both indicated that comammox successfully sorbed onto activated carbon. Media was fed in at a rate of 4.5 mL/hr and DO was controlled at approximately 0.05-0.12 mgO_2/L with aeration by an air/N_2 gas mixture. For the MABR, hollow fiber membrane strands ~2 mm in diameter were coated with poly-L-lysine. A large volume (~1 L) of late exponential phase comammox was then concentrated onto a polyethylene tangential

flow filter and washed off into ~50 mL of media. Poly-l-lysine coated fibers were then inoculated with the concentrated comammox culture with a ~30 minute soaking period. Subsquently, the comammox-inoculated fibers were then inoculated with anammox via another ~30 minute soaking period in anammox granular sludge that had been homogenized with a Bio-Gen (Cambridge, MA USA) Pro200 Electronic Tissue Grinder at 50% power for 1-2 minutes Media was fed at a rate of 15 mL/hr. Homogenous concentration of substrate was accomplished with rapid recirculation of the bulk liquid. After 89 days of operation, DO was controlled in the bulk media at 0 mg/L with a constant sparge of nitrogen gas. The reactor was then run at steady state for 93 days. Biofilm samples were taken and stored for both DNA extraction and fluorescent in-situ hybridization. Design, operation and molecular techniques used in previous work were also used in this study (Chapter 4).

5.4.4 Theoretical Models

Theoretical models built with AQUASIM were operated at varying ammonia and oxygen concentrations in order to understand how different loading conditions would affect the competition dynamics between AOB, canonical NOB, anammox, and comammox.[157] Two models were created to simulate co- and counter- diffusion reactor designs. In the co-diffusion model, the biofilm was modeled as a 1mm biofilm. The counter-diffusion model was designed with a 30 μm biofilm growing on a cylinder of 1 mm radius to simulate the MABR as that was the approximate thickness of biofilm on the membranes observed in the operating MABR (Figure 5-7). In addition to the biofilm compartment in the MABR model, a gas compartment, representing the interior of the hollow fiber membranes, was added. The base of the biofilm was linked to the gas compartment and oxygen was assumed to diffuse into the biofilm according to typical mass transfer coefficients and Henry's law constants and assuming a membrane area of

400,000 m^2.[20,120] In both models, the total volume of biomass was 100 m^3, the reactor volume was assumed to be 400 m^3 and the influent flowrate was 100 m^3/d. Biological kinetic parameters were taken from previous AQUASIM anammox models[20,116] with the exceptions of comammox kinetic constants which have been reported elsewhere,[17] and the nitrite half-inhibitions constants of the various organisms considered, which were measured either measured in this study or in similar related studies.[137] All kinetic, stoichiometric, and diffusion coefficients along with rate equations and reaction stoichiometries are available in supplementary information, (Tables C1-C4). Once the models were set-up, influent ammonia and oxygen loadings were varied independently in order to evaluate the impact of varying substrate concentration on reactor performance and population dynamics. In the co-diffusion model, oxygen loading was varied by changing the dissolved oxygen concentration in the bulk fluid whereas in the counter-diffusion model oxygen flowrate through the hollow fiber membranes in the gas compartment was varied.

5.5 RESULTS AND DISCUSSION

5.5.1 Nitrogen Removal Observed in Both Reactors

Performance of the ammonia-fed MABR and granular sludge reactors is shown in Figure 5-3. Both systems were inoculated with anammox and comammox and removed nitrogen as N_2 gas with some residual nitrogen left the system primarily as ammonia and effluent nitrite and nitrate concentrations at or near zero. This was unexpected as anammox produces some nitrate in its anabolic pathway,[8] and nitrate is usually found in the effluent of aerobic anammox reactors.[12,158] Recently, anammox-comammox co-operation in immobilized alginate beads was observed. Low nitrate concentrations were also observed in that system. In that study it was hypothesized that denitrifying species in the anammox enrichment may have used the alginate in the beads as a

carbon source for denitrification.[137] However, the materials that facilitated attachment in these systems, inorganic powdered activated carbon for the granular sludge system and poly-L-lysine in the MABR, are not biologically available to heterotrophic denitrifiers[159]. There was also no organic carbon fed to the system supporting heterotrophic growth and denitrification of organic carbon from the buffer component HEPES was unlikely as the chemical oxygen demand (COD) measurements of the influent and effluent of both systems revealed that no COD was consumed (Table C5), therefore analysis of the microbial populations present was performed in order to form a hypothesis around the fate of nitrate in both these systems.

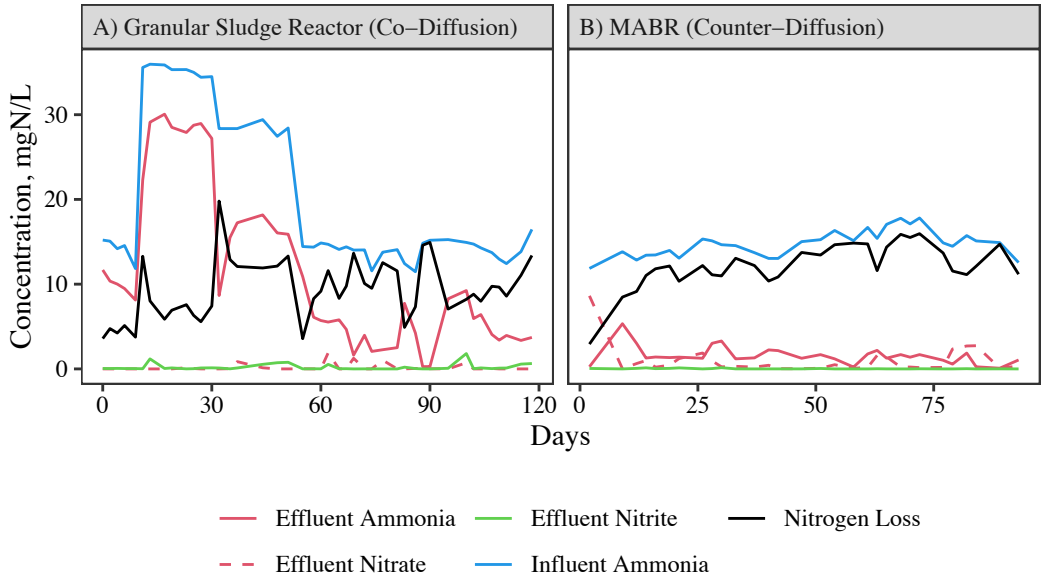

Figure 5-3. The long-term operational performance of both the granular sludge reactor and MABR inoculated with comammox and anammox.

The initial influent ammonia concentration into the granular sludge reactor (14 mgN-NH_3/L) appeared to be below the nitrogen removal potential of the co-culture, and therefore nitrogen loading was increased to establish an active seed culture and to evaluate the maximum removal possible by the anammox granular sludge. The nitrogen loading was then stepped back to similar levels fed to the MABR system in order to operate both reactors at similar conditions for better

comparison. The bulk fluid of the MABR was recirculated while being sparged with nitrogen gas to enforce anaerobic conditions in the bulk fluid and establish a healthy anammox culture. Without the addition of nitrogen gas, most influent ammonia was observed to be converted to nitrate (Figure C1). Once nitrogen gas was added, the concentration of nitrate in the influent dropped quickly, and nitrogen removal rate increased. The nitrogen removal observed in these systems as well as the absence of nitrate in the effluent prompted 16S rRNA gene sequencing and qPCR to explore the presence of aerobic and anaerobic ammonia oxidizing species in these reactors.

5.5.2 Comparing Measured Kinetic Parameters to Expected Values

The nitrite half-inhibition constant of AOB organism *N. europaea* ($k_i = 89 \pm 46 \frac{mgN-NO_2^-}{L}$) and the oxygen affinities of comammox for both ammonium ($k_{O_2,NH_4^+}^{CMX} = 0.131 \frac{mg}{L}$) and nitrite ($k_{O_2,NO_2^-}^{CMX} = 0.126 \frac{mg}{L}$) were determined as part of this study (**Error! Reference source not found.**). The nitrite half-inhibition constant of *N. europaea* was in line with similar studies.[160] However, the oxygen affinity of comammox during both ammonium and nitrite oxidation was lower than was expected. Close examinations of comammox *Nitrospira* genomes have suggested that oxidase enzymes used by comammox would have a high affinity for oxygen. Given this, the oxygen affinities as measured in this experiment are surprisingly poor, especially when compared to other ammonium oxidizers, such as AOA ($k_{O_2}^{AOA} = 0.093 - 0.0896 \frac{mg}{L}$)[20]. However, the affinity of comammox under oxygen-stressed conditions was not explored as part of this study. It could be that under oxygen-stressed conditions, a different terminal oxidase enzyme is responsible for comammox activity, thus fulfilling the previously predicted low oxygen affinities possessed by comammox.

Table 5-1. Oxygen uptake kinetics of N. inopinata

Oxygen (ammonia as substrate)		Oxygen (nitrite as substrate)	
Km (μM)	Vmax (fM per cell per hour)	Km (μM)	Vmax (fM per cell per hour)
4.11±3.52	4.96±1.33	3.93±0.65	5.37±1.69

5.5.3 Higher Abundance of Nitrifiers Leads to Higher Nitrogen Removal

The relative proportions of all known aerobic nitrifiers as detected with 16S sequencing are shown in Figure 5-4. *Nitrospira,* the genus which comammox belongs to, was found to be highly abundant in both the granular sludge reactor (12%) and the MABR (14%). Meanwhile the only AOB-containing genus found was *Nitrosomonas*, which was present in low abundances in both the granular sludge reactor (0.5%) and the MABR (2%). The OTU belonging to *Nitrospira* may contain both comammox and canonical NOB. Comammox are unique in that they have ammonia monooxygenase genes (*amoA*, *amoB*, and *amoC*), that are genetically distinct from those present in AOB or ammonia oxidizing archaea, and not present in canonical NOB. Previous work have designed qPCR primers that target all known *Nitrospira amoB* genes, which were used here to investigate if the *Nitrospira* belonged to comammox (Figure 5-5).[130]

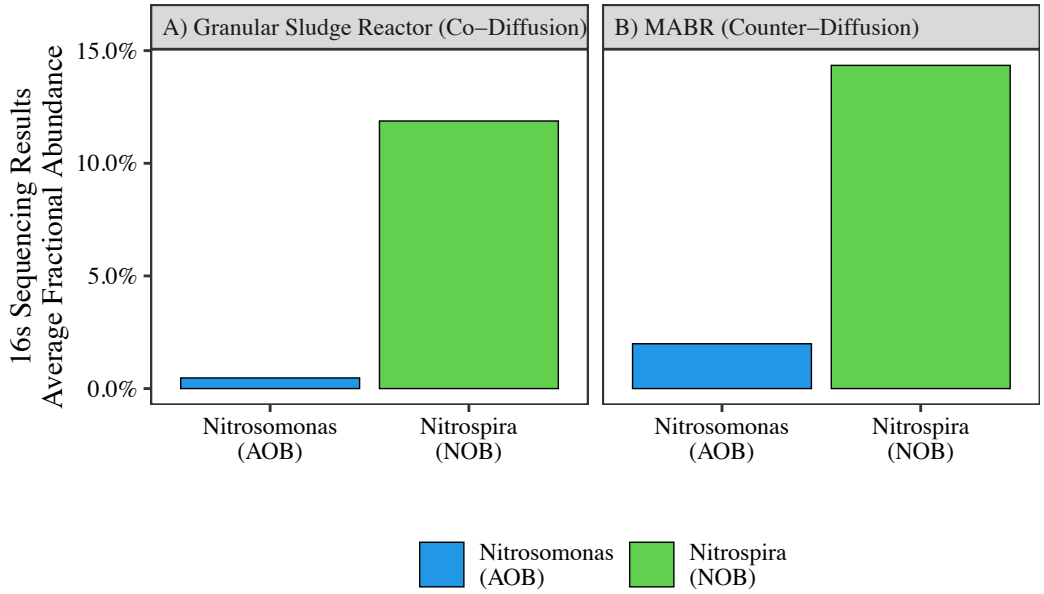

Figure 5-4. Final relative abundance of aerobic nitrifiers in biofilms present in both the granular sludge reactor (left) and MABR (right).

Comammox was found to be much more abundant in the MABR system than the granular sludge system. The number of copies of comammox *amoB* in the granular sludge reactor were so low that it was extrapolated from the calculated standard curve (Figure C2). However, the melt curves of all replicates were very similar to the positive control, suggesting that the amplification within the qPCR samples was due to the presence of the target comammox *amoB* sequence (Figure C3). Furthermore, gel electrophoresis revealed that the qPCR product was the same base pair length as the target sequence in samples from the granular sludge reactor on days 0, 31 and 118 (Figure C4).

These results suggest that comammox was present in both the granular sludge and MABRs after long periods of operation, though comammox signals were almost 300-fold higher in the MABR. Canonical AOB were also four times more successful in the MABR than the granular sludge reactor.

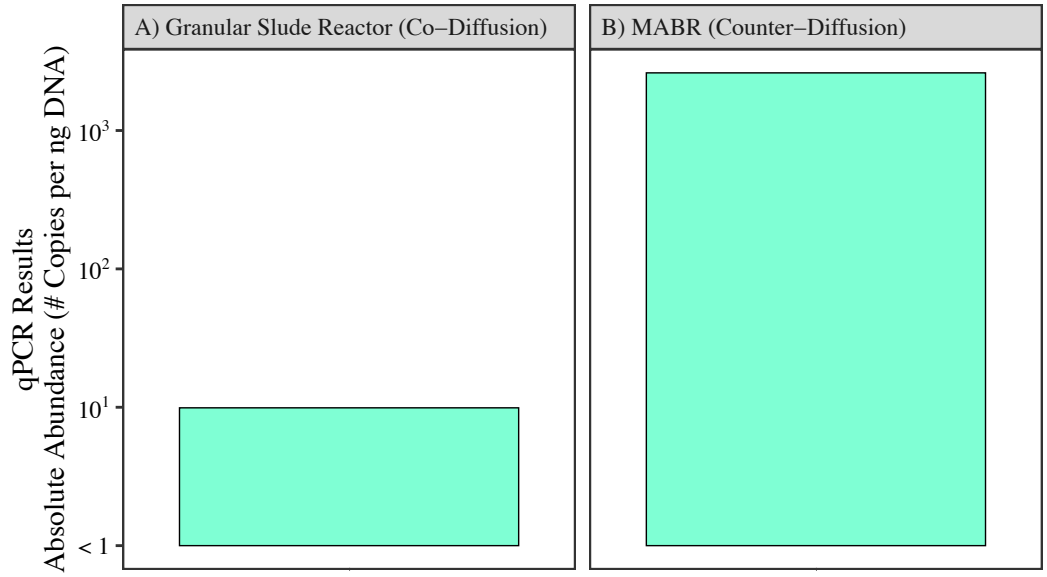

Figure 5-5. Abundance of comammox in both the granular sludge reactor (left) and the MABR (right) as detected by general qPCR *amoB Nitrospira* primers after operation was completed.

Though 16S sequencing showed a surprisingly low abundance of anammox, qPCR results with anammox 16S primers revealed anammox was clearly present in both systems, and more abundant in the co-diffusing granular sludge reactor than the MABR (Figure 5-6). Assuming 1-4 fgDNA/cell, the qPCR results that the estimated relative abundance of anammox was between 4.6%-2.9% in the granular sludge reactor and up to 0.14% in the MABR. The fluorescence signals in the FISH assays (Figure 5-7) were also quite high for anammox (red), so it is possible that the primers chose for 16S sequencing selected against anammox, causing the fractional abundance as detected by 16S rRNA sequencing to appear lower than it was in reality. During operation the anaerobic granular sludge likely had a larger anaerobic volume fraction than the counter-diffusing MABR, because it was inoculated with granules that had an established a community. In addition, the granular sludge reactor received a mixture of nitrogen gas and compressed air in order to control the system at a set oxygen concentration while the membrane fibers in the MABR were fed 100% compressed air. This likely led to a higher maximum

dissolved oxygen concentration in the MABR biofilm, which would inhibit anammox. The maximum oxygen concentration in the MABR biofilm supported a higher concentration of aerobic nitrifiers, like comammox and AOB, which were able to supply anammox with sufficient nitrite for 88% nitrogen removal, whereas the granular sludge system could only remove 76% nitrogen.

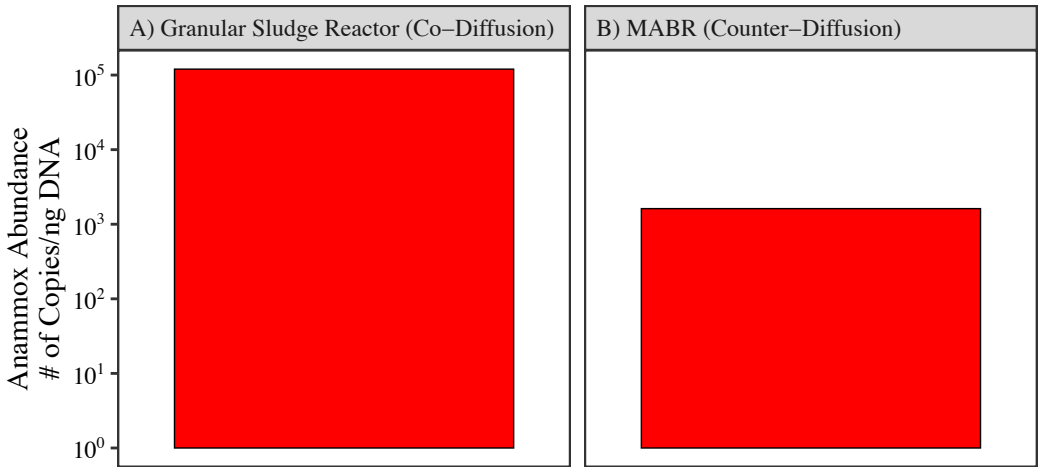

Figure 5-6. Anammox abundance in the granular sludge reactor (left) and MABR (right) as measured by qPCR targeting the 16S rRNA anammox gene.

5.5.4 Fish Microscopy Suggests a Possible Fate for Nitrate

FISH analysis was conducted to elucidate the spatial distribution of all functional groups and the observations suggested a compelling hypothesis explaining the absence of nitrate in the effluent of both reactors. Presence of AOB (blue), *Nitrospira* (green), and anammox (red) was observed in FISH microscopy of the biofilms from both reactors. In the counter-diffusing MABR biofilm, a distinct layer of AOB was observed through the center of the biofilm (Figure 5-7b). On the aerobic membrane-facing side of that layer, NOB (green) was found. On the anoxic bulk-fluid facing side of the AOB layer, both anammox (red) and *Nitrospira* (green) were found to co-exist. A similar phenomenon was observed in the co-diffusing granular sludge biofilm (Figure 5-7a),

where NOB were found to be present in both oxic and anoxic zones of the granular sludge biofilm while anammox was observed to be more abundant on the anoxic interior of the biofilm and AOB primarily localized in the oxic exterior of the granular sludge. Redox-stratification of AOB, NOB, and anammox in both MABR and granular sludge reactors is well documented,[161,162] and as a result the presence of *Nitropsira* in an anoxic region of the biofilm was surprising as both comammox and canonical NOB require oxygen for ammonia and/or nitrite oxidation.

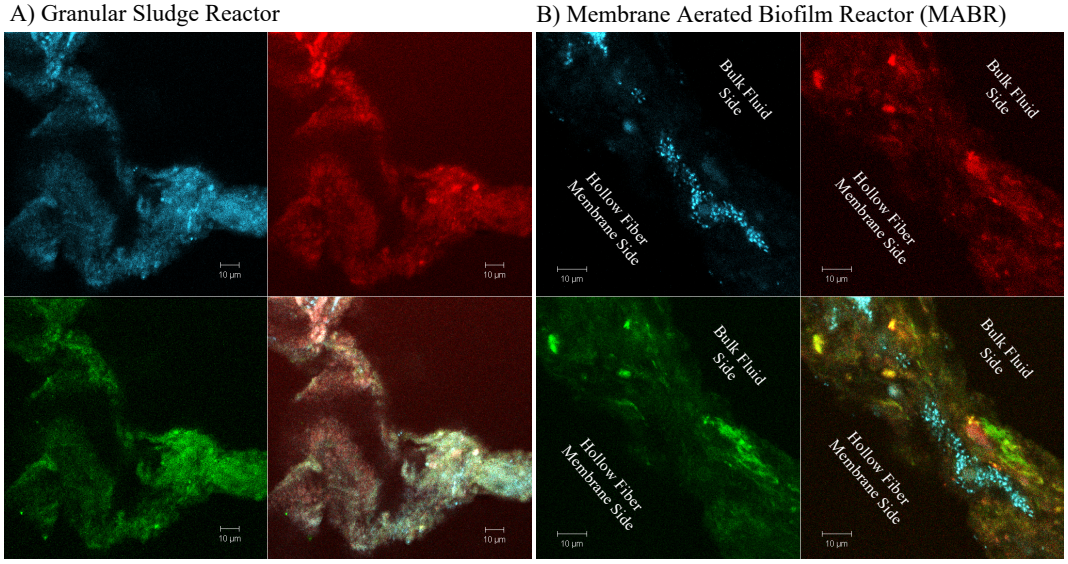

Figure 5-7. Fluorescent in-situ hybridization (FISH) microscopy of the biofilms from both the granular sludge reactor (left) and MABR (right) after operation was finished. Probes targeting anammox (Cy 3, red), AOB (Cy 5, blue), and *Nitrospira* (Fluorescein, green) were used.

It is possible that some of the NOB present in the anaerobic region of the biofilm are no longer active,[163] though inactive NOB would not explain the high abundance of *Nitrospira* present (Figure 5-4) that cannot be entirely accounted for by *Nitrospira* comammox (Figure 5-5). While the activity of NOB in anaerobic or microaerophilic conditions is atypical, *Nitrospira* was found to be highly abundant in nitrifying reactors controlled at low DO (0.12-0.24 mg/L)[123], and in addition more recently high concentrations of marine NOB *Nitrospina* have been observed in

oxygen and nitrate depleted zones of the ocean[146]. The presence of NOB in anoxic regions may suggest that they follow anaerobic lifestyle that might help to explain the absence of nitrate in the effluent without an externally supplied organic carbon source. Both canonical NOB *Nitrospira moscoviensis* and comammox *N. inopinata* have been observed to use formate to reduce nitrate to nitrite[18]. However, these observed anaerobic NOB metabolisms are heterotrophic, and require some form of COD. No COD consumption was measured in the reactor, but the robust population of known heterotrophs present (Figure C5) suggest the occurrence of some organic carbon cycling, possibly supported by decay material or alternatively by the carbon fixing autotrophs in the biofilm, like anammox. In fact, in co- and counter- diffusing systems very similar to these inoculated with ammonia oxidizing archaea instead of comammox, a high concentration of NOB in the anoxic regions of the biofilms was also observed[137]. In those systems, a syntrophy between anaerobic NOB and anammox was proposed in which anammox uses formate dehydrogenase to supply formate to *Nitrospira* for nitrate reduction to nitrite. Produced nitrite was then consumed by anammox for additional nitrite removal. It is likely that a similar phenomenon was observed in these environments.

5.5.5 Theoretical Co-operation of Comammox-Anammox at Varied Loading Conditions

In the co-diffusing granular sludge model nitrogen removal was greatest between 0.375 and 0.40 mg O_2/L when the influent ammonia concentration was held constant at 98 mgN/L (Figure 5-8a) because under these conditions comammox was able to produce the most nitrite for anammox. Above a DO setpoint of 0.45 mgO_2/L oxygen started to diffuse into the biofilm, inhibiting oxygen sensitive anammox in the granule interior (Figure 5-8b). As anammox are required in the system to consume nitrite, an increase in nitrite was observed to abruptly lower

nitrogen removal. The nitrite inhibition tests conducted on *N. europaea* in this study revealed that AOB have a higher tolerance for nitrite than has been reported for comammox (Figure C6, $k_{AOB,i,NO2}$= 89.6 mg N/L & $k_{CMX,i,NO2}$= 4.34 ± 2.67 mgN/L),[137] which led to dominance of AOB while nitrite concentration was elevated. As oxygen concentration increased, canonical NOB activity increased, which led to lowering inhibitory nitrite concentrations. Lower nitrite and ammonia concentrations favored comammox as they have higher affinity for ammonia and AOB, and were not inhibited at the low nitrite concentrations. AOB, NOB and comammox then all work together in a nitrification reactor.

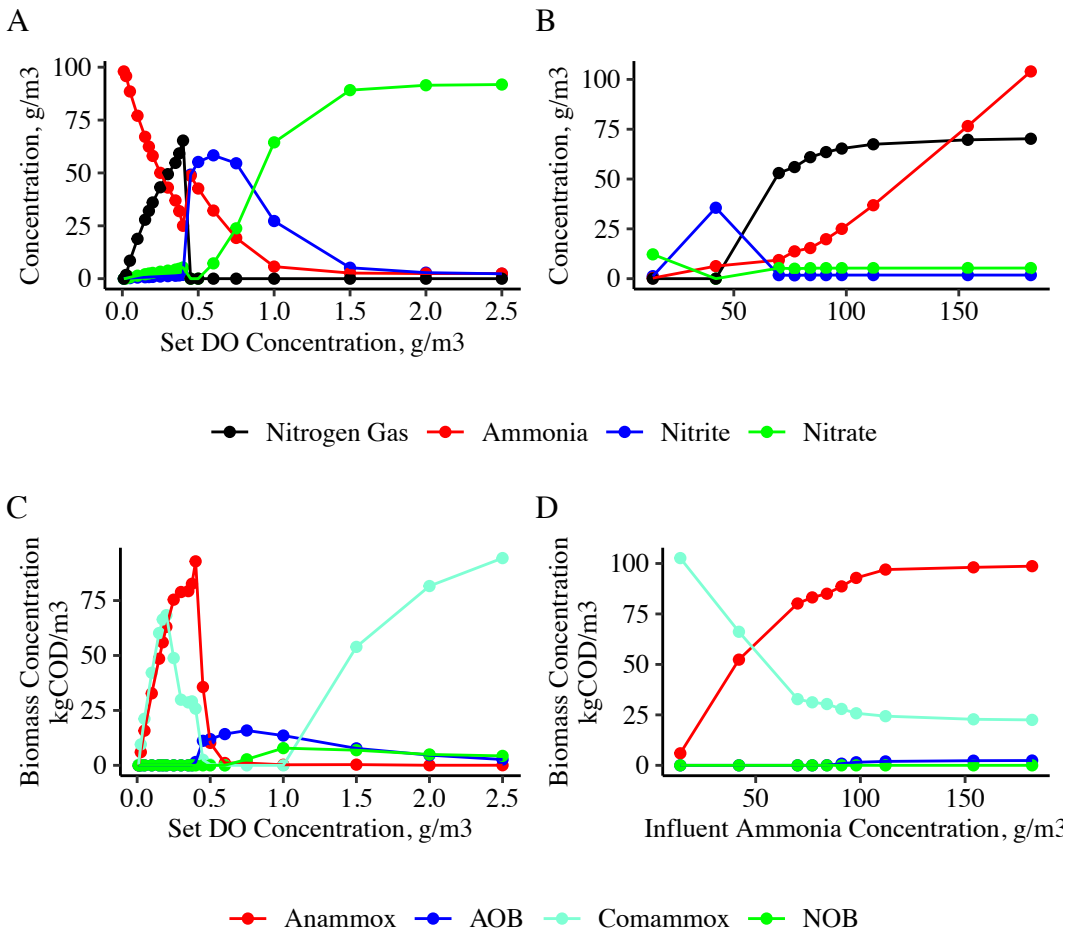

Figure 5-8. Theoretical performance (top) and microbial composition (bottom) of co-diffusing anammox granular sludge inoculated with comammox with changing dissolved oxygen (left) and influent ammonia concentrations (right).

The co-operation between comammox and anammox was consistent at most ammonia concentrations explored in this study at fixed oxygen concentration (0.4 mg/L) in the granular sludge reactor (Figure 5-8b). However, at low influent ammonia concentration (14 mgN/L) all ammonia was oxidized to nitrate and there was no anammox activity. At this low ammonia concentration the fixed oxygen supply provided more oxygen than required for full ammonia removal, and the residual oxygen inhibited anammox activity. When the granular sludge reactor was fed 42 mgN/L and controlled at 0.4 mg/L oxygen, nitrite was observed to accumulate. Although high nitrite and ammonia availability support anammox growth, oxygen concentrations were still at inhibitory levels for anammox and therefore net nitrogen removal remained low. Meanwhile the accumulated nitrite inhibited comammox, which are sensitive to nitrite at high enough concentration ($k_{CMX,i,NO2}$= 4.34 ± 2.67 mgN/L), and nitrite oxidation by comammox was inhibited. Since oxygen concentration was still too low to support canonical NOB, nitrite was left to accumulate. As influent ammonia concentration increased beyond 42 mgN/L, more oxygen was consumed, creating an anaerobic niche in the biofilm for anammox. Eventually, as ammonia concentration increased, maximum nitrogen removal was achieved (Figure 5-8d).

A higher maximum possible nitrogen removal and higher concentrations of comammox were observed in the counter-diffusing MABR model (83%) than in granular sludge, which is in alignment with experimental data (Figure 5-2, left), as well as other theoretical and experimental set-ups that explore AOB-anammox and AOA-anammox co-operation at co- and counter-diffusing conditions.[20,120,161] When influent ammonia concentration was fixed at 98 mgN/L at low oxygen loading, comammox and anammox grew together (Figure 5-9c). Comammox population reached a local maximum concentration at a loading rate of 2.1 g-O_2/m^2/d. As oxygen loading increased beyond that point, DO concentration at the membrane-biofilm interface

increased, and a population of AOB began to emerge, resulting in competition between AOB and comammox and the slight reduction of the comammox population. Nitrogen removal was greatest at the oxygen loading rate of 4.2 g-O_2/m^2/d (Figure 5-9a), where anammox and comammox co-existed with small populations of AOB and NOB, which is in alignment with observations from the bench-scale experiment (Figure 5-3). A small population of NOB was in competition with anammox for a small fraction of the nitrite, which the NOB converted to nitrate. This resulted in a slightly lower fractional nitrogen removal (83%) than is stoichiometrically possible by anammox and comammox alone (89%) and an effluent nitrate concentration of 16.7 mg N/L. As oxygen concentration increased beyond that ideal oxygen loading, AOB and NOB both began to outcompete comammox for ammonia, oxygen, and nitrite. Anammox became increasingly inhibited at these conditions as the aerobic fraction of the biofilm increased towards 100%. At high oxygen loading rates, comammox was observed to almost entirely take over the biofilm, as nearly all ammonia was consumed, resulting in low ammonia concentrations that select for the aerobic ammonia oxidizer with the highest affinity for ammonia being comammox. NOB and comammox both further oxidized the resulting nitrite to nitrate. At the highest loading rates explored in this theoretical study (>10 g-O2/m2/d), the comammox population diminished, as high oxygen concentrations allow NOB to be the dominant nitrite oxidizing organism, though comammox is still abundant and supplies nitrite to the NOB population.

When the influent ammonia concentration was varied, but the oxygen loading rate was fixed at 4.2 g-O_2/m^2/d, co-operation between anammox and comammox was observed at a wide range of concentrations (Figure 5-9d). As with the co-diffusing environment, low ammonia loading (14 mgN/L) resulted in almost 100% conversion of ammonia to nitrate due to the surplus of oxygen

inhibiting anammox (Figure 5-9b). As ammonia concentration increased, more oxygen was consumed, decreasing the aerobic volume fraction of the biofilm and providing a niche for anammox to consume some of the nitrite produced by comammox and some of the ammonia to achieve nitrogen removal.

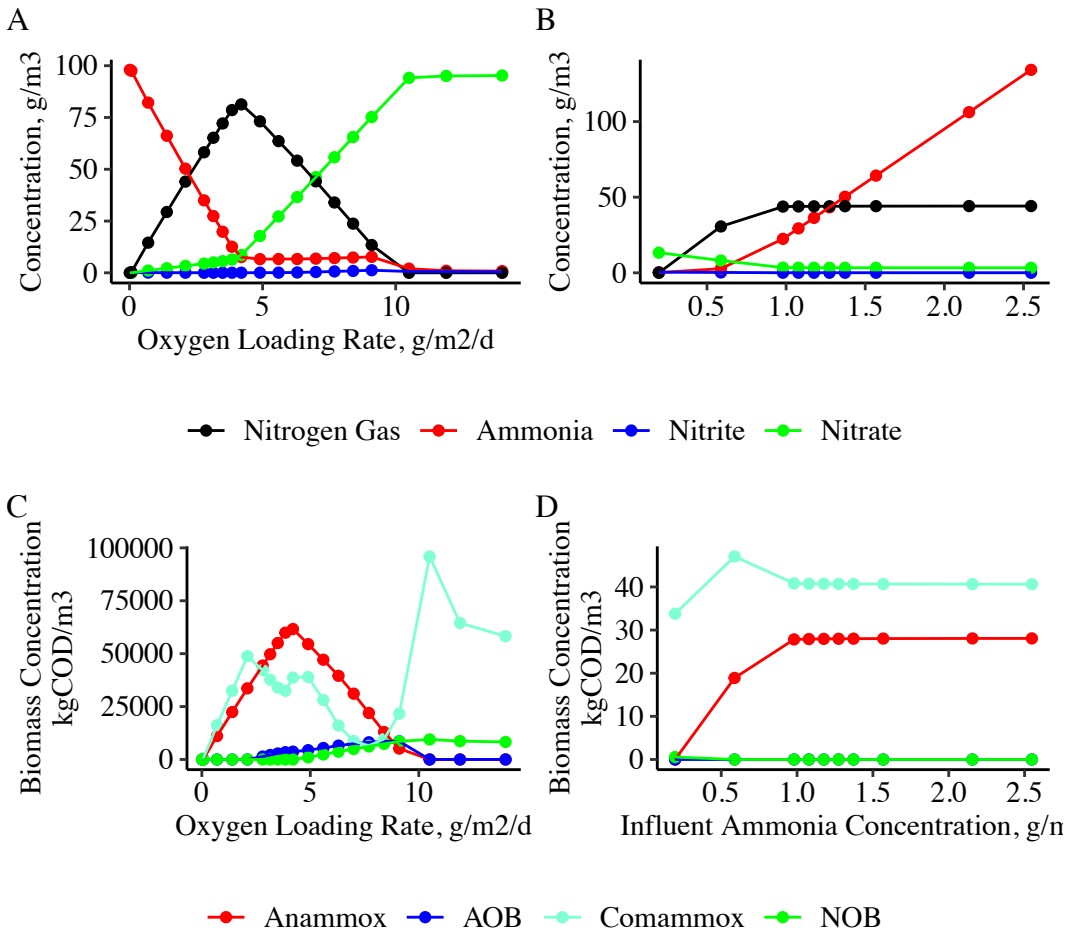

Figure 5-9. Theoretical performance and microbial composition of counter-diffusing anammox MABR inoculated with comammox with changing dissolved oxygen (left) and influent ammonia concentrations (right).

When comparing the co-diffusing and counter-diffusing models, it is clear that the MABR system was less sensitive to changing oxygen concentrations. For example, in order to achieve nitrogen removal >50% the co-diffusing anammox model predicted that DO would have to be controlled between 0.3-0.4 mg/L. Meanwhile, the MABR was able to achieve >50% nitrogen removal at a wide range of oxygen loading rates (2.8-5.6 $g/m^2/d$). This result suggests that not

only is higher nitrogen removal possible in an MABR in comparison to granular sludge, but such a system is easier to control as aeration rate does not have to be regulated in the same narrow range.

5.5.6 Comparison of Theoretical and Experimental Results

Theoretical models of these two reactors largely reflected experimental results, validating the prediction that co-operation between comammox and anammox would exist at a wide range of conditions. There are two notable differences between the theoretical and experimental results presented here. First, the theoretical results predict the presence of nitrite and/or nitrate in the effluent at all conditions leading to a predicted lower average fractional nitrogen removal than was observed in the MABR system. This minor mismatch supports our hypothesis that the nitrate might have been reduced to nitrite by an anaerobic *Nitrospira* population that served then as electron acceptor for anammox activity, thus increasing the fractional nitrogen removal above the model's predictions. This hypothesized metabolism is uncharacterized and the stoichiometries and kinetic constants would need to be determined to include in a theoretical model. In order to improve the accuracies of our models and better leverage this nitrogen cycling microbial populations to improve the efficiency of wastewater treatment, future studies are required to resolve the fate of nitrate in comammox-anammox dominated systems.

5.6 CONCLUSIONS

- Comammox-anammox nitrogen removal was observed to be more efficient in a counter-diffusing membrane aerated biofilm reactor (MABR) (88% nitrogen removal) when compared to a co-diffusing anammox granular sludge reactor (83%).

- Comammox and anammox were found in both the MABR and granular sludge systems, though comammox was more abundant in the MABR.
- Comammox appeared to almost entirely replace AOB as the nitrite-supplying partner to anammox and were able to continue to supply nitrite at lower ammonia concentrations, thus yielding higher overall nitrogen removal in the MABR.
- Theoretical models largely reflected the experimental results observed in this study, with the exception of the presence of nitrate and nitrite in the effluent and the lower predicted removal efficiency of the MABR. These discrepancies can be explained by the activity of a new nitrate-reducing pathway that the models are not yet able to describe
- In both systems, the absence of nitrite and nitrate in the effluents and the presence of *Nitrospira* in anaerobic regions of the biofilm suggests an anaerobic lifestyle for the *Nitrospira* present, in which they consume nitrate and potentially organic carbon leaked by autotrophic anammox.

5.7 SUPPORTING INFORMATION AVAILABLE

Supplemental figures and tables referred to in this chapter are available.in Appendix C.

Chapter 6. EVALUATING IMPACT OF ANAMMOX GRANULAR SLUDGE ON ION SELECTIVE ELECTRODES

6.1 INTRODUCTION

The magnitude of anthropogenic fluxes of reactive nitrogen (N) to the environment is currently roughly equivalent to the natural N fluxes. This development is primarily due to invention of the Haber-Bosch process, the fixation of atmospheric nitrogen gas to ammonium fertilizer, which is currently the source of 50% of nitrogen in human tissues[164,165]. As a consequence, managing the nitrogen cycle has been identified as one of the 14 Grand Engineering Challenges of this century[166]. This is readily apparent in the field of wastewater treatment, where poor nitrogen management can negatively impact aquatic ecosystems[167] and release potent greenhouse gases such as nitrous oxide[87]. Traditional nitrogen removal in wastewater treatment relies on nitrification-denitrification, which requires complete oxidation of ammonium to nitrate prior to denitrification. Oxidation to nitrate drives up oxygen demand which in turn increases the energy requirements.[5].

The application of anaerobic ammonium oxidation (anammox) granular sludge has been shown to roughly halve overall energy demand of a nitrogen removal system while potentially lowering greenhouse gases if compared to conventional nitrification denitrification[11]. Anammox nitrogen removal is most often accomplished in redox stratified spherical biofilms of 1-3mm in diameter.[118] In the aerobic shell, ammonia is partially converted to nitrite by aerobic ammonia oxidizing organisms.[37] Nitrite and ammonia then diffuse to the anoxic core of the granule where anammox bacteria convert it to di-nitrogen gas. Effective anammox nitrogen removal requires

careful management of the aerobic processes to ensure enough nitrite is supplied to anammox. As such, accurate online monitoring of ammonium would be a powerful tool to expand the operational versatility of anammox nitrogen removal.

Methods for online ammonium measurements involving colorimetrics take too long for effective online control (5-10 minutes/sample),[168] and UV-based methods requires costly instrumentation[169]. Ammonium ion selective electrodes (ISE) are a less expensive alternative and are already in use in some wastewater treatment plants[21,170]. Ion selective electrodes utilize ionophores (lipophilic complexing agents) that are doped into the membrane and reversibly and preferentially bind a specific ion in proportion to its concentration in the bulk fluid.[171] Changes bound-ionophores change the voltage potential when measured against a reference electrode, and the resulting calibration slope theoretically follows the Nernst Equation.[172] Unfortunately, ISE sensors do not perform consistently in the complex ionic environment present in wastewaters due to poor selectivity (interference from other molecules of similar size and charge)[173] and membrane damage[21,174]. The challenge of cross-interferences could potentially be met by installing a suite of sensors, sensitive to both the target and interfering ions, for which the signals are then fused using a machine-learning algorithm that includes chemical knowledge of the system[173,175], if challenges related to wastewater chemistry can be overcome.

6.2 PRELIMINARY WORK

Online measurement of ammonium using a suite of sensors was attempted in an operating anammox granular sludge reactor by measuring the concentrations of target ions, interfering ions, and anions in order to calibrate an algorithm for accurate online measurement of ammonium. Ammonium, potassium, and chloride sensors (Table 6-2) were initially calibrated

with a suite of standard solutions (10,000 µM, 1,000 µM, 100 µM, 10 µM, 5 µM KCl solutions and 10,000 µM, 1,000 µM, 100 µM, 10 µM, 5 µM, 1µM NH_4Cl) in which their performance was confirmed to be within manufacturer specification (Table 5-1). Sensors were then placed in the operating reactor (Figure 6-1) and fed ammonium and nitrite rich media (Table D1). Re-calibration was performed after 14 days to enable data corrections for drift and to evaluate sensors after long term exposure in the reactor. The second calibration was performed with a set of multi-analyte standards (Table 6-3). The second calibration revealed significant sensor decay in two of the three sensors (ammonium and potassium sensors). Both of these sensors are constructed with a PVC membrane, while the relatively unaffected chloride sensor utilizes a poly-crystalline membrane. It was therefore hypothesized that the membrane material is a key factor in sensor degradation within anammox granular sludge reactors. However, the mechanism by which active anammox granular sludge causes degradation of PVC-based sensors was unclear.

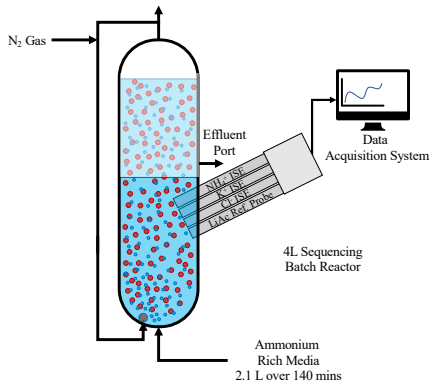

Table 6-1. Calibration slopes (mV/decade) of sensors before and after long-term exposure to active anammox biomass.

Sensor	Day 0	Day 14	Change in Slope
Chloride	-55.4 ± 0.6	-55.3 ± 0.3	0.1 ± 0.6
Ammonium	57.0 ± 0.2	49.3 ± 1.7	7.7 ± 1.7
Potassium	58.7 ± 0.3	53.5±0.4	5.2 ± 0.5

Figure 6-1. Sensors were placed in an anammox granular sludge reactor (left) where they were observed to degrade (right).

Table 6-2. Description of sensors used in Anammox reactor.				
Ion	Brand	Sensor Slope at 25 °C	Detection Limit	Type
NH_4^+	ELIT	54 ± 5 mV/decade	$2x10^{-6}$ M	Solid state, PVC membrane
K^+	ELIT	54 ± 5 mV/decade	$1x10^{-5}$ M	Solid state, PVC membrane
Cl^-	ELIT	-54 ± 5 mV/decade	$3x10^{-5}$ M	Solid state, poly-crystalline membrane

Table 6-3. Concentrations in µM in the multi-salt set of calibrating solution used after 14 days of exposure to active anammox granular sludge.			
Solution	1	2	3
$[NH_4^+]$	10000	1000	100
$[K^+]$	100	10	1
$[Na^+]$	5000	500	50
$[Ca^{2+}]$	10000	1000	100
$[Cl^-]$	23020.82	2302.082	230.2082
$[NO_3^-]$	12000	1200	120

Anammox granular sludge is complex biologically, chemically, and physically. Therefore, the observed sensor behavior prompted a holistic literature review of potential causes of sensor decay. From this review, a list of potential hypotheses explaining sensor decay was developed:

- Biofouling
    - Biofilm growth has been observed to reduce sensor accuracy in nitrogen removal systems [21].
- Anoxic conditions
    - It has been previously observed that low-oxic and anoxic conditions impact sensor performance,[174] though rates of sensor decay due to anoxic conditions have not been reported.
- Anammox granular sludge metabolites and media constituents

    - New metabolisms for the species in granular sludge are still being discovered, and the known metabolites have not been compared to the make-up of detergents that are known to damage sensors. NO in particular is highly reactive species known to be present in anammox granular sludge reactors.[176]
- Structural Membrane Damage
    - Sensor performance has been shown to decay after physical damage (i.e. piercing, cutting) to the membrane[177].

These hypotheses were then evaluated in context of the granular sludge reactor described in this work. After 14 days of operation, no biofilm growth was observed on the sensors in the reactor and they appeared relatively clean and visually similar to out-of-the-box sensors. This is likely because the biomass yield of anammox (0.3 gVSS/gN)[8] is much lower than the yield of denitrifying heterotrophs present in the previously cited biofouled sensor environment (1.5 gVSS/gN)[5,21]. Therefore, biofouling was eliminated as a potential source of sensor degradation. The anammox granular sludge reactor was operated at anoxic conditions in order to provide anammox the anaerobic environment they require for nitrogen removal, and therefore anoxia was identified as a potential risk factor to sensor performance. When a list of potentially inhibiting or damaging compounds to sensor membranes was compared to a list of known compounds present in anammox granular sludge reactors, (Tables D2-D3), no overlap was found. However, highly reactive NO was present in the reactor at low concentrations (~1ppm, Figure D5). The impact of high concentrations of NO on sensors was therefore evaluated over a short time horizon (Figure 6-2c) to attempt to accelerate any impact sustained low concentrations of NO would have on sensors. Finally, granular sludge, which is made up of soft 1-3mm particles that are continuously mixed during reactor operation, were well mixed in the reactor where they could make contact

with and impact the sensor membranes. Continuous abrasion by anammox granular sludge could have created micro scratches on the membrane causing a decrease in sensor performance. Therefore, probes were exposed to biologically inactivated granular sludge over a long-time horizon (Figure 6-2b) and compared to a control without inactive granular sludge (Figure 6-2a).

6.3 MATERIALS AND METHODS

6.3.1 Design of experimental setups

Ammonium, potassium and chloride sensors (Table 6-2) were tested in a control environment aerated with compressed air (Figure 6-2a) and compared to environments that were aerated together with biologically inactivated granular sludge (Figure 6-2b) and aerated with 1000 ppm NO balanced with nitrogen gas (Figure 6-2c).

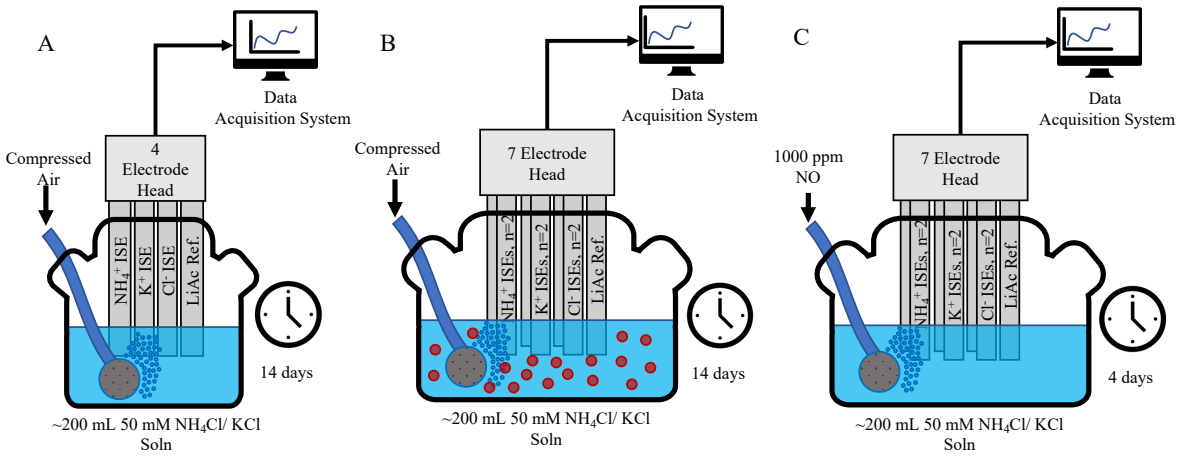

Figure 6-2. Schematics of the experimental conditions in which sensors were tested. (A) a control system aerated with compressed air, (B) a biologically inert granular sludge system mixed with compressed air,and (C) a system without granular sludge sparged with 1000 ppm nitric oxide

All three systems were conducted in bottles which conveniently fit the 4-6 8mm diameter sensors immersed in 2-4 cm of 50 mM NH_4Cl and 50 mM KCl, a controlled ionic strength solution to avoid sensor damage related to low ionic strength. The control (Figure 6-2a) included one of

each sensor to validate experimental results and confirm that under aerobic conditions without granular sludge, aeration alone would not cause sensor decay. The abiotic granular system (Figure 6-2b) and the NO exposed system included two of each sensor to measure variation in sensor decay (Figure 6-2c).

6.3.2 Abiotic granular sludge experiment

Granular sludge was biologically inactivated for several hours at pH=1. The selection of this biological inactivation method is described in the Appendix D. Biologically inactivated granular sludge was added to the previously described controlled ionic strength solution in a1:8 and aerated at a rate of ~1L/min/L working volume to match the conditions of the active granular sludge reactor. The system was then aerated with compressed air at 200 ml/min to match the ~1 L/min/1 L aeration rate in the operating granular sludge reactor. Sensors were calibrated with the 11 single-salt solutions noted above prior to the experiment, and after 41, 118, 144, 200, 260, 327, and 336 hours in order to track changes in sensor performance over time. Single salt solutions were used as opposed to the complex multi-salt solutions described in Table 6-3 as the complex solutions were designed to simultaneously calibrate and evaluate effect of interfering ions on sensor accuracy.

6.3.3 Nitric oxide experiment

The nitric oxide system (Figure 6-2c) was aerated with 1000 ppm nitric oxide mixed with N_2 gas for 20 ml/min for ~4 days in a fume hood to avoid local NO accumulation. The concentration of NO was set at 1000 times higher than the NO concentration in the operating reactor to accelerate any NO-driven degradation. A flowrate of 20 ml/min was chosen to maximize sensor exposure time to concentrated NO with a limited quantity of gas. Sensors remained in the environment

continuously during the experiment and were calibrated before and after the experiment with the 11 solutions noted previously.

6.3.4 Calibration of Sensors

ELIT TRA-IS1-B transmitters were used to isolate (high input impedance 1x amplifier) sensor signals, with output voltages recorded on a PC hard drive using a National Instruments USB-6218 Dataq board controlled with LabVIEW VI. 10 consecutive samples were taken for a single channel and then averaged. The resulting averaged value was logged and then the next channel was sampled. This resulted in a data point logging every six seconds (10 samples taken in each of the 9 channels at a sampling rate of 15 Hz). During calibration, a new data collection file was initialized on starting the data collection software. Prior to calibration, sensors were removed from and ammonium and chloride sensors were placed in 10 mM NH_4Cl and potassium sensors in 10 mM KCl for a 10 minute pre-conditioning period (following manufacturer guidelines). sensors were submerged in 1 cm of calibration solution for 15 minutes. Calibration proceeded from lowest concentration to highest with a milliQ dispensed via Millipore Advantage A10 (MillporeSigma Burlington, MA, USA) rinse and blot-dry with a Kimwipe™ between each calibration. After calibrations with all solutions in a single set was complete, data collection was stopped. The equilibrium of each sensor in a given calibration solution was determined using previously described methods[178] assuming an equilibrium threshold of 2 mV/min. The resulting calibration curve fit using the linear fit method available within the R stats package and the associated standard error was reported (Tables D3-D6). After calibration, the continuous signal data acquisition program was restarted using the previously mentioned LabVIEW software.

6.3.5 Data Analysis Methods

In the nitric oxide experiment, the calibrated slopes of the control and NO exposed sensors before and after the experiment were compared as there were only two calibrations performed per sensor. In the biologically inert system, the degree of sensor degradation was tracked over time (t) by calculating the change in slope (m), defined as:

$$\Delta m = m_{t=0} - m_t \qquad \text{Eqn 6-1}$$

6.4 RESULTS & DISCUSSION

6.4.1 Impact of Nitric Oxide on Sensors

After four days exposure to nitric oxide, very little change in performance was observed in the ammonium or potassium sensors when comparing the calibrated slope of the control sensors and the NO-exposed sensors. The (absolute) slope of the chloride sensors slightly increased after four days for both the NO-exposed chloride sensors and the control. This increase was not caused by the presence of NO gas because the increase in slope was observed for both the control and NO-exposed sensors.

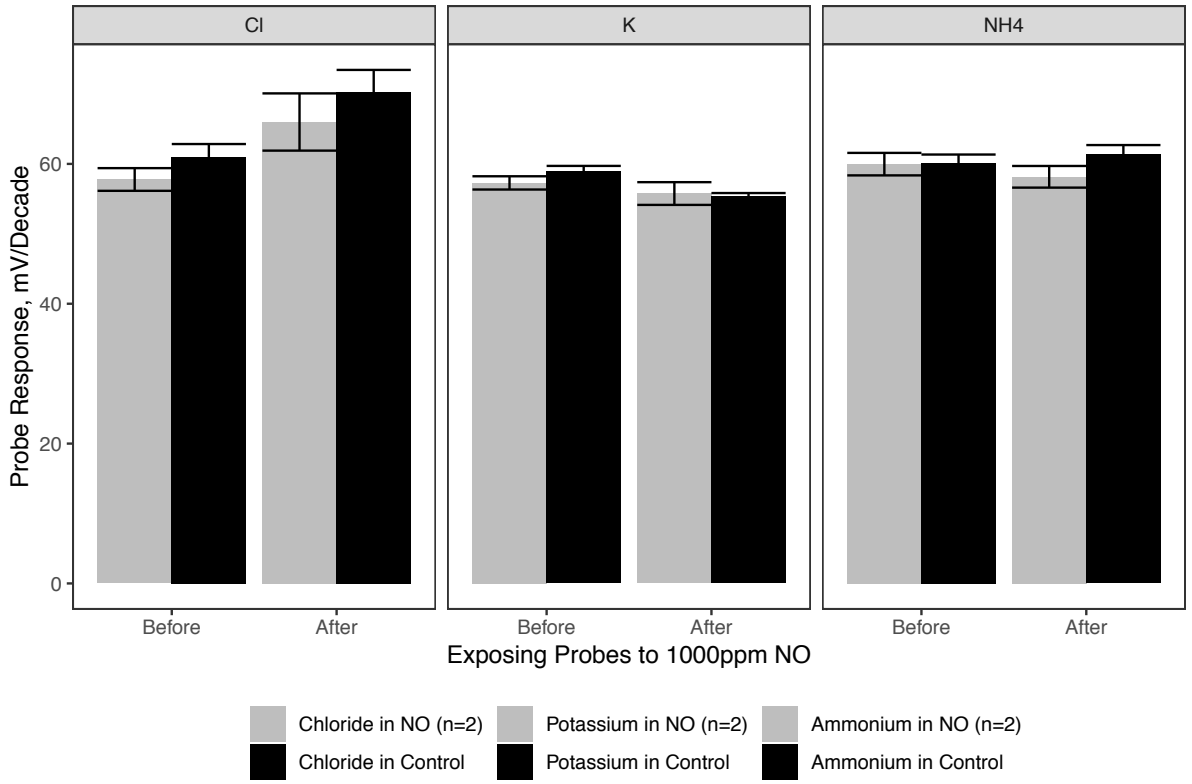

Figure 6-3. After approximately four days of exposure to 1000 ppm nitric oxide, little sensor decay was observed in the chloride (left), potassium (middle), or ammonium (right) sensors.

6.4.2 Physical Abrasion with Inactive Granular Sludge

The change in slope of the chloride, potassium, and ammonium sensors is shown in Figure 6-4. The poly-cystralline-based chloride sensor (Figure 6-4, left) was the least affected by the different environments as compared to the PVC-based ammonium and potassium sensors. The slope varied slightly throughout the duration of the experiment, but did not significantly change over the course of the experiment, as was observed in the active granular sludge reactor. This suggested that poly-crystalline based sensors are more resilient to physical abrasion than PVC sensors. Unfortunately, poly-crystalline membranes are limited in their application to halogenides, S_2^-, CN^-, SCN^-, and metals that can form low-solubility sulfides.[179]

The potassium sensors (Figure 6-4, middle) were affected by granular sludge. While in the control environment, the potassium sensor did not significantly decay. In the abiotic granular sludge systems, the potassium sensor significantly decayed (Replicate 1 = 0.33 ± 0.17 & Replicate 2 = 0.35 ± 0.15 mV/decade/day). In the active granular sludge system, sensor decay occurred at a very similar rate (0.256 ± 0.04 mV/decade/day). This suggested that potassium sensors are damaged by anammox granular sludge due to physical abrasion of the biofilm particles on the membrane surface.

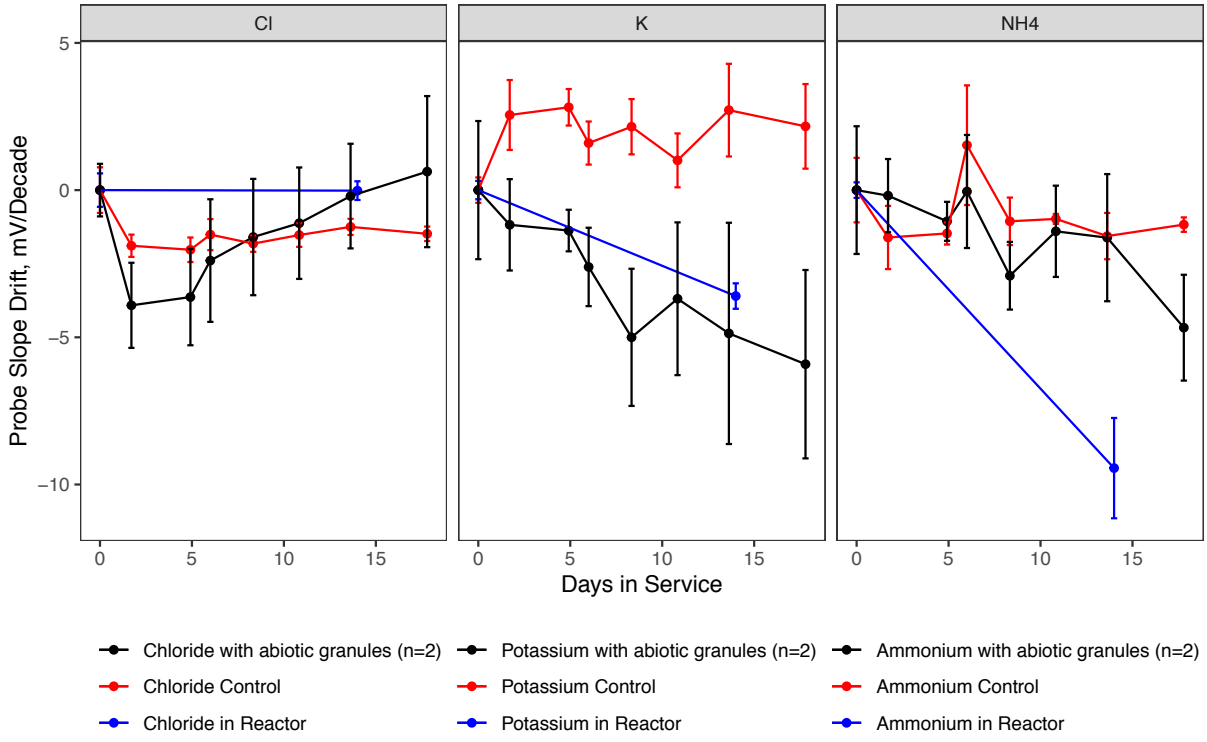

Figure 6-4. Sensor drift over time for ammonium, potassium, and chloride sensors in the abiotic granular system, operating reactor, and control.

Ammonium sensors(Figure 6-4, right) were more affected by active granular sludge than biologically inactivated granular sludge and in the control, no significant sensor decay was observed. In the inactivated granular sludge environment, significant decay of the ammonium sensors was not observed until the final calibration of the abiotic granules after 17 days of

operation (-0.32 mV/decade/day). Meanwhile, the ammonium sensor in the operating reactor was observed to decay much faster than either the control or the sensors in the abiotic granular system or even the potassium sensors (-0.67 mV/decade/day). This suggests that ammonium sensor decay was not primarily caused by physical abrasion. Short-term/high-concentration NO exposure did not cause any sensor decay. However, the sensors in the active granular sludge environment were exposed to low concentrations of NO for long periods of time. In this experimental design, it was assumed that by increasing the concentration of NO gas. If that assumption is not true, then it is possible that after a longer exposure time to NO, sensor decay would have been observed. Therefore, further work should focus on elucidating the long-term effects of NO and anaerobic or near-anaerobic conditions on ammonium sensors to better understand the potential impact these factors could have on sensor performance. Despite Nitric oxide had little to no effect on the sensors at the short time horizons explored here. Future work should explore probe degradation under longer exposure time to nitric oxide.

6.5 SUPPORTING INFORMATION AVAILABLE

Supplemental methods, figures, and tables referred to in this chapter are available.in Appendix D.

Chapter 7. CONCLUSIONS AND FUTURE OUTLOOK

This work endeavors to lower the financial and environmental burden of nitrogen removal in wastewater treatment through the implementation of anammox nitrogen removal at the low ammonium concentrations present in the mainstream. A detailed literature review is included (**chapter 2**) that gives the benefits and challenges associated with anammox nitrogen removal and motivates the need to pair anammox with a different nitrite-producing metabolism such as nitrate-dependent anaerobic methane oxidizing archaea (n-damo), ammonia oxidizing archaea (AOA), or complete ammonia oxidizing bacteria (comammox). A techno-economic feasibility analysis demonstrated that the implementation of a partial-nitritation/anammox system for nitrogen removal and an AnMBR system for organic carbon removal would theoretically reduce operational cost and greenhouse gas (GHG) emission drastically when compared to traditional treatment methods (**chapter 3**). The addition of n-damo to the combined nitrogen-carbon removal scheme yielded a very similar prediction both in savings and GHG reduction, while providing more operational flexibility. With the addition of n-damo it would no longer be necessary to stop nitrification at nitrite, which has been a bottleneck in implementing anammox at mainstream conditions. Many full-scale AnMBR, anammox, and nitrification reactors exist in full-scale wastewater treatment and anammox/n-damo reactors at bench scale have been shown to accomplish high-rate nitrogen removal.[13,43,180] However, these bench-scale anammox/n-damo setups must be scaled up. Given the potential economic and environmental benefit predicted by the model, future work should focus on implementing n-damo/anammox in pilot and full-scale wastewater treatment plants. The techno-economic feasibility study could be used to guide operations of a pilot plant and likewise be validated by measuring the energy demand and

greenhouse gas production of the plant. If it is found that pilot-scale results match the techno-economic model results, it would greatly motivate interest and investment in the design and operation of a full-scale wastewater treatment plant that efficiently removes nitrogen with nitrification/anammox/n-damo and carbon with an AnMBR system. Prior to implementation in a full or pilot scale system, it may prove valuable to investigate the impact of the microbial mediated production of hydrogen sulfide in anaerobic digestors that might inhibit microbes[181]. The sensitivity of microbes to sulfide varies from organism to organism and the concentration of sulfide exiting an anaerobic digester varies from plant to plant. While anammox sensitivity to sulfide has been shown,[182] n-damo sensitivity to sulfide has not been explored. If these preliminary toxification tests show sulfide would inhibit nitrogen removal, an scrubber on the digester gas line would be necessary to avoid hydrogen sulfide toxification.

This work also demonstrated the potential of two newly discovered ammonia oxidizing organisms to supply nitrite for anammox in nitrogen removal. Anammox with ammonia oxidizing archaea (AOA), and complete ammonium oxidizing bacteria (comammox). Pairing anammox with AOA was shown to replicate findings within marine oxygen minimum zones (OMZs), where anammox and AOA are known to co-operate to remove up to 50% of the nitrogen that is emitted from the ocean and ammonia and oxygen counter-diffuse in opposite directions (**chapter 4**). Furthermore, a population of comammox was found to emerge after long term nitrogen removal was observed. These results suggested that comammox and anammox can also co-operate together.

The potential of comammox and anammox was further explored in both theoretical models and experimental set-ups, and it was shown that in both co- and counter-diffusing reactors, comammox-anammox nitrogen removal was possible (Chapter 5), with higher nitrogen removal

and comammox abundances found in the MABR system. These results confirmed the hypothesis that the low affinities for ammonia that AOA and comammox possess make counter-diffusion favorable for AOA- or comammox-anammox nitrogen removal. This is because in a counter-diffusion environment, ammonia and oxygen diffuse in opposite directions, which means that in the aerobic fraction of the biofilm, ammonia concentrations are at their lowest. In that oxygen-rich ammonia poor region of the biofilm, the organisms with the highest affinity (AOA and comammox) were observed to survive. This is an exciting achievement because it suggests that anammox nitrogen removal is possible at the low ammonia concentrations similar to the conditions encountered in the mainstream. Future work should strive to continue to bring AOA-comammox-anammox nitrogen removal to mainstream conditions. These experiments were conducted at temperatures much warmer (30 °C – 35 °C) than typical wastewater (< 10 °C), as the higher temperatures are ideal for these organisms[17,27,57]. While AOA and anammox activity has been observed in arctic soils and sediments,[183,184] co-operation of these three species at low temperatures has not yet been observed in nature. Before scale-up of AOA-comammox-anammox is possible, the limiting effect that low temperatures have on the growth and activity of anammox, comammox, and AOA must be addressed.

In all four of the comammox and AOA inoculated anammox reactors studied in this work, anammox nitrogen removal was achieved without the accumulation of nitrite or nitrate in the effluent. This was an unexpected result as anammox produces some nitrate in its anabolic pathway during nitrogen removal and the comammox-anammox theoretical model predicted the accumulation of some nitrate in the effluent at all conditions. Another surprising and potentially related result was the high abundance of *Nitrospira* in the 16S rRNA gene sequencing that was unlikely to be entirely made up of *Nitrospira* comammox given the low abundances of

comammox detected by qPCR in some samples. Furthermore, FISH microscopy revealed the presence of NOB in anaerobic portions of the biofilm. It was then hypothesized that the *Nitrospira* in the system could be reducing nitrate produced by anammox. *Nitrospira* have been shown to use formate as an electron donor to reduce nitrate to nitrite.[18] Anammox could supply *Nitrospira* with nitrate from its anabolic pathway and formate from the reverse acetyl-coA pathway. The anammox species in these experiments have the genomic potential to produce and transport formate[144], and this work also showed that *Nitrospira inopinata* comammox was able to reduce nitrate to nitrite in the presence of formate. Furthermore, theoretical calculations suggested the rate of endogenous decay could not have supported denitrification of the nitrate produced by anammox in these systems (Tables B3-B5). Though it may be possible that the *Nitrospira* found in the anaerobic portion of the biofilms could have been inactive or dead as biofilm models have shown that inactive species can remain in a biofilm over 600 days after they have ceased activity.[163] If this is the case, an alternate explanation for the absence of nitrate is required. Future work should elucidate the mechanisms, kinetics, and stoichiometries used by anammox to supply organic carbon to other nitrogen cycling species in anammox biofilms, potentially with co-cultures of anammox and *Nitrospira* together in short-term batch experiments.

This work consistently observed that low ammonia concentration selected for co-operation between AOA or comammox and anammox. Therefore, online-control and measurement of ammonium is a very attractive technology even though it has been a long-standing challenge in the field of wastewater treatment. Accurate online measurement of ammonium with ion selective electrodes was attempted but failed in an anammox granular sludge reactor because the performance of polyvinyl chloride (PVC)-based ammonium and potassium probes were found to

decay relativly quickly. Therefore, this work began to demystify some of the causes behind the observed decay by comparing the decay rate of probes kept in a control solution, a compartment with inert granular sludge that had been biologically deactivated, and an anaerobic compartment with high concentrations of nitric oxide gas. Chloride probes, which have a poly-crystalline membrane, were not observed to decay in any of these environments while the two PVC probes tested, ammonium and potassium, were shown to decay in the presence of inactive granules after 14 days. When comparing the rate of decay of electrodes in inert and active granular sludge, the potassium electrode was found to decay at about the same rate in either environment, while the ammonium probe decayed much faster in the operating granular system than the inert granular system. Meanwhile, the probes that were exposed to anaerobic high nitric oxide did not appear to decay at all, though this experiment was only done for a short while (4 days). These results suggested three things: (1) Poly-crystalline membranes are much less sensitive to physical abrasion by granular biofilms, (2) PVC-based potassium probes are subject to damage when placed in granular sludge systems, and (3) PVC-based ammonium ISE probes are not as sensitive to physical abrasion damage as potassium probes. Granular sludge reactors are complex physical-chemical-biological systems. In this work, the physical aspect of a granular sludge reactor was isolated, and the decay of the ammonium probe appeared to be slower when granular sludge was inactive. That suggests that the cause of ammonium electrode decay is chemical in nature. Future work should explore the long-term chemical effects of anammox granular sludge on ammonium probes. This would be accomplished most efficiently by staying grounded in the ever-growing body of knowledge regarding anammox granular sludge metabolic potential. This could be accomplished by isolating various chemical and biological aspects of the operating granular sludge and testing the long-term performance of the ammonium probe. Furthermore,

while short-term anaerobic conditions are known to temporarily affect the probe signal, the impact of long-term anaerobic conditions on probe health is not well understood. Probes could be kept under anaerobic conditions or high nitric oxide conditions for a long period and the impact of probe performance could be evaluated. Additional work could also focus on better understanding the chemistry of the ionophores used in ion selective electrodes and the impact of anammox, granular sludge, and anaerobic conditions on these ionophores, potentially with the help of scanning electron microscopy.

REFERENCES

(1) Dodds, W. K.; Bouska, W. W.; Eitzmann, J. L.; Pilger, T. J.; Pitts, K. L.; Riley, A. J.; Schloesser, J. T.; Thornbrugh, D. J. Eutrophication of U.S. Freshwaters: Analysis of Potential Economic Damages. *Environ. Sci. Technol.* **2009**, *43* (1), 12–19.

(2) Edmonson, W. T.; Anderson, G. C.; Peterson, D. R. Artificial Eutrophication of Lake Washington1. *Limnol. Oceanogr.* **1956**, *1* (1), 47–53. https://doi.org/10.4319/lo.1956.1.1.0047.

(3) US EPA. *Inventory of U.S. Greenhouse Gas Emissions and Sinks: 1990-2013*; 2015.

(4) Pabi, S.; Reekie, L.; Amarnath, A.; Goldstein, R.; Reekie, L. *Electricity Use and Management in the Municipal Water Supply and Wastewater Industries*; 2013.

(5) Tchobanoglous, G.; Burton, F. L.; Stensel, H. D. *Wastewater Engineering: Treatment and Resource Recovery*, 4th ed.; McGraw Hill: New York, New York, 2014.

(6) US EPA. *Biosolids Technology Fact Sheet Use of Landfilling for Biosolids Management*; 2003.

(7) Giesen, A.; van Loosdrecht, M.; Pronk, M.; Robertson, S.; Thompson, A. Aerobic Granular Biomass Technology: Recent Performance Data, Lessons Learnt and Retrofitting Conventional Treatment Infrastructure. In *WEFTEC 2016 - 89th Water Environment Federation Annual Technical Exhibition and Conference*; Water Environment Federation, 2016; Vol. 3, pp 1913–1923. https://doi.org/10.2175/193864716819707139.

(8) Strous, M.; Kuenen, J. G.; Jetten, M. S. Key Physiology of Anaerobic Ammonium

Oxidation. *Appl. Environ. Microbiol.* **1999**, *65* (7), 3248–3250.

(9) Siegrist, H.; salzgeber Eugster, D. J.; Joss, A. Anammox Brings WWTP Closer to Energy Autarky Due to Increased Biogas Production and Reduced Aeration Energy for N·removal. *J. Title Water Sci. Technol. a J. Int. Assoc. Water Pollut. Res.* **2008**, *57* (3), 383–388.

(10) Strous, M.; Heijnen, J. J.; Kuenen, J. G.; Jetten, M. S. M. The Sequencing Batch Reactor as a Powerful Tool for the Study of Slowly Growing Anaerobic Ammonium-Oxidizing Microorganisms. *Appl. Microbiol. Biotechnol.* **1998**, *50* (5), 589–596. https://doi.org/10.1007/s002530051340.

(11) Cogert, K. I.; Ziels, R. M.; Winkler, M. K. H. Reducing Cost and Environmental Impact of Wastewater Treatment with Denitrifying Methanotrophs, Anammox, and Mainstream Anaerobic Treatment. *Environ. Sci. Technol.* **2019**. https://doi.org/10.1021/acs.est.9b04764.

(12) van der Star, W. R. L.; Abma, W. R.; Blommers, D.; Mulder, J.-W.; Tokutomi, T.; Strous, M.; Picioreanu, C.; van Loosdrecht, M. C. M. Startup of Reactors for Anoxic Ammonium Oxidation: Experiences from the First Full-Scale Anammox Reactor in Rotterdam. *Water Res.* **2007**, *41* (18), 4149–4163.

(13) Winkler, M. K.; Straka, L. New Directions in Biological Nitrogen Removal and Recovery from Wastewater. *Curr. Opin. Biotechnol.* **2019**, *57*, 50–55. https://doi.org/10.1016/J.COPBIO.2018.12.007.

(14) Hellinga, C.; Loosdrecht, M. C. M. Van; Heijnen, J. J.; Van Loosdrecht, M. C. M.;

Heijnen, J. J. Model Based Design of a Novel Process for Nitrogen Removal from Concentrated Flows. *Math. Comput. Model. Dyn. Syst.* **1999**, *5* (4), 351–371.

(15) Wett, B.; Podmirseg, S. M.; Gómez-Brandón, M.; Hell, M.; Nyhuis, G.; Bott, C.; Murthy, S. Expanding DEMON Sidestream Deammonification Technology Towards Mainstream Application. *Water Environ. Res.* **2015**, *87* (12), 2084–2089. https://doi.org/10.2175/106143015X14362865227319.

(16) Daims, H.; Lebedeva, E. V; Pjevac, P.; Han, P.; Herbold, C.; Albertsen, M.; Jehmlich, N.; Palatinszky, M.; Vierheilig, J.; Bulaev, A.; et al. Complete Nitrification by Nitrospira Bacteria. *Nature* **2015**, *528* (7583), 504–509. https://doi.org/10.1038/nature16461.

(17) Kits, K. D.; Sedlacek, C. J.; Lebedeva, E. V.; Han, P.; Bulaev, A.; Pjevac, P.; Daebeler, A.; Romano, S.; Albertsen, M.; Stein, L. Y.; et al. Kinetic Analysis of a Complete Nitrifier Reveals an Oligotrophic Lifestyle. *Nature* **2017**, *549* (7671), 269–272. https://doi.org/10.1038/nature23679.

(18) Koch, H.; Lücker, S.; Albertsen, M.; Kitzinger, K.; Herbold, C.; Spieck, E.; Nielsen, P. H.; Wagner, M.; Daims, H. Expanded Metabolic Versatility of Ubiquitous Nitrite-Oxidizing Bacteria from the Genus Nitrospira. *Proc. Natl. Acad. Sci. U. S. A.* **2015**, *112* (36), 11371–11376. https://doi.org/10.1073/pnas.1506533112.

(19) Russ, L.; Harhangi, H. R.; Schellekens, J.; Verdellen, B.; Kartal, B.; Op Den Camp, H. J. M.; Jetten, M. S. M. Genome Analysis and Heterologous Expression of Acetate-Activating Enzymes in the Anammox Bacterium Kuenenia Stuttgartiensis. *Arch. Microbiol.* **2012**, *194* (11), 943–948. https://doi.org/10.1007/s00203-012-0829-7.

(20) Straka, L. L.; Meinhardt, K. A.; Bollmann, A.; Stahl, D. A.; Winkler, M.-K. H. Affinity Informs Environmental Cooperation between Ammonia-Oxidizing Archaea (AOA) and Anaerobic Ammonia-Oxidizing (Anammox) Bacteria. *ISME J.* **2019**, *13* (8), 1997–2004. https://doi.org/10.1038/s41396-019-0408-x.

(21) Cecconi, F.; Reifsnyder, S.; Ito, Y.; Jimenez, M.; Sobhani, R.; Rosso, D. ISE-Ammonium Sensors in WRRFs: Field Assessment of Their Influencing Factors. *Environ. Sci. Water Res. Technol.* **2019**, *5* (4), 737–746. https://doi.org/10.1039/c8ew00763b.

(22) Broda, E. Two Kinds of Lithotrophs Missing in Nature. *Z. Allg. Mikrobiol.* **2007**, *17* (6), 491–493. https://doi.org/10.1002/jobm.19770170611.

(23) Van der Star, W. R. L. Growth and Metabolism of Anammox Bacteria, TUDelft, 2008.

(24) Mulder, A.; Graaf, A. A.; Robertson, L. A.; Kuenen, J. G. Anaerobic Ammonium Oxidation Discovered in a Denitrifying Fluidized Bed Reactor. *FEMS Microbiol. Ecol.* **1995**, *16* (3), 177–184. https://doi.org/10.1111/j.1574-6941.1995.tb00281.x.

(25) Kuypers, M. M. M.; Silekers, A. O.; Lavik, G.; Schmid, M.; Jøorgensen, B. B.; Kuenen, J. G.; Sinninghe Damsté, J. S.; Strous, M.; Jetten, M. S. M. Anaerobic Ammonium Oxidation by Anammox Bacteria in the Black Sea. *Nature* **2003**, *422* (6932), 608–611. https://doi.org/10.1038/nature01472.

(26) Kuypers, M. M. M.; Lavik, G.; Woebken, D.; Schmid, M.; Fuchs, B. M.; Amann, R.; Jørgensen, B. B.; Jetten, M. S. M. Massive Nitrogen Loss from the Benguela Upwelling System through Anaerobic Ammonium Oxidation. *Proc. Natl. Acad. Sci. U. S. A.* **2005**, *102* (18), 6478–6483. https://doi.org/10.1073/pnas.0502088102.

(27) Lotti, T.; Kleerebezem, R.; Hu, Z.; Kartal, B.; Jetten, M. S. M.; van Loosdrecht, M. C. M. Simultaneous Partial Nitritation and Anammox at Low Temperature with Granular Sludge. *Water Res.* **2014**, *66*, 111–121. https://doi.org/10.1016/j.watres.2014.07.047.

(28) Dalsgaard, T.; Canfield, D. E.; Petersen, J.; Thamdrup, B.; Acuña-González, J. N2 Production by the Anammox Reaction in the Anoxic Water Column of Golfo Dulce, Costa Rica. *Nature* **2003**, *422* (6932), 606–608. https://doi.org/10.1038/nature01526.

(29) Kartal, B.; Geerts, W.; Jetten, M. S. M. Cultivation, Detection, and Ecophysiology of Anaerobic Ammonium-Oxidizing Bacteria. In *Methods in Enzymology*; Academic Press Inc., 2011; Vol. 486, pp 89–108. https://doi.org/10.1016/B978-0-12-381294-0.00004-3.

(30) Lam, P.; Jensen, M. M.; Lavik, G.; McGinnis, D. F.; Muller, B.; Schubert, C. J.; Amann, R.; Thamdrup, B.; Kuypers, M. M. M. Linking Crenarchaeal and Bacterial Nitrification to Anammox in the Black Sea. *Proc. Natl. Acad. Sci.* **2007**, *104* (17), 7104–7109. https://doi.org/10.1073/pnas.0611081104.

(31) Füssel, J.; Lam, P.; Lavik, G.; Jensen, M. M.; Holtappels, M.; Günter, M.; Kuypers, M. M. M. Nitrite Oxidation in the Namibian Oxygen Minimum Zone. *ISME J.* **2012**, *6* (6), 1200–1209. https://doi.org/10.1038/ismej.2011.178.

(32) Egli, K.; Bosshard, F.; Werlen, C.; Lais, P.; Siegrist, H.; Zehnder, A. J. B.; Van Der Meer, J. R. Microbial Composition and Structure of a Rotating Biological Contactor Biofilm Treating Ammonium-Rich Wastewater without Organic Carbon. *Microb. Ecol.* **2003**, *45* (4), 419–432. https://doi.org/10.1007/s00248-002-2037-5.

(33) Rysgaard, S.; Glud, R. N.; Risgaard-Petersen, N.; Dalsgaard, T. Denitrification and

Anammox Activity in Arctic Marine Sediments. *Limnol. Oceanogr.* **2004**, *49* (5), 1493–1502. https://doi.org/10.4319/lo.2004.49.5.1493.

(34) Oshiki, M.; Shimokawa, M.; Fujii, N.; Satoh, H.; Okabe, S. Physiological Characteristics of the Anaerobic Ammonium-Oxidizing Bacterium "Candidatus Brocadia Sinica." *Microbiology* **2011**, *157* (6), 1706–1713. https://doi.org/10.1099/mic.0.048595-0.

(35) Raudkivi, M.; Zekker, I.; Rikmann, E.; Vabamäe, P.; Kroon, K.; Tenno, T. Nitrite Inhibition and Limitation - The Effect of Nitrite Spiking on Anammox Biofilm, Suspended and Granular Biomass. *Water Sci. Technol.* **2017**, *75* (2), 313–321. https://doi.org/10.2166/wst.2016.456.

(36) Strous, M.; Pelletier, E.; Mangenot, S.; Rattei, T.; Lehner, A.; Taylor, M. W.; Horn, M.; Daims, H.; Bartol-Mavel, D.; Wincker, P.; et al. Deciphering the Evolution and Metabolism of an Anammox Bacterium from a Community Genome. *Nature* **2006**, *440* (7085), 790–794. https://doi.org/10.1038/nature04647.

(37) Winkler, M. K. H.; Kleerebezem, R.; Van Loosdrecht, M. C. M. Integration of Anammox into the Aerobic Granular Sludge Process for Main Stream Wastewater Treatment at Ambient Temperatures. *Water Res.* **2012**, *46* (1), 136–144. https://doi.org/10.1016/j.watres.2011.10.034.

(38) IPCC. *Climate Change 2013: The Physical Science Basis - The Physical Science Basis*; 2013.

(39) Massara, T. M.; Malamis, S.; Guisasola, A.; Baeza, J. A.; Noutsopoulos, C.; Katsou, E. A Review on Nitrous Oxide (N2O) Emissions during Biological Nutrient Removal from

Municipal Wastewater and Sludge Reject Water. *Sci. Total Environ.* **2017**, *596–597*, 106–123. https://doi.org/10.1016/J.SCITOTENV.2017.03.191.

(40) Wiesmann, U. Biological Nitrogen Removal from Wastewater. *Advances in biochemical engineering/biotechnology*. 1994, pp 113–154. https://doi.org/10.1007/bfb0008736.

(41) Haroon, M. F.; Hu, S.; Shi, Y.; Imelfort, M.; Keller, J.; Hugenholtz, P.; Yuan, Z.; Tyson, G. W. Anaerobic Oxidation of Methane Coupled to Nitrate Reduction in a Novel Archaeal Lineage. *Nature* **2013**, *500* (7464), 567–570. https://doi.org/10.1038/nature12375.

(42) Luesken, F. A.; Sánchez, J.; van Alen, T. A.; Sanabria, J.; Op den Camp, H. J. M.; Jetten, M. S. M.; Kartal, B. Simultaneous Nitrite-Dependent Anaerobic Methane and Ammonium Oxidation Processes. *Appl. Environ. Microbiol.* **2011**, *77* (19), 6802–6807. https://doi.org/10.1128/AEM.05539-11.

(43) Shi, Y.; Hu, S.; Lou, J.; Lu, P.; Keller, J.; Yuan, Z. Nitrogen Removal from Wastewater by Coupling Anammox and Methane-Dependent Denitrification in a Membrane Biofilm Reactor. *Environ. Sci. Technol.* **2013**, *47* (20), 11577–11583. https://doi.org/10.1021/es402775z.

(44) Xie, G.-J.; Cai, C.; Hu, S.; Yuan, Z. Complete Nitrogen Removal from Synthetic Anaerobic Sludge Digestion Liquor through Integrating Anammox and Denitrifying Anaerobic Methane Oxidation in a Membrane Biofilm Reactor. *Environ. Sci. Technol.* **2017**, *51* (2), 819–827. https://doi.org/10.1021/acs.est.6b04500.

(45) Hu, S.; Zeng, R. J.; Haroon, M. F.; Keller, J.; Lant, P. A.; Tyson, G. W.; Yuan, Z. A Laboratory Investigation of Interactions between Denitrifying Anaerobic Methane

Oxidation (DAMO) and Anammox Processes in Anoxic Environments. *Sci. Rep.* **2015**, *5*, 8706. https://doi.org/10.1038/srep08706.

(46) Winkler, M.-K. . H.; Ettwig, K. F. F.; Vannecke, T. P. W. P. W.; Stultiens, K.; Bogdan, A.; Kartal, B.; Volcke, E. I. P. I. P. Modelling Simultaneous Anaerobic Methane and Ammonium Removal in a Granular Sludge Reactor. *Water Res.* **2015**, *73*, 323–331. https://doi.org/10.1016/j.watres.2015.01.039.

(47) Chen, X.; Guo, J.; Shi, Y.; Hu, S.; Yuan, Z.; Ni, B.-J. Modeling of Simultaneous Anaerobic Methane and Ammonium Oxidation in a Membrane Biofilm Reactor. *Environ. Sci. Technol.* **2014**, *48* (16), 9540–9547. https://doi.org/10.1021/es502608s.

(48) Könneke, M.; Bernhard, A. E.; de la Torre, J. R.; Walker, C. B.; Waterbury, J. B.; Stahl, D. A. Isolation of an Autotrophic Ammonia-Oxidizing Marine Archaeon. *Nature* **2005**, *437* (7058), 543–546. https://doi.org/10.1038/nature03911.

(49) Qin, W.; Amin, S. A.; Martens-Habbena, W.; Walker, C. B.; Urakawa, H.; Devol, A. H.; Ingalls, A. E.; Moffett, J. W.; Armbrust, E. V.; Stahl, D. A. Marine Ammonia-Oxidizing Archaeal Isolates Display Obligate Mixotrophy and Wide Ecotypic Variation. *Proc. Natl. Acad. Sci. U. S. A.* **2014**, *111* (34), 12504–12509. https://doi.org/10.1073/pnas.1324115111.

(50) Bollmann, A.; French, E.; Laanbroek, H. J. Isolation, Cultivation, and Characterization of Ammonia-Oxidizing Bacteria and Archaea Adapted to Low Ammonium Concentrations. *Methods Enzymol.* **2011**, *486*, 55–88. https://doi.org/10.1016/B978-0-12-381294-0.00003-1.

(51) Tourna, M.; Stieglmeier, M.; Spang, A.; Könneke, M.; Schintlmeister, A.; Urich, T.; Engel, M.; Schloter, M.; Wagner, M.; Richter, A.; et al. Nitrososphaera Viennensis, an Ammonia Oxidizing Archaeon from Soil. *Proc. Natl. Acad. Sci. U. S. A.* **2011**, *108* (20), 8420–8425. https://doi.org/10.1073/pnas.1013488108.

(52) De La Torre, J. R.; Walker, C. B.; Ingalls, A. E.; Könneke, M.; Stahl, D. A. Cultivation of a Thermophilic Ammonia Oxidizing Archaeon Synthesizing Crenarchaeol. *Environ. Microbiol.* **2008**, *10* (3), 810–818. https://doi.org/10.1111/j.1462-2920.2007.01506.x.

(53) Zhalnina, K. V.; Dias, R.; Leonard, M. T.; De Quadros, P. D.; Camargo, F. A. O.; Drew, J. C.; Farmerie, W. G.; Daroub, S. H.; Triplett, E. W. Genome Sequence of Candidatus Nitrososphaera Evergladensis from Group I.1b Enriched from Everglades Soil Reveals Novel Genomic Features of the Ammonia-Oxidizing Archaea. *PLoS One* **2014**, *9* (7). https://doi.org/10.1371/journal.pone.0101648.

(54) Lehtovirta-Morley, L. E.; Stoecker, K.; Vilcinskas, A.; Prosser, J. I.; Nicol, G. W. Cultivation of an Obligate Acidophilic Ammonia Oxidizer from a Nitrifying Acid Soil. *Proc. Natl. Acad. Sci. U. S. A.* **2011**, *108* (38), 15892–15897. https://doi.org/10.1073/pnas.1107196108.

(55) Jung, M. Y.; Kim, J. G.; Sinninghe Damsté, J. S.; Rijpstra, W. I. C.; Madsen, E. L.; Kim, S. J.; Hong, H.; Si, O. J.; Kerou, M.; Schleper, C.; et al. A Hydrophobic Ammonia-Oxidizing Archaeon of the Nitrosocosmicus Clade Isolated from Coal Tar-Contaminated Sediment. *Environ. Microbiol. Rep.* **2016**, *8* (6), 983–992. https://doi.org/10.1111/1758-2229.12477.

(56) Sauder, L. A.; Albertsen, M.; Engel, K.; Schwarz, J.; Nielsen, P. H.; Wagner, M.; Neufeld, J. D. Cultivation and Characterization of Candidatus Nitrosocosmicus Exaquare, an Ammonia-Oxidizing Archaeon from a Municipal Wastewater Treatment System. *ISME J.* **2017**, *11* (5), 1142–1157. https://doi.org/10.1038/ismej.2016.192.

(57) French, E.; Kozlowski, J. A.; Mukherjee, M.; Bullerjahn, G.; Bollmann, A. Ecophysiological Characterization of Ammonia-Oxidizing Archaea and Bacteria from Freshwater. *Appl. Environ. Microbiol.* **2012**, *78* (16), 5773–5780. https://doi.org/10.1128/AEM.00432-12.

(58) Park, H.-D.; Noguera, D. R. Characterization of Two Ammonia-Oxidizing Bacteria Isolated from Reactors Operated with Low Dissolved Oxygen Concentrations. *J. Appl. Microbiol.* **2007**, *102* (5), 1401–1417. https://doi.org/10.1111/j.1365-2672.2006.03176.x.

(59) Beach, N. K.; Noguera, D. R. Design and Assessment of Species-Level QPCR Primers Targeting Comammox. *Front. Microbiol.* **2019**, *10* (JAN), 36. https://doi.org/10.3389/fmicb.2019.00036.

(60) van Kessel, M. A. H. J.; Speth, D. R.; Albertsen, M.; Nielsen, P. H.; Op den Camp, H. J. M.; Kartal, B.; Jetten, M. S. M.; Lücker, S. Complete Nitrification by a Single Microorganism. *Nature* **2015**, *528* (7583), 555–559. https://doi.org/10.1038/nature16459.

(61) Pabi, S.; Reekie, L.; Amarnath, A.; Goldstein, R.; Reekie, L.; Electric Power Research Institute. *Electricity Use and Management in the Municipal Water Supply and Wastewater Industries*; 2013.

(62) Liu, C.; Li, S.; Zhang, F. The Oxygen Transfer Efficiency and Economic Cost Analysis of

Aeration System in Municipal Wastewater Treatment Plant. *Energy Procedia* **2011**, *5*, 2437–2443. https://doi.org/10.1016/j.egypro.2011.03.419.

(63) Hall, J. E. Sewage Sludge Production, Treatment and Disposal in the European Union. *Water Environ. J.* **1995**, *9* (4), 335–343. https://doi.org/10.1111/j.1747-6593.1995.tb00950.x.

(64) Daelman, M. R. J. *Emissions of Methane and Nitrous Oxide from Full-Scale Municipal Wastewater Treatment Plants*; 2014.

(65) Ahn, J. H.; Kim, S.; Park, H.; Rahm, B.; Pagilla, K.; Chandran, K. N_2O Emissions from Activated Sludge Processes, 2008−2009: Results of a National Monitoring Survey in the United States. *Environ. Sci. Technol.* **2010**, *44* (12), 4505–4511. https://doi.org/10.1021/es903845y.

(66) Schreiber, F.; Wunderlin, P.; Udert, K. M.; Wells, G. F. Nitric Oxide and Nitrous Oxide Turnover in Natural and Engineered Microbial Communities: Biological Pathways, Chemical Reactions, and Novel Technologies. *Front. Microbiol.* **2012**, *3*, 372. https://doi.org/10.3389/fmicb.2012.00372.

(67) Chandran, K.; Stein, L. Y.; Klotz, M. G.; van Loosdrecht, M. C. M. Nitrous Oxide Production by Lithotrophic Ammonia-Oxidizing Bacteria and Implications for Engineered Nitrogen-Removal Systems. *Biochem. Soc. Trans.* **2011**, *39* (6), 1832–1837. https://doi.org/10.1042/BST20110717.

(68) Chen, S.; Harb, M.; Sinha, P.; Smith, A. L. Emerging Investigators Series: Revisiting Greenhouse Gas Mitigation from Conventional Activated Sludge and Anaerobic-Based

Wastewater Treatment Systems. *Environ. Sci. Water Res. Technol.* **2018**, *4* (11), 1739–1758. https://doi.org/10.1039/C8EW00545A.

(69) *Innovative Wastewater Treatment & Resource Recovery Technologies: Impacts on Energy, Economy and Environment*, 1st ed.; Lema, J. M., Suarez, S., Eds.; IWA Publishing, 2017. https://doi.org/https://doi.org/10.2166/9781780407876.

(70) van Loosdrecht, M. C. M.; Salem, S. Biological Treatment of Sludge Digester Liquids. *Water Sci. Technol.* **2006**, *53* (12), 11. https://doi.org/10.2166/wst.2006.401.

(71) Lackner, S.; Gilbert, E. M.; Vlaeminck, S. E.; Joss, A.; Horn, H.; van Loosdrecht, M. C. M. Full-Scale Partial Nitritation/Anammox Experiences – An Application Survey. *Water Res.* **2014**, *55*, 292–303. https://doi.org/10.1016/J.WATRES.2014.02.032.

(72) Sliekers, A. O.; Third, K. A.; Abma, W.; Kuenen, J. G.; Jetten, M. S. M. CANON and Anammox in a Gas-Lift Reactor. *FEMS Microbiol. Lett.* **2003**, *218* (2), 339–344.

(73) van Dongen, U.; Jetten, M. S.; van Loosdrecht, M. C. The SHARON-Anammox Process for Treatment of Ammonium Rich Wastewater. *Water Sci. Technol.* **2001**, *44* (1), 153–160.

(74) Kim, D.-J.; Lee, D.-I.; Keller, J. Effect of Temperature and Free Ammonia on Nitrification and Nitrite Accumulation in Landfill Leachate and Analysis of Its Nitrifying Bacterial Community by FISH. *Bioresour. Technol.* **2006**, *97* (3), 459–468. https://doi.org/10.1016/J.BIORTECH.2005.03.032.

(75) Kartal, B.; Kuenen, J. G.; van Loosdrecht, M. C. M. Sewage Treatment with Anammox.

Science **2010**, *328* (5979), 702–703. https://doi.org/10.1126/science.1185941.

(76) Cao, Y.; Kwok, B.; Yong, W.; Chua, S.; Wah, Y.; Ghani, Y. Cao Y, Kwok BH, Yong WH, Chua SC, Wah YL, Ghani YA: Mainstream Partial Nitritation–ANAMMOX Nitrogen Removal in the Largest Full-Scale Activated Sludge Process in Singapore: Process Analysis. In *WEF/IWA Nutrient Removal and Recovery 2013: Trends in Resource Recovery and use*; Vancouver, Canada.

(77) van Kessel, M. A.; Stultiens, K.; Slegers, M. F.; Guerrero Cruz, S.; Jetten, M. S.; Kartal, B.; Op den Camp, H. J. Current Perspectives on the Application of N-Damo and Anammox in Wastewater Treatment. *Curr. Opin. Biotechnol.* **2018**, *50*, 222–227. https://doi.org/10.1016/J.COPBIO.2018.01.031.

(78) Wang, D.; Wang, Y.; Liu, Y.; Ngo, H. H.; Lian, Y.; Zhao, J.; Chen, F.; Yang, Q.; Zeng, G.; Li, X. Is Denitrifying Anaerobic Methane Oxidation-Centered Technologies a Solution for the Sustainable Operation of Wastewater Treatment Plants? *Bioresour. Technol.* **2017**, *234*, 456–465. https://doi.org/10.1016/J.BIORTECH.2017.02.059.

(79) Smith, A. L.; Skerlos, S. J.; Raskin, L. Psychrophilic Anaerobic Membrane Bioreactor Treatment of Domestic Wastewater. *Water Res.* **2013**, *47* (4), 1655–1665. https://doi.org/10.1016/j.watres.2012.12.028.

(80) Chu, L.-B.; Yang, F.-L.; Zhang, X.-W. Anaerobic Treatment of Domestic Wastewater in a Membrane-Coupled Expended Granular Sludge Bed (EGSB) Reactor under Moderate to Low Temperature. *Process Biochem.* **2005**, *40*, 1063–1070. https://doi.org/10.1016/j.procbio.2004.03.010.

(81) Ho, J.; Sung, S. Methanogenic Activities in Anaerobic Membrane Bioreactors (AnMBR) Treating Synthetic Municipal Wastewater. *Bioresour. Technol.* **2010**, *101* (7), 2191–2196. https://doi.org/10.1016/j.biortech.2009.11.042.

(82) Wen, C.; Huang, X.; Qian, Y. *Domestic Wastewater Treatment Using an Anaerobic Bioreactor Coupled with Membrane Filtration*; 1999; Vol. 35.

(83) Smith, A. L.; Stadler, L. B.; Cao, L.; Love, N. G.; Raskin, L.; Skerlos, S. J. Navigating Wastewater Energy Recovery Strategies: A Life Cycle Comparison of Anaerobic Membrane Bioreactor and Conventional Treatment Systems with Anaerobic Digestion. *Environ. Sci. Technol.* **2014**, *48* (10), 5972–5981. https://doi.org/10.1021/es5006169.

(84) Wan, J.; Gu, J.; Zhao, Q.; Liu, Y. COD Capture: A Feasible Option towards Energy Self-Sufficient Domestic Wastewater Treatment. *Sci. Rep.* **2016**, *6* (1), 25054. https://doi.org/10.1038/srep25054.

(85) US EIA. Electricity Power Monthly. Table 5.6.A. Average Price of Electricity to Ultimate Customers by End-Use Sector https://www.eia.gov/electricity/monthly/epm_table_grapher.php?t=epmt_5_6_a (accessed Jan 29, 2018).

(86) Pretel, R.; Robles, A.; Ruano, M. V.; Seco, A.; Ferrer, J. Environmental Impact of Submerged Anaerobic MBR (SAnMBR) Technology Used to Treat Urban Wastewater at Different Temperatures. *Bioresour. Technol.* **2013**, *149*, 532–540. https://doi.org/10.1016/j.biortech.2013.09.060.

(87) Hobson, J. CH4 and N2O Emissions from Waste Water Handling. *Good Pract. Guid.*

Uncertain. Manag. ... **2000**.

(88) Xie, G. J.; Liu, T.; Cai, C.; Hu, S.; Yuan, Z. Achieving High-Level Nitrogen Removal in Mainstream by Coupling Anammox with Denitrifying Anaerobic Methane Oxidation in a Membrane Biofilm Reactor. *Water Res.* **2018**, *131*, 196–204. https://doi.org/10.1016/j.watres.2017.12.037.

(89) Daelman, M. R. J. J.; van Voorthuizen, E. M.; van Dongen, U. G. J. M. J. M.; Volcke, E. I. P. P.; van Loosdrecht, M. C. M. M. Methane Emission during Municipal Wastewater Treatment. *Water Res.* **2012**, *46* (11), 3657–3670. https://doi.org/10.1016/j.watres.2012.04.024.

(90) Ding, Z.-W.; Ding, J.; Fu, L.; Zhang, F.; Zeng, R. J. Simultaneous Enrichment of Denitrifying Methanotrophs and Anammox Bacteria. *Appl. Microbiol. Biotechnol.* **2014**, *98* (24), 10211–10221. https://doi.org/10.1007/s00253-014-5936-8.

(91) Fu, L.; Zhang, F.; Bai, Y.-N.; Lu, Y.-Z.; Ding, J.; Zhou, D.; Liu, Y.; Zeng, R. J. Mass Transfer Affects Reactor Performance, Microbial Morphology, and Community Succession in the Methane-Dependent Denitrification and Anaerobic Ammonium Oxidation Co-Culture. *Sci. Total Environ.* **2019**, *651*, 291–297. https://doi.org/10.1016/j.scitotenv.2018.09.184.

(92) Lotti, T.; Kleerebezem, R.; Hu, Z.; Kartal, B.; de Kreuk, M. K.; van Erp Taalman Kip, C.; Kruit, J.; Hendrickx, T. L. G.; van Loosdrecht, M. C. M. Pilot-Scale Evaluation of Anammox-Based Mainstream Nitrogen Removal from Municipal Wastewater. *Environ. Technol.* **2015**, *36* (9), 1167–1177. https://doi.org/10.1080/09593330.2014.982722.

(93) Kits, K. D.; Jung, M.-Y.; Vierheilig, J.; Pjevac, P.; Sedlacek, C. J.; Liu, S.; Herbold, C.; Stein, L. Y.; Richter, A.; Wissel, H.; et al. Low Yield and Abiotic Origin of N2O Formed by the Complete Nitrifier Nitrospira Inopinata. *Nat. Commun.* **2019**, *10* (1), 1836. https://doi.org/10.1038/s41467-019-09790-x.

(94) Hink, L.; Gubry-Rangin, C.; Nicol, G. W.; Prosser, J. I. The Consequences of Niche and Physiological Differentiation of Archaeal and Bacterial Ammonia Oxidisers for Nitrous Oxide Emissions. *ISME J.* **2018**, *12* (4), 1084–1093. https://doi.org/10.1038/s41396-017-0025-5.

(95) Quan, X.; Zhang, M.; Lawlor, P. G.; Yang, Z.; Zhan, X. Nitrous Oxide Emission and Nutrient Removal in Aerobic Granular Sludge Sequencing Batch Reactors. *Water Res.* **2012**, *46* (16), 4981–4990. https://doi.org/10.1016/j.watres.2012.06.031.

(96) Castro-Barros, C. M.; Daelman, M. R. J.; Mampaey, K. E.; van Loosdrecht, M. C. M.; Volcke, E. I. P. Effect of Aeration Regime on N2O Emission from Partial Nitritation-Anammox in a Full-Scale Granular Sludge Reactor. *Water Res.* **2015**, *68*, 793–803. https://doi.org/10.1016/j.watres.2014.10.056.

(97) Ali, M.; Rathnayake, R. M. L. D.; Zhang, L.; Ishii, S.; Kindaichi, T.; Satoh, H.; Toyoda, S.; Yoshida, N.; Okabe, S. Source Identification of Nitrous Oxide Emission Pathways from a Single-Stage Nitritation-Anammox Granular Reactor. *Water Res.* **2016**, *102*, 147–157. https://doi.org/10.1016/j.watres.2016.06.034.

(98) Kampschreur, M. J.; van der Star, W. R. L.; Wielders, H. A.; Mulder, J. W.; Jetten, M. S. M.; van Loosdrecht, M. C. M. Dynamics of Nitric Oxide and Nitrous Oxide Emission

during Full-Scale Reject Water Treatment. *Water Res.* **2008**, *42* (3), 812–826. https://doi.org/10.1016/j.watres.2007.08.022.

(99) Lotti, T.; Kleerebezem, R.; Lubello, C.; van Loosdrecht, M. C. M. Physiological and Kinetic Characterization of a Suspended Cell Anammox Culture. *Water Res.* **2014**, *60*, 1–14. https://doi.org/10.1016/j.watres.2014.04.017.

(100) Xie, W.-M.; Ni, B.-J.; Li, W.-W.; Sheng, G.-P.; Yu, H.-Q.; Song, J. Formation and Quantification of Soluble Microbial Products and N2O Production by Ammonia-Oxidizing Bacteria (AOB)-Enriched Activated Sludge. *Chem. Eng. Sci.* **2012**, *71*, 67–74. https://doi.org/10.1016/J.CES.2011.12.032.

(101) Pijuan, M.; Torà, J.; Rodríguez-Caballero, A.; César, E.; Carrera, J.; Pérez, J. Effect of Process Parameters and Operational Mode on Nitrous Oxide Emissions from a Nitritation Reactor Treating Reject Wastewater. *Water Res.* **2014**, *49*, 23–33. https://doi.org/10.1016/J.WATRES.2013.11.009.

(102) Voss, M.; Bange, H. W.; Dippner, J. W.; Middelburg, J. J.; Montoya, J. P.; Ward, B. The Marine Nitrogen Cycle: Recent Discoveries, Uncertaintiesand the Potential Relevance of Climate Change. *Philos. Trans. R. Soc. B Biol. Sci.* **2013**, *368* (1621). https://doi.org/10.1098/rstb.2013.0121.

(103) Gruber, N.; Galloway, J. N. An Earth-System Perspective of the Global Nitrogen Cycle. *Nature*. Nature Publishing Group January 17, 2008, pp 293–296. https://doi.org/10.1038/nature06592.

(104) Arrigo, K. R. Marine Microorganisms and Global Nutrient Cycles. *Nature*. Nature

Publishing Group September 15, 2005, pp 349–355. https://doi.org/10.1038/nature04159.

(105) Devol, A. H. Nitrogen Cycle: Solution to a Marine Mystery. *Nature*. Nature Publishing Group April 10, 2003, pp 575–576. https://doi.org/10.1038/422575a.

(106) Van De Graaf, A. A.; Mulder, † Arnold; De Bruijn, P.; Jetten, M. S. M.; Robertson, L. A.; Gijs Kuenen, A. J. *Anaerobic Oxidation of Ammonium Is a Biologically Mediated Process Downloaded From*; 1995; Vol. 61.

(107) Li, M.; Gu, J. D. Community Structure and Transcript Responses of Anammox Bacteria, AOA, and AOB in Mangrove Sediment Microcosms Amended with Ammonium and Nitrite. *Appl. Microbiol. Biotechnol.* **2013**, *97* (22), 9859–9874. https://doi.org/10.1007/s00253-012-4683-y.

(108) Lam, P.; Lavik, G.; Jensen, M. M.; van de Vossenberg, J.; Schmid, M.; Woebken, D.; Gutiérrez, D.; Amann, R.; Jetten, M. S. M.; Kuypers, M. M. M. Revising the Nitrogen Cycle in the Peruvian Oxygen Minimum Zone. *Proc. Natl. Acad. Sci. U. S. A.* **2009**, *106* (12), 4752–4757. https://doi.org/10.1073/pnas.0812444106.

(109) Pitcher, A.; Villanueva, L.; Hopmans, E. C.; Schouten, S.; Reichart, G.-J.; Sinninghe Damsté, J. S. Niche Segregation of Ammonia-Oxidizing Archaea and Anammox Bacteria in the Arabian Sea Oxygen Minimum Zone. *ISME J.* **2011**, *5* (12), 1896–1904. https://doi.org/10.1038/ismej.2011.60.

(110) Yan, J.; Haaijer, S. C. M.; Op den Camp, H. J. M.; van Niftrik, L.; Stahl, D. A.; Könneke, M.; Rush, D.; Sinninghe Damsté, J. S.; Hu, Y. Y.; Jetten, M. S. M. Mimicking the Oxygen Minimum Zones: Stimulating Interaction of Aerobic Archaeal and Anaerobic Bacterial

Ammonia Oxidizers in a Laboratory-Scale Model System. *Environ. Microbiol.* **2012**, *14* (12), 3146–3158. https://doi.org/10.1111/j.1462-2920.2012.02894.x.

(111) Martens-Habbena, W.; Berube, P. M.; Urakawa, H.; de la Torre, J. R.; Stahl, D. A. Ammonia Oxidation Kinetics Determine Niche Separation of Nitrifying Archaea and Bacteria. *Nature* **2009**, *461* (7266), 976–979. https://doi.org/10.1038/nature08465.

(112) Rittmann, B. E.; McCarty, P. L. *Environmental Biotechnology : Principles and Applications*; McGraw Hill, 2001.

(113) Liu, Y.; Ngo, H. H.; Guo, W.; Peng, L.; Pan, Y.; Guo, J.; Chen, X.; Ni, B. J. Autotrophic Nitrogen Removal in Membrane-Aerated Biofilms: Archaeal Ammonia Oxidation versus Bacterial Ammonia Oxidation. *Chem. Eng. J.* **2016**, *302*, 535–544. https://doi.org/10.1016/j.cej.2016.05.078.

(114) Liu, T.; Hu, S.; Yuan, Z.; Guo, J. High-Level Nitrogen Removal by Simultaneous Partial Nitritation, Anammox and Nitrite/Nitrate-Dependent Anaerobic Methane Oxidation. *Water Res.* **2019**, *166*. https://doi.org/10.1016/j.watres.2019.115057.

(115) Cao, Y.; van Loosdrecht, M. C. M.; Daigger, G. T. Mainstream Partial Nitritation–Anammox in Municipal Wastewater Treatment: Status, Bottlenecks, and Further Studies. *Applied Microbiology and Biotechnology*. Springer Verlag February 1, 2017, pp 1365–1383. https://doi.org/10.1007/s00253-016-8058-7.

(116) Volcke, E. I. P.; Picioreanu, C.; De Baets, B.; van Loosdrecht, M. C. M. The Granule Size Distribution in an Anammox-Based Granular Sludge Reactor Affects the Conversion-Implications for Modeling. *Biotechnol. Bioeng.* **2012**, *109* (7), 1629–1636.

https://doi.org/10.1002/bit.24443.

(117) Lotti, T.; van der Star, W. R. L.; Kleerebezem, R.; Lubello, C.; van Loosdrecht, M. C. M. The Effect of Nitrite Inhibition on the Anammox Process. *Water Res.* **2012**, *46* (8), 2559–2569. https://doi.org/10.1016/j.watres.2012.02.011.

(118) Winkler, M.-K. H.; Kleerebezem, R.; Strous, M.; Chandran, K.; van Loosdrecht, M. C. M. Factors Influencing the Density of Aerobic Granular Sludge. *Appl. Microbiol. Biotechnol.* **2013**, *97* (16), 7459–7468. https://doi.org/10.1007/s00253-012-4459-4.

(119) Blackburne, R.; Vadivelu, V. M.; Yuan, Z.; Keller, J. Kinetic Characterisation of an Enriched Nitrospira Culture with Comparison to Nitrobacter. *Water Res.* **2007**. https://doi.org/10.1016/j.watres.2007.01.043.

(120) Terada, A.; Lackner, S.; Tsuneda, S.; Smets, B. F. Redox-Stratification Controlled Biofilm (ReSCoBi) for Completely Autotrophic Nitrogen Removal: The Effect of Co- versus Counter-Diffusion on Reactor Performance. *Biotechnol. Bioeng.* **2007**, *97* (1), 40–51. https://doi.org/10.1002/bit.21213.

(121) Xiaoyan Sun; Guangming Jiang; Philip L. Bond; Jurg Keller; Zhiguo Yuan. A Novel and Simple Treatment for Control of Sulfide Induced Sewer Concrete Corrosion Using Free Nitrous Acid. *Water Res.* **2015**, No. 70, 279–287.

(122) Annavajhala, M. K.; Kapoor, V.; Santo-Domingo, J.; Chandran, K. Comammox Functionality Identified in Diverse Engineered Biological Wastewater Treatment Systems. *Environ. Sci. Technol. Lett.* **2018**, *5* (2), 110–116. https://doi.org/10.1021/acs.estlett.7b00577.

(123) Park, H. D.; Noguera, D. R. Nitrospira Community Composition in Nitrifying Reactors Operated with Two Different Dissolved Oxygen Levels. *J. Microbiol. Biotechnol.* **2008**.

(124) Parada, A. E.; Needham, D. M.; Fuhrman, J. A. Every Base Matters: Assessing Small Subunit RRNA Primers for Marine Microbiomes with Mock Communities, Time Series and Global Field Samples. *Environ. Microbiol.* **2016**, *18* (5), 1403–1414. https://doi.org/10.1111/1462-2920.13023.

(125) Quince, C.; Lanzen, A.; Davenport, R. J.; Turnbaugh, P. J. Removing Noise From Pyrosequenced Amplicons. *BMC Bioinformatics* **2011**, *12* (1), 38. https://doi.org/10.1186/1471-2105-12-38.

(126) Edgar, R. C. Search and Clustering Orders of Magnitude Faster than BLAST. *Bioinformatics* **2010**. https://doi.org/10.1093/bioinformatics/btq461.

(127) Maidak, B. L.; Olsen, G. J.; Larsen, N.; Overbeek, R.; McCaughey, M. J.; Woese, C. R. The RDP (Ribosomal Database Project). *Nucleic Acids Res.* **1997**, *25* (1), 109–110. https://doi.org/10.1093/nar/25.1.109.

(128) Edgar, R. SINTAX: A Simple Non-Bayesian Taxonomy Classifier for 16S and ITS Sequences. *bioRxiv* **2016**, 074161. https://doi.org/10.1101/074161.

(129) Edgar, R. C. UNOISE2: Improved Error-Correction for Illumina 16S and ITS Amplicon Sequencing. *bioRxiv* **2016**, 081257. https://doi.org/10.1101/081257.

(130) Cotto, I.; Dai, Z.; Huo, L.; Anderson, C. L.; Vilardi, K. J.; Ijaz, U.; Khunjar, W.; Wilson, C.; De Clippeleir, H.; Gilmore, K.; et al. Long Solids Retention Times and Attached

Growth Phase Favor Prevalence of Comammox Bacteria in Nitrogen Removal Systems. *Water Res.* **2020**, *169*. https://doi.org/10.1016/j.watres.2019.115268.

(131) Tsushima, I.; Kindaichi, T.; Okabe, S. Quantification of Anaerobic Ammonium-Oxidizing Bacteria in Enrichment Cultures by Real-Time PCR. *Water Res.* **2007**, *41* (4), 785–794. https://doi.org/10.1016/j.watres.2006.11.024.

(132) Hamersley, M. R.; Lavik, G.; Woebken, D.; Rattray, J. E.; Lam, P.; Hopmans, E. C.; Sinninghe Damsté, J. S.; Krüger, S.; Graco, M.; Gutiérrez, D.; et al. Anaerobic Ammonium Oxidation in the Peruvian Oxygen Minimum Zone. *Limnol. Oceanogr.* **2007**. https://doi.org/10.4319/lo.2007.52.3.0923.

(133) Qin, W.; Zheng, Y.; Zhao, F.; Wang, Y.; Urakawa, H.; Martens-Habbena, W.; Liu, H.; Huang, X.; Zhang, X.; Nakagawa, T.; et al. Alternative Strategies of Nutrient Acquisition and Energy Conservation Map to the Biogeography of Marine Ammonia-Oxidizing Archaea. *ISME J.* **2020**, 1–15. https://doi.org/10.1038/s41396-020-0710-7.

(134) Louca, S.; Doebeli, M.; Parfrey, L. W. Correcting for 16S RRNA Gene Copy Numbers in Microbiome Surveys Remains an Unsolved Problem. *Microbiome* **2018**, *6* (1), 41. https://doi.org/10.1186/s40168-018-0420-9.

(135) Van Teeseling, M. C. F.; Mesman, R. J.; Kuru, E.; Espaillat, A.; Cava, F.; Brun, Y. V.; Vannieuwenhze, M. S.; Kartal, B.; Van Niftrik, L. Anammox Planctomycetes Have a Peptidoglycan Cell Wall. *Nat. Commun.* **2015**, *6* (1), 1–6. https://doi.org/10.1038/ncomms7878.

(136) Pan, Y.; Ni, B. J.; Liu, Y.; Guo, J. Modeling of the Interaction among Aerobic

Ammonium-Oxidizing Archaea/Bacteria and Anaerobic Ammonium-Oxidizing Bacteria. *Chem. Eng. Sci.* **2016**, *150*, 35–40. https://doi.org/10.1016/j.ces.2016.05.002.

(137) Gottshall, E. Y.; Bryson, S.; Cogert, K. I.; Landreau, M.; Sedlacek, C. J.; Stahl, D. A.; Daims, H.; Winkler, M. Sustained Nitrogen Loss in a Symbiotic Association of Comammox Nitrospira and Anammox Bacteria. *Manuscr. Prep.* **2020**.

(138) Roots, P.; Wang, Y.; Rosenthal, A. F.; Griffin, J. S.; Sabba, F.; Petrovich, M.; Yang, F.; Kozak, J. A.; Zhang, H.; Wells, G. F. Comammox Nitrospira Are the Dominant Ammonia Oxidizers in a Mainstream Low Dissolved Oxygen Nitrification Reactor. *Water Res.* **2019**, *157*, 396–405. https://doi.org/10.1016/j.watres.2019.03.060.

(139) Camejo, P. Y.; Santo Domingo, J.; McMahon, K. D.; Noguera, D. R. Genome-Enabled Insights into the Ecophysiology of the Comammox Bacterium "Candidatus Nitrospira Nitrosa." *mSystems* **2017**, *2* (5). https://doi.org/10.1128/msystems.00059-17.

(140) Freitag, A.; Rudert, M.; Bock, E. Growth of *Nitrobacter* by Dissimilatoric Nitrate Reduction. *FEMS Microbiol. Lett.* **1987**, *48* (1–2), 105–109. https://doi.org/10.1111/j.1574-6968.1987.tb02524.x.

(141) Marais, G. v R.; Ekama, G. A. The Activated Sludge Process – Part 1: Steady State Behaviour. *WATER SA* **1976**, *2* (4).

(142) Pandey, C. B.; Kumar, U.; Kaviraj, M.; Minick, K. J.; Mishra, A. K.; Singh, J. S. DNRA: A Short-Circuit in Biological N-Cycling to Conserve Nitrogen in Terrestrial Ecosystems. *Science of the Total Environment*. Elsevier B.V. October 10, 2020, p 139710. https://doi.org/10.1016/j.scitotenv.2020.139710.

(143) Yu, X.; Niks, D.; Ge, X.; Liu, H.; Hille, R.; Mulchandani, A. Synthesis of Formate from CO2 Gas Catalyzed by an O2-Tolerant NAD-Dependent Formate Dehydrogenase and Glucose Dehydrogenase. *Biochemistry* **2019**, *58* (14), 1861–1868. https://doi.org/10.1021/acs.biochem.8b01301.

(144) Oshiki, M.; Shinyako-Hata, K.; Satoh, H.; Okabe, S. Draft Genome Sequence of an Anaerobic Ammonium-Oxidizing Bacterium, "Candidatus Brocadia Sinica." *Genome Announc.* **2016**, *3* (2). https://doi.org/10.1128/genomeA.00267-15.

(145) Lawson, C. E.; Wu, S.; Bhattacharjee, A. S.; Hamilton, J. J.; McMahon, K. D.; Goel, R.; Noguera, D. R. Metabolic Network Analysis Reveals Microbial Community Interactions in Anammox Granules. *Nat. Commun.* **2017**, *8* (1), 1–12. https://doi.org/10.1038/ncomms15416.

(146) Sun, X.; Kop, L. F. M.; Lau, M. C. Y.; Frank, J.; Jayakumar, A.; Lücker, S.; Ward, B. B. Uncultured Nitrospina-like Species Are Major Nitrite Oxidizing Bacteria in Oxygen Minimum Zones. *ISME J.* **2019**, *13* (10), 2391–2402. https://doi.org/10.1038/s41396-019-0443-7.

(147) Beman, J. M.; Leilei Shih, J.; Popp, B. N. Nitrite Oxidation in the Upper Water Column and Oxygen Minimum Zone of the Eastern Tropical North Pacific Ocean. *ISME J.* **2013**, *7* (11), 2192–2205. https://doi.org/10.1038/ismej.2013.96.

(148) Abma, W. R.; Schultz, C. E.; Mulder, J. W.; van der Star, W. R. L.; Strous, M.; Tokutomi, T.; van Loosdrecht, M. C. M. Full-Scale Granular Sludge Anammox Process. *Water Sci. Technol.* **2007**, *55* (8–9), 27–33. https://doi.org/10.2166/wst.2007.238.

(149) Jetten, M. S. M.; Strous, M.; van de Pas-Schoonen, K. T.; Schalk, J.; van Dongen, U. G. J. M.; van de Graaf, A. A.; Logemann, S.; Muyzer, G.; van Loosdrecht, M. C. M.; Kuenen, J. G. The Anaerobic Oxidation of Ammonium. *FEMS Microbiol. Rev.* **1998**, *22* (5), 421–437. https://doi.org/10.1111/j.1574-6976.1998.tb00379.x.

(150) Kartal, B.; Kuypers, M. M. M.; Lavik, G.; Schalk, J.; Op den Camp, H. J. M.; Jetten, M. S. M.; Strous, M. Anammox Bacteria Disguised as Denitrifiers: Nitrate Reduction to Dinitrogen Gas via Nitrite and Ammonium. *Environ. Microbiol.* **2007**, *9* (3), 635–642. https://doi.org/10.1111/j.1462-2920.2006.01183.x.

(151) Straka, L.; Summers, A.; Stahl, D. A.; Winkler, M. K. H. Kinetic Implication of Moving Warm Side-Stream Anaerobic Ammonium Oxidizing Bacteria to Cold Mainstream Wastewater. *Bioresour. Technol.* **2019**, *288*, 121534. https://doi.org/10.1016/j.biortech.2019.121534.

(152) Jung, M. Y.; Park, S. J.; Min, D.; Kim, J. S.; Rijpstra, W. I. C.; Damsté, J. S. S.; Kim, G. J.; Madsen, E. L.; Rhee, S. K. Enrichment and Characterization of an Autotrophic Ammonia-Oxidizing Archaeon of Mesophilic Crenarchaeal Group I.1a from an Agricultural Soil. *Appl. Environ. Microbiol.* **2011**, *77* (24), 8635–8647. https://doi.org/10.1128/AEM.05787-11.

(153) Sakoula, D.; Koch, H.; Frank, J.; Jetten, M. S.; Kessel, M. A. van; Lücker, S. Enrichment and Physiological Characterization of a Novel Comammox Nitrospira Indicates Ammonium Inhibition of Complete Nitrification. *bioRxiv* **2020**, 2020.06.08.136465. https://doi.org/10.1101/2020.06.08.136465.

(154) Uri, N.; Constantine, T.; Sandino, J.; Willoughby, A.; Nielsen, P. H. Going Bubbleless: Design and Start-up of the Full-Scale MABR Demonstration at the Ejby Mølle WRRF. In *The 16th IWA Leading Edge Conference on Water and Wastewater Technologies*; Edinborough, UK, 2019; pp 3803–3808.

(155) Pellicer-Nàcher, C.; Sun, S.; Lackner, S.; Terada, A.; Schreiber, F.; Zhou, Q.; Smets, B. F. Sequential Aeration of Membrane-Aerated Biofilm Reactors for High-Rate Autotrophic Nitrogen Removal: Experimental Demonstration. *Environ. Sci. Technol.* **2010**, *44* (19), 7628–7634. https://doi.org/10.1021/es1013467.

(156) Gong, Z.; Yang, F.; Liu, S.; Bao, H.; Hu, S.; Furukawa, K. Feasibility of a Membrane-Aerated Biofilm Reactor to Achieve Single-Stage Autotrophic Nitrogen Removal Based on Anammox. *Chemosphere* **2007**, *69* (5), 776–784. https://doi.org/10.1016/j.chemosphere.2007.05.023.

(157) Reichert, P. Aquasim - A Tool for Simulation and Data Analysis of Aquatic Systems. In *Water Science and Technology*; Pergamon Press Inc, 1994; Vol. 30, pp 21–30. https://doi.org/10.2166/wst.1994.0025.

(158) Lotti, T.; Kleerebezem, R.; Hu, Z.; Kartal, B.; de Kreuk, M. K.; van Erp Taalman Kip, C.; Kruit, J.; Hendrickx, T. L. G.; van Loosdrecht, M. C. M. Pilot-Scale Evaluation of Anammox-Based Mainstream Nitrogen Removal from Municipal Wastewater. *Environ. Technol. 36* (9–12), 1167–1177. https://doi.org/10.1080/09593330.2014.982722.

(159) Yoshida, T.; Nagasawa, T. ε-Poly-L-Lysine: Microbial Production, Biodegradation and Application Potential. *Applied Microbiology and Biotechnology*. Springer July 1, 2003, pp

21–26. https://doi.org/10.1007/s00253-003-1312-9.

(160) Limpiyakorn, T.; Kurisu, F.; Sakamoto, Y.; Yagi, O. Effects of Ammonium and Nitrite on Communities and Populations of Ammonia-Oxidizing Bacteria in Laboratory-Scale Continuous-Flow Reactors. *FEMS Microbiol. Ecol.* **2007**, *60* (3), 501–512. https://doi.org/10.1111/j.1574-6941.2007.00307.x.

(161) Wang, R.; Terada, A.; Lackner, S.; Smets, B. F.; Henze, M.; Xia, S.; Zhao, J. Nitritation Performance and Biofilm Development of Co- and Counter-Diffusion Biofilm Reactors: Modeling and Experimental Comparison. *Water Res.* **2009**, *43* (10), 2699–2709. https://doi.org/10.1016/j.watres.2009.03.017.

(162) Winkler, M. K. H.; Kleerebezem, R.; Kuenen, J. G.; Yang, J.; van Loosdrecht, M. C. M. Segregation of Biomass in Cyclic Anaerobic/Aerobic Granular Sludge Allows the Enrichment of Anaerobic Ammonium Oxidizing Bacteria at Low Temperatures. *Environ. Sci. Technol.* **2011**, *45* (17), 7330–7337. https://doi.org/10.1021/es201388t.

(163) Picioreanu, C.; Kreft, J.-U.; Van Loosdrecht, M. C. M. Particle-Based Multidimensional Multispecies Biofilm Model Downloaded From. *Appl. Environ. Microbiol.* **2004**, *70* (5), 3024–3040. https://doi.org/10.1128/AEM.70.5.3024-3040.2004.

(164) Erisman, J. W.; Sutton, M. A.; Galloway, J.; Klimont, Z.; Winiwarter, W. How a Century of Ammonia Synthesis Changed the World. *Nat. Geosci.* **2008**, *1* (10), 636–639. https://doi.org/10.1038/ngeo325.

(165) Kanter, D. R.; Bartolini, F.; Kugelberg, S.; Leip, A.; Oenema, O.; Uwizeye, A. Nitrogen Pollution Policy beyond the Farm. *Nat. Food* **2019**. https://doi.org/10.1038/s43016-019-

0001-5.

(166) National Academy of Engineering. Grand Challenges - Manage the Nitrogen Cycle http://www.engineeringchallenges.org/9132.aspx (accessed Jan 1, 2016).

(167) Pelley, J. Taming Toxic Algae Blooms. *ACS Cent. Sci.* **2016**, *2* (5), 270–273. https://doi.org/10.1021/acscentsci.6b00129.

(168) International Standards Organization. *Water Quality - Determination of Ammonium - Part 1 : Manual Spectrometric Method*; 1984.

(169) Manap, H.; Dooly, G.; O'Keeffe, S.; Lewis, E. Ammonia Detection in the UV Region Using an Optical Fiber Sensor. In *Proceedings of IEEE Sensors*; 2009; pp 140–145. https://doi.org/10.1109/ICSENS.2009.5398215.

(170) Kaelin, D.; Rieger, L.; Eugster, J.; Rottermann, K.; Bänninger, C.; Siegrist, H. Potential of In-Situ Sensors with Ion-Selective Electrodes for Aeration Control at Wastewater Treatment Plants. *Water Sci. Technol.* **2008**, *58* (3), 629–637. https://doi.org/10.2166/wst.2008.433.

(171) Ortuño, J. A.; Tomás-Alonso, F.; Rubio, A. M. Ion-Selective Electrodes Based on Ionic Liquids. In *Ionic Liquids in Separation Technology*; Elsevier Ltd, 2014; pp 275–299. https://doi.org/10.1016/B978-0-444-63257-9.00009-2.

(172) Ruzicka, J. *The Seventies-Golden Age for Ion Selective Electrodes*; UTC, 1997; Vol. 74.

(173) Snauffer, A. M.; Chauhan, U.; Cogert, K.; Winkler, M. K. H.; Mueller, A. V. Data Fusion for Environmental Process Control: Maximizing Useful Information Recovery under Data

Limited Constraints. *IEEE Sensors Lett.* **2019**, *3* (1). https://doi.org/10.1109/LSENS.2018.2889274.

(174) Brinkhoff, H. C. *Analysis of the Nitrate Content of Surface Water and Effluent Water. Application of a Plastic-Membrane Nitrate-Selective Electrode in Water Quality Monitors*; UTC, 1975; Vol. 79.

(175) Mueller, A. V.; Hemond, H. F. Statistical Generation of Training Sets for Measuring NO3-, NH4+ and Major Ions in Natural Waters Using an Ion Selective Electrode Array. *Environ. Sci. Process. Impacts* **2016**, *18* (5), 590–599. https://doi.org/10.1039/c6em00043f.

(176) Kampschreur, M. J.; van der Star, W. R. L.; Wielders, H. A.; Mulder, J. W.; Jetten, M. S. M.; van Loosdrecht, M. C. M. Dynamics of Nitric Oxide and Nitrous Oxide Emission during Full-Scale Reject Water Treatment. *Water Res.* **2008**, *42* (3), 812–826. https://doi.org/10.1016/J.WATRES.2007.08.022.

(177) Radu, A.; Anastasova-Ivanova, S.; Paczosa-Bator, B.; Danielewski, M.; Bobacka, J.; Lewenstam, A.; Diamond, D. Diagnostic of Functionality of Polymer Membrane - Based Ion Selective Electrodes by Impedance Spectroscopy. *Anal. Methods* **2010**, *2* (10), 1490–1498. https://doi.org/10.1039/c0ay00249f.

(178) Mueller, A. V.; Hemond, H. F. Towards an Automated, Standardized Protocol for Determination of Equilibrium Potential of Ion-Selective Electrodes. *Anal. Chim. Acta* **2011**, *690* (1), 71–78. https://doi.org/10.1016/j.aca.2011.02.011.

(179) Pechenkina, I. A.; Mikhelson, K. N. Materials for the Ionophore-Based Membranes for

Ion-Selective Electrodes: Problems and Achievements (Review Paper). *Russ. J. Electrochem.* **2015**, *51* (2), 93–102. https://doi.org/10.1134/S1023193515020111.

(180) Chang, S. Anaerobic Membrane Bioreactors (AnMBR) for Wastewater Treatment. *Adv. Chem. Eng. Sci.* **2014**, *04* (01), 56–61. https://doi.org/10.4236/aces.2014.41008.

(181) Hilton, B. L.; Oleszkiewicz, J. A. Sulfide-Induced Inhibition of Anaerobic Digestion. *J. Environ. Eng.* **1988**, *114* (6), 1377–1391. https://doi.org/10.1061/(ASCE)0733-9372(1988)114:6(1377).

(182) Carvajal-Arroyo, J. M.; Sun, W.; Sierra-Alvarez, R.; Field, J. A. Inhibition of Anaerobic Ammonium Oxidizing (Anammox) Enrichment Cultures by Substrates, Metabolites and Common Wastewater Constituents. *Chemosphere* **2013**, *91* (1), 22–27. https://doi.org/https://doi.org/10.1016/j.chemosphere.2012.11.025.

(183) Rysgaard, S.; Glud, R. N.; Risgaard-Petersen, N.; Dalsgaard, T. Denitrification and Anammox Activity in Arctic Marine Sediments. *Limnol. Oceanogr.* **2004**, *49* (5), 1493–1502. https://doi.org/10.4319/lo.2004.49.5.1493.

(184) Alves, R. J. E.; Wanek, W.; Zappe, A.; Richter, A.; Svenning, M. M.; Schleper, C.; Urich, T. Nitrification Rates in Arctic Soils Are Associated with Functionally Distinct Populations of Ammonia-Oxidizing Archaea. *ISME J.* **2013**, *7* (8), 1620–1631. https://doi.org/10.1038/ismej.2013.35.

(185) U.S. EIA. United States Electricity Profile 2016. Table 1: 2016 Summary statistics (United States) https://www.eia.gov/electricity/state/unitedstates/index.php (accessed Sep 21, 2018).

(186) Thermodynamic Tables Project., K.; Angus, S. (Selby); Armstrong, B.; Reuck, K. M. de. *International Thermodynamic Tables of the Fluid State*; Butterworths: Oxford, 1971.

(187) Pricing | Methanex Corporation https://www.methanex.com/our-business/pricing (accessed Apr 13, 2019).

(188) U.S. Natural Gas Prices https://www.eia.gov/dnav/ng/ng_pri_sum_dcu_nus_m.htm (accessed Apr 13, 2019).

(189) Setzmann, U.; Wagner, W. A New Equation of State and Tables of Thermodynamic Properties for Methane Covering the Range from the Melting Line to 625 K at Pressures up to 100 MPa. *J. Phys. Chem. Ref. Data* **1991**. https://doi.org/10.1063/1.555898.

(190) Sander, R. Henry's Law Constants. In *NIST Chemistry WebBook, NIST Standard Reference Database Number 69*; Mallard, P. J. L. and W. G., Ed.; National Institute of Standards and Technology: Gaithersburg MD, 20899. https://doi.org/10.18434/T4D303.

(191) Daelman, M. R. J.; Van Eynde, T.; van Loosdrecht, M. C. M.; Volcke, E. I. P. Effect of Process Design and Operating Parameters on Aerobic Methane Oxidation in Municipal WWTPs. *Water Res.* **2014**, *66*, 308–319. https://doi.org/10.1016/J.WATRES.2014.07.034.

(192) Gouveia, J.; Plaza, F.; Garralon, G.; Fdz-Polanco, F.; Peña, M. Long-Term Operation of a Pilot Scale Anaerobic Membrane Bioreactor (AnMBR) for the Treatment of Municipal Wastewater under Psychrophilic Conditions. *Bioresour. Technol.* **2015**, *185*, 225–233. https://doi.org/10.1016/J.BIORTECH.2015.03.002.

(193) Daims, H.; Lücker, S.; Wagner, M. A New Perspective on Microbes Formerly Known as

Nitrite-Oxidizing Bacteria. *Trends in Microbiology*. 2016. https://doi.org/10.1016/j.tim.2016.05.004.

(194) Raskin, L.; Stromley, J. M.; Rittmann, B. E.; Stahl, D. A. Group-Specific 16S RRNA Hybridization Probes to Describe Natural Communities of Methanogens. *Appl. Environ. Microbiol.* **1994**. https://doi.org/10.1128/aem.60.4.1232-1240.1994.

(195) Schmid, M. C.; Maas, B.; Dapena, A.; Van De Pas-Schoonen, K.; Van De Vossenberg, J.; Kartal, B.; Van Niftrik, L.; Schmidt, I.; Cirpus, I.; Kuenen, J. G.; et al. Biomarkers for in Situ Detection of Anaerobic Ammonium-Oxidizing (Anammox) Bacteria. *Applied and Environmental Microbiology*. 2005. https://doi.org/10.1128/AEM.71.4.1677-1684.2005.

(196) Henze, M.; Gujer, W.; Mino, T.; van Loosedrecht, M. Activated Sludge Models ASM1, ASM2, ASM2d and ASM3. *Water Intell. Online* **2015**. https://doi.org/10.2166/9781780402369.

(197) Picioreanu, C.; Van Loosdrecht, M. C. M.; Heijnen, J. J. Modelling the Effect of Oxygen Concentration on Nitrite Accumulation in a Biofilm Airlift Suspension Reactor. *Water Sci. Technol.* **1997**. https://doi.org/10.1016/S0273-1223(97)00347-8.

(198) Hao, X.; Heijnen, J. J.; Van Loosdrecht, M. C. M. Sensitivity Analysis of a Biofilm Model Describing a One-Stage Completely Autotrophic Nitrogen Removal (CANON) Process. *Biotechnol. Bioeng.* **2001**. https://doi.org/10.1002/bit.10105.

(199) VISHNIAC, W.; SANTER, M. The Thiobacilli. *Bacteriol. Rev.* **1957**, *21* (3), 195–213.

(200) Hach USA. What is the recommended cleaning for a Ion Selective Electrodes (ISE) with

PVC membranes? https://support.hach.com/app/answers/answer_view/a_id/1020187/~/what-is-the-recommended-cleaning-for-a-ion-selective-electrodes-%28ise%29-with-pvc (accessed Aug 20, 2020).

(201) The Dow Chemical Company. *Product Information: KATHON™ CG Preservative* .

(202) Hach USA. Electrode Cleaning Solution for Regular Maintenance, 500 mL https://www.hach.com/electrode-cleaning-solution-for-regular-maintenance-500-ml/product-details?id=7640205099 (accessed Aug 20, 2020).

(203) Borer Chemie AG. *Deconex 11 Universal: Mildly Alkaline Cleaning Concentrate for Laboratory Glassware - with Activated Chlorine*; Zuchwil, 2008.

(204) Hach USA. Electrode Cleaning Solution for Minerals/Inorganic Samples, 500 mL https://www.hach.com/electrode-cleaning-solution-for-minerals-inorganic-samples-500-ml/product-details?id=7640206882 (accessed Aug 20, 2020).

(205) Sun, Y.; Guan, Y.; Zeng, D.; He, K.; Wu, G. Metagenomics-Based Interpretation of AHLs-Mediated Quorum Sensing in Anammox Biofilm Reactors for Low-Strength Wastewater Treatment. *Chem. Eng. J.* **2018**, *344*, 42–52. https://doi.org/10.1016/j.cej.2018.03.047.

(206) Kartal, B.; Maalcke, W. J.; De Almeida, N. M.; Cirpus, I.; Gloerich, J.; Geerts, W.; Op Den Camp, H. J. M.; Harhangi, H. R.; Janssen-Megens, E. M.; Francoijs, K. J.; et al. Molecular Mechanism of Anaerobic Ammonium Oxidation. *Nature* **2011**, *479* (7371), 127–130. https://doi.org/10.1038/nature10453.

(207) Van Der Star, W. R. L.; Van De Graaf, M. J.; Kartal, B.; Picioreanu, C.; Jetten, M. S. M.; Van Loosdrecht, M. C. M. Response of Anaerobic Ammonium-Oxidizing Bacteria to Hydroxylamine. *Appl. Environ. Microbiol.* **2008**, *74* (14), 4417–4426. https://doi.org/10.1128/AEM.00042-08.

(208) Ma, C.; Jensen, M. M.; Smets, B. F.; Thamdrup, B. Pathways and Controls of N 2 O Production in Nitritation−Anammox Biomass. **2017**. https://doi.org/10.1021/acs.est.7b01225.

(209) Lawson, C. E.; de Graaf, R. M.; Nuijten, G.; Jacobson, T. B.; Pabst, M.; Stevenson, D. M.; Jetten, M. S. M.; Noguera, D. R.; McMahon, K. D.; Amador-Noguez, D.; et al. Autotrophic and Mixotrophic Metabolisms of an Anammox Bacterium Revealed by in Vivo 13C and 2H Metabolic Network Mapping. *bioRxiv* **2020**, 835298. https://doi.org/10.1101/835298.

APPENDIX A

Supplemental Information for

Chapter 3:

Reducing Cost and Environmental Impact of Wastewater Treatment with Denitrifying Methanotrophs, Anammox, and Mainstream Anaerobic Treatment

Number of Pages: 33
Number of Figures: 10
Number of Tables: 14

Table of Contents:

Supplemental Methods: Preliminary Calculations for Cost Estimations	A3
Table A1: Preliminary Calculations for Cost Estimations	A3
Supplemental Methods: Description of Models & Sample Calcuations	A6
Table A2. Summary of cost factors from Table A1.	A8
Table A3. Key Metabolism stoichiometric constants and biomass yields used in this model.	A8
Table A4. Additional constants required for model calculations.	A9
Figure A1. Replication of Scenario A taken from Figure 1 of the manuscript	A9
Table A5. Fractional conversions for scenario A, f_{Z_Y}	A10
Table A6. The following cost and equivalent GHG emissions are reported from ScenarioA.R when using the input used in this sample calculation	A14
Figure A2. Replication of Scenario B taken from Figure 1 of the manuscript	A14
Table A7. Fractional conversions for scenario B, f_{Z_Y}	A14
Table A8. The following metrics are reported from ScenarioB.R when using the input used in this sample calculation	A16
Figure A3. Replication of Scenario C taken from Figure 1 of the manuscript	A17
Table A9. Fractional conversions for scenario C, f_{Z_Y}	A17
Table A10. The following metrics are reported from ScenarioC.R when using the input used in this sample calculation	A20
Table A11. Fractional conversions for scenario D, $\boldsymbol{f_{Z_Y}}$	A21
Figure A4. Replication of Scenario D taken from Figure 1 of the manuscript	A21
Table A12. The following metrics are reported from ScenarioD.R when using the input used in this sample calculation	A24
Figure A5. Replication of Scenario E taken from Figure 1 of the manuscript	A25
Table A13. Fractional conversions for scenario E, $\boldsymbol{f_{Z_Y}}$	A25
Table A14. The following metrics are reported from ScenarioE.R when using the input used in this sample calculation	A28
Supplemental Results: Individual Cost Factor Results from the Model	A29
Figure A6. Comparison of oxygen demand in scenarios B (2.1), C (2.2), D (2.3), and E (2.4) to the base case scenario A (Modified Ludzack-Ettinger, MLE, also referred to as conventional nitrification/denitrification).	A29

Figure A7. Comparison of sludge produced in Scenarios B (3.1), C (3.2), D (4.3), and E (3.4) to the base case scenario A (Modified Ludzack-Ettinger, MLE, also referred to as conventional nitrification/denitrification). A30
Figure A8. Comparison of methane production in Scenarios B (4.1), C (4.2), D (4.3), and E (4.4) to the base case scenario A (Modified Ludzack-Ettinger, MLE, also referred to as conventional nitrification/denitrification). A31
Supplemental Results: Sensitivity Study of Pumping Demand on Results A32
Figure A9. Sensitivity of GHG emissions to varying pumping demands in scenarios B-D. GHG emissions are measured as the kg CO_2 per day averted by utilizing one of the theoretical scenarios B-D instead of conventional nitrification/dentrification. A32
Figure A10. Sensitivity of GHG emissions to varying pumping demands in scenarios B-D. GHG emissions are measured as dollars saved per day averted by utilizing one of the theoretical scenarios B-D instead of conventional nitrification/dentrification. A33

SUPPLEMENTAL METHODS: PRELIMINARY CALCULATIONS FOR COST ESTIMATIONS

In addition to the sample calculation above, an estimation of sludge handling cost was used in the preparation of this manuscript. The calculations involved in that estimation are given below:

Table A1. Preliminary Calculations for Cost Estimations

Description	*Value*	*Units*	*Citation or Calculation*
Sludge Handling Costs			
Typical Sludge Solids Content	21.50%		[6]
Mass of sludge to landfill	4.65	kg wet sludge to landfill	1 / % Solids Content
Cost to landfill sludge	11	$/Mg wet	[6]
Cost to landfill 1 kg biomass produced	$ (0.05)	$/kgVSS produced	Landfilled Wet Sludge x Cost/Mg to Landfill / 1000
Plant Flowrate	60	10^3 m^3/day	This study
	15.9	MGD	This study
Cost of electricity to the plant	0.078	$/kWh	[185]
Fraction of Energy for Solids Handling in a Typical Plant	0.3	unitless	[4]
Typical Fraction of VSS in TSS, Mass Basis	0.75	unitless	[5]
Conventional Plant Energy Demand, 7-16 MGD on Volume Basis	2000	kWh/MG	[4]
Conventional Plant Energy Demand, Daily Basis	31701	kWh/day	Plant Energy Demand Volume Basis x Plant Flowrate
Conventional Plant Sludge Production, Volume Basis	248	kgTSS/10^3 m^3	[5]
Conventional Plant Sludge Production, Daily Basis	14880	kgTSS/day	Plant Sludge Production (flowrate basis) x Plant Flowrate
Conventional Plant VSS Production, Daily Basis	11160	kgVSS/day	Plant Sludge Production (daily basis) x Fraction VSS in TSS
Conventional Plant Sludge from Digester, Daily Basis	4241	kgVSS/day	Daily VSS Production x Fraction VSS to Landfill

Energy Required for Solids Handling, Daily Basis	9510	kWh/day	Daily Plant Energy Demand x Typical Fraction of Energy for Biosolids Handling
Table A1 (cont). Preliminary Calculations for Cost Estimations			
Energy Required for Solids Handling, VSS Basis	*2.24*	*kWh/kgVSS*	*Daily Energy Required for Solids Handling / Daily VSS from digester*
Cost of Energy for Solids Handling	$ (0.17)	$/kgVSS	Electricity Cost x Energy Required for Solids Handling
Total Cost of Solids Handling	**$ (0.23)**	**$/kgVSS**	**Energy Cost + Cost to Landfill**
Cost of Oxygen Supply			
Energy Demand of Aeration	*1.5*	*kWh/kgO_2 Dissolved*	[5]
Cost of Aeration	**$ (0.12)**	**$/kg$O_2$**	**Energy Demand of Aeration x Cost of Electricity**
Cost of Energy for AnMBR Operation			
Energy Demand of AnMBR Operation	*190*	*kWh/ 10^3 m^3*	[86]
Cost of Energy for AnMBR Operation	**$(14.82)**	**$/$10^3$ m^3**	**AnMBR Energy Demand x Flowrate x Cost of Electricity**
Cost of Anaerobic Mixing			
Typical Energy Demand of Biological Nitrogen Removal Mixing, 10 MGD Plant	1100	kWh/d	[4]
Typical Energy Demand of Biological Nitrogen Removal Mixing, 20 MGD Plant	2100	kWh/d	[4]
Interpolated BNR Mixing Energy Demand of This Plant, daily basis	1580	kWh/d	Interpolate between 10 & 20 MGD values at 15.8 MGD
Anaerobic Mixing Energy, volume basis	*26.3*	*kWh/th m^3*	*BNR Mixing Energy Demand / Flowrate, assumed to be similar for all anaerobic tanks*
Cost of Energy for Anaerobic Tank Mixing	**$(2.05)**	**$/$10^3$ m^3**	**AnMBR Energy Demand x Flowrate x Cost of Electricity**
Cost of External COD			
Specific Weight of Methanol	0.786	kgCH3OH/L	[186]
Cost of Methanol	$1.30	$/gal	[187]

COD in Methanol, weight basis	1.5	kgCOD/kgCH3OH	Stoichiometry of Combustion Reaction
CO_2 released oxiding methanol, COD basis	*0.92*	*$kgCO_2/kgCOD$*	*Stoichiometry of Combustion Reaction*
Table A1 (cont). Preliminary Calculations for Cost Estimations			
COD in Methanol, volume basis	4.46	kgCOD/gal CH3OH	COD in Methanol x Specific Weight x 3.78 L/gal
Cost of External COD, Methanol (Scenario A, Base Case Only)	**$ (0.29)**	**$/kgCOD as CH3OH**	**Cost of Methanol x COD in Methanol, volume basis**
COD in Methane, weight basis	4	$kgCOD/kgCH_4$	Stoichiometry of Combustion Reaction
CO_2 released oxiding methane, COD basis	*0.69*	*$kgCO_2/kgCOD$*	*Stoichiometry of Combustion Reaction*
Cost of Natural Gas	$5.04	$/th ft^3	[188]
Density of Methane Gas at 0 °C	0.717	kg/m^3	[189]
Cost of COD, Methane (Scenarios D&E, ndamo only)	**$ (0.03)**	$/kgCOD	**Cost of Natural gas x Density of Methane x 0.0353 th ft^3/m^3 / COD in 1 kg CH_4**
Cost Saved through Methane Recovery			
Concentration Methane in Biogas	0.65	Volume fraction	[5]
Biogas Density at STP	0.86	kg/m^3	[5]
Lower Heating Value of Biogas	22400	kJ/m^3	[5]
	6.22	kWh/m^3	Lower Heating Value of Biogas x 0.00028 kWh/kJ
Cogen Plant Efficiency	20%	unitless	[5]
Mass Methane in Biogas	0.56	$kgCH_4$/m^3 biogas	Concentration Methane in Biogas x Biogas Density
Energy recovered from cogen plant, Volume basis	1.24	kWh/m^3 biogas	Lower Heating Value of Biogas x Plant Efficiency
Energy recovered from cogen plant, mass methane basis	*2.2*	*$kWh/kgCH_4$*	*Energy recovered from cogen plant, volume basis / Mass methane in Biogas*
Cost saved through methane recovery	**$ 0.17**	**$/kgCH4 produced**	Cogen energy per kg CH_4 x Electricity Cost

SUPPLEMENTAL METHODS: DESCRIPTION OF MODELS & SAMPLE CALCULATIONS

The following document is intended to describe in detail the models created for the five carbon and nitrogen removal scenarios (Modified Luzak-Ettinger, HRAS/anammox, AnMBR/anammox, HRAS/anammox & n-damo, and AnMBR/anammox & n-damo) described in detail in Figure 3-1. Equations are provided with the associated R script file name and line number in the code to better enable model users to interact with the code directly. (e.g. ScenarioX.R line #)
The following key metrics are returned from these models:
Total oxygen demand
Sludge discharge volume
Methane available for energy recovery
External Carbon Addition Required
Greenhouse Gas Emissions

The models were written in R code using RStudio IDE operating on MacOSX High Sierra. The code for these models is available online with instructions on how to run these models here:
https://github.com/cogerk/ndamo-econ

Definitions
In the definitions given below, **Z** represents a constituent (e.g. N for total nitrogen, COD for chemical oxygen demand, O2 for oxygen, etc.) and **Y** represents an organism or process (e.g. AOB for ammonium oxidizing bacteria or AnMBR for anaerobic membrane bioreactor, etc.)
Q, WWTP capacity, [th m^3/day]
$c_{\mathbf{Z}in}$, Concentration of **Z** in influent, [g-**Z**/ m^3]
$L_{Z_{stream}}$, Total load of **Z** in a given stream (i.e. influent, centrate), [kg-**Z**/d]
$MW_{\mathbf{Z}}$, Molecular weight of **Z**
$S_{\mathbf{Z_Y}}$, Stoichiometric coefficient of **Z** in metabolism of organism **Y,** [mol-**Z**]
Y_Y, Biomass yield of organism **Y,** [g-VSS/g-Substrate]
f_{Z_Y}, Fractional conversion of constituent **Z** by organism **Y**
O_{2_Y}, Total oxygen demand by organism **Y,** [kg-O_2/d]
$COD_{req'd}$, mass of COD required for heterotrophic organisms, [kg-COD/d]
COD_{bal}, COD required for nitrogen removal minus COD available, [kg-COD/d]
CO_{2_Y}, mass of carbon dioxide produced by organism or process **Y**, [kg-CO_2/d]
$CH_{4_{prod}}$, Mass of methane produced from anaerobic digestion, [kg-CH_4/d]
$CH_{4_{burn}}$, Mass of methane available to burn for energy regeneration, [kg-CH_4/d]
$CH_{4_{MOB,ox}}$, Mass of methane oxidized by methanotrophs,
V_X, Volumetric measure of component **Z**, [m^3/d]
ρ_X, Density of component **Z,** [kg/m3]
c_l^*, Concentration of component **Z** in liquid at gas-vapor equilibrium
e_Y, Electrical demand of process **Y** on weight or volume basis, [kWh/kg-**Z**] or [kWh/m^3]
E_Y, Electrical demand/production due to process **Y** on daily basis, [kWh/d]
η_Y, Efficiency of process **Y**, [%]
ΔH_{C_Z}, Heat of combustion or energy density of **Z**, [kWh/kg-**Z**]
C_Y, Cost per unit of a given metric calculated in this study, [$/cost factor unit]
x_Z, Volume fraction of **Z** in gas [%]

BG, Biogas production from sludge [m^3/kgVSS destroyed]

Model Assumptions

The following assumptions were made in this model:

pH and temperature were assumed to be ideal for microbial reactions, meaning this is a stoichiometry-based model where:

100% of COD was removed

Scenarios A, C, and E achieved a nitrogen removal of 100%.

In scenarios B and D, the maximum amount of nitrogen was removed, but some nitrate remained in the effluent according to following Anammox stoichiometry (defined per 1N-mol):

$$NH_4^+ + 1.3\,NO_2^- \rightarrow N_2 + 0.3\,NO_3^- \qquad \text{reaction A-1)}$$

$$\frac{2\,mol - N_2N}{1\,molNH_4^+ - N + 1.3\,molNO_2^- - N} = 87\%$$

The biomass yield of n-damo archaea was assumed to be the same as n-damo bacteria as calculated by Winkler et al.[46]

According to literature recommendation 59% of sludge by weight was reduced in anaerobic sludge digestion (AD).[5]

$$f_{x_{AD}} = 0.59$$

Biogas production from the anerobic digester was assumed to be:[5]

$$BG = 0.75\frac{m^3\ biogas}{kgVSS\ destroyed}$$

Biogas density is assumed to be: [5]

$$\rho_{BG} = 0.86\frac{kg}{m^3}$$

Methane concentration in biogas is assumed to be:[5]

$$x_{CH_4} = 62\ \%\ by\ vol$$

Dissolved methane concentration from the AnMBR was assumed to be 1.5 times that of the saturation concentration calcuated with Henry's law with constant H = 0.0015 mol/kg•atm.[83,190] Assuming 62%v/v methane concnentration in the biogas,[5] this yielded a dissolved methane concentration of:

$$1.5 \times c_l^* = 1.5HPx_{biogas_{CH_4}}MW_{CH_4}\rho_{H_2O} = \qquad \text{(equation A-1)}$$

$$1.5 \times 0.0015\frac{mol}{kg\ atm} \times 1\ atm \times 0.62 \times 16\frac{gCH_4}{mol\ CH_4} \times 1000\frac{kg}{m^3} \qquad \text{scenarioC.R\& scenarioE.R line 40}$$

$$=$$

$$22.4\frac{gCH_4}{m^3} = 0.0224\frac{kg}{m^3}$$

To reflect a "worse case" for GHG emissions, if COD concentration was so low such that less than $22.4\ gCH_4/m^3$was produced from biogas, it was assumed all produced methane is dissolved even though this is not in line with equilibrium concentration predictions.

Centrate was returned to the mainstream from anaerobic sludge digestion and according to literature it was assumed to contain 25% of the total nitrogen load[5].

$$N_{cent} = 0.25$$

Carbon dioxide consumption by autotrophs was considered negligible.

Biogenic CO2 emissions from heterotrophs were not considered according to IPCC guidelines.[38]

According to literature results from Daelman et al. driven by the kinetics of methane oxidizing bacteria, it was assumed that aerobic methanotrophs were only active when methane concentration exceeded 5 mgCOD/L and that they remove 90% of methane present.[191]

$$c_{\min_{CH_4}} = 5\frac{mgCOD}{L};\ x_{CH_{4_{ox}}} = 0.9$$

Methane stripped from the nitrification reactor was assumed to be too dilute for energy recovery and was considered a greenhouse gas emission.

CO2 emissions due to electrical demand were determined with the most recent United States Electrical Profile published by the U.S. Energy and Information Administration (EIA) where the emission of carbon dioxide is given as 1,041 lbsCO_2/MWh or:[185]

$$\frac{kgCO_2}{kWh} = 0.4722\frac{kgCO_2}{kWh}$$

The global warming potential of methane was considered to be34 times that of carbon dioxide as per IPCC guidelines.[38]

$$CO_{2_{\mathrm{eq}_{CH_4}}} = 34$$

Cost factors for all metrics considered were estimated using calculations outlined in Table A1 and summarized again here as variables:

Table A2. Summary of cost factors from Table A1.

Description	**Variable**	**Value, unit**
Anaerobic Mixing	C_{ana}	\$ (2.18), \$/th m^3
Sludge Handling Costs	C_{solids}	\$ (0.23), \$/kgVSS
Oxygen Demand	C_{O_2}	\$ (0.12) \$/kg O_2 Dissolved
AnMBR Operation	C_{AnMBR}	\$ (14.82), \$/th m^3
COD Addition, Methanol	C_{CH_3OH}	\$ (0.29), \$/kgCOD
COD Addition, Methane	$C_{CH_4,added}$	\$ (0.03), \$/kgCOD
Methane Prodcution	$C_{CH_4,prod}$	\$ 0.17

Organism Characteristics

Table A3. Key Metabolism stoichiometric constants and biomass yields used in this model.

Process	**Key stoichiometric coefficients, S_{Z_Y}**	**Biomass Yield, Y_Y**	**Reference**
Heterotrophic Denitrification[5]	5 gCOD/gN	0.30 gVSS/gCOD	(Tchobanoglous G, Burton FL, & Stensel HD, 2014)
Heterotrophic Oxidation[5]	1 gO_2/gCOD	0.45 gVSS/gCOD	(Tchobanoglous G, Burton FL, & Stensel HD, 2014)[5]
Ammonium Oxidation[5]	1.5 molO_2/molNH_4	0.12 gVSS/gNH_4-N	(Tchobanoglous G, Burton FL, & Stensel HD, 2014)[5]
Nitrite Oxidation[5]	0.5 molO_2/molNO_2	0.05 gVSS/ gNO_2-N	(Tchobanoglous G, Burton FL, & Stensel HD, 2014)[5]
Anammox[5]	0.3 molNO_3/molNH_4[a] 1.3 molNO_2/molNH_4[a]	0.13 gVSS/ gNH_4-N[b]	(a) (Tchobanoglous, Burton FL, & Stensel HD, 2014)[5] (b) (Strous, Kuenen, & Jetten, 1999)[8]

Table A3 cont. Key Metabolism stoichiometric constants and biomass yields used in this model.			
N-Damo Archaea	0.25 mol CH_4/ molNO_2[a]	0.071 gCOD/ gCOD[b]	(a) (Haroon et al.,, 2014) [41] (b) (Winkler et al., 2015) [46]
Anaerobic Membrane Bioreactor	N/A	0.036 gCOD/ gCOD	(Gouveia et al., 2015)[192]

Constants

Table A4. Additional constants required for model calculations.		
Description	**Value**	**Reference**
Biomass conversion of VSS to COD, *n*	1.48 gVSS/gCOD	(Marais & Ekama, 1976)[141]
Universal gas constant, R	$0.082 \frac{m^3\ atm}{kmol\ K}$	

Sample Calculations

The following sample calculation was performed for all four scenarios given the following conditions:

$$Q = 40 \frac{th\ m^3}{d}$$

$$c_{N_{in}} = 40 \frac{mgN}{L}$$

$$c_{COD_{in}} = 100 \frac{mgCOD}{L}$$

Scenario A – Conventional Nitrification/Denitrification

In scenario A, a traditional MLE system, it was assumed that 100% of the influent nitrogen is completely nitrified and denitrified for 100% nitrogen removal and 100% of COD was consumed by heterotrophs.

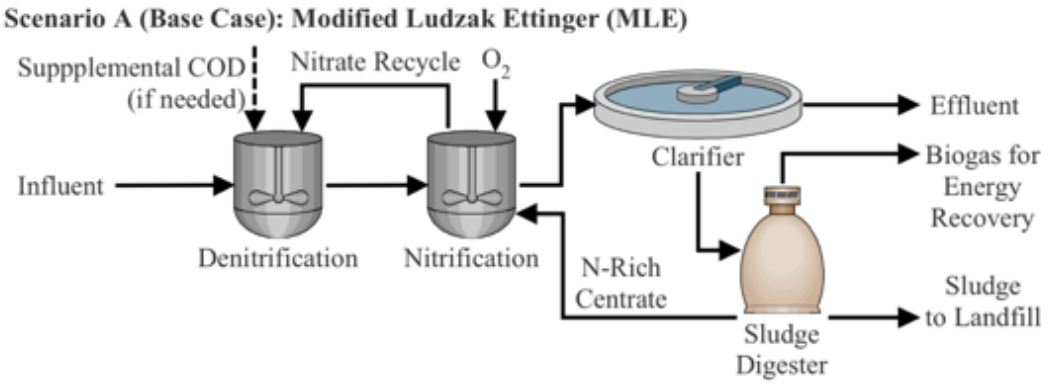

Figure A1. Replication of Scenario A taken from Figure 3-1 of the manuscript

The fractional conversion of constituent **Z** by organism **Y** in this scenario**,** f_{Z_Y}, were given in the table 3 below:

Table A5. Fractional conversions for scenario A, f_{Z_Y}			
Organism, Y	**AOB**	**NOB**	**Denitrifying Heterotrophs (Y is HET)**
Nitrogen (Z is N)	1	1	1
Scenario A.R Line #	20	21	28

Step 1) Total Contaminant Load
The COD load in the influent was calculated as:

$$L_{COD} = c_{COD_{in}} Q = 100\frac{mgCOD}{L} \times 40\frac{th\ m^3}{d} = 4000\frac{kgCOD}{d}$$ (equation A-2) scenarioA.R line 8

The nitrogen load in the influent was calculated as the total nitrogen load in the influent.

$$L_{N_{in}} = c_{N_{in}} \times Q = 40\frac{mgN}{L} \times 40\frac{ML}{d} = 1600\frac{kgN}{d}$$ (equation A-3) scenarioA.R line 9

The centrate from the anaerobic sludge digester (AD) was returned to the nitrification reactor for additional removal. It was assumed that 25% of total nitrogen load of the system resides in the centrate sidestream:

$$L_{N_{cent}} = N_{cent} \times L_{N_{in}} = 0.25\ \times 1600\frac{kgN}{d} = 400\frac{kgN}{d}$$ (equation A-4) scenarioA.R line 10

Therefore:

$$L_N = L_{N_{in}} + L_{N_{cent}} = 1600\frac{kgN}{d} + 400\frac{kgN}{d} = 2000\frac{kgN}{d}$$ (equation A-5) scenarioA.R line 11

Step 2) Nitrification
Oxygen demand by AOB and NOB is calculated as:

$$O_{2_{AOB}} = f_{N_{AOB}} L_N s_{O_{2_{AOB}}} \frac{MW_{O_2}}{MW_N} = 1 \times 2000\ \frac{kgN}{d} \times 1.5\frac{kmol\ O_2}{kmol_N} \times \frac{32kg/kmol}{14\ kg/kmol} = 6857\frac{kgO_2}{d}$$ (equation A-6) scenarioA.R line 22

$$O_{2_{NOB}} = f_{N_{NOB}} L_N s_{O_{2_{NOB}}} \frac{MW_{O_2}}{MW_N} = 1 \times 2000\ \frac{kgN}{d} \times 0.5\frac{kmol\ O_2}{kmol_N} \times \frac{32kg/kmol}{16kg/kmol} = 2286\frac{kgO_2}{d}$$ (equation A-7) scenarioA.R line 23

Sludge production by AOB and NOB is calculated as:

$$p_{x_{AOB}} = f_{N_{AOB}} L_N Y_{AOB} =$$ (equation A-8) scenarioA.R line 24

$$1 \times 2000\ \frac{kgN}{d} \times 0.12 \frac{kgVSS}{kgN} = 240 \frac{kgVSS}{d}$$

$$p_{x_{NOB}} = f_{N_{NOB}} L_N Y_{NOB} = \quad \text{(equation A-9)}$$
$$1 \times 2000\ \frac{kgN}{d} \times 0.05 \frac{kgVSS}{kgN} = 240 \frac{kgVSS}{d} \quad \text{scenarioA.R line 25}$$

Step 3) Denitrification

In order to remove nitrogen, COD was required in a 1:5 N/C ratio ($s_{COD_{DENIT}}$) for denitrification and therefore the total COD required was calculated as:

$$COD_{req'd} = f_{N_{DENIT}} L_N s_{COD_{DENIT}} = \quad \text{(equation A-10)}$$
$$1 \times 2000\ \frac{kgN}{d} \times 5 \frac{gCOD}{gN} = 10000 \frac{kgCOD}{d} \quad \text{scenarioA.R line 29}$$

The biomass yield of denitrifying heterotrophs was calculated as:

$$p_{x_{DENIT}} = COD_{req'd} Y_{DENIT} = \quad \text{(equation A-11)}$$
$$10000 \frac{kgCOD}{d} \times 0.3 \frac{kgVSS}{kg} = 3000 \frac{kgVSS}{d} \quad \text{scenarioA.R line 30}$$

In order to determine whether additional COD needs to be externally supplied to remove the nitrogen in the influent a COD balance was preformed:

$$COD_{bal} = COD_{req'd} - L_{COD} = \quad \text{(equation A-12)}$$
$$10000 \frac{kgCOD}{d} - 4000 \frac{kgCOD}{d} = 6000 \frac{kgCOD}{d} \quad \text{scenarioA.R line 31}$$

At these conditions, ($COD_{bal} > 0$) additional COD was required, therefore:

$$COD_{added} = COD_{bal} = 6000 \frac{kgCOD}{d} \quad \text{(equation A-13)}$$
$$\text{scenarioA.R line 33}$$

However, if $COD_{bal} < 0$ (at higher COD/N ratios) there is more COD than can be removed by denitrification ($COD_{bal} < 0$), and:

$$COD_{added} = 0 \quad \text{(equation A-14)}$$
$$\text{scenarioA.R line 32}$$

Furthermore, if $COD_{bal} < 0$, additional oxygen will be required for heterotrophic oxidation of the remaining COD (after denitrification):

$$O_{2_{HET}} = COD_{bal} \quad \text{(equation A-15)}$$
$$\text{scenarioA.R lines 35-36}$$

Finally, the the biomass yield of aerobic heterotrophs was calculated as follows:

$$p_{x_{HET}} = COD_{bal} Y_{HET} \quad \text{(equation A-16)}$$
$$\text{scenarioA.R line 37-38}$$

Step 4) Anaerobic Digestion

The total sludge load into the AD was the sum of all biomass yields from all organisms:

$$p_{x_{TOT}} = \sum p_{x_Y} = \quad \text{(equation A-17)}$$
$$\text{scenarioA.R line 62}$$

$$240 + 100 + 3000 + 0 = 3340 \frac{kgVSS}{d}$$

The sludge load from the AD (total sludge handling demand of the MLE system) was determined using the assumed sludge reduction factor defined above:

$$p_{x_{out}} = p_{x_{TOT}} \times \left(1 - f_{x_{AD}}\right) = \quad \text{(equation A-18)}$$
$$3340 \frac{kgVSS}{d} \times (1 - 0.59) = 1369 \frac{kgVSS}{d} \quad \text{scenarioA.R line 63}$$

Digested COD was assumed to be coverted to biogas in a ratio of 0.74 m^3/kgVSS destroyed so volume of biogas produced is calculated as:

$$Biogas_{vol} = \left(p_{x_{TOT}} - p_{x_{out}}\right) \times BG \quad \text{(equation A-19)}$$
$$(3340 - 1369) \frac{kgVSS}{d} \times 0.75 \frac{kgCH_4}{kgCOD} \quad \text{scenarioA.R lines 64}$$
$$= 1478 \frac{m^3 biogas}{d}$$

As calculated in Table A1, mass of methane in biogas is estimated given biogas density, ρ_{BG}=0.86 kg/m^3, and methane concentration in biogas, x_{CH_4}=0.62

$$CH_{4_{burn}} = V_{biogas} \times \rho_{BG} \times x_{CH_4} = \quad \text{(equation A-20)}$$
$$1478 \frac{m^3 biogas}{d} \times 0.62 \frac{m^3\ CH_4}{m^3\ biogas} \times 0.86 \frac{kg}{m^3} \quad \text{scenarioA.R lines 65}$$
$$= 788 \frac{kg\ CH_4}{d}$$

Step 5) Electrical Demand

The electrical demand due to sludge thickening and aeration were considered. The electrical demand for aeration was based on the total oxygen demand of the system

$$O_{2_{TOT}} = \sum O_{2_Y} = \quad \text{(equation A-22)}$$
$$6857 + 2286 = 9143 \frac{kgO_2}{d} \quad \text{scenarioA.R line 76}$$

From this the electrical demand due to aeration was estimated as follows:

$$E_{O_2} = O_{2,TOT}\, e_{O_2} = 9143 \frac{kgO_2}{d} \times 1.5 \frac{\text{kWh}}{\text{kg}O_2} \quad \text{(equation A-23)}$$
$$= 13700 \frac{kWh}{d} \quad \text{scenarioA.R line 80}$$

The electrical demand from the sludge dewatering system was based on the mass of sludge leaving the digester:

$$E_{Solids} = p_{x_{out}} e_{solids} \quad \text{(equation A-24)}$$
$$= 1369 \frac{kgVSS}{d} \times 2.24 \frac{\text{kWh}}{\text{kgVSS}} \quad \text{scenarioA.R line 81}$$
$$= 3070 \frac{kWh}{d}$$

The electrical demand required for mixing the denitrification tank was from biogas in the combined heat and power plant (CHP) is based on the mass of methane produced in the digester and estimated as follows:

$$E_{mix} = Q \times e_{base} = \quad \text{(equation A-25)}$$
$$= 40 \times 10^3 \frac{m^3}{d} \times 28 \frac{kWh}{10^3 m^3} = 1120 \frac{kWh}{d} \quad \text{scenarioA.R line 82}$$

The electricity recovered from biogas in the combined heat and power plant (CHP) is based on the mass of methane produced in the digester and estimated as follows:

$$E_{CHP} = -CH_{4_{burn}} e_{cogen} \quad \text{(equation A-26)}$$
$$= -788 \frac{kgCH_4}{d} \times 2.2 \frac{kWh}{kgCH_4} = -1730 \frac{kWh}{d} \quad \text{scenarioA.R line 84}$$

The total GHG emission is calculated as the non-biogenic CO_2 produced from electrical consumption as reported by the U.S. Energy & Information Administration and the biogenic CO_2 produced from external COD added. The amount of CO_2 produced per kg methanol added is calculated in Table A1:

$$CO_{2_{TOT}} = \frac{kgCO_2}{kWh} \sum E_Y + COD_{added} \times s_{CH_3OH/CO_2} \quad \text{(equation A-27)}$$
$$\text{scenarioA.R line 86}$$
$$= (13700 + 3070 + 1120 - 1730) \frac{kWh}{d} \times 0.47 \frac{kgCO_2}{kWh}$$
$$+ 6000 \times 0.92$$
$$= 13100 \frac{kgCO_2}{d}$$

Step 6) Scenario A Cost Estimation

The key cost factors were combined together by multiplying them each by an estimated cost per units calculated in Table A1. They are then added together to provide a base cost factor. This does not represent the operational cost of the plant, but instead provides a value that can be compared to the other scenarios to estimate how much would be saved using the other theoretical systems examined in this study. In this scenario, methanol is used as the additive COD if required for denitrification.

$$Cost_A = CH_{4_{burn}} \times C_{CH_4,prod} + COD_{added} \times C_{COD_{CH_3OH}} \quad \text{(equation A-28)}$$
$$+ p_{x_{out}} \times C_{solids} + O_{2_{TOT}} \times C_{O_2} + C_{ana} \times Q = \quad \text{scenarioA.R line 89}$$
$$788 \frac{kgCH_4}{d} \times \frac{\$0.17}{kgCH_4} + 6000 \frac{kgCOD}{d} \times -\frac{\$0.29}{kgCOD_{CH_3OH}}$$
$$+ 1369 \frac{kgVSS}{d} \times -\frac{\$0.23}{kgVSS} + 9143 \frac{kgO_2}{d} \times -\frac{\$0.12}{kgO_2}$$
$$+ \frac{\$2.18}{th\ m^3} \times 60 \frac{th\ m^3}{d} = -\frac{\$3080}{d}$$

Step 7) Scenario A Summary

Table A6. The following cost and equivalent GHG emissions are reported from ScenarioA.R when using the input used in this sample calculation		
Metric	**Combined Cost of Key Metrics**	**GHG Emissions**
Variable	$Cost_{compare,A}$	$CO_{2_{TOT}}$
ScenarioA.R Line #(s)	98	97
Value	-$3080/d	13100 kgCO_2/d

Scenario B – HRAS/Anammox

In scenario B it was assumed that all COD was removed aerobically by heterotrophs. Furthermore, it was assumed enough of the influent nitrogen was partially nitrified from ammonium to nitrite by AOB in order to supply anammox with a stoichiometric ratio of nitrite:ammonium, calculated with the anammox metabolic reaction:

$$NH_4^+ + 1.3\,NO_2^- \rightarrow N_2 + 0.3\,NO_3^- \qquad \text{(reaction A-1)}$$

The fraction of influent ammonium undergoing partial nitrification by AOB is then calculated as:

$$f_{N_{AOB}} = \frac{1.3\ kgNO_2^- - N}{1\ kgNH_4^+ - N + 1.3 kgNO_2^- - N} = 0.565 \qquad \text{(equation A-29)}$$

The rest of the influent ammonium is then anaerobically oxidized by anammox, therefore:

$$f_{N_{ANAMX}} = 1 - f_{N_{AOB}} \qquad \text{(equation A-30)}$$
$$= 1 - 0.565 = 0.435$$

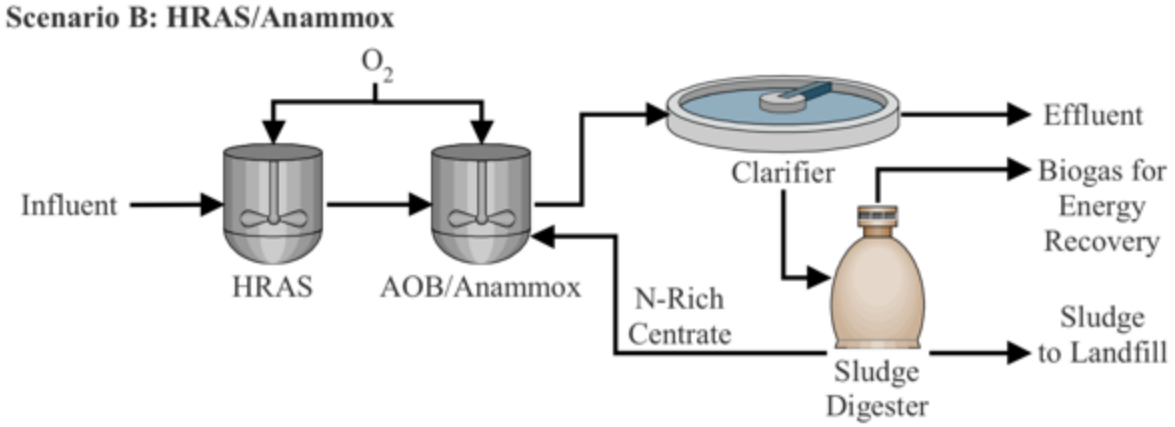

Figure A2. Replication of Scenario B taken from Figure 1 of the manuscript

The fractional conversion of constituent **Z** by organism **Y** in this scenario, f_{Z_Y}, are given in the table 5 below:

Table A7. Fractional conversions for scenario B, f_{Z_Y}				
Organism, Y	**AOB**	**NOB**	**Anammox (Y is ANAMX)**	**Heterotrophs (Y is HET)**
Nitrogen (Z is N)	0.565	0	0.435	N/A
COD	N/A	N/A	N/A	1
Scenario B.R Line #	20	21	28	16

Step 1) Total Contaminant Load
Calculated identically to scenario A using equations SI-1 thru SI-4 (scenarioB.R lines 8-11).
Step 2) High Rate Activated Sludge for COD Removal
Biomass yield and oxygen demand were calculated with equations SI-15 and SI-16,respectively (but using total COD load L_{COD} instead of the COD balance).

$$p_{x_{HET}} = L_{COD} Y_{DENIT} = 4000 \frac{kgCOD}{d} \times 0.45 \frac{kgVSS}{kgCOD} = 1800 \frac{kgVSS}{d}$$ scenarioB.R line 16

$$O_{2_{HET}} = L_{COD} = 4000 \frac{kgO_2}{d}$$ scenarioB.R line 17

Step 2) Nitrification
Biomass yield and oxygen demand were calculated by equations SI-6 thru 9 utilizing the fractional conversion calculated in SI-29 and given in Table A7:

$$O_{2_{AOB}} = f_{N_{AOB}} L_N s_{O_{2_{AOB}}} \frac{MW_{O_2}}{MW_N} = 0.565 \times 2000 \times 1.5 \times \frac{32}{14}$$ scenarioB.R line 22

$$= 3874 \frac{kgO_2}{d}$$

$$p_{x_{AOB}} = f_{N_{AOB}} L_N Y_{AOB} = 0.565 \times 2000 \times 0.12 = 136 \frac{kgVSS}{d}$$ scenarioB.R line 24

Because it was assumed there is no NOB activity in this scenario, $O_{2_{NOB}} = 0$, $p_{x_{NOB}} = 0$ (scenarioB.R line 23 & 25)
Step 3) Anammox
Sludge production by anammox was calculated according to equation A-8:

$$p_{x_{ANAMX}} = f_{N_{ANAMX}} L_N Y_{ANAMX} =$$ scenarioB.R line 32

$$0.435 \times 2000 \frac{kgN}{d} \times 0.13 \frac{kgVSS}{kgN} = 113 \frac{kgVSS}{d}$$

Step 4) Anaerobic digester
This system was identical to scenario A. Sludge handling demand and methane available for energy recovery were calculated with equations SI-17 thru SI-20:

$$p_{x_{out}} = 839\ kgVSS/d$$ scenarioB.R line 62 & 63

$$V_{biogas} = 907 \frac{m^3}{d}$$ scenarioB.R line 64 & 6

$$CH_{4_{burn}} = 483 \frac{kgCH_4}{d}$$

Step 5) Electrical Demand
The electrical demands were considered in the same way as done in scenario A with equations SI-21 thru SI-27.

$$O_{2_{TOT}} = 7870 \frac{kgO_2}{d}$$ scenarioB.R line 75

$$E_{O_2} = 11800 \frac{kWh}{d}$$ scenarioB.R line 79

$$E_{solids} = 1880 \frac{kWh}{d}$$ scenarioB.R line 80

$$E_{CHP} = -1060\frac{kWh}{d}$$ scenarioB.R line 82

$$CO_{2_{TOT}} = 5940\ \frac{kgCO_2}{d}$$ scenarioB.R line 83

Step 6) Cost Estimation

As in scenario A, the key cost factors were combined with a modified version of equation A-28. Because there is no denitrification, no external COD will be added in this scenario, so that term was not included.

$$Cost_B = CH_{4_{burn}} \times C_{CH_4,prod} + p_{x_{out}} \times C_{solids} + O_{2_{TOT}} \times C_{O_2} = \quad \text{scenarioB.R line 88}$$
$$483\frac{kgCH_4}{d} \times \frac{\$0.17}{kgCH_4} + 839\frac{kgVSS}{d} \times -\frac{\$0.23}{kgVSS}$$
$$+ 7870\frac{kgO_2}{d} \times -\frac{\$0.12}{kgO_2} = \frac{\$1031}{day}$$

The most effective way to consider this number is in comparison to the combined cost metrics from a conventional nitrification/denitrification system at the same conditions (flowrate, nitrogen and carbon concentration). That is done as follows:

$$Cost_{compare} = -(Cost_A - Cost_B) = -\left(\frac{-\$3080}{d} - \frac{-\$1030}{day}\right)$$ (equation A-31) masterrun.R line 111

$$= \frac{\$2050}{day}(\$\ are\ saved)$$

Therefore, we roughly estimate that operating an HRAS/anammox system as the same conditions would save $2050. The same comparison is made for GHG emissions:

$$GHG_{compare} = -(GHG_A - GHG_B)$$ masterrun.R line 106

$$= -\left(\frac{13100\ kg\ CO_2}{d} - \frac{5940\ kg\ CO_2}{day}\right)$$
$$= -7180\ (emissions\ averated)$$

Step 7) Scenario Summary

Table A8. The following metrics are reported from ScenarioB.R when using the input used in this sample calculation

Metric	**Combined Cost of Key Metrics**	**Comparitive Cost**	**GHG Emissions**	**Comparitive GHG Emissions**
Variable	$Cost_B$	$Cost_{compare}$	GHG_b	$GHG_{compare}$
Location in Code	ScenarioB.R Line 95	masterrun.R Line 111	ScenarioB.R Line 94	masterrun.R Line 106
Value	-$1030/d	$2050/d (saved)	5940 $kgCO_2$/d	7180 $kgCO_2$/d (GHG Redcued)

Scenario C – AnMBR/Anammox

In scenario C, nitrogen removal was calculated identically to the AOB/Anammox scenario in scenario B. 100% COD removal was assumed to be achieved by an AnMBR system.

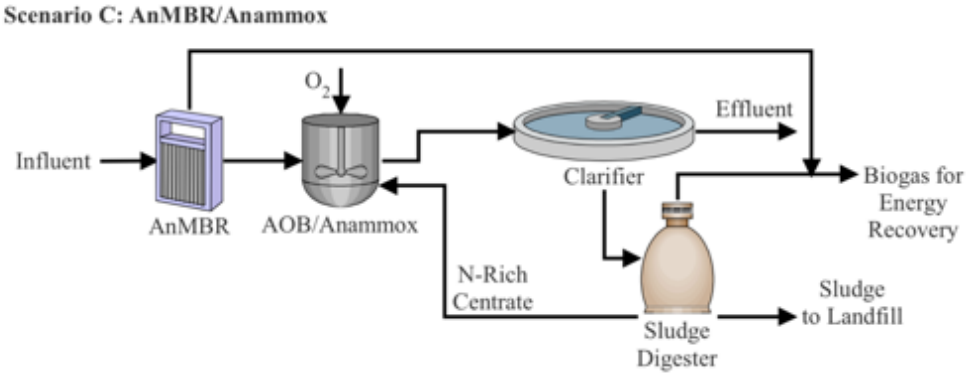

Figure A3. Replication of Scenario C taken from Figure 1 of the manuscript

Table A9. Fractional conversions for scenario C, f_{Z_Y}				
Organism, Y	**AOB**	**NOB**	**Anammox (Y is ANAMX)**	**AnMBR**
Nitrogen (Z is N)	0.565	0	0.435	N/A
COD	N/A	N/A	N/A	1
Scenario C.R Line #	20	21	28	35

Step 1) Total Contaminant Load

This was calculated identically to scenario A using equations SI-1 thru SI-4 (scenarioC.R lines 8-11).

Step 2) Nitrification & Anammox for Nitrogen Removal

Biomass yield and oxygen demand were calculated identically to scenario B with equations SI-6 thru 9 and the fractional conversion calculated in SI-29 and given in table 7, therefore $O_{2_{AOB}} = 3874\frac{kgO_2}{d}$, $p_{x_{AOB}} = 136\frac{kgVSS}{d}$, & $p_{x_{ANAMX}} = 113\frac{kgVSS}{d}$ (scenarioC.R lines 22, 24 & 29)

Step 2) Nitrification & Anammox for Nitrogen Removal

Sludge production from the AnMBR was calculated by equation A-8 as follows:

$$p_{x_{AnMBR}} = f_{COD_{AnMBR}} L_{COD} Y_{AnMBR} n = 1 \times 4000\frac{kgCOD}{d} \times 0.036\frac{kgCOD}{kgCOD} \times 1.48\frac{kgVSS}{kgCOD} = 213\frac{kgVSS}{d}$$ scenarioC.R line 36

COD was assumed to be converted to methane by equation as follows:

$$CH_{4_{prod}} = f_{COD_{AnMBR}} L_{COD}(1 - Y_{AnMBR})\frac{kgCH_4}{kgCOD} =$$ (equation A-32) scenarioC.R line 39

$$1 \times 4000 \frac{kgCOD}{d} \times \left(1 - 0.036 \frac{kgCOD}{kgCOD}\right) \times 4$$
$$= 15424 \frac{kgCH_4}{d}$$

Step 2) Nitrification & Anammox for Nitrogen Removal

The mass of dissolved methane was determined using the saturated dissolved methane concentration determined in equation A-1 and the following:

$$L_{CH_{4_{diss,sat}}} = Qc_l^* = \quad \text{(equation A-33) scenarioC.R line 41}$$
$$40 \frac{ML}{d} \times 0.0224 \frac{kgCH_4}{m^3} \times 10^3 \frac{m^3}{ML} = 896 \frac{kgCH_4}{d}$$

The amount of methane available for energy recovery from the AnMBR was adjusted by removing the fraction of methane that was dissolved:

$$CH_{4_{burn_{AnMBR}}} = CH_{4_{prod_{AnMBR}}} - L_{CH_{4_{diss}}} = \quad \text{(equation A-34) scenarioC.R line 42}$$
$$15424 \frac{kgCH_4}{d} - 896 \frac{kgCH_4}{d} = 14528 \frac{kgCH_4}{d}$$

NOTE: If less methane was produced than could be dissolved at equilibrium ($CH_{4_{prod}} < L_{CH_{4_{diss}}}$) , it was assumed that all methane was captured in the dissolved phase for simplicity in order to simulate a "worst case scenario" for comparison to the base case.

$$L_{CH_{4_{diss}}} = CH_{4_{prod_{AnMBR}}}; \; CH_{4_{burn_{AnMBR}}} = 0 \quad \text{(equation A-35) scenarioC.R line 43-44}$$

Step 5) Fate of Dissolved Methane in Nitrification Reactor

Based on results from Daelman et al., 2014[191] it was assumed that at low methane concentrations ($c_{\mathrm{CH_4}} < 5 \frac{mgCOD}{L}$), methane would be 100% stripped from the reactor. At high methane concentrations, methane would be 90% oxidized by aerobic methanotrophs and the remaining 10% would be stripped out[191].

$$CH_{4_{MOB,ox}} = 0.9 \times L_{CH_{4_{diss,sat}}} = \quad \text{(equation A-36) scenarioC.R line 52}$$
$$0.9 \times 896 \frac{kgCH_4}{d} = 806 \frac{kgCH_4}{d}$$

The residual dissolved methane was then calculated as:

$$L_{CH_{4_{diss}}} = L_{CH_{4_{diss,sat}}} - CH_{4_{MOB,ox}} = \quad \text{(equation A-37) scenarioC.R line 56}$$
$$896 \frac{kgCH_4}{d} - 806 \frac{kgCH_4}{d} = 90 \frac{kgCH_4}{d}$$

Sludge produced by MOBs was calculated with a modified version of equation A-8, $p_{x_{MOB}} = 56.7 \frac{kgVSS}{d}$ (scenarioC.R line 58).

Oxygen demand of MOBs was determined by converting methane consumed to chemical oxygen demand (COD).

$$O_{2_{MOB}} = CH_{4_{MOB,ox}} s_{O_{2_{MOB}}} = \quad \text{(equation A-38) scenarioC.R line 57}$$
$$806 \frac{kgCH_4}{d} \times 0.25 \frac{kgO_2}{kgCH_4} = 201 \; kg \; O_2$$

Step 6) Anaerobic digester

This system was calculated identically to scenario A. Sludge handling demand and methane available for energy recovery were calculated with equations SI-17 thru SI-20.

$$p_{x_{out}} = 213\ kgVSS/d$$ scenarioC.R line 63

$$V_{biogas} = 229\frac{kgCH_4}{d}; CH_{4_{prod_{AD}}} = 122\frac{kgCH_4}{d}$$ scenarioC.R line 64 & 65

with the addendum that the total methane available for energy regeneration was the sum of methane from both the AnMBR and the AD:

$$CH_{4_{burn}} = CH_{4_{prod_{AD}}} + CH_{4_{burn_{AnMBR}}} = 122 + 14500 = 14700\frac{kgCH_4}{d}$$ (equation A-39) scenarioC.R line 66

Step 7) Electrical Demand

The electrical demand is considered in the same way as in scenario A with equations SI-21 thru SI-27.

$$O_{2_{TOT}} = 4080\frac{kgO_2}{d}$$ scenarioC.R line 76

$$E_{O_2} = 6110\frac{kWh}{d}$$ scenarioC.R line 80

$$E_{solids} = 7600\frac{kWh}{d}$$ scenarioC.R line 81

$$E_{CHP} = -32200\frac{kWh}{d}$$ scenarioC.R line 84

In addition to these demands, the electrical energy for scouring and mixing of the AnMBR was determined on a volumetric basis:

$$E_{AnMBR} = Q \times e_{AnMBR} = 40\frac{10^3 m^3}{d} \times 190\frac{kWh}{10^3 m^3} = 7600\frac{kWh}{d}$$ (equation A-40) scenarioC.R line 83

The total emissions were then calculated as the sum of the electrical demands and sources calculated above plus the amount of dissolved methane exiting the system adjusted to CO2 equivalents.

$$CO_{2_{TOT}} = \frac{kgCO_2}{kWh}\sum E_Y + \frac{CO_2}{CH_{4_{eq}}} L_{CH_{4_{diss}}} = (-18000)\frac{kWh}{d} \times 0.47\frac{kgCO_2}{kWh} + 90 \times 34\frac{kgCO_2}{kgCH_4} = -5450\frac{kgCO_2}{d}$$ (equation A-41) scenarioC.R line 85

Step 8) Cost Estimation

As in scenario A, the key cost factors were combined with a modified version of equation A-28. Because there is no denitrification, no external COD will be added in this scenario, so that term is not included. The cost of electricity used operating an AnMBR is included.

$$Cost_C = CH_{4_{burn}} \times C_{CH_4,prod} + p_{x_{out}} \times C_{solids} + O_{2_{TOT}} \times C_{O_2} + Q \times C_{AnMBR} =$$ scenarioC.R line 88

$$14700\frac{kgCH_4}{d}\times\frac{\$0.17}{kgCH_4}+\ 212\ \frac{kgVSS}{d}\times-\frac{\$0.23}{kgVSS}$$
$$+\ 4080\frac{kgO_2}{d}\times-\frac{\$0.12}{kgO_2}+40\ \frac{th\ m^3}{d}\times-\frac{\$14.82}{th\ m^3}$$
$$=\frac{\$1400}{d}$$

This value is positive because so much energy is generated from biogas cogeneration from mainstream anaerobic digestion. It does not suggest that this WRRF would make money or that it is energy positive, because these calculations only include the key metrics that would be most greatly affected by the theoretical technologies examined in this study. The most effective way to consider this number is in comparison to the combined cost metrics from a conventional nitrification/denitrification system at the same conditions (flowrate, nitrogen and carbon concentration). That is done as follows:

masterrun.R line 112

$$Cost_{compare}=Cost_A-Cost_C=-\left(\frac{-\$3080}{d}-\frac{\$1400}{day}\right)$$
$$=\frac{\$4470}{day}\ (cost\ saved)$$

The same comparison is made for GHG emissions:

masterrun.R line 107

$$GHG_{compare}=-(GHG_A-GHG_C)$$
$$=-\left(\frac{13100\ kg\ CO_2}{d}-\frac{5450\ kg\ CO_2}{day}\right)$$
$$=18565\ (emissions\ averated)$$

Step 9) Scenario Summary

Table A10. The following metrics are reported from ScenarioC.R when using the input used in this sample calculation

Metric	**Combined Cost of Key Metrics**	**Comparitive Cost**	**GHG Emissions**	**Comparitive GHG Emissions**
Variable	$Cost_C$	$Cost_{compare}$	GHG_C	$GHG_{compare}$
Location in Code	ScenarioC.R Line 97	masterrun.R Line 112	ScenarioC.R Line 96	masterrun.R Line 107
Value	-$3080/d	$4470/d ($ saved)	-5450 kgCO_2/d	-18565 kgCO2/d (GHG Reduced)

Scenario D – HRAS/Anammox & N-Damo

In scenario D it was assumed that all COD was removed aerobically by heterotrophs. Furthermore, it was assumed enough of the influent nitrogen underwent nitrification in order to supply anammox and n-damo with a stoichiometric ratio of nitrate and ammonium, calculated with the anammox and n-damo metabolic reactions:

$$Anammox: NH_4^+ + 1.3\,NO_2^- \rightarrow N_2 + 0.3\,NO_3^- \quad \text{(reaction A-1)}$$
$$N-damo:\ 0.3\,NO_3^- \rightarrow\ 0.3\,NO_2^- \quad \text{(reaction A-2)}$$
$$Overall:\ NH_4^+ + NO_2^- \rightarrow N_2$$

The fraction of influent ammonium undergoing nitrification was then calculated as:

$$f_{N_{NOB}} = f_{N_{AOB}} = \frac{1\,kgNO_2^- - N}{1\,kgNH_4^+ - N + 1\,kgNO_2^- - N} = 0.5 \quad \text{(equation A-42) scenarioD.R line 21}$$

The rest of the influent ammonium was then anaerobically oxidized by anammox, therefore:

$$f_{N_{ANAMX}} = 1 - f_{N_{AOB}} = 0.5 \quad \text{(equation A-43) scenarioB.R line 29}$$

N-damo will reduce all nitrate produced from the nitrification reactor as well as the nitrate produced by anammox (stoichiometric coefficient in reaction A-1 of 0.3).

$$f_{N_{NDAMO}} = f_{N_{NOB}} + 0.3 = 0.8 \quad \text{(equation A-44) scenarioC.R line 30}$$

Table A11. Fractional conversions for scenario D, f_{Z_Y}

Organism, Y	AOB	NOB	Anammox (Y is ANAMX)	N-damo (Y is NDAMO)	Heterotrophs (Y is HET)
Nitrogen (Z is N)	0.5	0.5	0.435	0.8	N/A
COD	N/A	N/A	N/A	N/A	1
Scenario D.R Line #	20	21	28	29	15

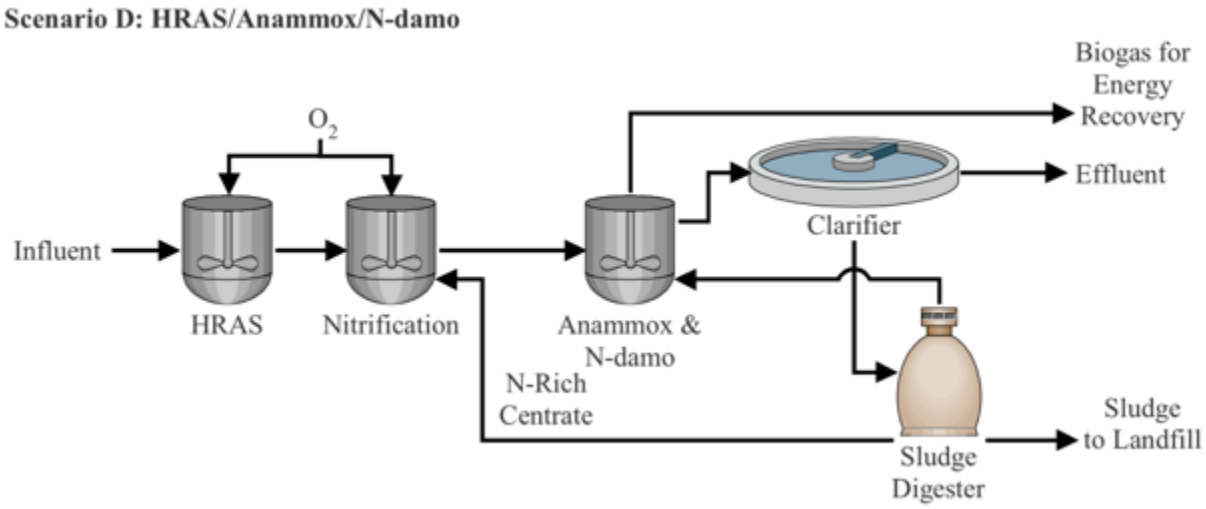

Figure A4. Replication of Scenario D taken from Figure 1 of the manuscript

The addition of n-damo will increase the total oxygen demand by 16% as compared to an anammox system. In partial nitritation/anammox system, 1 mole nitrogen requires 0.84 mole O_2 in order for AOB to convert 56% ($f_{N_{AOB,scenario\,B}}$, Table A9) to nitrite for anammox. (Recall AOB require 1.5 molO_2/molNH_4, Table A3):

$$0.84\ \frac{mol\ O_2}{mol\ NH_4} = 1\ mol\ NH_4 \times 0.56\ \times \frac{1.5\ mol\ O_2}{1\ mol\ NH_4}$$ (equation A-45)

Meanwhile, in an nitrification/anammox/n-damo system, 1 mole nitrogen will require 1 mol O2 in order for AOB & NOB to completely convert 50% ($f_{N_{AOB,}}$ & $f_{N_{NOB\,scenario\,D}}$, Table A11) of influent ammonium to nitrate for n-damo. (Recall NOB requires an additional 0.5 molO_2/molNH_4, Table A3 and therefore complete nitrification requires 2 molO_2/molNH_4)

$$1\ \frac{mol\ O_2}{mol\ NH_4} = 1\ mol\ NH_4 \times 0.50\ \times \frac{2\ mol\ O_2}{1\ mol\ NH_4}$$ (equation A-46)

Therefore, there is a 16% increase in oxygen demand with the addition of n-damo:

$$16\% = \frac{1 - 0.84}{1}$$ (equation A-47)

Step 1) Total Contaminant Load
Calculated identically to scenario A using equations SI-1 thru SI-4 (scenarioD.R lines 8-11).
Step 2) High Rate Activated Sludge for COD Removal
Calculated identically to scenario B using equations SI-15 thru SI-16. (scenarioD.R lines 16-17).
Therefore: $p_{x_{HET}} = 1800\frac{kgVSS}{d}$, $O_{2_{HET}} = 4000\frac{kgO_2}{d}$.

Step 3) Nitrification
Given the above defined fractional conversions, biomass yield and oxygen demand were calculated for each nitrfier (AOB and NOB) via equations SI-6 thru 9:

$$O_{2_{AOB}} = 3429\frac{kgO_2}{d}, \qquad O_{2_{NOB}} = 1143\frac{kgO_2}{d}$$ scenarioD.R lines 22 & 23

$$p_{x_{AOB}} = 120\frac{kgVSS}{d}, \qquad p_{x_{NOB}} = 50\frac{kgVSS}{d}$$ scenarioD.R lines 24 & 25

Step 4) Anammox & N-Damo
Biomass yield of anammox was calculated via modifying equation A-8:

$$p_{x_{ANAMX}} = 130\frac{kgVSS}{d}$$ scenarioD.R line 31

The above defined fractional conversion for n-damo and the n-damo stoichiometric coefficient of methane was used to determine the total mass of methane consumed as well as sludge produced by n-damo:

$$L_{CH_{4_{cons}}} = L_N f_{N_{NDAMO}} s_{CH_{4_{NDAMO}}} \frac{MW_{CH_4}}{MW_N} =$$ (equation A-48) scenarioD.R line 30

$$2000 \times 0.8 \times 0.25 \times \frac{16}{14} = 457\frac{kgCH_4}{d}$$

$$p_{x_{NDAMO}} = \frac{L_{CH_{4cons}} Y_{ANAMX}}{\frac{kgCH_4}{kgCOD}} n = \quad \text{(equation A-49)}$$ scenarioD.R line 32

$$\frac{457\frac{kgCH_4}{d} \times 0.071\frac{kgCOD}{kgCOD}}{4} \times 1.48\frac{kgVSS}{kgCOD} = 12.1\frac{kgVSS}{d}$$

Step 5) Anaerobic Digester

This system was calculated identically to scenario A. Sludge handling demand and methane available for energy recovery were calculated with equations SI-17 thru SI-20.

$$p_{x_{out}} = 866\, kgVSS/d$$ scenarioD.R line 62 & 63

$$V_{biogas} = 936\frac{m3}{d};\ CH_{4_{prod}} = 498\frac{kgCH_4}{d}$$ scenarioD.R line 64

Step 6) Methane Balance

Methane available for energy recovery must be adjusted since n-damo will consume some as an electron donor:

$$CH_{4_{burn}} = CH_{4_{prod}} - L_{CH_{4cons}} = \quad \text{(equation A-50)}$$ scenarioD.R line 69

$$3368 - 457 = 41\frac{kgCH_4}{d}$$

In this example calculation, there was enough methane available for n-damo ($CH_{4_{burn}} > 0$) and:

$$COD_{added} = 0$$ (equation A-51) scenarioD.R line 71

NOTE: At low COD/N ratios, this may not be the case. Therefore if $CH_{4_{burn}} < 0$:

$$COD_{added} = \frac{-CH_{4_{burn}}}{\frac{kgCH_4}{kgCOD}}$$ (equation A-52) scenarioD.R line 72

$$CH_{4_{burn}} = 0$$ (equation A-53) scenarioD.R line 73

Step 7) Electrical Demand

The electrical demands were considered in the same way as in scenario A with equations SI-21 thru SI-27.

$$E_{base} = 10160\frac{kgO_2}{d}$$ scenariD.R line 79

$$O_{2_{TOT}} = 8571\frac{kgO_2}{d}$$ scenarioD.R line 76

$$E_{O_2} = 12900\frac{kWh}{d}$$ scenarioD.R line 80

$$E_{solids} = 140\frac{kWh}{d}$$ scenarioD.R line 81

$$E_{mix} = 1120\frac{kWh}{d}$$ scenarioD.R line 82

$$E_{CHP} = -90.5\frac{kWh}{d}$$ scenarioD.R line 84

$$CO_{2_{TOT}} = 7440\ \frac{kgCO_2}{d}$$ scenarioD.R line 85

Step 8) Cost Estimation

Key cost factors were combined with a modified version of equation A-27. If external COD addition is required, it would be in the form as methane in natural gas, so that term is modified for the cost of natural gas.

$$Cost_D = CH_{4_{burn}} \times C_{CH_4,prod} + p_{x_{out}} \times C_{solids} + O_{2_{TOT}} \times C_{O_2} + COD_{added} \times C_{CH_4,added} =$$ scenarioD.R line 88

$$41.1\frac{kgCH_4}{d} \times \frac{\$0.17}{kgCH_4} + 866\ \frac{kgVSS}{d} \times -\frac{\$0.19}{kgVSS} + 8571\frac{kgO_2}{d} \times -\frac{\$0.12}{kgO_2} + 0\frac{kgCOD}{d} \times -\frac{\$0.13}{kgCOD} = \frac{-\$1280}{d}$$

As with all other scenarios, this is compared to the base case as follows:

$$Cost_{compare} = Cost_A - Cost_D = \frac{-\$3080}{d} - \frac{-\$1280}{day} = \frac{\$1790}{day}\ (cost\ saved)$$ masterrun.R line 113

The same comparison is made for GHG emissions: masterrun.R line 108

$$GHG_{compare} = -(GHG_A - GHG_B) = -\left(\frac{13100\ kg\ CO_2}{d} - \frac{7440\ kg\ CO_2}{day}\right) = -5680\ (emissions\ averated)$$

Step 9) Scenario Summary

Table A12. The following metrics are reported from ScenarioD.R when using the input used in this sample calculation

Metric	**Combined Cost of Key Metrics**	**Comparitive Cost**	**GHG Emissions**	**Comparitive GHG Emissions**
Variable	$Cost_D$	$Cost_{compare}$	GHG_D	$GHG_{compare}$
Location in Code	ScenarioD.R Line 97	masterrun.R Line 113	ScenarioD.R Line 96	masterrun.R Line 108
Value	-$1280/d	$4470/d ($ saved)	7440 kgCO_2/d	5680 kgCO2/d (GHG Reduced)

Scenario E – AnMBR/Anammox & N-Damo

In scenario E it was assumed 100% of COD was removed by an AnMBR system, and 100% of nitrogen was removed with n-damo and anammox identically to scenario D.

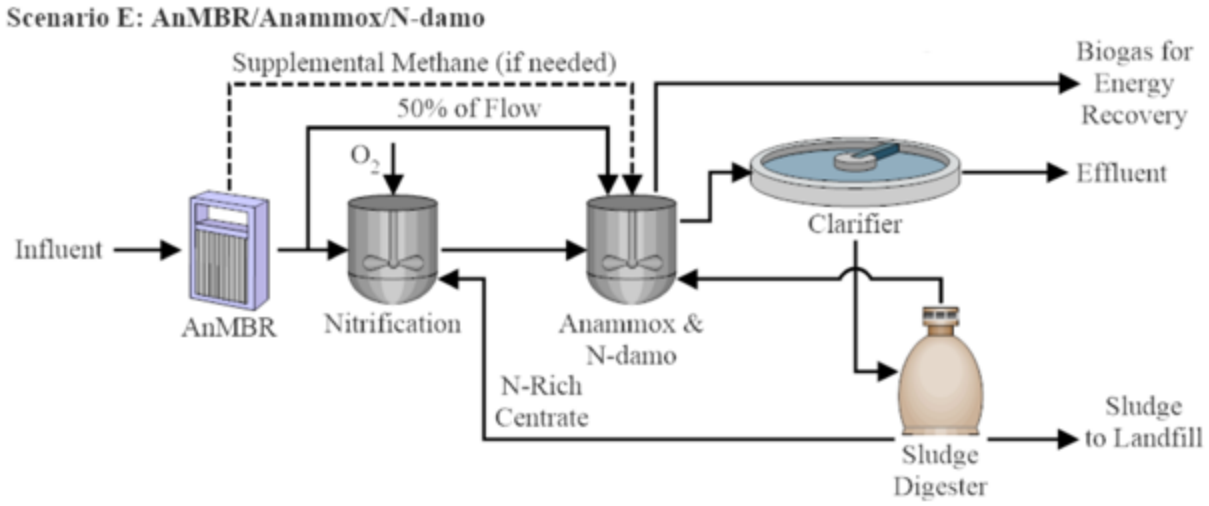

Figure A5. Replication of Scenario E taken from Figure 1 of the manuscript

Table A13. Fractional conversions for scenario E, f_{Z_Y}					
Organism, Y	**AOB**	**NOB**	**Anammox (Y is ANAMX)**	**N-damo (Y is NDAMO)**	**AnMBR**
Nitrogen (Z is N)	0.5	0.5	0.435	0.8	N/A
COD	N/A	N/A	N/A	N/A	1
Scenario E.R Line #	20	21	28	29	35

Step 1) Total Contaminant Load
This was calculated identically to scenario A using equations SI-1 thru SI-4 (scenarioC.R lines 8-11).
Step 2) Nitrification, Anammox & N-damo (Nitrogen Removal)
The nitrification, anammox and n-damo sludge production and oxygen/methane consumption were identical to scenario D and calculated via equations SI-6 thru 8 and SI-36 thru SI-38 (scenarioE.R lines 22-25 & 30-32) and thus $O_{2_{AOB}} = 3429\frac{kgO_2}{d}$; $O_{2_{NOB}} = 1143\frac{kgO_2}{d}$; $p_{x_{AOB}} = 120\frac{kgVSS}{d}$; $p_{x_{NOB}} = 50\frac{kgVSS}{d}$; $L_{CH_{4_{cons}}} = 457\frac{kgCH_4}{d}$; $p_{x_{ANAMX}} = 130\frac{kgVSS}{d}$; $p_{x_{NDAMO}} = 12\frac{kgVSS}{d}$.
Step 3) Mainstream Anaerobic Membrane Bioreactor
The sludge and methane production from the AnMBR is calculated identically to scenario C with equations SI-8 & SI-32 (scenarioE.R lines 36 & 37), and thus: $p_{x_{AnMBR}} = 213\frac{kgVSS}{d}$; $CH_{4_{prod_{AnMBR}}} = 15424\frac{kgCH_4}{d}$.
Step 4) Dissolved vs. Gaseous Methane & CO2 Production
Calculated nearly identically to scenario C with equations SI-33 thru SI-35. (scenarioE.R lines 42-44): $L_{CH_{4_{diss}}} = 893\frac{kgCH_4}{d}$; $CH_{4_{burn_{AnMBR}}} = 14500\frac{kgCH_4}{d}$

However, unlike scenario C, 50% of the flow from the AnMBR is diverted to anammox/n-damo reactor, and half was diverted to the nitrification reactor as per the fractional conversions defined in table 9. Dissolved methane into the nitrification and anammox/n-damo reactor was therefore calculated as:

$$L_{CH_4diss_{NIT}} = f_{NOB_N} L_{CH_4diss} = 0.5 \times 893 \frac{kgCH_4}{d} = 446.5 \frac{kgCH_4}{d}$$

(equation A-54) scenarioE.R line 45

$$L_{CH_4diss_{AMX}} = L_{CH_4diss} - L_{CH_4diss_{NIT}} = 2976 \frac{kgCH_4}{d} - 1488 \frac{kgCH_4}{d} = 446.5 \frac{kgCH_4}{d}$$

(equation A-55) scenarioE.R line 46

Step 6) Fate of Dissolved Methane in Nitrification Reactor (50% of AnMBR Flow)
The same assumption regarding methane stripping and consumption by MOBs from scenario C was used here, therefore equations SI-8 and SI-34 thru SI-38 were used to calculate the methane/oxygen consumed by MOBs, the sludge produced by MOBs, and the residual dissolved methane from the nitrification reactor (scenarioE.R lines 52, 57 thru 59): $CH_{4_{MOB,ox}} = 1339 \frac{kg}{d}$; $L_{CH_4diss_{From\ NIT}} = 45 \frac{kg}{d}$; $O_{2_{MOB}} = 100\ kg\ O_2$; $p_{x_{MOB}} = 28 \frac{kg}{d}$;

Step 7) Anaerobic Digester
This system was identical to scenario C with sludge handling demand and methane available for energy recovery were calculated with equations SI-17 thru SI-20 and SI-39 (scenarioE.R lines 62 thru 66) as follows: $p_{x_{out}} = 227 \frac{kgVSS}{d}$; $CH_{4_{dig}} = 131 \frac{kg}{d}$;

Step 8) Methane Balance
It was assumed that n-damo would first consume methane from the already dissolved methane available from the AnMBR before consuming methane gas, therefore the methane balance was calculated as:

$$L_{CH_4} = \left(L_{CH_4diss_{AMX}} \right) - L_{CH_4cons} = 446 - 457 = -10 \frac{kgCH_4}{d}$$

(equation A-56) scenarioE.R line 68

Additional methane was provided from the anaerobic digester, and there is no residual methane available in the liquid phase:

$$CH_{4_{burn}} = CH_{4_{burn}} + L_{CH_4} = 14700 \frac{kgCH_4}{d}$$
$$L_{CH_4} = 0$$

(equation A-57) scenarioE.R lines 66-71

NOTE: If additional methane was required beyond what the anaerobic digester can provide ($CH_{4_{burn}} < 0$), it was added externally and calculated as:

$$COD_{added} = \frac{-CH_{4_{burn}}}{s_{O_2burn}}$$
$$CH_{4_{burn}} = 0$$

scenarioE.R lines 72-73

If there was enough methane available in the liquid phase ($L_{CH_4} < 0$), The residual methane was then treated like a greenhouse gas.

Step 8) Electrical Demand

The electrical demand was determined identically to in scenario C with equations SI-21 thru SI-27 & SI-40.

$$O_{2_{TOT}} = 4670\frac{kgO_2}{d}$$ scenarioE.R line 76

$$E_{O_2} = 7000\frac{kWh}{d}$$ scenarioE.R line 79

$$E_{Solids} = 508\frac{kWh}{d}$$ scenarioE.R line 80

$$E_{mix} = 1120\frac{kWh}{d}$$ scenarioC.R line 82

$$E_{AnMBR} = 7600\frac{kWh}{d}$$ scenarioE.R line 81

$$E_{CHP} = -32200\frac{kWh}{d}$$ scenarioB.R line 82

The total emissions were then calculated as the sum of the electrical demands and sources calculated above plus the amount of dissolved methane exiting the system and the amount of stripped methane leaving the nitrification reactor adjusted to CO_2 equivalents.

$$CO_{2_{TOT}} = \frac{kgCO_2}{kWh}\sum E_Y + \frac{CO_2}{CH_{4_{eq}}}\left(L_{CH_{4_{diss}}} + L_{CH_{4_{diss_{From\,NIT}}}}\right)$$ (equation A-58) scenarioE.R line 83

$$= (-16000)\frac{kWh}{d} \times 0.47\frac{kgCO_2}{kWh} + (0+45) \times 34\frac{kgCO_2}{kgCH_4} = -6000\frac{kgCO_2}{d}$$

Step 9) Cost Estimation

Key cost factors were combined with a modified version of equation A-28. If external COD addition is required, it would be in the form as methane in natural gas, so that term is modified for the cost of natural gas. The cost of electricity required to operate an AnMBR is also included.

$$Cost_E = CH_{4_{burn}} \times C_{CH_4,prod} + p_{x_{out}} \times C_{solids} + O_{2_{TOT}} \times C_{O_2} + COD_{added} \times C_{CH_4,added} + Q \times C_{AnMBR} =$$ scenarioE.R line 88

$$14700\frac{kgCH_4}{d} \times \frac{\$0.17}{kgCH_4} + 254\ \frac{kgVSS}{d} \times -\frac{\$0.23}{kgVSS} + 4670\frac{kgO_2}{d} \times -\frac{\$0.12}{kgO_2} + 0\frac{kgCOD}{d} \times -\frac{\$0.13}{kgCOD} + 40\frac{th\ m^3}{d} \times -\frac{\$14.82}{th\ m^3} + 40\frac{th\ m^3}{d} \times -\frac{\$2.18}{th\ m^3} = \$1240$$

As with all other scenarios, this is compared to the base case as follows:

$$Cost_{compare} = Cost_A - Cost_E = \frac{-\$3080}{d} - \frac{\$1240}{day} = \frac{\$4310}{day}\ (cost\ saved)$$ masterrun.R line 97

The same comparison is made for GHG emissions: masterrun.R line 108

$$GHG_{compare} = -(GHG_A - GHG_E)$$
$$= -\left(\frac{13100\ kg\ CO_2}{d} - \frac{-6000\ kg\ CO_2}{day}\right)$$
$$= -19100\ (emissions\ averated)$$

Step 10) Scenario Summary

Table A14. The following metrics are reported from ScenarioE.R when using the input used in this sample calculation

Metric	**Combined Cost of Key Metrics**	**Comparitive Cost**	**GHG Emissions**	**Comparitive GHG Emissions**
Variable	$Cost_E$	$Cost_{compare}$	GHG_E	$GHG_{compare}$
Location in Code	ScenarioE.R Line 97	masterrun.R Line 114	ScenarioE.R Line 96	masterrun.R Line 109
Value	-$1240/d	$4310/d ($ saved)	-6000 $kgCO_2/d$	19100 $kgCO2/d$ (GHG Reduced)

Supplemental Results: Individual Cost Factor Results from the Model

To dig into the contribution of individual cost factors on the overall cost comparion results for each scenario, plots were made comparing the relative % increase or decrease of each cost factor considered similar to Figures 4 & 5 in the study. Those plots are provided here:

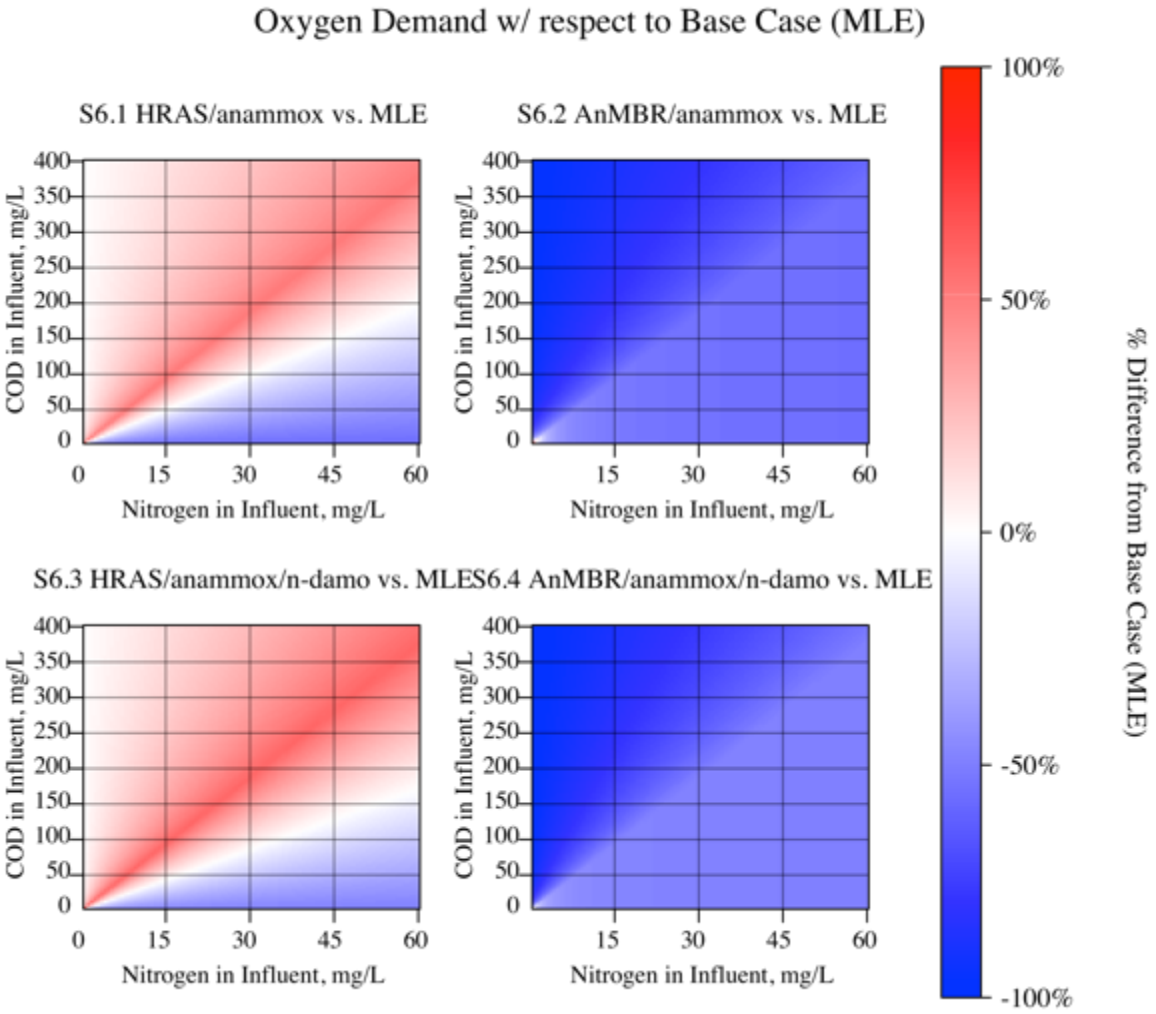

Figure A6. Comparison of oxygen demand in scenarios B (2.1), C (2.2), D (2.3), and E (2.4) to the base case scenario A (Modified Ludzack-Ettinger, MLE, also referred to as conventional nitrification/denitrification). Percentage increase or decrease in oxygen demand was shown in red (high) and blue (low) respectively as defined by the color key.

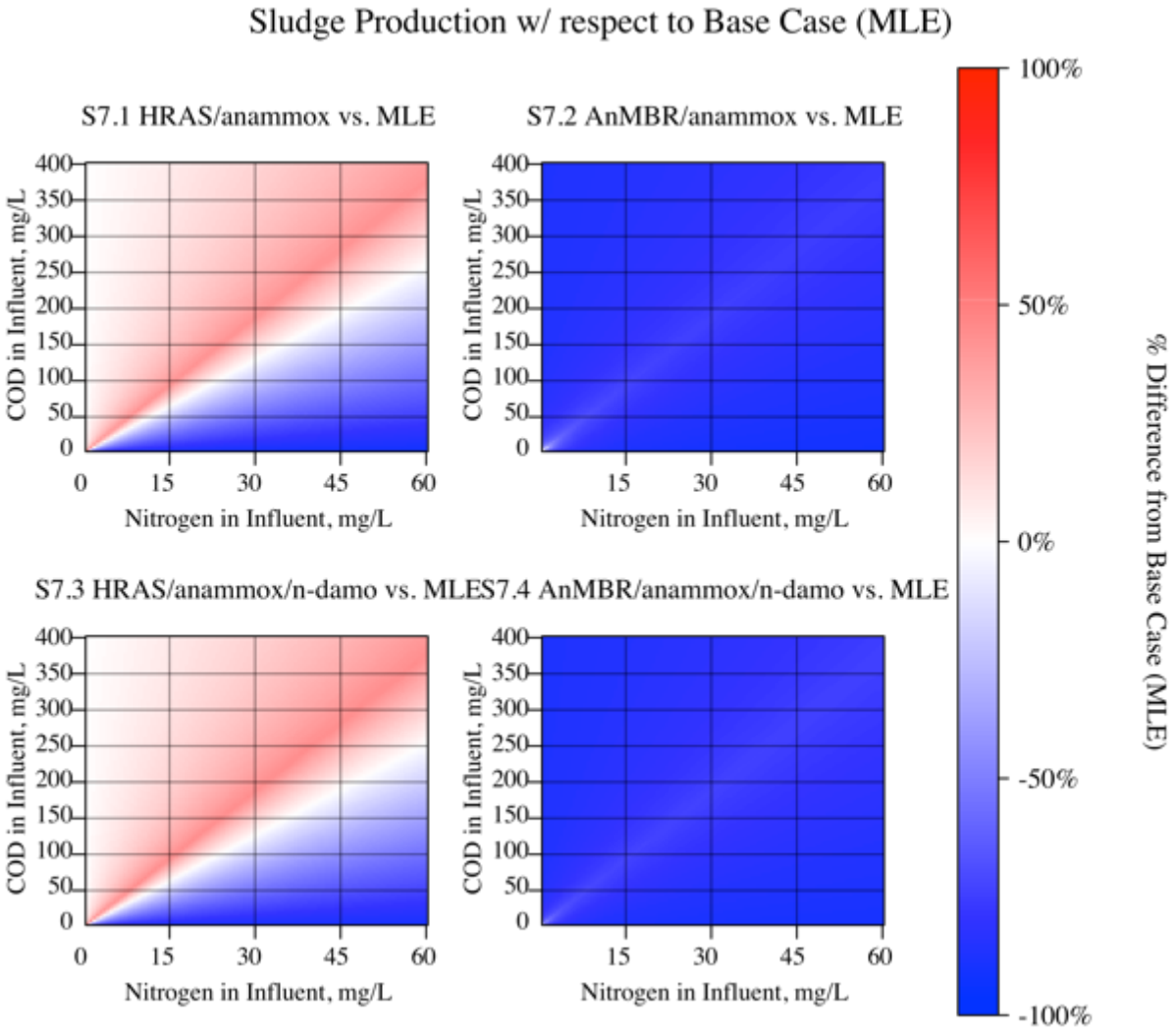

Figure A7. Comparison of sludge produced in Scenarios B (3.1), C (3.2), D (4.3), and E (3.4) to the base case scenario A (Modified Ludzack-Ettinger, MLE, also referred to as conventional nitrification/denitrification). Percentage increase or decrease in sludge discharge was shown in red (high) and blue (low) respectively as defined by the color key.

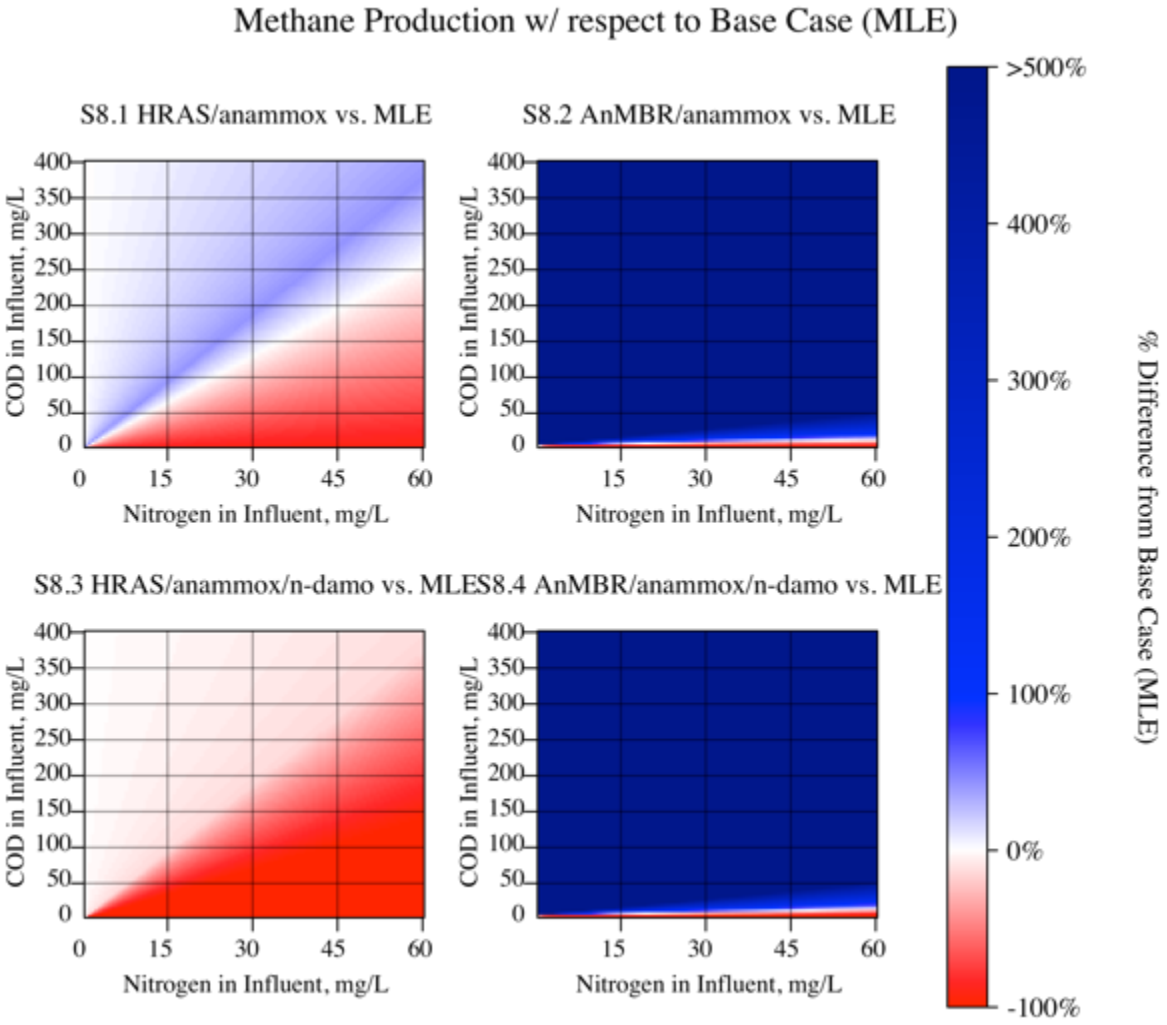

Figure A8. Comparison of methane production in Scenarios B (4.1), C (4.2), D (4.3), and E (4.4) to the base case scenario A (Modified Ludzack-Ettinger, MLE, also referred to as conventional nitrification/denitrification). Biogas production is of benefit to plant operational costs. Red is associated with a negative impact and therefore is chosen here to represent a percent decrease in methane production and blue is chosen to represent a percent increase in methane production as opposed to figures 2, 3, and 5.

External Carbon Addition

If there was not enough carbon for denitrification, the base case required exogenous carbon. In all other scenarios, nitrogen was removed via the autotrophic anammox metabolism and the only organic carbon source required, if any, was provided from biogas produced on-site. At all conditions considered in this study enough biogas was produced to supply n-damo with adequate methane for complete nitrogen removal, so no carbon addition was required for scenarios B-E, while at low COD/N ratios, carbon addition as methanol was required in scenario A. This binary conclusion resulted in a simple addition or exclusion of the cost of external carbon when calculating the cost factor and so this graph is omitted here.

SUPPLEMENTAL RESULTS: SENSITIVITY STUDY OF PUMPING DEMAND ON RESULTS

A conventional nitrification/denitrification WRRF of the size in in this study (15.8 MGD, 60 th m^3/day) has a daily electrical demand between 2000-1700 kWh/MG and typically 52% and 30% of that electrical demand was devoted to the already accounted for aeration and biosolids processing, respectively.[4] The remaining 18%, representing other electrical demands such as pumping requirements, is roughly 90 kWh/th m^3. It was assumed that this value did not vary significantly when calculating the primary results in this model. In practice, the energy required for pumping could vary between scenarios. In this sensitivity study, the 90 kWh/th m^3 factor was included in calculating the electrical demand of the conventional system (base case, scenario A) while it was varied between 45-450 kWh/th m3 (50-500% of base case) in the other four scenarios examined (scenarios B-D).

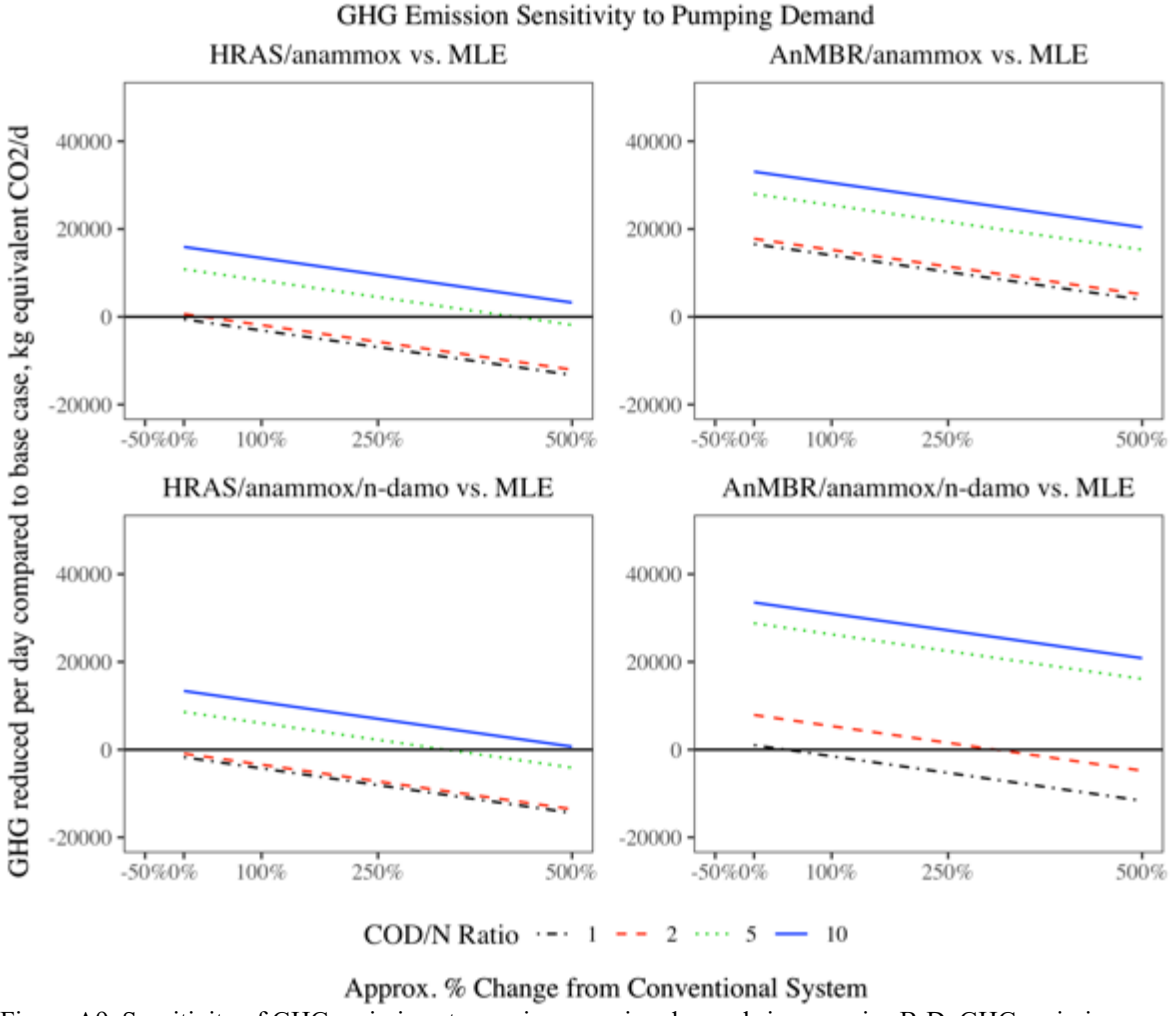

Figure A9. Sensitivity of GHG emissions to varying pumping demands in scenarios B-D. GHG emissions are measured as the kg CO_2 per day averted by utilizing one of the theoretical scenarios B-D instead of conventional nitrification/dentrification. This is plotted against the % increase or decrease in pumping demand as compared to the base case.

The difference in GHG emissions and operational cost between the base case and the four scenarios was compared at four different COD/N ratios and plotted in Figures A9 & A10

respectively. At each COD/N ratio examined, COD concentration was held constant at 100 mg/L. As pumping demand increased, the relative GHG emissions averted or dollars saved decreased, which makes sense as both these values are tied to total electrical demand. It was found in both instances that at most COD/N ratios, the overall result (more or fewer GHGs than the base case) changed at the extremes of the sensitivity study if at all. The response of GHG emissions averted or dollars saved was only mildly sensitive to overall pumping demand. It can be inferred from this that the results in this study (figures 2 & 3 in the main manuscript) still hold value even though the pumping demand is not included in the cost as pumping demand would only have a mild impact on overall results.

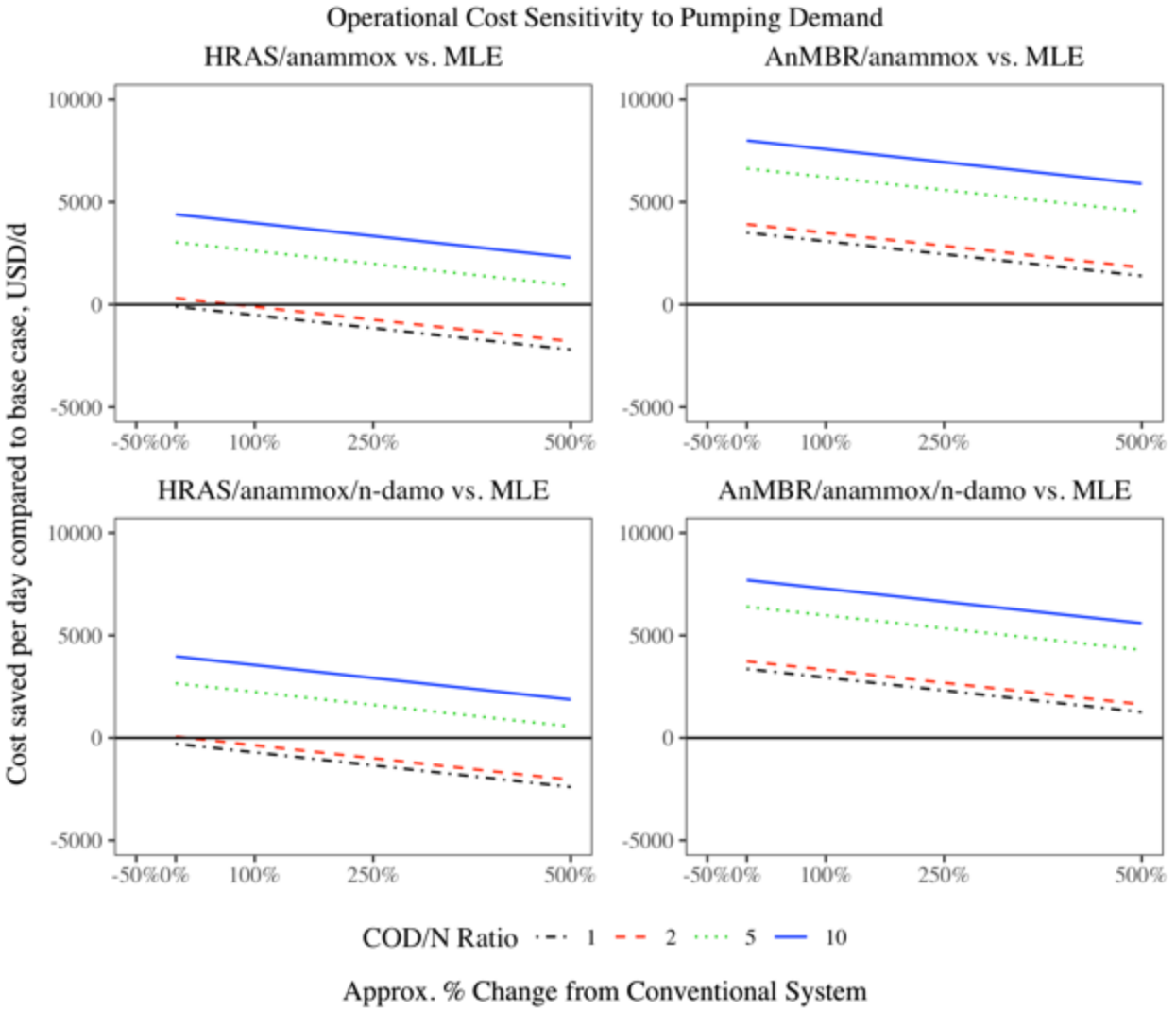

Figure A10. Sensitivity of GHG emissions to varying pumping demands in scenarios B-D. GHG emissions are measured as dollars saved per day averted by utilizing one of the theoretical scenarios B-D instead of conventional nitrification/dentrification. This is plotted against the % increase or decrease in pumping demand as compared to the base case.

APPENDIX B

Supplemental Information for

Chapter 4:

Replicating an Oxygen Minimum Zone in a Laboratory Microscosm Elucidates Partnerships between Anammox, Ammonia Oxidizing Archaea, and *Nitrospira*

Number of Pages: 15
Number of Figures: 15
Number of Tables: 5

Table of Contents:

Figure B1. Figure B1. Distribution of SYBR™ green-stained DW1 AOA culture after PAC addition was observed (a) immediately after addition and (b) 24 hours later. The decrease in cell density in the liquid phase and increase in density on the black PAC particles was observed. (c) PAC was also attached to anammox granules and (d) observed to remain attached after 2 weeks of 100 rpm shaking. B3
Table B1. qPCR Primers and conditions B3
Table B2. FISH Probes used in this study B4
Figure B2. Total performance over time of the counter-diffusing environment B4
Figure B3. Gel electrophoresis of the qPCR product of DNA from the co-diffusion system biofilm taken after operation and general comammox amoB primers. A very faint band is visible indicating the presence of DNA of the same length as the target sequence. Other samples not relevant to this study were run on this gel and were cropped out of the image. B5
Figure B4. 16s sequencing results showing the population dynamics of aerobic nitrifiers in the co-diffusion environment over the length of operation (n=2). B6
Figure B5. Live dead stain performed on a segment of the membrane fibers present in the counter-diffusing system. Live cells are stained with propidium iodide and dead cells are stained with SYTO 9 (green). B7
Figure B6. Relative abundances of top 6 most abundant phylums as determined from 16s sequencing for the co- and counter- diffusione enivronments. B8
Figure B7. Standard curve using cmx_amoB-148F and cmx_amoB_485R primers with plasmid containing target sequence taken from N. inopinata genome. B9
Figure B8. Melting curves of a positive control (grey) compared to five different replicates of DNA extracted from granules in the co-diffusing environment (black) B9

immediately after operation ceased using cmx_amoB-148F and cmx_amoB_485R primers.
Figure B9. Melting curves of a positive control (grey) compared to two replicates of DNA extracted from biofilm around hollow fiber membranes (black) in the counter-diffusing environment immediately after operation ceased using cmx_amoB-148F and cmx_amoB_485R primers. B10
Figure B10. Standard curve using AMX-808-F and AMX-1040-R primers with anammox 16s plasmid. B10
Figure B11. Melting curves of a positive control (light grey) compared to two different replicates of DNA extracted from granules in the co-diffusing environment (dark grey) immediately after operation ceased using AMX-808-F and AMX-1040-R primers. B11
Figure B12. Melting curves of a positive control (grey) compared to three replicates of DNA extracted from biofilm around hollow fiber membranes (black) in the counter-diffusing environment immediately after operation ceased using AMX-808-F and AMX-1040-R primers. B11
Figure B13. Standard curve using nvs_amoA-F and nvs_amoA-R primers with N. viennensis amoA plasmid. B12
Figure B14. Melting curves of a positive control (light grey) compared to three different replicates of DNA extracted from granules in the co-diffusing environment (dark grey) immediately after operation ceased using nvs_amoA-F and nvs_amoA-R primers. After 45 cycles, some small amplification was detected so these samples were run for an additional 5 cycles, resulting in stronger melting curve signals than would have been observed though the Cq values were so low as to indicate effectively no presence of AOA. B12
Figure B15. Melting curves of a positive control (light grey) compared to three replicates of DNA extracted from biofilm around hollow fiber membranes (dark grey) immediately after operation ceased using nvs_amoA-F and nvs_amoA-R primers. The negative sample was not included in the final analysis presented. B13
Table B3. Constants used in calculations in Tables B4 & B5 B13
Table B4. Summary of COD calculations performed in Table B5. B14
Table B5. Comparison of theoretical formate required to COD supplied via endogenous decay reveals a COD deficit that cannot be accounted for by decay alone. B15

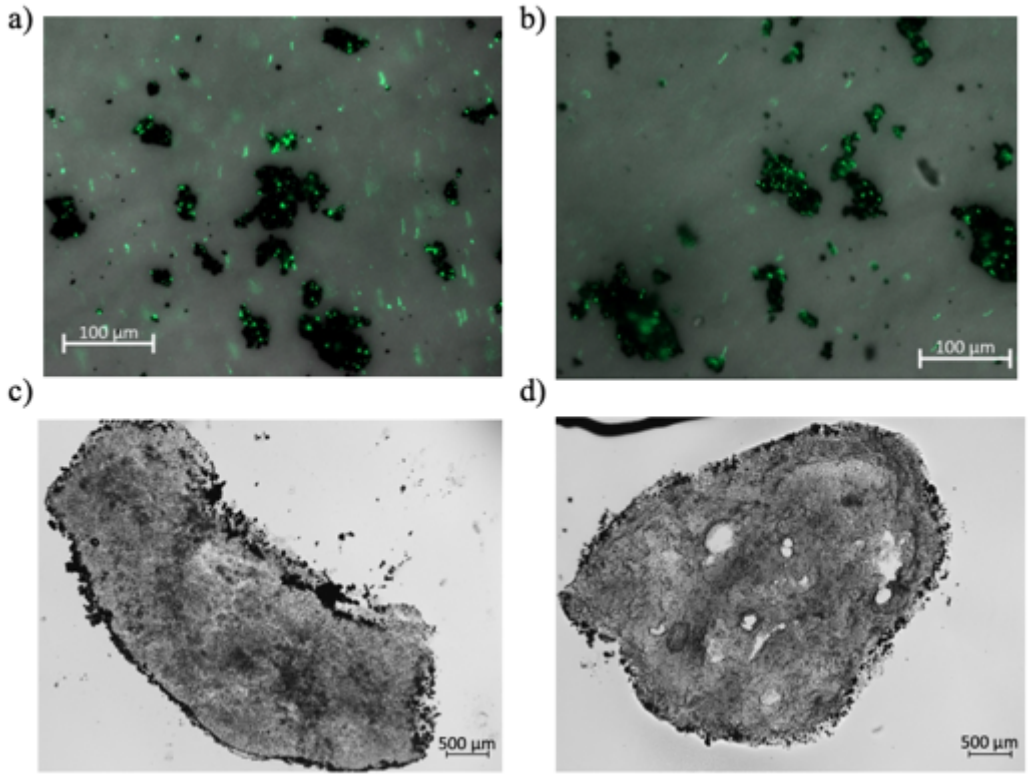

Figure B1. Distribution of SYBR™ green-stained DW1 AOA culture after PAC addition was observed (a) immediately after addition and (b) 24 hours later. The decrease in cell density in the liquid phase and increase in density on the black PAC particles was observed. (c) PAC was also attached to anammox granules and (d) observed to remain attached after 2 weeks of 100 rpm shaking.

Table B1. qPCR Primers and conditions			
Name	5'-3' Sequence	Annealing Temp/# Cycles	Citation
cmx_amoB-148F	TGG TAY GAY ACN GAA TGG G	52 °C/40	[130]
cmx_amoB_485R	CCC GTG ATR TCC ATC CA		
AMX-808-F	ARC YGT AAA CGA TGG GCA CTA A	58 °C /40	[132]
AMX-1040-R	CAG CCA TGC AAC ACC TGT RAT A		
nvs_amoA-F	AGTATTCTCCGTGTCACAGT	63 °C /45	This study
nvs_amoA-R	GTCCCTGACGAGCAAC		

Table B2. FISH Probes used in this study				
Organism	Name	Sequence (5'-3')	Probe	Citation
Nitrospira	Ntsp662	GGA ATT CCG CGC TCC TCT	Flourescein	[193]
General Archaea	ARC915	GTG CTC CCC CGC CAA TTC CT	Cyanine 3	[194]
Anammox	AMX368	CCT TTC GGG CAT TGC GAA	Cyanine 5	[195]

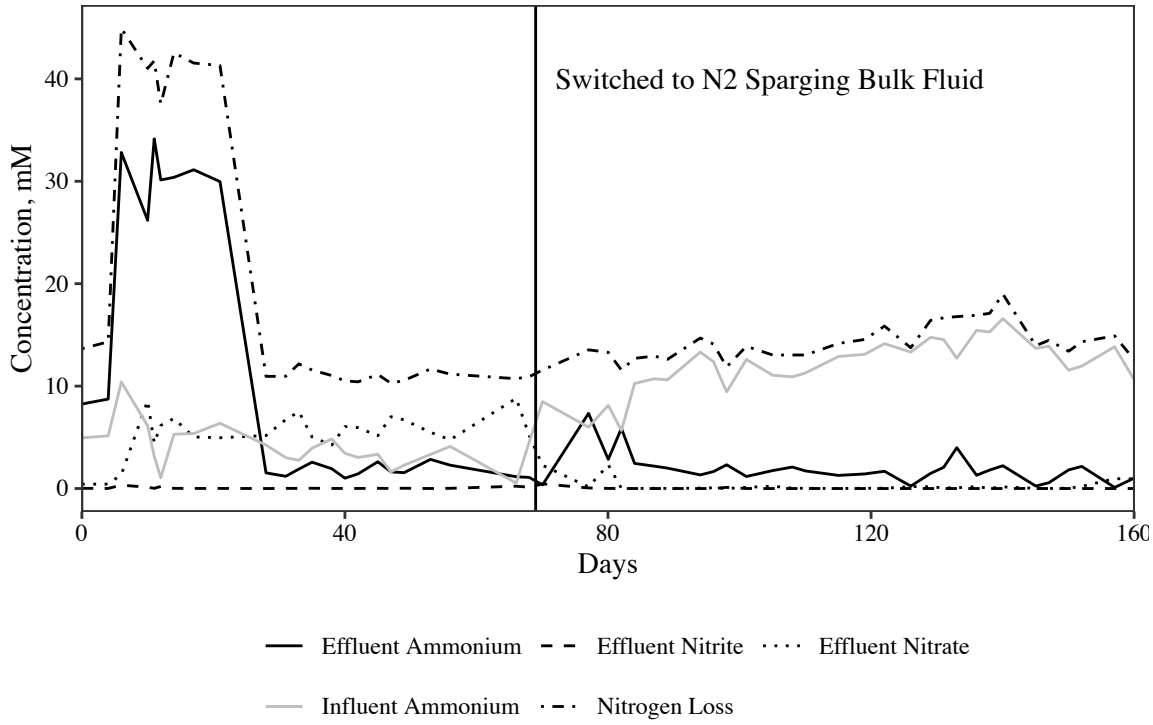

Figure B2. Total performance over time of the counter-diffusing environment

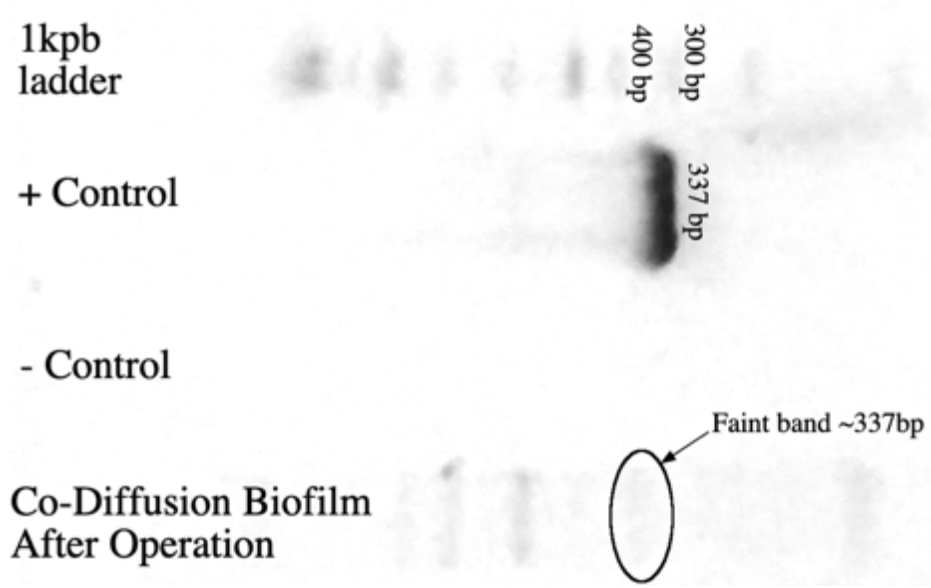

Figure B3. Gel electrophoresis of the qPCR product of DNA from the co-diffusion system biofilm taken after operation and general comammox amoB primers. A very faint band is visible indicating the presence of DNA of the same length as the target sequence. Other samples not relevant to this study were run on this gel and were cropped out of the image.

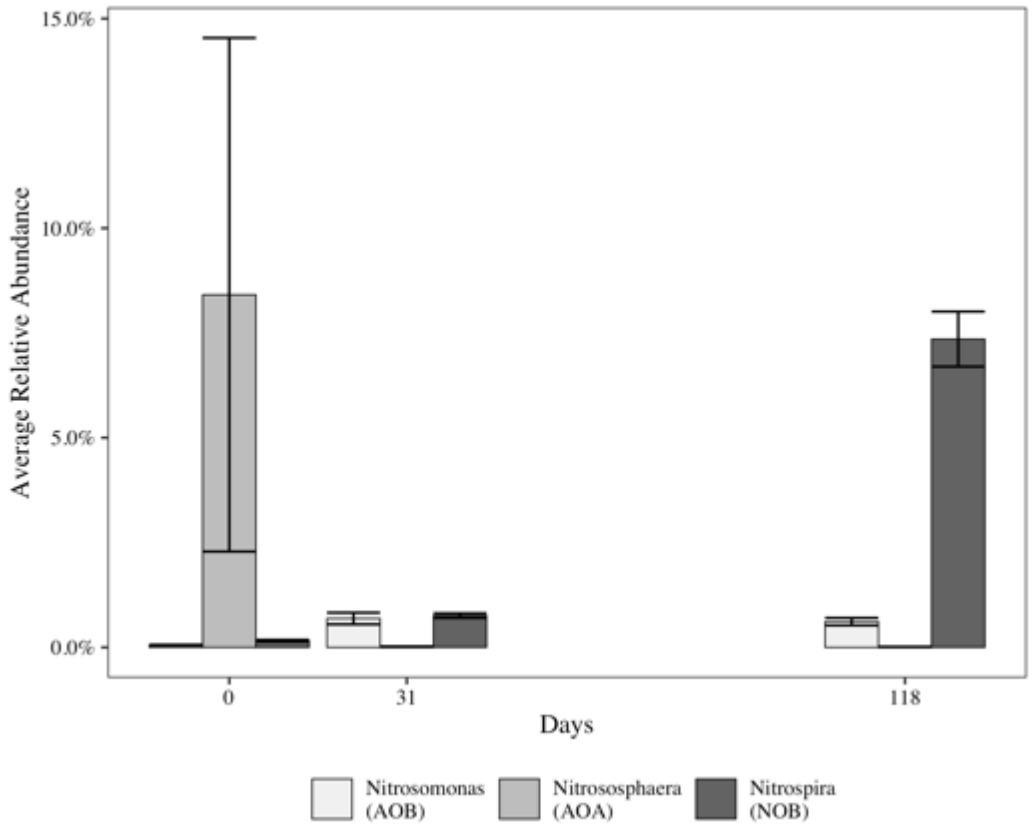

Figure B4. 16s sequencing results showing the population dynamics of aerobic nitrifiers in the co-diffusion environment over the length of operation (n=2).

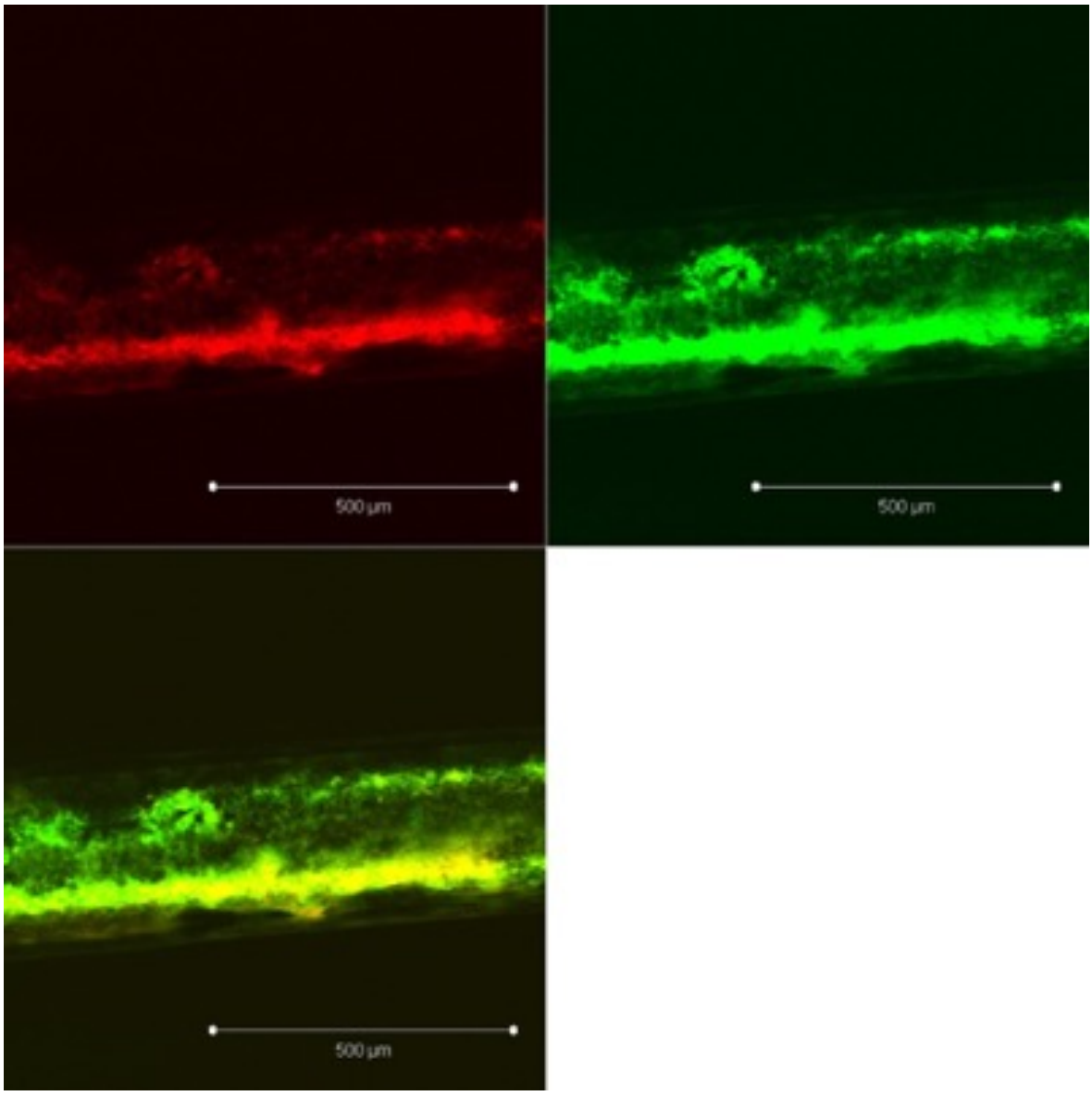

Figure B5. Live dead stain performed on a segment of the membrane fibers present in the counter-diffusing system. Live cells are stained with propidium iodide and dead cells are stained with SYTO 9 (green).

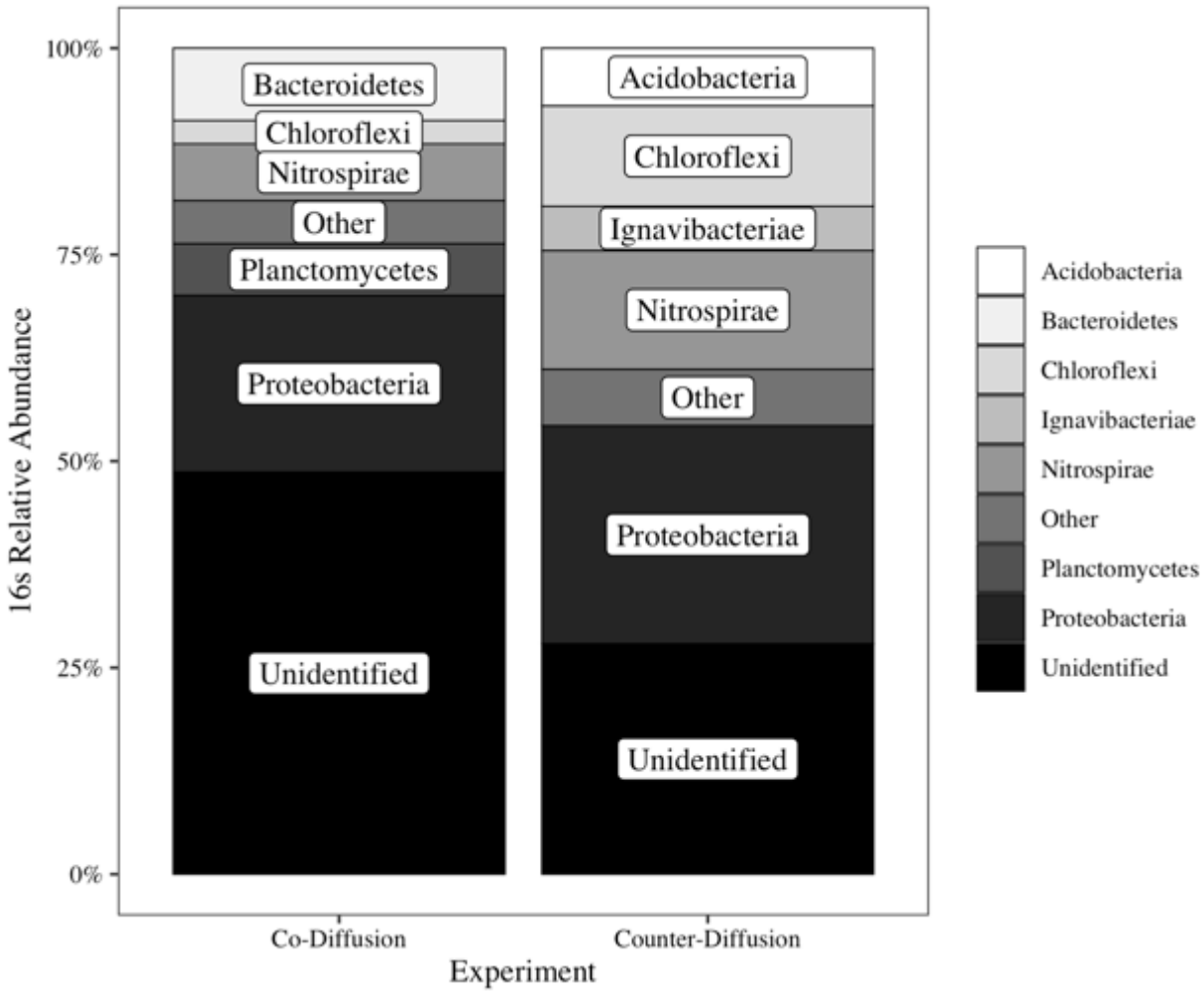

Figure B6. Relative abundances of top 6 most abundant phylums as determined from 16s sequencing for the (n=2, 874 OTUs) co- and (n=1, 425 OTUs) counter- diffusion enivronments.

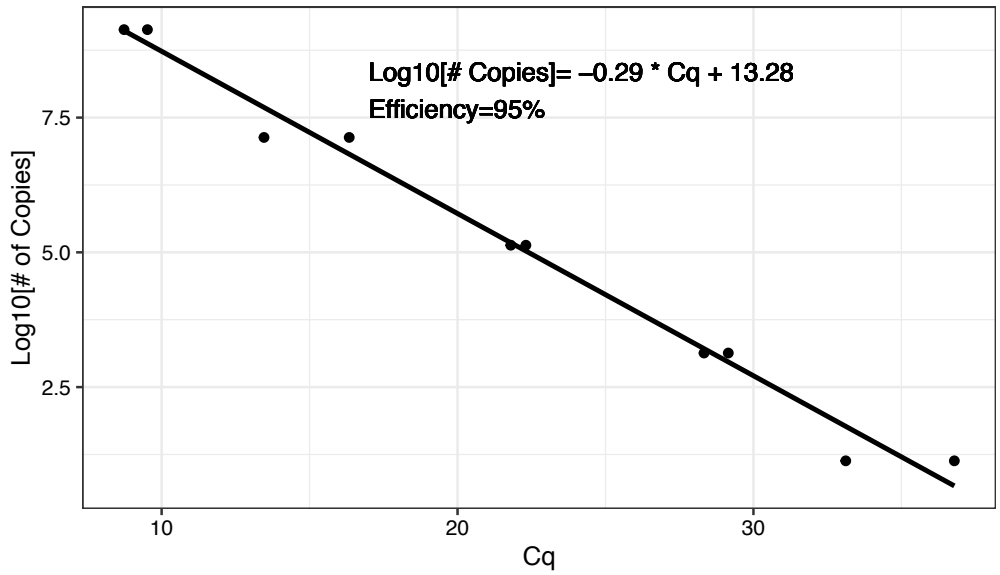

Figure B7. Standard curve using cmx_amoB-148F and cmx_amoB_485R primers with plasmid containing target sequence taken from N. inopinata genome.

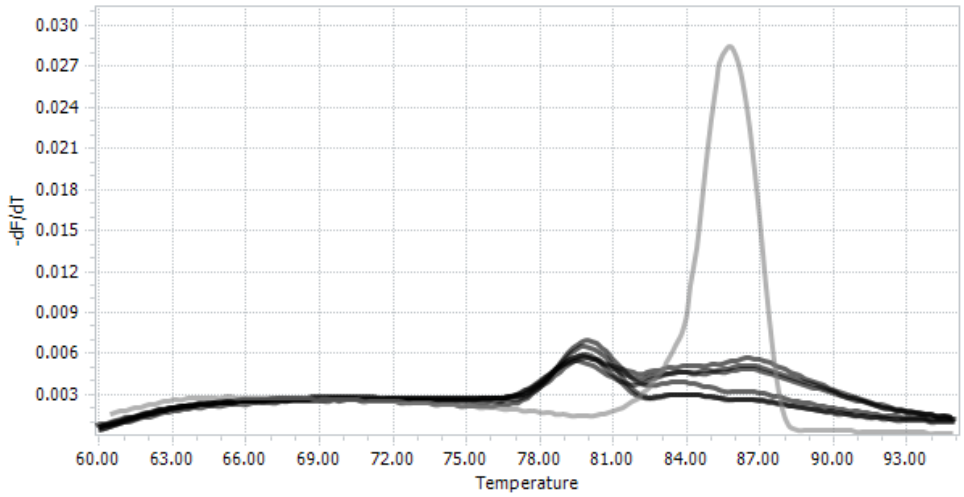

Figure B8. Melting curves of a positive control (grey) compared to five different replicates of DNA extracted from granules in the co-diffusing environment (black) immediately after operation ceased using cmx_amoB-148F and cmx_amoB_485R primers.

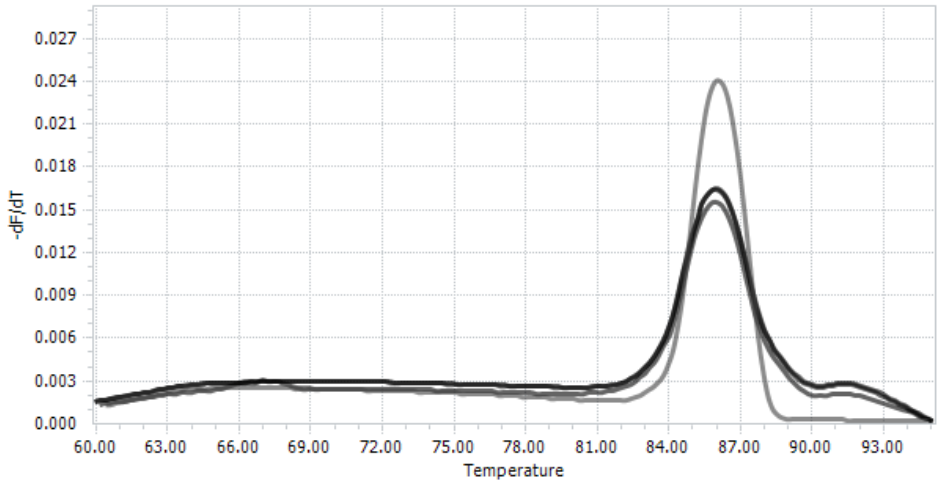

Figure B9. Melting curves of a positive control (grey) compared to two replicates of DNA extracted from biofilm around hollow fiber membranes (black) in the counter-diffusing environment immediately after operation ceased using cmx_amoB-148F and cmx_amoB_485R primers.

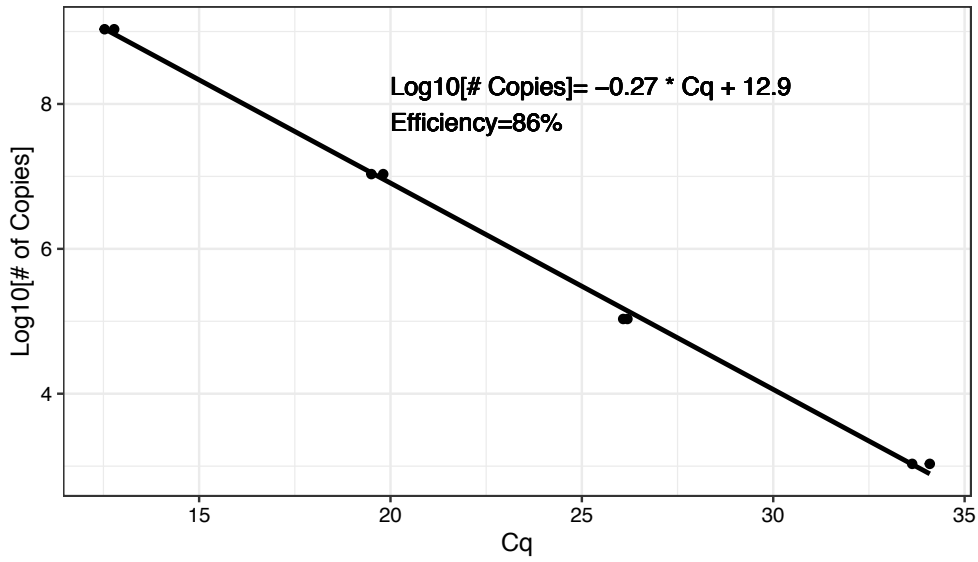

Figure B10. Standard curve using AMX-808-F and AMX-1040-R primers with anammox 16s plasmid.

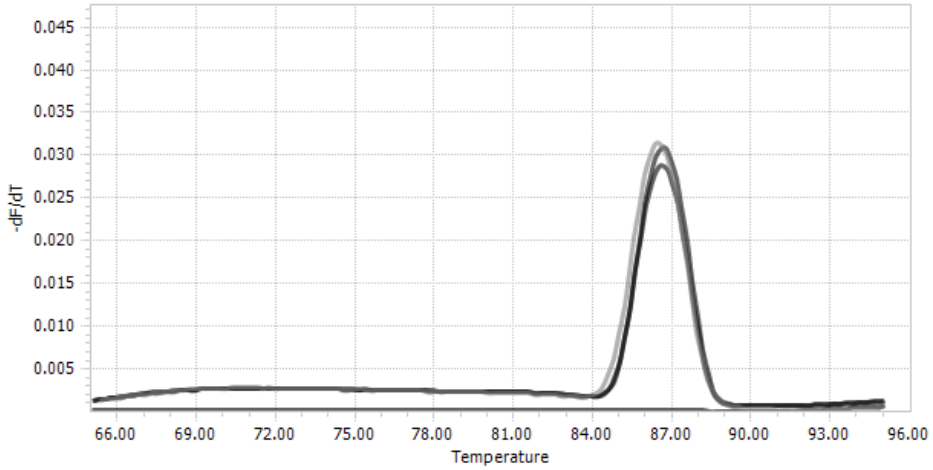

Figure B11. Melting curves of a positive control (light grey) compared to two different replicates of DNA extracted from granules in the co-diffusing environment (dark grey) immediately after operation ceased using AMX-808-F and AMX-1040-R primers.

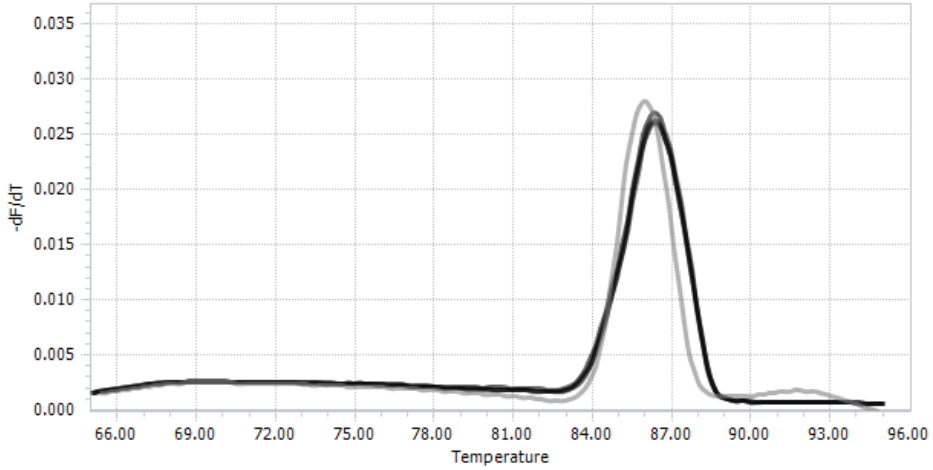

Figure B12. Melting curves of a positive control (grey) compared to three replicates of DNA extracted from biofilm around hollow fiber membranes (black) in the counter-diffusing environment immediately after operation ceased using AMX-808-F and AMX-1040-R primers.

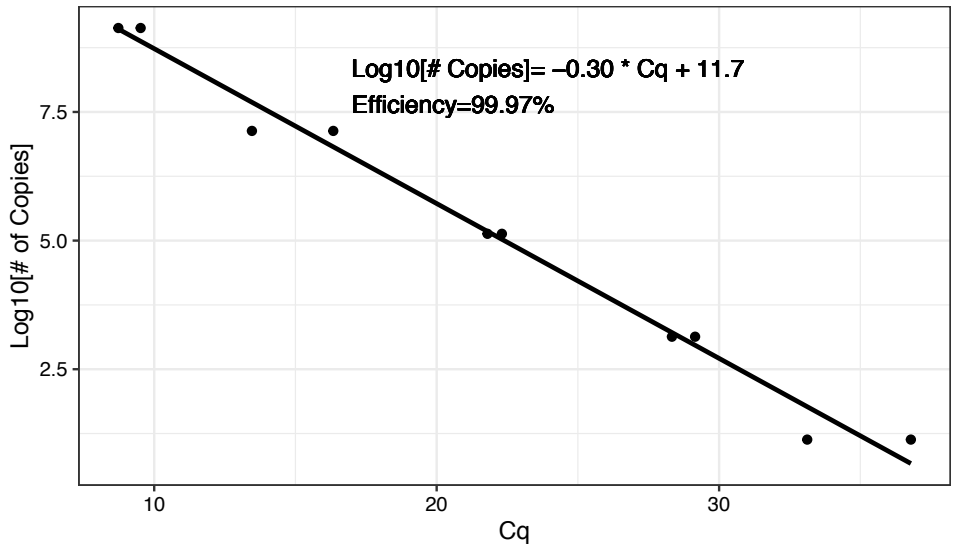

Figure B13. Standard curve using nvs_amoA-F and nvs_amoA-R primers with N. viennensis amoA plasmid.

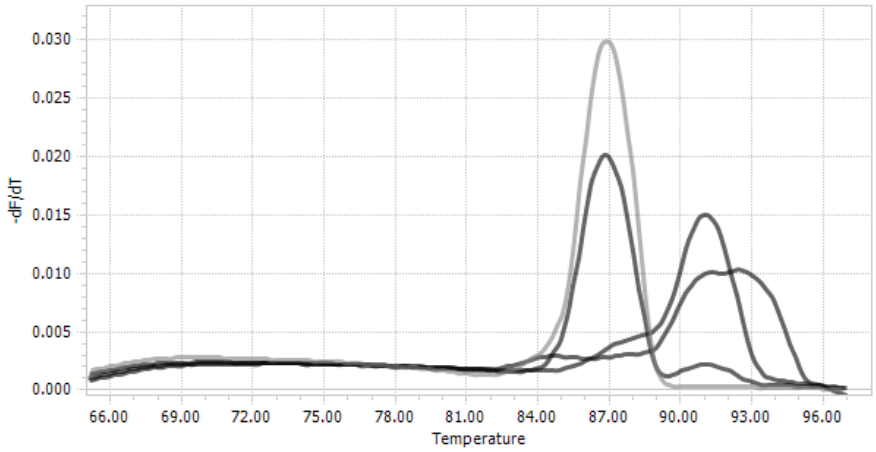

Figure B14. Melting curves of a positive control (light grey) compared to three different replicates of DNA extracted from granules in the co-diffusing environment (dark grey) immediately after operation ceased using nvs_amoA-F and nvs_amoA-R primers. After 45 cycles, some small amplification was detected so these samples were run for an additional 5 cycles, resulting in stronger melting curve signals than would have been observed though the Cq values were so low as to indicate effectively no presence of AOA.

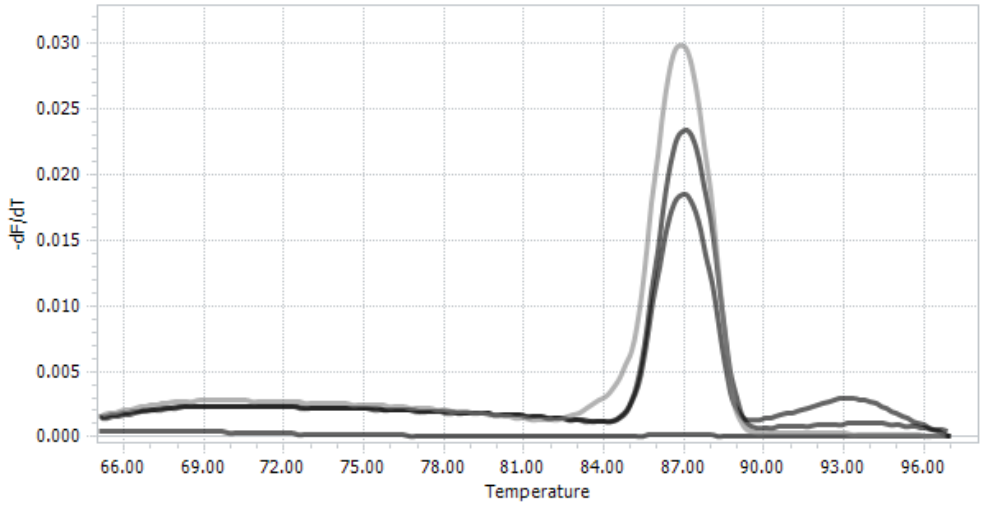

Figure B15. Melting curves of a positive control (light grey) compared to three replicates of DNA extracted from biofilm around hollow fiber membranes (dark grey) immediately after operation ceased using nvs_amoA-F and nvs_amoA-R primers. The negative sample was not included in the final analysis presented.

Table B3. Constants used in calculations in Tables B4 & B5				
Description	**Value**	**Variable Name**	**Units**	**Source**
Counter-Diffusing Mesocosm Flowrate	4.5		ml/hr	This Study
	0.108	Q	L/d	
Anammox Stoichiometric Ratios	0.13	$S_{NO3,AMX}$	mole NO_3^-/ mole N consumed	8
	0.43	$S_{NH3,AMX}$	mole NH_3/mole N consumed	
Nitrospira Formate Stoichiometry	0.9	$S_{NO3,NOB}$	mol NO_3^- : mol $HCOO^-$	18
COD of Formate	8	COD_{HCOO^-}	g O_2 : mol formate	Calculated

Table B4. Summary of COD calculations performed in Table B5.		
Description	**Variable Name**	**Calculation**
Days	D_i	None
NH_3 influent, mM	$NH_{3,in}$	Measured Value
NH_3 effluent, mM	$NH_{3,out}$	Measured Value
TON* effluent, mM	TON_{out}	Measured Value
Nitrogen Removed, mmol **	N_{rem}	$\left[NH_{3,in,avg} - \left(NH_{3,out} + TON_{out}\right)_{avg}\right] \times (D_i - D_{i-1}) \times Q$
Anammox Produced NO_3^-, mmol	$NO_{3,AMX}$	$N_{rem} \times S_{NO3,AMX}$
Theoretical Formate Required, gCOD	$COD_{Req,NOB}$	$NO_{3,AMX} \times S_{NO3,NOB} \times COD_{HCOO^-}$
Anammox Growth, mgVSS	$X_{G,AMX}$	$N_{rem} \times S_{NH3,AMX} \times Y_{AMX} \times 14 \frac{mgN}{mmol}$
AOA Growth, mgVSS	$X_{G,AOA}$	$N_{rem} \times \left(1 - S_{NH3,AMX}\right) \times Y_{AOA} \times 14 \frac{mgN}{mmol}$
Total Anammox, gVSS	$X_{Tot,AMX}$	$X_{Tot,AMX,i-1} + X_{G,AMX,i} - X_{D,AMX,i}$
Total AOA, gVSS	$X_{Tot,AOA}$	$X_{Tot,AOA,i-1} + X_{G,AOA,i} - X_{D,AOA,i}$
Anammox Decay, gVSS	$X_{D,AMX}$	$X_{Tot,AMX} \times b_{AMX} \times (D_i - D_{i-1})$
AOA Decay, gVSS	$X_{D,AOA}$	$X_{Tot,AOA} \times b_{AOA} \times (D_i - D_{i-1})$
COD Produced via decay, gCOD	COD_{Decay}	$\left(X_{Tot,AOA} + X_{Tot,AMX}\right) \times n$
% COD Deficit		$\frac{COD_{Decay} - COD_{Req,NOB}}{COD_{Req,NOB}} \times 100\%$
* TON = Total oxidized nitrogen, Nitrite + Nitrate ** avg indicates the average of these values at Day = D_i and Day = D_{i-1}		

Table B5. Comparison of theoretical formate required in to COD supplied via endogenous decay reveals a COD deficit that cannot be accounted for by decay alone in MABR.														
Day	NH_3 influent mM	NH_3 effluent mM	TON* effluent mM	Nitrogen Removed mmol	Anammox Produced NO_3^- mmol	Theoretical Formate Required mmol	Anammox Growth mgVSS	AOA Growth mgVSS	Total Anammox gVSS	Total AOA gVSS	Anammox Decay gVSS	AOA Decay gVSS	COD Produced via decay mgCOD	% COD Deficit
0	0.03	0.19	0.83											
7	0.52	0.02	0.97	0.39	0.05	0.37	0.16	0.37	0.16	0.37	0.03	0.13	0.16	-57%
10	0.20	0.17	0.95	0.16	0.02	0.15	0.07	0.16	0.07	0.16	0.00	0.02	0.03	-82%
12	0.42	0.00	0.83	0.11	0.01	0.10	0.04	0.10	0.04	0.10	0.00	0.01	0.01	-88%
14	0.18	0.00	0.91	0.12	0.02	0.11	0.05	0.12	0.05	0.12	0.00	0.01	0.01	-88%
17	0.16	0.00	0.92	0.24	0.03	0.23	0.10	0.23	0.10	0.23	0.01	0.03	0.04	-82%
19	0.14	0.00	0.90	0.16	0.02	0.15	0.07	0.16	0.07	0.16	0.00	0.02	0.02	-88%
24	0.10	0.00	1.05	0.46	0.06	0.43	0.19	0.44	0.19	0.44	0.02	0.11	0.13	-69%
26	0.12	0.01	1.01	0.20	0.03	0.19	0.08	0.19	0.08	0.19	0.00	0.02	0.02	-88%
28	0.17	0.01	0.85	0.17	0.02	0.16	0.07	0.16	0.07	0.16	0.00	0.02	0.02	-88%
31	0.08	0.01	0.99	0.26	0.03	0.24	0.11	0.24	0.11	0.24	0.01	0.04	0.04	-82%
35	0.13	0.02	0.93	0.37	0.05	0.34	0.15	0.35	0.15	0.35	0.01	0.07	0.08	-76%
38	0.15	0.00	0.93	0.25	0.03	0.24	0.11	0.24	0.11	0.24	0.01	0.04	0.04	-82%
40	0.12	0.00	0.93	0.17	0.02	0.16	0.07	0.16	0.07	0.16	0.00	0.02	0.02	-88%
45	0.09	0.00	1.01	0.47	0.06	0.44	0.20	0.45	0.20	0.45	0.02	0.11	0.13	-69%
49	0.10	0.00	1.04	0.40	0.05	0.38	0.17	0.38	0.17	0.38	0.01	0.08	0.09	-76%
52	0.12	0.00	1.13	0.32	0.04	0.30	0.13	0.30	0.13	0.30	0.01	0.05	0.05	-82%
56	0.02	0.01	0.98	0.42	0.06	0.40	0.18	0.41	0.18	0.41	0.02	0.08	0.10	-76%
59	0.11	0.01	1.17	0.33	0.04	0.30	0.14	0.31	0.14	0.31	0.01	0.05	0.06	-82%
61	0.15	0.00	1.19	0.23	0.03	0.21	0.10	0.22	0.10	0.22	0.00	0.02	0.03	-88%
63	0.28	0.01	1.20	0.21	0.03	0.20	0.09	0.20	0.09	0.20	0.00	0.02	0.02	-88%
66	0.09	0.01	1.21	0.33	0.04	0.30	0.14	0.31	0.14	0.31	0.01	0.05	0.06	-82%
68	0.13	0.00	1.22	0.24	0.03	0.22	0.10	0.23	0.10	0.23	0.00	0.02	0.03	-88%
70	0.16	0.01	1.36	0.25	0.03	0.23	0.10	0.24	0.10	0.24	0.00	0.02	0.03	-88%
75	0.02	0.00	1.00	0.58	0.08	0.55	0.25	0.56	0.25	0.56	0.03	0.14	0.17	-69%
77	0.04	0.00	1.03	0.21	0.03	0.20	0.09	0.20	0.09	0.20	0.00	0.02	0.02	-88%
80	0.13	0.00	0.96	0.29	0.04	0.28	0.12	0.28	0.12	0.28	0.01	0.04	0.05	-82%
82	0.15	0.02	1.02	0.18	0.02	0.17	0.08	0.17	0.08	0.17	0.00	0.02	0.02	-88%
87	0.01	0.07	1.06	0.50	0.06	0.47	0.21	0.48	0.21	0.48	0.02	0.12	0.14	-69%
90	0.07	0.07	0.90	0.28	0.04	0.26	0.12	0.27	0.12	0.27	0.01	0.04	0.05	-82%

APPENDIX C

Supplemental Information for
Chapter 5:

Comammox and Anammox Co-operate in both Co-Diffusing Granular Sludge and Counter-Diffusing Membrane Aerated Biofilm Reactors

Number of Pages: 10
Number of Figures: 6
Number of Tables: 5

Table of Contents:

Figure C1. Performance of the MABR reactor during the entire operation.	C2
Table C1. Influent and effluent COD measurements from both reactors.	C2
Figure C2. Comammox qPCR standard curve	C3
Figure C3. Comammox qPCR melt curves for granular sludge reactor samples taken at the the end of operation (N=3) (dark grey) compared to a positive control (light grey).	C3
Figure C4. Gel electrophoresis of the qPCR amplification products of samples from the granular sludge reactor before, during, and after operation shows that comammox was present throughout operation of this reactor.	C4
Figure C5. Relative abundances of top 6 most abundant phylums as determined from 16s sequencing for the granular sludge reactor and MABR.	C5
Figure C6. Nitrite inhibition curve of *Nitrosomonas europaea.* The inhibition curve fit to this data revealed a nitrite inhibition constant of 89 ± 46 mgN/L-NO_2^-.	C6
Table C1. Definitions	C6
Table C2. Reaction Kinetics	C7
Table C3. Stoichiometric matrix	C8
Table C4. Stoichiometric, kinetic and diffusion parameters	C9
Table C5. COD Measurements in both reactor systems.	C10

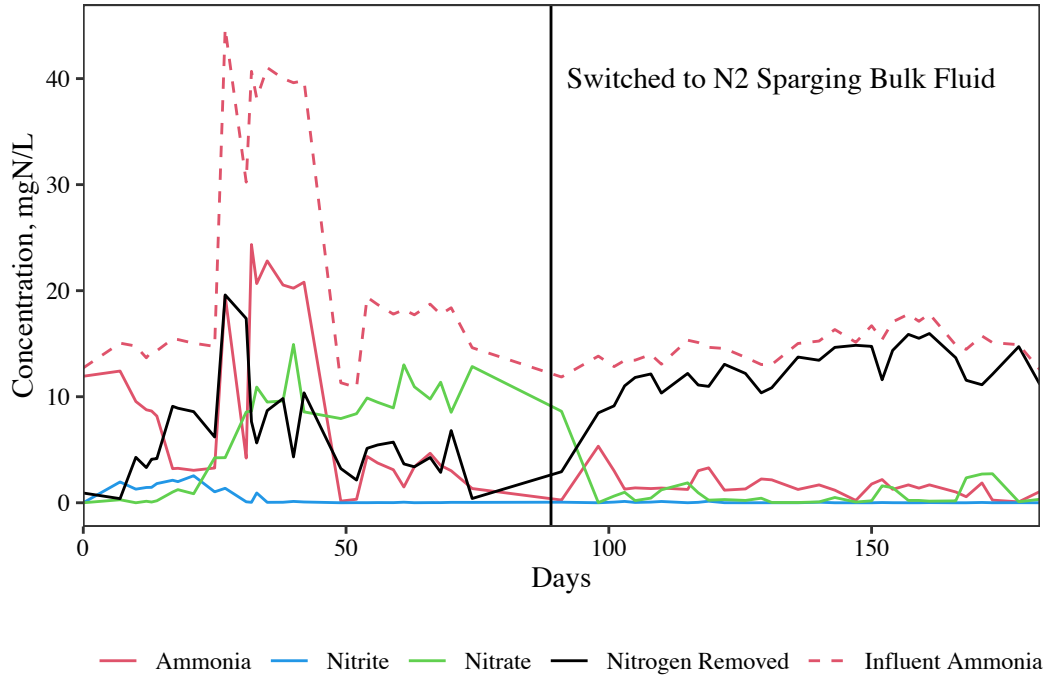

Figure C1. Performance of the MABR reactor during the entire operation.

Table C1. Influent and effluent COD measurements from both reactors.		
Reactor	Influent (mgCOD/L)	Effluent (mgCOD/L)
MABR	1010	1010
Granular Sludge	1000	1000

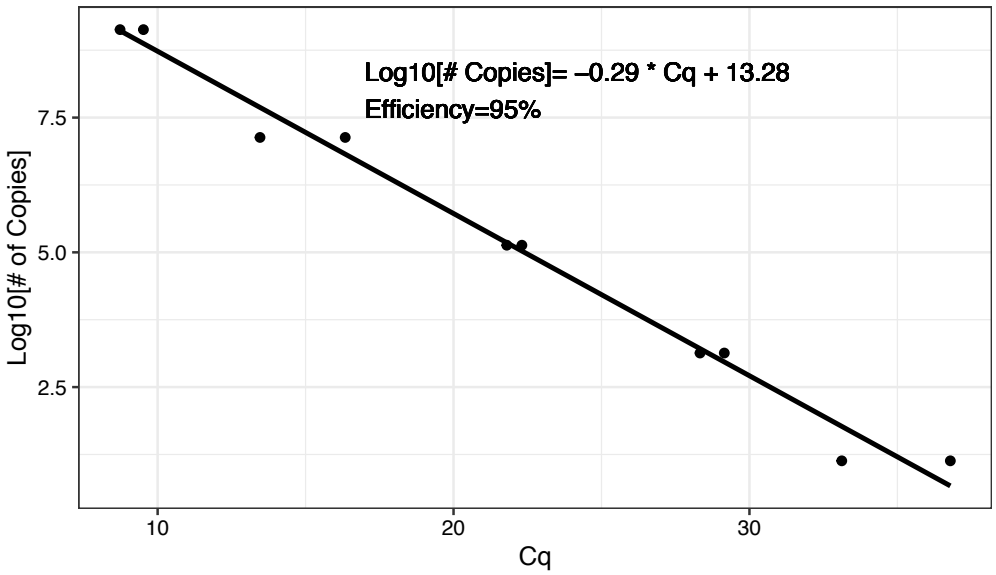

Figure C2. Comammox qPCR standard curve

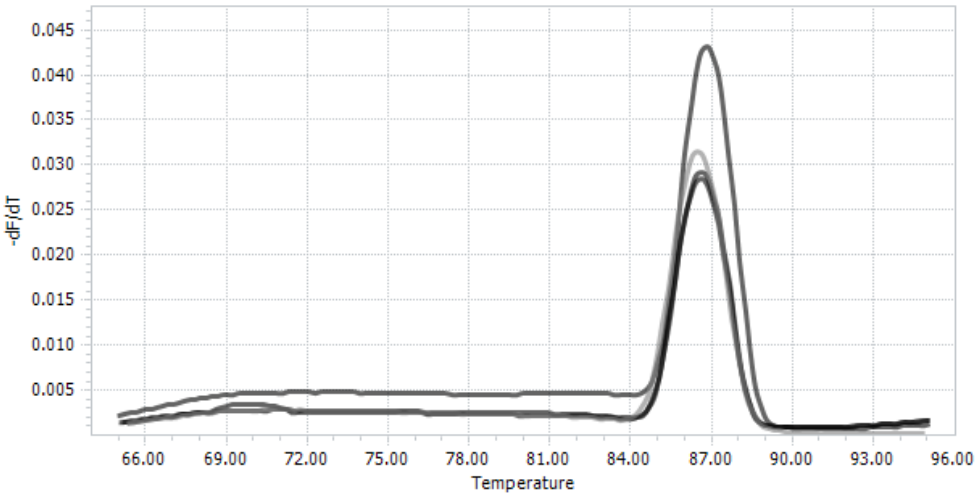

Figure C3. Comammox qPCR melt curves for granular sludge reactor samples taken at the the end of operation (N=3) (dark grey) compared to a positive control (light grey).

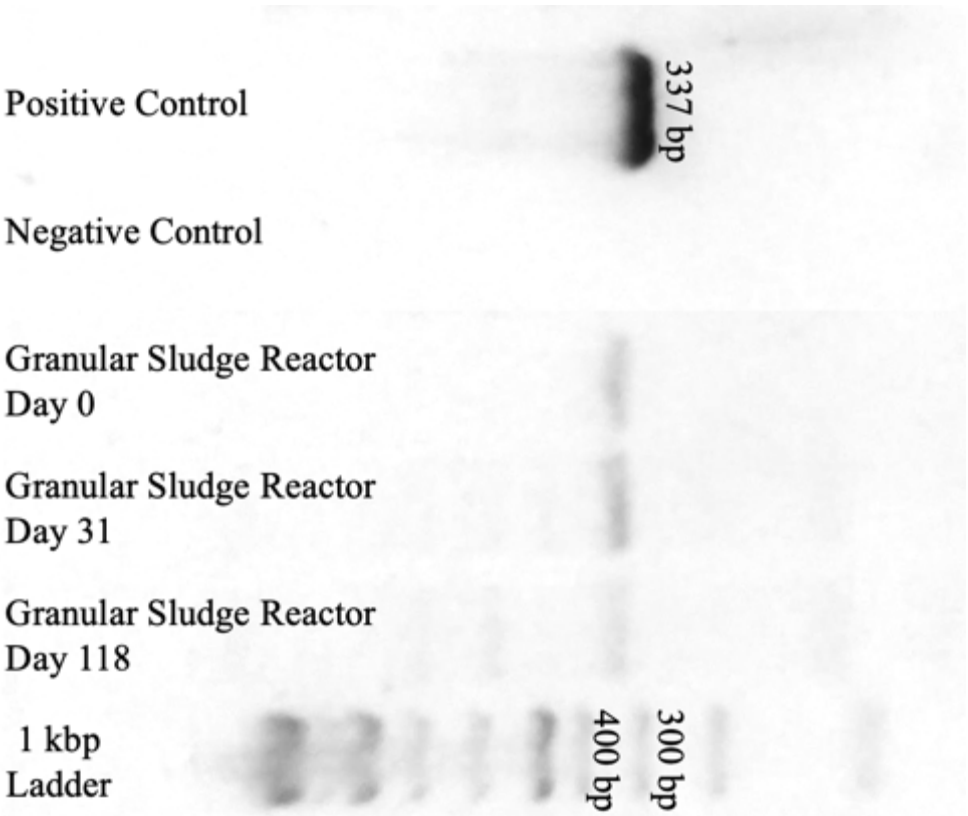

Figure C4. Gel electrophoresis of the qPCR amplification products of samples from the granular sludge reactor before, during, and after operation shows that comammox was present throughout operation of this reactor.

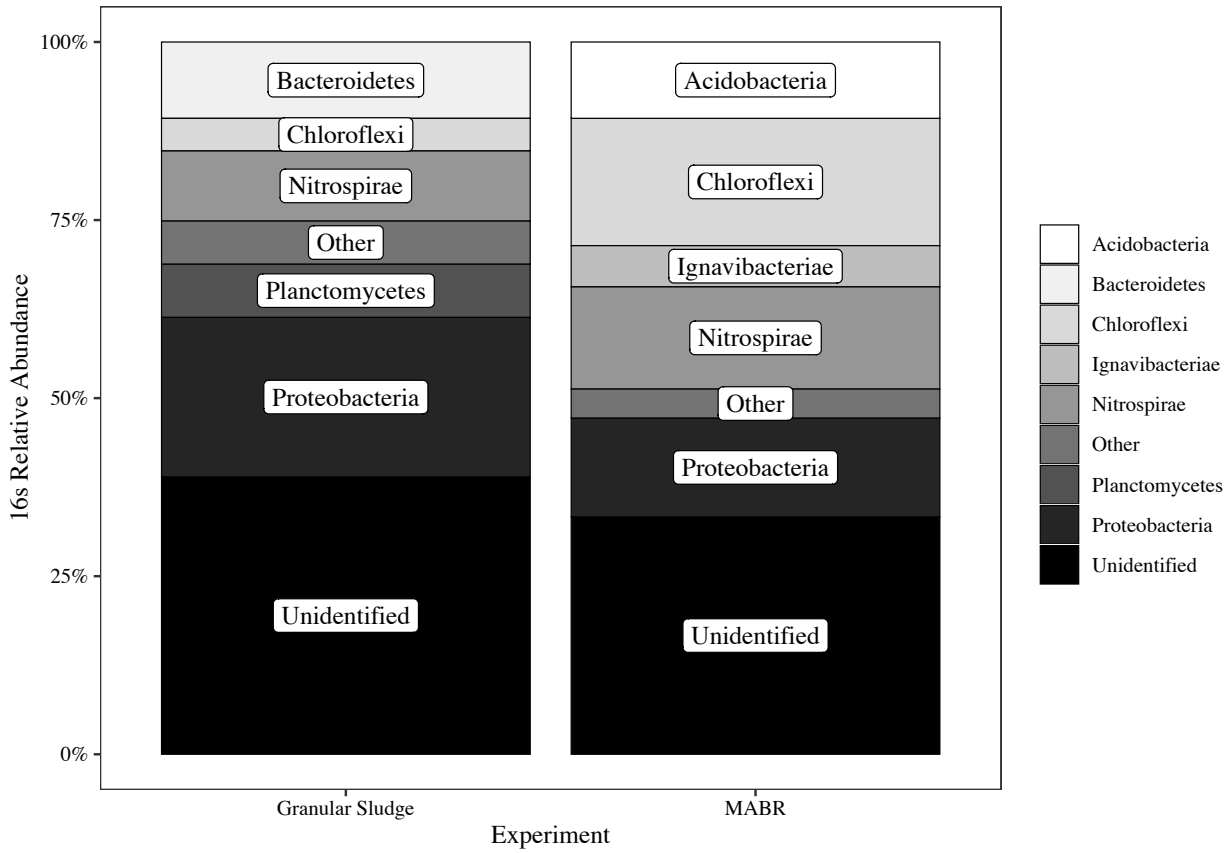

Figure C5. Relative abundances of top 6 most abundant phylums as determined from 16s sequencing for the granular sludge reactor and MABR.

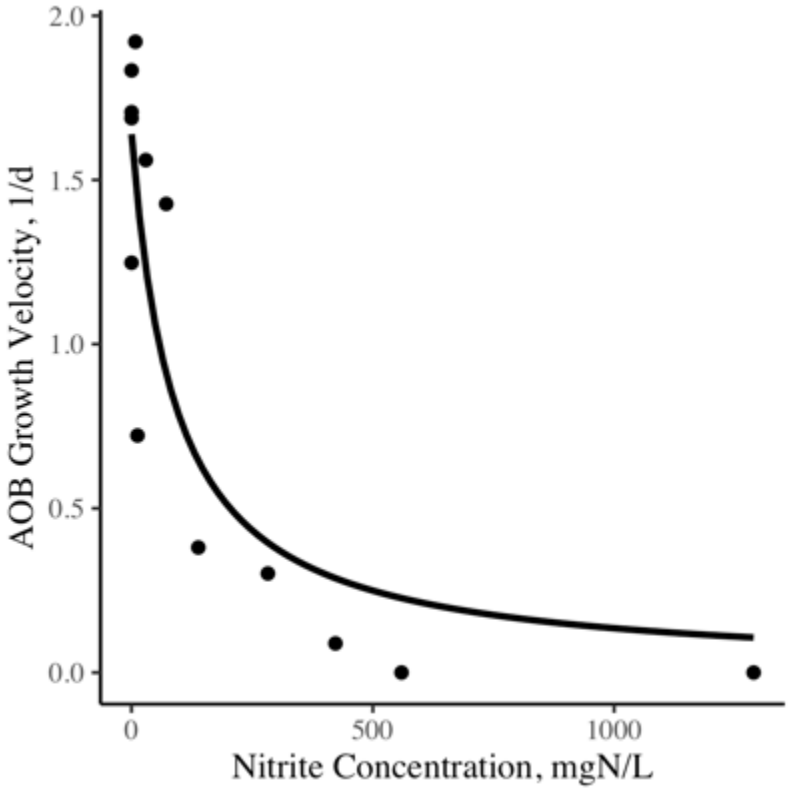

Figure C6. Nitrite inhibition curve of *Nitrosomonas europaea.* The inhibition curve fit to this data revealed a nitrite inhibition constant of 89 ± 46 mgN/L-NO_2^-.

Table C1. Definitions

AMX	Anaerobic Ammonium Oxidizing organism (anammox)
AOB	Ammonium Oxidizing Bacteria
NOB	Nitrite Oxidizing Bacteria
CMX	Complete Ammonium Oxidizing bacteria (Comammox)
S_S	Concentration of organic substrate, gCOD m^{-3}

Table C2. Reaction Kinetics

Process	Rate
Anammox	
Growth	$\mu_{max}^{AMX} \cdot \frac{S_{NH_4^+}}{S_{NH_4^+} + k_{NH_4^+}^{AMX}} \cdot \frac{S_{NO_2^-}}{S_{NO_2^-} + k_{NO_2^-}^{AMX}} \cdot \frac{k_{i,NO_2^-}^{AMX}}{S_{NO_2^-} + k_{i,NO_2^-}^{AMX}} \cdot \frac{k_{i,O_2}^{AMX}}{S_{O_2} + k_{i,O_2}^{AMX}} \cdot X_{AMX}$
Death	$b_{AMX} \cdot X_{AMX}$
AOB	
Growth	$\mu_{max}^{AOB} \cdot \frac{S_{NH_4^+}}{S_{NH_4^+} + k_{NH_4^+}^{AOB}} \cdot \frac{S_{O_2}}{S_{O_2} + k_{O_2}^{AOB}} \cdot \frac{k_{i,NO_2^-}^{AOB}}{S_{NO_2^-} + k_{i,NO_2^-}^{AOB}} \cdot X_{AOB}$
Death	$b_{AOB} \cdot X_{AOB}$
Comammox	
Growth on Ammonium*	$\mu_{max}^{CMX} \cdot \frac{S_{NH_4^+}}{S_{NH_4^+} + k_{NH_4^+}^{CMX}} \cdot \frac{S_{O_2}}{S_{O_2} + k_{O_2,NH_4^+}^{CMX}} \cdot \frac{k_{i,NO_2^-}^{CMX}}{S_{NO_2^-} + k_{i,NO_2^-}^{CMX}} \cdot \frac{S_{NH_4^+}}{S_{NH_4^+} + S_{NO_2^-}} \cdot X_{CMX}$
Growth on Nitrite*	$\mu_{max}^{CMX} \cdot \frac{S_{NO_2^-}}{S_{NO_2^-} + k_{NO_2^-}^{AMX}} \cdot \frac{S_{O_2}}{S_{O_2} + k_{O_2,NO_2^-}^{CMX}} \cdot \frac{k_{i,NO_2^-}^{CMX}}{S_{NO_2^-} + k_{i,NO_2^-}^{CMX}} \cdot \frac{S_{NO_2^-}}{S_{NH_4^+} + S_{NO_2^-}} \cdot X_{CMX}$
Death	$b_{CMX} \cdot X_{CMX}$
NOB	
Growth**	$\mu_{max}^{NOB} \cdot \frac{S_{NO_2^-}}{S_{NO_2^-} + k_{NO_2^-}^{AMX}} \cdot \frac{S_{O_2}}{S_{O_2} + k_{O_2,NO_2^-}^{CMX}} \cdot X_{NOB}$
Death	$b_{NOB} \cdot X_{NOB}$

* Because comammox can oxidize either ammonium or nitrite The ratio of either $NH_4^+ : NH_4^+ + NO_2^-$ or $NO_2^- : NH_4^+ + NO_2^-$ in the reaction rate allows us to assume preference for these two processes is dependent on concentration of the nitrogen substrate while distributing X_{CMX}.

** A binary switching factor (not shown) is also used in this reaction to ensure that this process will be 0 when ammonium concentration is 0 to avoid numerical errors.

Table C3. Stoichiometric matrix

Component → / Process ↓	$S_{NH_4^+}$ $\frac{gN}{m^3}$	$S_{NO_2^-}$ $\frac{gN}{m^3}$	$S_{NO_3^-}$ $\frac{gN}{m^3}$	S_{N_2} $\frac{gN}{m^3}$	S_{O_2} $\frac{g}{m^3}$	S_S $\frac{gCOD}{m^3}$	X_I $\frac{gCOD}{m^3}$	X_{AN} $\frac{gCOD}{m^3}$	X_{AOB} $\frac{gCOD}{m^3}$	X_{CMX} $\frac{gCOD}{m^3}$	X_{NOB} $\frac{gCOD}{m^3}$
Anammox											
Growth	$-{}^{1}/_{Y_{AMX}} - i_{NXB}^{AMX}$	$-{}^{1}/_{Y_{AMX}} - 1/1.14$	$1/1.14$	${}^{2}/_{Y_{AMX}}$				1			
Death	$i_{NXB}^{AMX} - f_i i_{NXI} - (1-f_i) i_{NSS}$					$1-f_i$	f_i	-1			
AOB											
Growth	$-{}^{1}/_{Y_{AOB}} - i_{NXB}$	${}^{1}/_{Y_{AOB}}$			$1 - {}^{3.43}/_{Y_{AOB}}$				1		
Death	$i_{NXB} - f_i i_{NXI} - (1-f_i) i_{NSS}$					$1-f_i$	f_i		-1		
Comammox											
Growth on Ammonium	$-{}^{1}/_{Y_{CMX}} - i_{NXB}$	${}^{1}/_{Y_{CMX}}$			$1 - {}^{3.43}/_{Y_{CMX}}$					1	
Growth on Nitrite	$-i_{NXB}$	$-{}^{1}/_{Y_{CMX}}$	${}^{1}/_{Y_{CMX}}$		$1 - {}^{1.14}/_{Y_{CMX}}$					1	
Death	$i_{NXB} - f_i i_{NXI} - (1-f_i) i_{NSS}$					$1-f_i$	f_i			-1	
NOB											
Growth	$-i_{NXB}$	$-{}^{1}/_{Y_{NOB}}$	${}^{1}/_{Y_{NOB}}$		$1 - {}^{1.14}/_{Y_{NOB}}$						1
Death	$i_{NXB} - f_i i_{NXI} - (1-f_i) i_{NSS}$					$1-f_i$	f_i				-1

Table C4. Stoichiometric, kinetic and diffusion parameters

Parameter	Value	Unit	Description	Reference
Stoichiometric Parameters				
Y_{AMX}	0.17	gCOD gN^{-1}	Yield of anammox on ammonium	[10]
Y_{AOB}	0.09	gCOD gN^{-1}	Yield of AOB on ammonium	[48]
Y_{CMX}	0.174	gCOD gN^{-1}	Yield of comammox on ammonium/nitrite	[17]
Y_{NOB}	0.057	gCOD gN^{-1}	Yield of NOB on nitrite	[17]
f_i	0.08	gCOD $gCOD^{-1}$	Inert content in biomass	[196]
i_{NXB}	0.083	gN $gCOD^{-1}$	Nitrogen content in active biomass	[197]
i_{NXB}^{AMX}	0.058	gN $gCOD^{-1}$	Nitrogen content in active anammox biomass	[197]
i_{NXI}	0.06	gN $gCOD^{-1}$	Nitrogen content in inert biomass	[196]
i_{NSS}	0.03	gN $gCOD^{-1}$	Nitrogen content in organic substrate	[196]
Kinetic Parameters				
μ_{max}^{AMX}	0.18	d^{-1}	Maximum growth rate of anammox	[20]
μ_{max}^{AOB}	1.36	d^{-1}	Maximum growth rate of AOB	[20,112]
μ_{max}^{CMX}	0.294	d^{-1}	Maximum growth rate of comammox	[17]
μ_{max}^{NOB}	0.79	d^{-1}	Maximum growth rate of NOB	[14]
$k_{NH_4^+}^{AMX}$	1.8	gN m^{-3}	Ammonium half-saturation constant for anammox	[20]
$k_{NO_2^-}^{AMX}$	0.67	gN m^{-3}	Nitrite half-saturation constant for anammox	[20]
k_{i,O_2}^{AMX}	0.01	g m^{-3}	Oxygen half-inhibition constant for anammox	[198]
$k_{i,NO_2^-}^{AMX}$	400	gN m^{-3}	Nitrite half-inhibition constant for anammox	[117]
$k_{O_2}^{AOB}$	0.5	g m^{-3}	Oxygen half-saturation constant for AOB	[112]
$k_{NH_4^+}^{AOB}$	2.19	gN m^{-3}	Ammonium half-saturation constant for AOB	[112]
$k_{i,NO_2^-}^{AOB}$	89.4	gN m^{-3}	Nitrite half-inhibition constant for AOB	This Study
$k_{NH_4^+}^{CMX}$	0.0091	gN m^{-3}	Ammonium half-saturation constant for comammox	[17]
$k_{NO_2^-}^{CMX}$	6.65	gN m^{-3}	Nitrite half-saturation constant for comammox	[17]
$k_{O_2,NH_4^+}^{CMX}$	0.131	g m^{-3}	Oxygen half- saturation constant for ammonium oxidation by comammox	This study
$k_{O_2,NO_2^-}^{CMX}$	0.126	g m^{-3}	Oxygen half-saturation constant for nitrite oxidation by comammox	This Study

Table C4 (cont)				
$k_{i,NO_2^-}^{CMX}$	4.34	g m^{-3}	Nitrite half-saturation constant for nitrite oxidation by comammox	[137]
$k_{O_2}^{NOB}$	0.9	g m^{-3}	Oxygen half-saturation constant for canonical *Nitrospira* NOB	[119]
$k_{NO_2^-}^{NOB}$	0.54	gN m^{-3}	Nitrite half-saturation constant for canonical *Nitrospira* NOB	[119]
b_{AMX}	0.027	d^{-1}	Specific biomass decay rate of anammox	Assumed to 5-15% of μ, similar to previous studies [20,116]
b_{AOB}	0.19	d^{-1}	Specific biomass decay rate of AOB	
b_{CMX}	0.022	d^{-1}	Specific biomass decay rate of comammox	
b_{NOB}	0.12	d^{-1}	Specific biomass decay rate of NOB	
Diffusion Coefficients				
$D_{NH_4^+}$	0.00015	m^2 d^{-1}	Diffusion coefficient of ammonium in water	[197]
$D_{NO_3^-}$	0.00014	m^2 d^{-1}	Diffusion coefficient of nitrate in water	[197]
$D_{NO_2^-}$	0.00014	m^2 d^{-1}	Diffusion coefficient of nitrite in water	[197]
D_{N_2}	0.00022	m^2 d^{-1}	Diffusion coefficient of N_2 gas in water	[197]
D_{O_2}	0.00022	m^2 d^{-1}	Diffusion coefficient of O_2 gas in water	[197]
$D_{NH_4^+}$	0.00015	m^2 d^{-1}	Diffusion coefficient of ammonium in water	[197]

Table C5. COD Measurements in both reactor systems.		
Reactor	Influent (mgCOD/L)	Effluent (mgCOD/L)
Granular Sludge Reactor	1000	1000
MABR	1010	1010

APPENDIX D

Supplemental Information for
Chapter 6:

Evaluating Impact of Anammox Granular Sludge Conditions on Ion Selective Electrodes

Number of Pages: 12
Number of Figures: 5
Number of Tables: 6

Table of Contents:

D.1 - Testing Methods to Biologically Inactivate Anammox Granular Sludge	D2
Figure D1. Granules observed to break down when sonicated with high speed sonicating tip.	D3
Figure D2. Granules immediately after treatment while aerating (t=0 hrs)	D4
Figure D3. Granules after 24 hours of aeration following inactivation treatments are shown. Autoclaved and bleached granules was observed to breakdown. Sonicated granules clumped together (clump shown inside red circle). Minimal change was observed in pH treated granules.	D4
Figure D4. Increase in total ammonia, nitrite, and nitrate after 24 hours of aeration in each bottle. Very little change in nitrite and nitrate was observed indicating successful inactivation.	D5
Figure D5. Nitric oxide concentration during one cycle of anammox sequencing batch reactor operation.	D7
Table D1. Makeup of ammonium Media fed to Operating Anammox Granular Sludge System	D7
Table D2. Chemicals Known to Damage ISEs	D7
Table D3. Incomplete List of Potential Chemicals Present in Anammox Granular Sludge with approximate concentrations where possible.	D8
Table D4. Electrode calibration curves in the active granular sludge reactor calcuated with the linear method function in the R stats package. Values are reported as ± SE.	D10
Table D5. Electrode calibration curves in inactive granular sludge calcuated with the linear method function in the R stats package. Values are reported as ± SE.	D10
Table D6. Electrode calibration curves in inactive granular sludge calcuated with the linear method function in the R stats package. Values are reported as ± SE.	D11

D.1 - Testing Methods to Biologically Inactivate Anammox Granular Sludge

D.1.1 Motivation

To isolate the physical impact of granular sludge on ion selective membranes it was necessary to make the granular sludge chemically and biologically inert while retaining its physical properties.

D.1.2 Methods

Five inactivation treatment methods were evaluated to biologically inactivate the sludge samples (i.e., kill all cells present) while keeping the granular sludge intact.

i. *Autoclaving* – 5 mL sludge was autoclaved on a short cycle (30 minutes)
ii. *Bleaching* – 5 mL sludge was soaked in a 10% bleach and tap water solution for 1-2 hours
iii. *Low pH* – 5 mL sludge was soaked in tap water adjusted to pH = 1 with HCl for 1-2 hours (inhibition of anammox begins at pH < 6.3, so any pH significantly below that threshold should be adequate for cell death)[8,32]
iv. *Low Rate Sonication* – A tube of 2.5 mL biomass was placed in a bath sonicator at full power (70 watts) for 5 minutes
v. *High Rate Sonication* – A tip sonicator was used on 2.5 mL of biomass for 5 minutes at half power (10 watts)

Granules that remained intact after the inactivation treatment methods described (*i* - *v*) were placed in a controlled ionic strength solution (50 mM NH_4Cl, 50 mM KCl)) to avoid sensor damage related to low ionic strength. The granular sludge was subsequently aerated with compressed air for 24 hours to apply some shear pressure to the sample and evaluate how each of the inactivation treatments (*i* - *v)* affected the structural integrity of granules. The granules were visually evaluated before and after aeration. The change in ammonium, nitrite, and nitrate over that 24-hour period were measured to check for biological activity.

D.1.3 Results and Discussion

D.1.3.1 Visual Transformations After Inactivation Treatment

High rate sonication with the tip sonicator (treatment *v*) for 5 minutes caused granules to shear apart almost entirely (Figure D1). Therefore, these granules did not undergo the 24 hour aeration treatment like the other four granular samples.

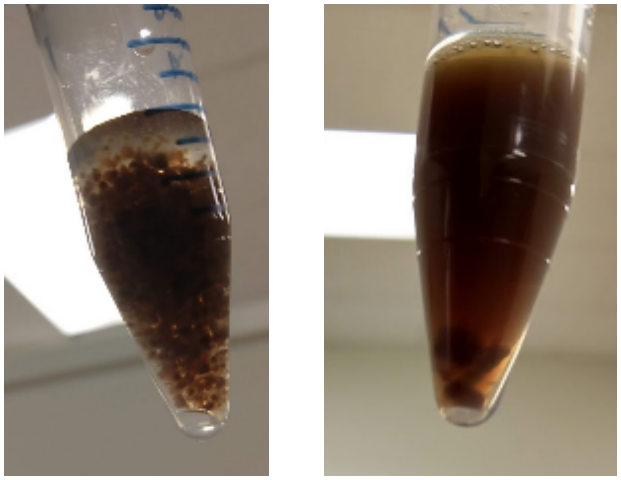

Before After

Figure D1. Granules observed to break down when sonicated with high speed sonicating tip.

Immediately after leaving the autoclave, the autoclaved biomass was found to have partially broken apart (water was cloudy). Bleached biomass turned white. On visual inspection, no significant drop in biomass level in the bottle was observed in the pH treated or bath sonicated samples (Figure D2).

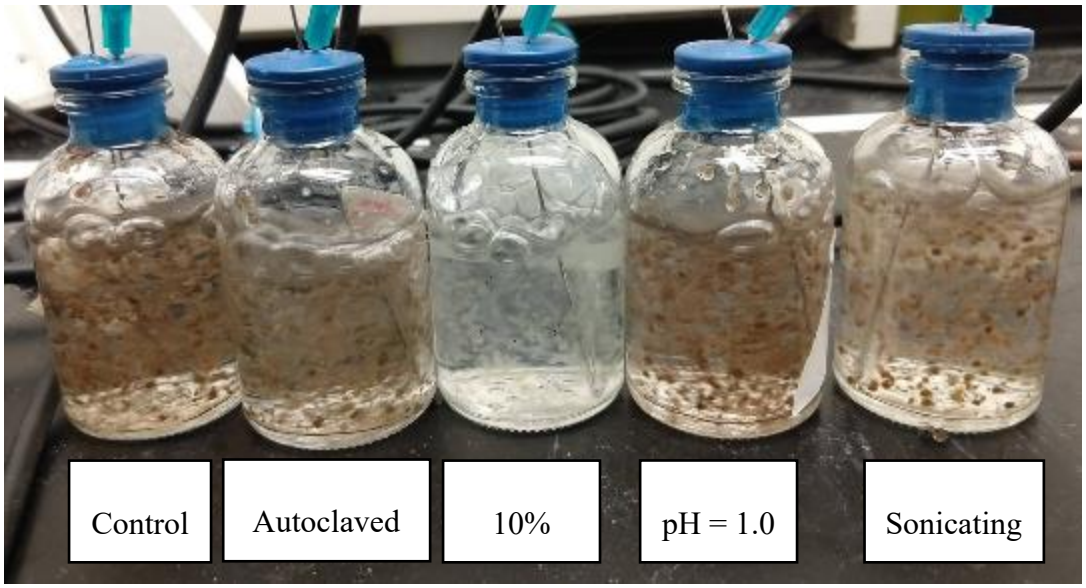

Figure D2. Granules immediately after the inactivation treatments while aerating (t=0 hrs)

After 24 hours of aeration, a drop in biomass level within the bottle was observed in the autoclaved and bleached samples. The sonicated biomass was observed to form clumps, perhaps due to additional EPS production caused by stressing organisms by sonication. Meanwhile, very little if any biomass level drop was observed in the control and pH treated samples (Figure D3).

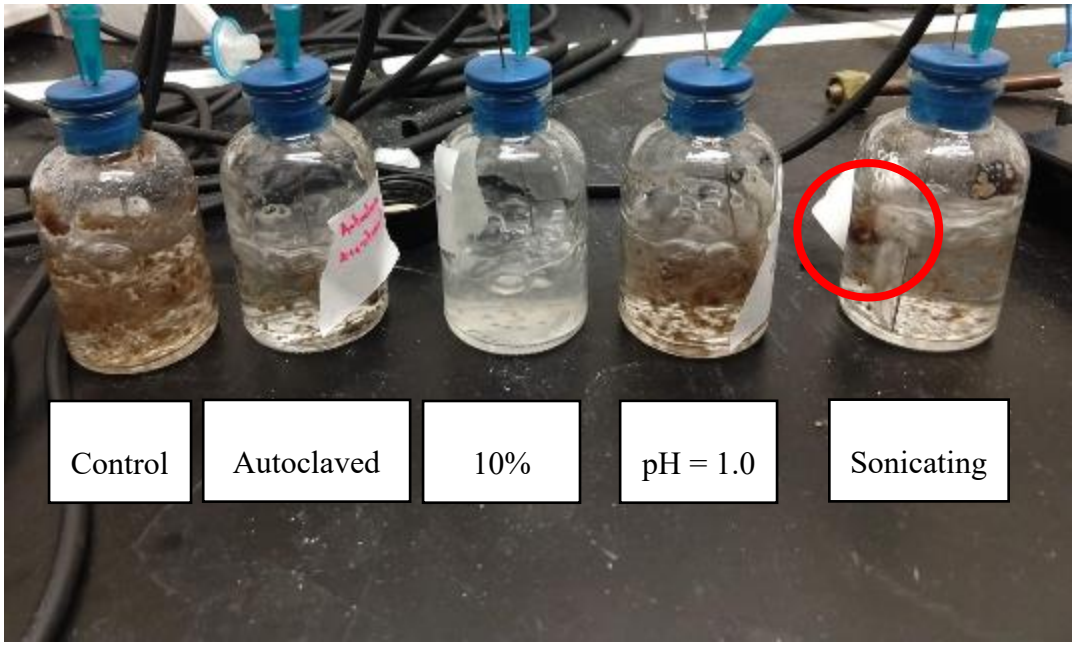

Figure D3. Granules after 24 hours of aeration following inactivation treatments are shown. Autoclaved and bleached granules was observed to breakdown. Sonicated granules clumped together (clump shown inside red circle). Minimal change was observed in pH treated granules.

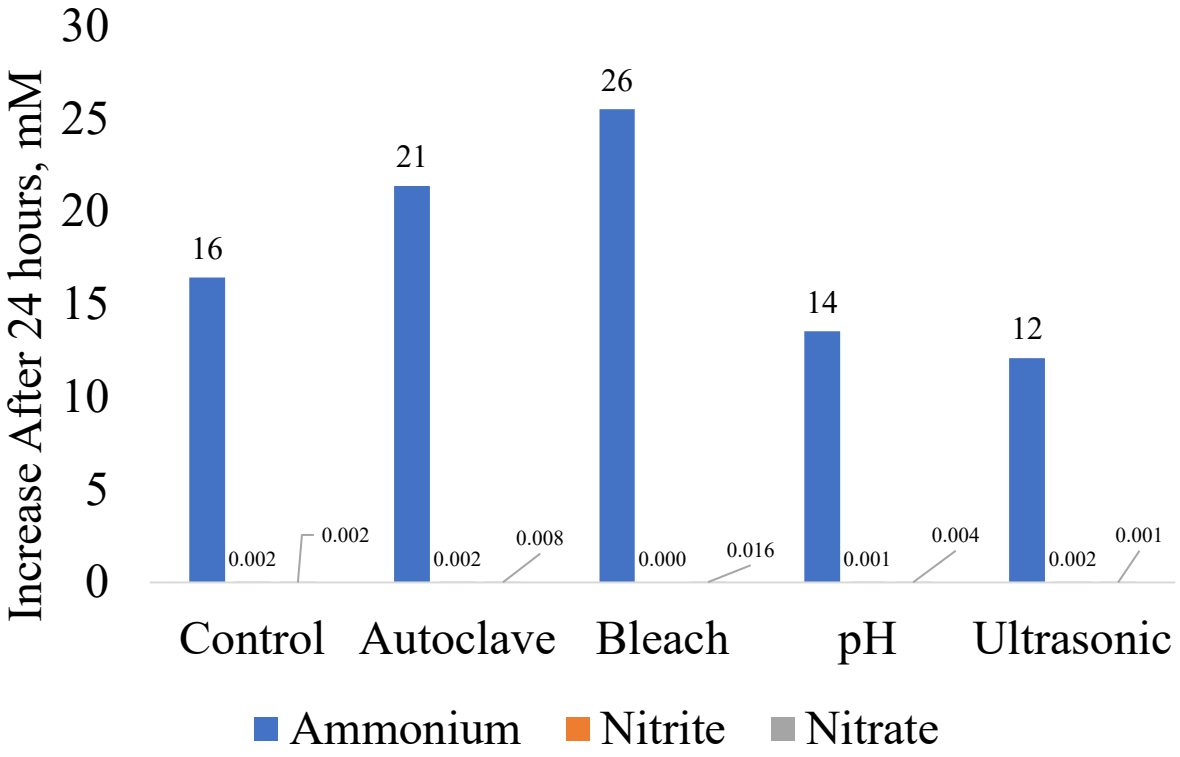

Figure D4. Increase in total ammonia, nitrite, and nitrate after 24 hours of aeration in each bottle. Very little change in nitrite and nitrate was observed indicating successful inactivation.

No de-ammonification or nitrification was observed in the samples, including the control. This may be because the biomass was placed in the controlled ionic solution, which had much higher concentrations of NH_4Cl and KCl than is typical of an anammox granular sludge system. The additional osmotic pressure likely inhibited the living cells in the control and caused some cell decay. Cell decay would result ammonification which is the release of nitrogen that was bound as part of cell material in the form of ammonia and ammonium. This hypothesis is suggested by the increase in ammonia concentration measured after 24 hours of aeration (Figure D4). Further work, such as a live dead stain of sample before and after treatment, would be required to confirm this hypothesis.

D.1.4 Conclusions

pH treatment was identified as the most effective method to biologically inactivate cells for the probe abrasion experiment. Significant biomass loss was observed in the autoclaved sample. Bleaching changed the color of the biomass and likely changes the physical properties of the biofilm matrix significantly that it turned from the red color typical of anammox granular sludge to a white and translucent color after treatment. Ultrasonic treatment did not cause breakdown of biomass but did cause biomass to clump together, which does not accurately represent anammox granular sludge in an operating reactor.

D.2 – Anammox Reactor Operational Detail

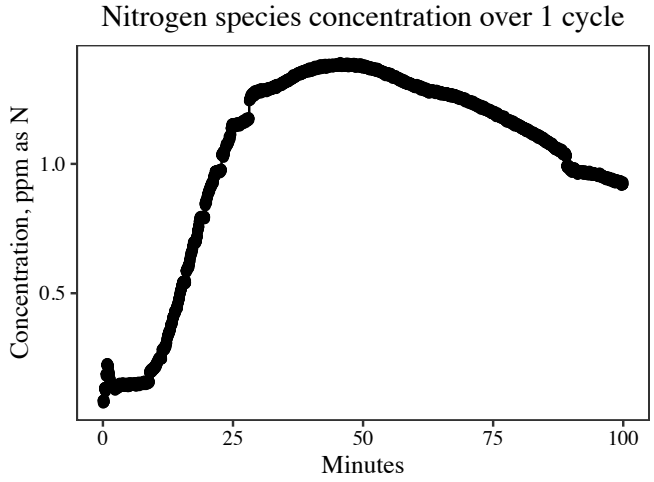

Figure D5. Nitric oxide concentration during one cycle of anammox sequencing batch reactor operation.

Table D1. Makeup of ammonium Media fed to Operating Anammox Granular Sludge System	
Chemical	Concentration
NH_4Cl	17.9 mM
$NaNO_2$	8.9 mM
NaCl	10 mM
KCl	0.1 mM
$CaCl_2.H_2O$	1 mM
$MgSO_4.7H_2O$	0.2 mM
$NaHCO_3$	4 mM
Trace Elements*	1.75 mL/L
*Vishniac solution was used for trace elements.[199]	

Table D2. Chemicals Known to Damage ISEs
Harsh Cleaning Reagents[200]
KATHON™ CG [201,202]
Thiazolinones
DECONEX ®11[203,204]
Surfactants
High Concentration Alkalis
Inorganic Chlorine Carriers
10% Phosphoric Acid

Table D3. Incomplete List of Potential Chemicals Present in Anammox Granular Sludge with approximate concentrations where possible.		
Chemical	Concentration Estimation	Reference
Ammonia/Ammonium	< 1 mM	This study, effluent measurement
Nitrite	< 1 mM	
Nitrate	< 1 mM	
Magnesium	~ 0.2 mM	This study, Reactor Influent concentration
Calcium	~ 1 mM	
Calcium	~ 10 mM	
Sodium	~ 20 mM	
Bicarbonate	~4 mM	
Sulfate	~ 0.2 mM	
EDTA	~ 20 µM	
Iron	~ 3 µM	
Zinc	~ 1 µM	
Molydate	~ 2 µM	
Copper	~ 1 µM	
Cobalt	~ 1 µM	
Di-basic Phosphate	~ 2 µM	
Potassium	~ 2 µM	
HEPES	~ 7 µM	
S-Adenosy-L-methionine (Quorum Quenching)	< 1e-9 ng/L	[205]
Homoserines Lactones (Quorum Sensing)	< 1e-9 ng/L	
Extracellular Poly-Saccharides	~ 5 mg/L	
Humic Acids	~ 5 mg/L	
Hydrazine	Not measured directly, N labeling experiment	[206]
Hydroxylamine	< 0 mgN/L	[207]

Table D3 cont. Incomplete List of Potential Chemicals Present in Anammox Granular Sludge with approximate concentrations where possible.		
Chemical	Concentration Estimation	Reference
Nitrous Oxide	0.6 ppm	[208]
Nitric oxide	~ 1 ppm	This study (Figure D5.)
Hydrophobic Amino Acids	Not measured directly, proteomics experiment	[209]
Pyruvate	Not measured directly, C labeling experiment	
Acetyl-CoA	Not measured directly, C labeling experiment	
Peptides	Not measured directly, C labeling experiment	

D.3 – Electrode Calibration Curves

Table D4. Electrode calibration curves in the active granular sludge reactor calcuated with the linear method function in the R stats package. Values are reported as ± SE.		
Electrodes in Active Anammox Bioreactor		
Days Exposed	Electrode	Calibration Curve
0	Ammonium	(55.9 ± 1.03) log10[NH_4^+] + (347. ± 4.36)
	Potassium	(57.3 ± 0.03) log10[K^+] + (467.8 ± 0.1)
	Chloride	(-51.7 ± 0.07) log10[Cl^-] + (10.6 ± 0.23)
14	Ammonium	(49.3 ± 0.06) log10[NH_4^+] + (347.1 ± 0.18)
	Potassium	(53.8 ± 0.02) log10[K^+] + (462.3 ± 0.04)
	Chloride	(-55.2 ± 0.12) log10[Cl^-] + (-17.2 ± 0.33)

Table D5. Electrode calibration curves in high concentration NO calcuated with the linear method function in the R stats package. Values are reported as ± SE.			
Electrodes in High NO Experiment			
0	Ammonium	Control (No NO)	(59.8 ± 0.22) log10[NH_4^+] + (356.5 ± 0.69)
	Ammonium	Replicate 1	(60.8 ± 0.17) log10[NH_4^+] + (351.8 ± 0.57)
	Ammonium	Replicate 2	(58.3 ± 0.11) log10[NH_4^+] + (521.1 ± 0.44)
	Potassium	Control (No NO)	(54.6 ± 0.58) log10[K^+] + (468.4 ± 1.91)
	Potassium	Replicate 1	(56.8 ± 0.14) log10[K^+] + (572.2 ± 0.45)
	Potassium	Replicate 2	(56.1 ± 0.13) log10[K^+] + (555.6 ± 0.44)
	Chloride	Control (No NO)	(-54.1 ± 0.13) log10[Cl^-] + (-14.4 ± 0.35)
	Chloride	Replicate 1	(-52.7 ± 0.15) log10[Cl^-] + (3.7 ± 0.5)
	Chloride	Replicate 2	(-47.5 ± 0.21) log10[Cl^-] + (18.9 ± 0.7)
4	Ammonium	Control (No NO)	(59.7 ± 0.34) log10[NH_4^+] + (356.7 ± 1.05)
	Ammonium	Replicate 1	(59.3 ± 0.15) log10[NH_4^+] + (372.9 ± 0.59)
	Ammonium	Replicate 2	(57.4 ± 0.14) log10[NH_4^+] + (519.1 ± 0.49)
	Potassium	Control (No NO)	(55.4 ± 0.08) log10[K^+] + (471.7 ± 0.27)
	Potassium	Replicate 1	(55.6 ± 0.13) log10[K^+] + (572.5 ± 0.44)
	Potassium	Replicate 2	(55.6 ± 0.1) log10[K^+] + (547.3 ± 0.35)
	Chloride	Control (No NO)	(-53.9 ± 0.14) log10[Cl^-] + (-11.5 ± 0.39)
	Chloride	Replicate 1	(-51.9 ± 0.15) log10[Cl^-] + (7.4 ± 0.47)
	Chloride	Replicate 2	(-50.1 ± 0.19) log10[Cl^-] + (10.9 ± 0.6)

Table D6. Electrode calibration curves in inactive granular sludge calcuated with the linear method function in the R stats package. Values are reported as ± SE.			
Electrodes in Inactive Granular Sludge			
0	Ammonium	Control (No NO)	(58.2 ± 0.1) log10[NH_4^+] + (362.5 ± 0.36)
	Ammonium	Replicate 1	(58.3 ± 0.11) log10[NH_4^+] + (371.7 ± 0.43)
	Ammonium	Replicate 2	(54.3 ± 0.1) log10[NH_4^+] + (537.6 ± 0.42)
	Potassium	Control (No NO)	(55.4 ± 0.08) log10[K^+] + (473.4 ± 0.28)
	Potassium	Replicate 1	(55.5 ± 0.18) log10[K^+] + (579. ± 0.64)
	Potassium	Replicate 2	(54.9 ± 0.23) log10[K^+] + (557.1 ± 0.79)
	Chloride	Control (No NO)	(-53.7 ± 0.15) log10[Cl^-] + (-8.1 ± 0.45)
	Chloride	Replicate 1	(-49.3 ± 0.2) log10[Cl^-] + (11.6 ± 0.71)
	Chloride	Replicate 2	(-51.5 ± 0.15) log10[Cl^-] + (5. ± 0.52)
1.7	Ammonium	Control (No NO)	(57.3 ± 0.08) log10[NH_4^+] + (351.2 ± 0.25)
	Ammonium	Replicate 1	(57.7 ± 0.07) log10[NH_4^+] + (357.7 ± 0.27)
	Ammonium	Replicate 2	(54.2 ± 0.08) log10[NH_4^+] + (519.2 ± 0.32)
	Potassium	Control (No NO)	(57.4 ± 0.18) log10[K^+] + (472.8 ± 0.56)
	Potassium	Replicate 1	(56.4 ± 0.08) log10[K^+] + (569.3 ± 0.29)
	Potassium	Replicate 2	(56.8 ± 0.13) log10[K^+] + (552.4 ± 0.45)
	Chloride	Control (No NO)	(-54.6 ± 0.09) log10[Cl^-] + (-2.9 ± 0.25)
	Chloride	Replicate 1	(-45. ± 0.18) log10[Cl^-] + (20.9 ± 0.62)
	Chloride	Replicate 2	(-49.2 ± 0.12) log10[Cl^-] + (10.8 ± 0.43)
4.9	Ammonium	Control (No NO)	(56.8 ± 0.07) log10[NH_4^+] + (344.3 ± 0.21)
	Ammonium	Replicate 1	(54. ± 0.16) log10[NH_4^+] + (338.6 ± 0.57)
	Ammonium	Replicate 2	(51.3 ± 0.17) log10[NH_4^+] + (493.6 ± 0.66)
	Potassium	Control (No NO)	(56.7 ± 0.14) log10[K^+] + (467.4 ± 0.44)
	Potassium	Replicate 1	(57.2 ± 0.16) log10[K^+] + (559.2 ± 0.65)
	Potassium	Replicate 2	(56.5 ± 0.09) log10[K^+] + (538.3 ± 0.36)
	Chloride	Control (No NO)	(-53.9 ± 0.1) log10[Cl^-] + (-3.5 ± 0.32)
	Chloride	Replicate 1	(-45.9 ± 0.2) log10[Cl^-] + (21. ± 0.71)
	Chloride	Replicate 2	(-49.4 ± 0.17) log10[Cl^-] + (13.4 ± 0.58)
6	Ammonium	Control (No NO)	(61.8 ± 0.58) log10[NH_4^+] + (356.9 ± 2.25)
	Ammonium	Replicate 1	(60.9 ± 0.47) log10[NH_4^+] + (354.1 ± 1.66)
	Ammonium	Replicate 2	(55.1 ± 0.12) log10[NH_4^+] + (497.8 ± 0.49)
	Potassium	Control (No NO)	(54.3 ± 0.19) log10[K^+] + (459.4 ± 0.63)
	Potassium	Replicate 1	(50.4 ± 0.29) log10[K^+] + (536.5 ± 0.99)
	Potassium	Replicate 2	(54.8 ± 0.1) log10[K^+] + (527.7 ± 0.35)
	Chloride	Control (No NO)	(-50.2 ± 0.16) log10[Cl^-] + (5.2 ± 0.5)
	Chloride	Replicate 1	(-50.5 ± 0.22) log10[Cl^-] + (9.9 ± 0.69)
	Chloride	Replicate 2	(-53.4 ± 0.16) log10[Cl^-] + (4.6 ± 0.49)

Table D6 Cont. Electrode calibration curves in high concentration NO calculated with the linear method function in the R stats package. Values are reported as ± SE.			
8.3	Ammonium	Control (No NO)	(57.2 ± 0.08) log10[NH_4^+] + (343.8 ± 0.25)
	Ammonium	Replicate 1	(54. ± 0.07) log10[NH_4^+] + (333.9 ± 0.25)
	Ammonium	Replicate 2	(51.3 ± 0.13) log10[NH_4^+] + (484.6 ± 0.5)
	Potassium	Control (No NO)	(67.4 ± 1.61) log10[K^+] + (498.3 ± 5.64)
	Potassium	Replicate 1	(54.9 ± 0.14) log10[K^+] + (547.1 ± 0.45)
	Potassium	Replicate 2	(55. ± 0.13) log10[K^+] + (527.6 ± 0.42)
	Chloride	Control (No NO)	(-53.2 ± 0.13) log10[Cl^-] + (-1.5 ± 0.41)
	Chloride	Replicate 1	(-47. ± 0.27) log10[Cl^-] + (21.1 ± 0.92)
	Chloride	Replicate 2	(-50.5 ± 0.23) log10[Cl^-]+ (14.2 ± 0.75)
10.8	Ammonium	Control (No NO)	(56.5 ± 0.1) log10[NH_4^+] + (339.3 ± 0.34)
	Ammonium	Replicate 1	(54.4 ± 0.17) log10[NH_4^+] + (332.2 ± 0.59)
	Ammonium	Replicate 2	(51.5 ± 0.19) log10[NH_4^+] + (482. ± 0.73)
	Potassium	Control (No NO)	(55. ± 0.14) log10[K^+] + (459.6 ± 0.43)
	Potassium	Replicate 1	(54.7 ± 0.12) log10[K^+] + (542.7 ± 0.42)
	Potassium	Replicate 2	(53.3 ± 0.15) log10[K^+] + (520.4 ± 0.5)
10.8	Chloride	Control (No NO)	(-54.2 ± 0.11) log10[Cl^-] + (-4.2 ± 0.34)
	Chloride	Replicate 1	(-50.8 ± 0.28) log10[Cl^-] + (11.8 ± 0.89)
	Chloride	Replicate 2	(-53.2 ± 0.22) log10[Cl^-] + (7.8 ± 0.71)
13.6	Ammonium	Control (No NO)	(56.1 ± 0.11) log10[NH_4^+] + (336.3 ± 0.36)
	Ammonium	Replicate 1	(52.8 ± 0.2) log10[NH_4^+] + (325.7 ± 0.73)
	Ammonium	Replicate 2	(50.9 ± 0.2) log10[NH_4^+] + (480.2 ± 0.77)
	Potassium	Control (No NO)	(58.6 ± 0.17) log10[K^+] + (468. ± 0.51)
	Potassium	Replicate 1	(56.2 ± 0.21) log10[K^+] + (544.8 ± 0.67)
	Potassium	Replicate 2	(55.3 ± 0.26) log10[K^+] + (518.2 ± 0.81)
	Chloride	Control (No NO)	(-54.1 ± 0.12) log10[Cl^-] + (-3.7 ± 0.37)
	Chloride	Replicate 1	(-49.3 ± 0.28) log10[Cl^-] + (18.1 ± 0.9)
	Chloride	Replicate 2	(-51.4 ± 0.23) log10[Cl^-] + (13.5 ± 0.74)
17.8	Ammonium	Control (No NO)	(56.3 ± 0.08) log10[NH_4^+] + (336.8 ± 0.28)
	Ammonium	Replicate 1	(51.9 ± 0.14) log10[NH_4^+] + (317.7 ± 0.53)
	Ammonium	Replicate 2	(48.6 ± 0.14) log10[NH_4^+] + (469.1 ± 0.54)
	Potassium	Control (No NO)	(55.8 ± 0.16) log10[K^+] + (461.9 ± 0.5)
	Potassium	Replicate 1	(49.9 ± 0.17) log10[K^+] + (525.7 ± 0.6)
	Potassium	Replicate 2	(51. ± 0.15) log10[K^+] + (510.2 ± 0.53)
	Chloride	Control (No NO)	(-55.2 ± 0.06) log10[Cl^-] + (-8.1 ± 0.19)
	Chloride	Replicate 1	(-48. ± 0.23) log10[Cl^-] + (20.6 ± 0.79)
	Chloride	Replicate 2	(-53.3 ± 0.2) log10[Cl^-] + (7.5 ± 0.68)

Kathryn Cogert
Curriculum Vitae

Phone: +1 (360) 927-6052
Email: cogerk@uw.edu

Educational History

June 2015 – Current *University of Washington* *Seattle, WA*

PhD Candidate in Civil and Environmental Engineering

Advisor: Mari H.K. Winkler

Thesis: Pairing Anaerobic Ammonia Oxidation with Newly Discovered Nitrite-Supplying Metabolisms for Enhanced Mainstream Nitrogen Removal

Sept. 2008 – June 2012 *University of Washington* *Seattle, WA*

B.S. in Chemical Engineering, 2012

Relevant Work Experience

June 2015 – Current *University of Washington* *Seattle, WA*

Graduate Research Assistant

Research: Biological Nitrogen Removal Processes:

(1) Pairing ammonium oxidizing organisms with anammox granular sludge

- Designed and operated automated anammox sequencing batch reactor utilizing LabVIEW software and compactRIO controller.
- Conducted assays to measure nitrogen conversion rates and kinetic parameters of ammonium oxidizing species.
- Developed novel inoculation techniques utilizing activated carbon as attachment medium for suspended cultures onto biofilm surfaces.
- Conducted molecular microbiological techniques to assess microbial ecology.
- Designed theoretical comammox-anammox models using AQUASIM software

(2) Techno-econonomic feasibility analysis of theoretical anammox, n-damo and anMBR systems

- Created theoretical models to evalute the potential operational cost and greenhouse gas emission reduction associated with various theoretical carbon and nitrogen removing wastewater treatment schema in R studio: https://github.com/cogerk/ndamo-econ

(3) Online Ammonium Measurement and Control

- Evaluated potential of multiple different online-ammonium measurement algorithms.
- Designed and operated short-term ammonium control scheme.
- Evaluated long-term performance of ion selective electrodes in anammox granular sludge.

Kathryn Cogert | University of Washington | Email: cogerk@uw.edu

July 2012 – Aug. 2014 *E3 Energy Partners* *Seattle, WA*

Process Engineer

- Commisioned 10 MMGPY biodiesel plant.
- Evaluated grantees and grants for Gates Foundation (i.e. Janicki Fecal Sludge Boiler/Generator Module)

March 2011 – Oct. 2011 *E3 Energy Partners* *Seattle, WA*

Engineering Intern

- Calculated mass and energy balance of silica production plant
- Performed R&D on viability of industrial fishing waste to omega oil production

June 2010 – Sept. 2010 *EdeniQ* *Visalia, CA*

Engineering Intern

- Modeled of Saccharification and Fermentation in Pilot Plant
- Document control for 40 MMGPY bioethanol plant design

Teaching Experience

June 2015 – Current *University of Washington* *Seattle, WA*

Guest Lecturer

Taught guest lectures for the courses:

- *Microbial Ecology (CEE 498 Spring 2016 & 2017)*
- *Wastewater Resuse and Resource Recovery (CEE 482 Winter 2020)*

Peer-Reviewed Publications

Cogert, K. I.; Ziels, R. M.; Winkler, M. K. H. Reducing Cost and Environmental Impact of Wastewater Treatment with Denitrifying Methanotrophs, Anammox, and Mainstream Anaerobic Treatment. *Environ. Sci. Technol.* **2019**. https://doi.org/10.1021/acs.est.9b04764.

Snauffer, A. M.; Chauhan, U.; **Cogert, K.;** Winkler, M. K. H.; Mueller, A. V. Data Fusion for Environmental Process Control: Maximizing Useful Information Recovery under Data Limited Constraints. *IEEE Sensors Lett.* **2019**, *3* (1). https://doi.org/10.1109/LSENS.2018.2889274.

Honors and Awards

1. International Conference on Nitrification, Top 3 Abstracts, 2019
2. Environmental Protection Agency Science to Achieve Results Fellowship, 2017-2019
3. National Science Foundation Graduate Research Fellowship, Honorable Mention, 2016
4. National Science Foundation Graduate Research Fellowship, Honorable Mention, 2015

5. Engineer in Training Certification, Washington State, #33415, 2013
6. UW Science and Technology Showcase, 1st Place, $1,000, "OmniOff", 2012
7. Honorable Mention, Environmental Innovation Challenge, $2,500, "OmniOff" 2012
8. Campus Sustainability Fund Grant, $1,600, 2012

Social Innovation Fast Pitch Competition, 2nd Place, University Division, $2,000, "Biodiesel Cooperative: Fostering Tomorrow's Energy Innovators", 2011

Volunteer and Professional Society Participation

Feb 2015 – June 2015 *Winkler Lab* *Seattle, WA*
University of Washington

Research Volunteer

- Programming automated control of granular sludge reactors.
- Managing set-up of granular sludge reactors.
- Reviewed model of PAO/GAO competition in granular sludge.

Feb 2011 – June 2012 *Biodiesel Cooperative* *Seattle, WA*
University of Washington

Founding Member

- Attained $10,000+ in funding for a student-run on-campus biodiesel production facility.

Feb 2011 – June 2012 *Engineers Without Borders* *Seattle, WA*
University of Washington

Publicity Directory

- Organized Silent Auction for Dessert and Wine event in 2010. Broke previous fundraising records by raising $30,000.
- Wrote quarterly newsletter to keep stakeholders involved and up-to-date with organizational activities

Conference Proceeding and Other Non-Journal Articles

Cogert, K. I.; Landreau, M.; Bryson, S.; Stahl, D. A.; Winkler, M.-K. H. Development of Archaeon-Anammox Granular Sludge Using Activated Carbon. In *International Conference on Nitrification 6*; Xiamen, China, 2019.

Cogert, K. I., Williamson, Grant., Siedlik, M., Wang, N., 'OmniOff: 2012 Business Plan". Seattle: Environmental Innovation Challenge, 2012. Web Access: http://foster.uw.edu/wp-content/uploads/2015/02/eic-omnioff.pdf

Cogert, K. I.. 'OmniOff: A Superior Nonstick Nontoxic Cookware". Environmental Innovation Challenge. Seattle Center, Seattle, WA. January 2012. Honorable Mention.

Cogert, K. I.. 'Biodiesel Cooperative: Fostering Tomorrow's Energy Innovators'. Social Innovation Fast Pitch. Fischer Pavillion, Seattle, WA. September 2011. 2nd Place.

Cogert, K. I., 'Biodiesel Cooperative: Fostering Tomorrow's Energy Innovators'. Environmental Innovation Challenge. Seattle Center, Seattle WA. March 2011.